THE UNIVERSITY
of EDINBURGH

Towards differentiation of mouse Embryonic Stem Cells to Thymic Epithelial Progenitor Cells

Xin Jin

Thesis presented for the degree of Doctor of Philosophy

The University of Edinburgh

2013

Declaration

The work presented in this thesis is my own, except where otherwise stated.

Xin Jin

Acknowledgement

Firstly, I would like to thank my supervisor Professor Clare Blackburn for giving me such an opportunity for doing this PhD project, for her academic guidance, patience and valuable writing comments. I would also like to thank all members of the Blackburn lab for their generous help, especially to Nick, Alison, Craig and Terri who almost act as my secondary supervisory board to teach me everything from basic lab techniques to the academic thinking. To Frances, who arranged everything well and saved me a lot of trouble in mouse organizing. I would also like to thank Dr G. Morrison, University of Cambridge, for sharing her protocol for generating anterior definitive endoderm from mouse ES cells ahead of publication. Thanks to all the service units in ISCR and CRM, including Simon Monard in FACS tutoring and help for cell sorting, thanks to Joe Mee and Sally Inverarity for help with kidney capsule grafting work, thanks to Ron Wilkie for help with teratomas analysis. Thanks to Dr. John West for kind help with statistics analysis and guidance during my thesis correction.

Thanks to my parents for their endless love and financial support. Finally, special thanks to Miss Yue Kang, for her love, care, encouragement and wisdom.

Abstract

The thymus is the major site for T-cell generation and thus is important for the adaptive immune system. Development of a properly selected, functional T-cell repertoire relies on interactions between developing T cells and a series of functionally distinct thymic stroma cell types including the cortical and medullary thymic epithelial cells (TECs). The thymus is one of the first organs to degenerate in normal healthy ageing. Related to this, there is strong interest in developing protocols for improving thymus function in patients by cell replacement or regenerative therapies. Thymic epithelial progenitor cells (TEPCs) represent a potential source of cells for thymus transplantation. However, the only source of these cells for transplantation is currently fetal thymus tissue. If TEPCs could be generated from pluripotent cells, this could provide an alternative source of cells for transplantation. The work described in this thesis therefore had two central aims (i) to test the stability of thymic epithelial progenitor cells *in vivo* and (ii) to investigate the possibility of generating TEPCs or TECs from mouse embryonic stem (ES) cells.

The forkhead transcription factor, *Foxn1*, is essential for the development of a functionally mature thymic epithelium, but is not necessary for formation of the thymic primordium or for medullary thymic epithelial sub-lineage specification. By reactivating Foxn1 expression postnatally in mice carrying a revertible hypomorphic allele of *Foxn1*, $Foxn1^{R}$, I herein demonstrate that TEPCs that can express only low levels of Foxn1 mRNA can persist postnatally in the thymic rudiment in mice until at least 6 months of age, and retain the potential to give rise to both cortical and medullary thymic epithelial cells (cTECs and mTECs). These data demonstrate that the TEPC-state is remarkably stable *in vivo* under conditions of low Foxn1 expression.

In parallel with this work, I confirmed the possibility of generating Foxn1-expressing cells from mouse ES cells by using a Foxn1 reporter cell line. As the thymic epithelium has a single origin in the third pharyngeal pouch (3pp) endoderm, I then tested whether or not TEPCs and /or TECs were generated during ES cell differentiation via existing protocols for generating anterior definitive endoderm differentiation cells from mouse ES cells. From this work, I showed that genes expressed in the 3pp and/or TEPC,-including *Plet-1*, *Tbx1*, *Hoxa3* and *Pax9,* were induced by differentiation of ES cells using these protocols. I further showed that cells expressing both Plet-1, a marker of foregut endoderm and 3pp, and EpCAM, a marker of proliferating epithelial cells, were induced using a novel protocol (2i ADE) for generating ES cells from ADE. However, gene expression analysis and functional testing suggested that the majority of these cells were non-thymus lineage. I subsequently developed a novel protocol which combined this 2i ADE protocol with co-culturing of the differentiating ES cells with fetal thymic lobes, and demonstrated that this further induced 3pp and TEPC related genes. Finally, I modified the culture conditions in this protocol to conditions predicted to better support TEPC/TEC, and showed that in these conditions, the TEPC-specific markers *Foxn1* and *IL-7* were induced more strongly than in any other conditions tested. The data presented in this thesis therefore represent an advance towards an optimized protocol for successfully generating TEPCs from ES cells *in vitro*.

Abbreviation

4-OHT	4-hydroxy-tamoxifen
3pp	Third pharyngeal pouch
ADE	Anterior definitivce endoderm
AFE	Anterior foregut endoderm
AVE	Anterior visceral endoderm
BM	Bone marrow
BSA	Bovine serum albumin
CMJ	Cortico-medullary junction
CoROC	Compact reaggregate organ culture
cTEC	Cortical thymic epithelial cell
DC	Dendritic cell
DE	definitive endoderm
DN	Double negative
DP	CD4 and CD8 double positive T cells
EB	Embryoid body
EpCAM	Epithelial cell adhesion molecule
EpiSC	Epiblast stem cell
ES cell	Embryonic stem cell
ESC	Embryonic stem cell
eYFP	enhanced Yellow Fluorescent Protein
FACS	Fluorescence-activated cell sorting
FCS	Fetal calf serum
Fgf	Fibroblast growth factor
FTL	Fetal thymic lobe
IC	Isotype control
ICM	Inner cell mass
IL	Interleukin
IP	Intraperitoneal
IRES	Internal ribosome entry site
K	Keratin
KGF	Keratinocyte growth factor
mAb	monoclonal antibodies
MEF	mouse embryonic fibroblast
MHC	Major histocompatibilty complex
MHCII	Major histocompatibilty complex class II
mTEC	Medullary thymic epithelial cell
NCC	Neural Crest Cell
NK	Natural killer
PBS	Phosphate buffered saline
qRT-PCR	Quantitative real-time polymerase chain reaction
R	*Foxn1*^{R} allele
R26	ROSA26 locus

SP	CD4 or CD8 single positve T cells
Tam	Tamoxifen
TCR	T cell receptor
TEC	Thymic epithelial cell
TEPC	Thymic epithelial progenitor cell
TN	Triple negative
U	Units
UEA	*Ulex europaeus* agglutinin

Table of Contents

Chapter 1: Introduction

1.1 Thymus

The thymus is located in the central compartment of the thoracic cavity, above the heart and below the sternum, and is the primary site for T-cell development (Miller 1961). The thymus has two functionally identical lobes. Each lobe can be histologically divided into two main compartments, the cortex and the medulla, and is surrounded by a mesenchymal capsule. The cortex and medulla each contain distinct thymic epithelial cell (TEC) types. Together with other non-epithelial cells, such as dendritic cells, macrophages and mesenchymal cells, these cells produce the unique microenvironment needed to support T-cell differentiation. (Figure 1.1). They are collectively termed the thymic stroma, which comprises five percent of the cells in the thymus. The remaining ninety five percent are developing T cells, or thymocytes (Nowell, Farley et al. 2007).

1.1.1 Thymocytes

Bone-marrow derived haematopoietic progenitor cells enter the thymus through the large vessels located at the cortico-medullary junction (CMJ) region. They then travel first through the cortex and then the medulla, and finally exit the thymus through the vasculature to the peripheral immune system (Petrie 2002).

The earliest T-cell progenitors do not express CD4 or CD8, and are therefore called double negative (DN) cells. Four different DN stage can be identified based on CD25 and CD44 expression. (DN1: $CD44^{+}CD25^{-}$; DN2: $CD44^{+}CD25^{+}$; DN3: $CD44^{-}CD25^{+}$; DN4: $CD44^{-}CD25^{-}$)(Godfrey, Kennedy et al. 1993). These cells give rise to $CD4^{+}CD8^{+}$ double positive cells, which undergo positive selection to become single

positive $CD4^+$ or $CD8^+$ cells (Petrie 2003)(Figure 1.1).

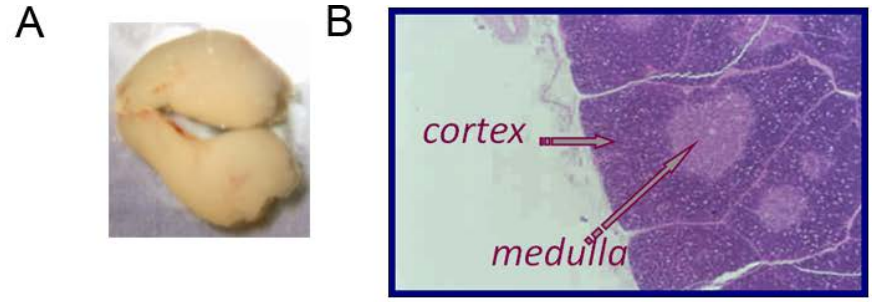

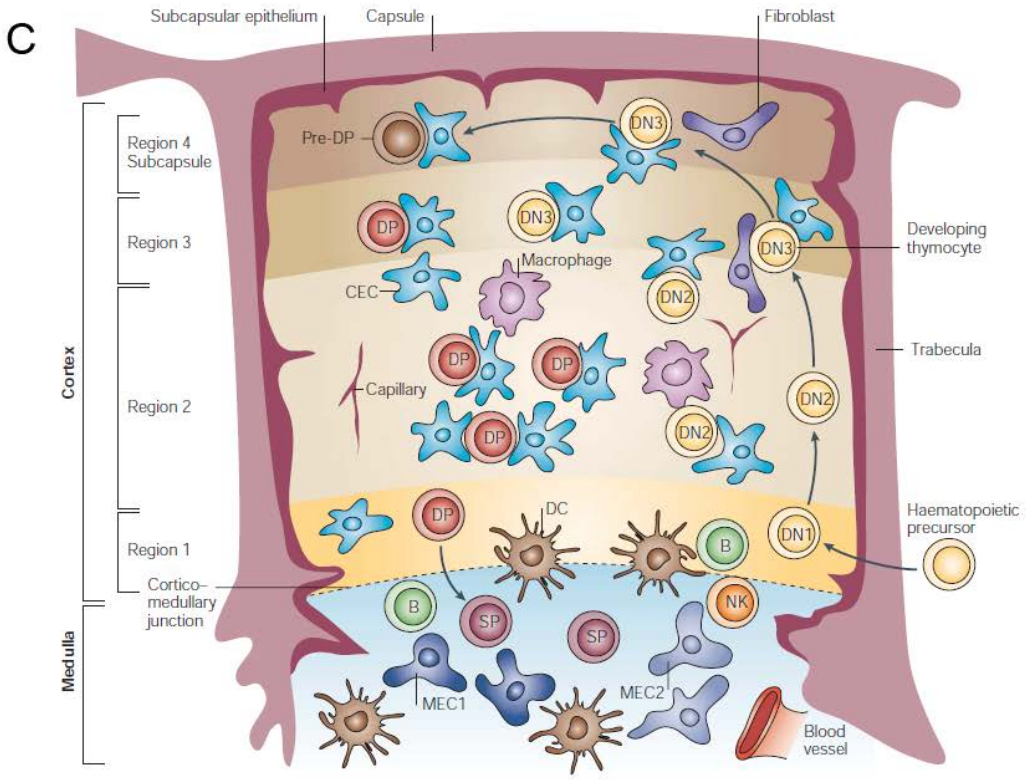

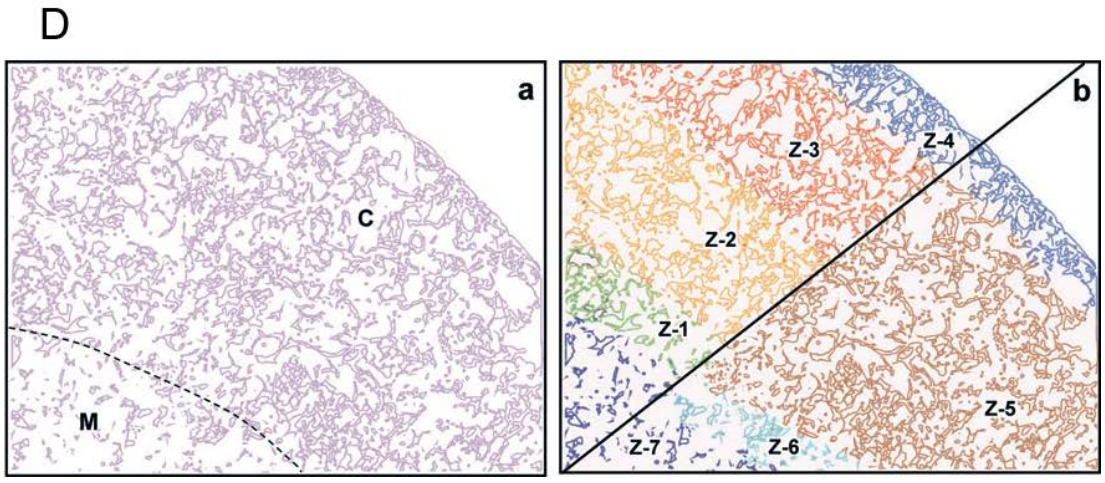

Figure 1.1 Thymus structure and function A) Image shows thymus dissected from a six week old C57BL/6 mouse (Nowell, Bredenkamp et al. 2011). **B**) Haematoxylin and eosin staining of a human thymus section. Arrows indicate cortex and medulla (Image from M. Ritter). **C**) Thymus structure and T-cell development process (Blackburn and Manley 2004) See text for explanation. **D)** Zones of thymocyte maturation. (a) shows the histologically defined cortical and medullary regions. (b) shows intrathymic zones identified on the basis of thymocyte maturation stage. Z-1, Z-2 and Z-3 are the areas predominantly containing DN1, DN2 and DN3 thymocytes, respectively. In Z-4, DN3 cells become pre-DP cells. IZ-5, also contains DP thymocytes, and in Z-6, thymocytes become immature SP cells. In Z-7, thymocytes become mature SP cells (Petrie and Zuniga-Pflucker 2007).

During their migration, the developing T cells, or thymocytes, interact with the different cell components of the thymus. First, they become committed to the T-cell fate and then, through positive selection, thymocytes with the ability to recognize self-MHC, are selected to survive and expand. Subsequently, through a process termed “negative selection”, T-cells which are self-reactive are eliminated. In this way, a diverse repertoire of peripheral T-cells is generated (Starr, Jameson et al. 2003).

TECs play an important role during the whole of T-cell development. When bone marrow (BM)-derived progenitor cells first seed the thymus, T-cell lineage commitment requires Notch (N1) receptor-mediated signalling (Radtke, Wilson et al. 1999; Wilson, MacDonald et al. 2001). There are two main classes of transmembrane bound ligands for Notch signalling, one is Jagged 1 and 2, and the other is Delta-like (DL) 1, 3 and 4 (Maillard, Fang et al. 2005). It would be interesting to address which ligand plays an essential role through Notch signalling in supporting the normal T-cell development. All these ligands can be detected within the functional TECs, except DL3 (Harman, Jenkinson et al. 2003). Meanwhile, *Jagged 1*$^{-/-}$ and *Jagged 2*$^{-/-}$ mice have normal T-cell development (Jiang, Lan et al. 1998; Mancini, Mantei et al. 2005) and thus DL3, Jagged1 and 2 are excluded from the candidates. Although overexpression of DL1 in stromal cells can support T-cell development in vitro (Schmitt and Zúñiga-Pflücker 2002), conditional inactivation of DL1 in either thymic epithelial cells or thymocytes does not inhibit T-cell development in vivo (Hozumi, Negishi et al. 2004). Recent study also shows that the expression of DL1 in TECs cannot be detected (Koch, Fiorini et al. 2008). Therefore, focus is changed to DL4. Inactivation of *DL4* in TECs leads to a complete block of T cell development coupled with the ectopic appearance of immature B cells, while loss of DL4 in hematopoietic progenitors doesn’t affect T-cell development. Furthermore, the

phenotype of *DL4* inactivation in TECs is consistent with the inactivation of N1 in BM-derived progenitor cells. Together, these observations suggest that, in the T cell lineage, commitment from the pro-T-cell to Pre-T-cell stage requires that DL4 is expressed in TECs to activate N1-mediated signalling in BM-derived progenitors (Koch, Fiorini et al. 2008). TECs also support T-cell development through expression of Interleukin-7 (IL-7). IL-7 is a pleiotropic cytokine that is produced by thymic and bone marrow stromal cells (Fry and Mackall 2002). IL-7 expression is initiated in the thymic-fated domain of the early primordium by E11.5 and shows differences in localization and frequency of expression in fetal and adult TECs (Zamisch, Moore-Scott et al. 2005). Mutation of the receptor of IL-7 (IL-7R) leads to a block in thymocyte expansion occurring before the onset of T cell receptor gene rearrangement at the DN stage (Peschon, Morrissey et al. 1994). IL-7 signaling also promotes the survival of DN thymocytes undergoing transition to double positive (DP) thymocytes (Trigueros, Hozumi et al. 2003) and proliferation of positively selected single positive (SP) thymocytes (Hare, Jenkinson et al. 2000). Therefore, IL-7 expressed by TECs is essential for T-cell development.

1.1.2 Thymic epithelial cells

Thymic epithelial cells (TECs) form a 3 three dimensional network structure within the thymus (van Ewijk, Wang et al. 1999). There are a variety of different TEC types within both the cortex and the medulla, based on morphology and antibody staining profile. Ultrastructural morphology studies demonstrated six types of epithelial cells within the human thymus (Vandewijngaert, Kendall et al. 1984). Later on, through a series of international workshops, the staining patterns of approximately 50 TEC-specific monoclonal antibodies (mAb) on multiple species including human and mouse, were tested. From this, seven clusters of thymic epithelial staining patterns (CTES) were identified and used to designate individual mAb (Table 1.1)(Kampinga,

Berges et al. 1989; Boyd, Tucek et al. 1993).

1.1.2.1 Subcapsular epithelium and cortical epithelium

The subcapsular epithelium separates the outer capsule, which is mainly composed of connective tissue, from the inner thymic epithelium. It also separates the lobulated cortex from the trabeculae, which penetrate from the capsule into the cortex to the cortico-medullary junction. The subcapsular epithelium is mainly composed of the type 1 epithelial cells, and is reactive to CTES II mAbs (Boyd, Tucek et al. 1993).

The thymic cortex proper lies directly under the subcapsular epithelium and can be separated into three main epithelial types: type II, type III and type IV. They were identified based on their electron lucency, and are described as “pale”, “intermediate” and “dark”, respectively (Vandewijngaert, Kendall et al. 1984). Their locations and morphological characteristics are summarized in Table 1.2. Although all cortical epithelial cells are reactive to CTES III mAbs, Type II and III could be distinguished from Type IV by strong expression of MHC Class II (Boyd, Tucek et al. 1993). The high expression of MHC Class II could be consistent with the possible role of these cell types in mediating positive selection of developing thymocytes. The cytoplasm of Type II and Type III cells was found to be able to completely surround lymphocytes (Vandewijngaert, Kendall et al. 1984) and thus is identical to the description of “thymic nurse cells” which were thought to play a role in positive selection of thymocytes (Wekerle and Ketelsen 1980; Ritter, Sauvage et al. 1981).

Antibodies for detecting different cytokeratins can also be used to classify different type of thymic epithelial cells. For example, a $K8^{+}K5^{-}K14^{-}K18^{+}$ phenotype broadly identifies cortical thymic epithelial cells, with exception of a small population of cTECs at the cortico-medullary junction, which is $K8^{+}K5^{+}K14^{-}K18^{+}$ (Klug, Carter et

al. 1998; Klug, Carter et al. 2002).

1.1.2.2 Medullary epithelium

Medullary epithelium also contains a variety of thymic epithelial cell types. These are generally reactive to CTES II and IV mAbs (Table 1.1), although Type III, Type V and Type VI were also found in the medulla through ultrastructural analysis. Based on their morphology as described in Table 1.2, Type V cells are classified as undifferentiated cells and Type VI are proposed as differentiated cells that can express hormones in supporting thymocytes development (Vandewijngaert, Kendall et al. 1984). All medullary epithelial cells are MHC Class I positive, but are variable for MHC Class II expression (Boyd, Tucek et al. 1993). In contrast to cortical epithelium, medullary thymic epithelial cells are predominantly $K8^{-}K5^{+}K14^{+}K18^{-}$ (Klug, Carter et al. 1998; Klug, Carter et al. 2002).

CTES group	Specificity
I	**Panepithelium**
II	**Subcapsule/perivascular, medulla** Medullary-network, Hassall's Corpuscles (HC) Subcapsule/perivascular (II.A thick; II.B thin)
III	**Cortex** III.A: pan cortex III.B: pan cortex, infrequent subset medulla III.C: pan cortex, subset leucocytes: III.C.1 macrophages III.C.2 thymocytes
IV	**Medulla** Pan medullary, HC
V	**Hassall's Corpuscles** V.A: HC V.B: HC, myeloid cells V.C: HC, associated medullary Ep V.D: HC, associated medullary Ep, subset leukocytes V.E: HC, associated medullary Ep, subcapsular Ep
VI	**Type 1 Epithelium**
XX	**Miscellaneous** XX.A Minority subcapsule, majority cortical and medullary Ep XX.B Minority of cortical and medullary Ep XX.C Minority medullary Ep, cortical thymocytes

Table 1.1 Cluster of thymic staining patterns. Summarized by Boyd et al (Examples and related references were not listed here)(Boyd, Tucek et al. 1993).

	Morphological characteristics	Location
Type 1 "subcapsular, perivascular"	basal lamina heterochromatic nucleus long cisternae of RER well-developed Golgi complex micropinocytotic vesicles	beneath capsule around capillaries in cortex and cortico-medullary junction region
Type 2 "pale"	round euchromatic nucleus well-developed Golgi complex short profiles of RER electron-dense granules tubular structures	scattered in cortex and medulla predominant in outer cortex
Type 3 "intermediate"	spectrum in morphology between type 2 and type 4 euchromatic or heterochromatic, irregularly shaped nucleus dilated cisternae of nucleus and RER	mid cortex, deep cortex, medulla
Type 4 "dark"	heterochromatic, electron-dense, irregularly shaped nucleus dilated cisternae of nucleus and RER residual bodies, swollen mitochondria	deep cortex scattered in medulla and around Hassall's corpuscules
Type 5 "undifferentiated"	rounded nucleus with some heterochromatin polyribosomes small bundles of tonofilaments small desmosomes	in groups in cortico-medullary region scattered in medulla
Type 6 "large-medullary"	large, rounded nucleus, either eu- or heterochromatic sometimes RER well developed abundant tonofilaments tubular structures	scattered in medulla adjacent to large Hassall's corpuscules part of small Hassall's corpuscules

Table 1.2 Morphological characteristics and location of types of epithelial cells in the human thymus (Wijngaert, Kendall et al. 1984)

1.1.3 Non-epithelial stroma cells

In addition to the epithelial cells, the thymus stroma also contains bone marrow (BM)-derived dendritic cells and macrophages (Boyd, Tucek et al. 1993). Dendritic cells mainly reside in the CMJ and medulla and display strong expression of MHC Class II (Duijvestijn and Hoefsmit 1981; Boyd, Tucek et al. 1993). These cells play an important role in negative selection stage of the T cell repertoire (Ardavi´n 1997). Recently, a study by Dudakov and colleagues showed that dendritic cells also secrete IL-23 in response to thymus damage, and that this secreted IL-23 further induces the lymphoid tissue inducer (LTi)-like cells to secret IL-22, which enhances the proliferation and survival of TECs. This study therefore reveals a crucial role for dendritic cells in endogenous thymic repair (Dudakov, Hanash et al. 2012), in addition to their role in negative selection

Within the thymus, macrophages mainly reside in the cortex and CMJ region. The morphology of the macrophages varies depending on their location, and they also show varying levels of MHC Class II expression. (Milicevic, Milicevic et al. 1987; Boyd, Tucek et al. 1993). It has been demonstrated that macrophages play an important role in removal of the apoptosed thymocytes within thymus through phagocytosis and subsequent DNA degradation (Odaka and Mizuochi 2002; Esashi, Sekiguchi et al. 2003).

Neural crest (NC) – derived mesenchymal cells form the outer layer of the thymus capsule. NC cells which migrate into the thymus eventually differentiate into pericytes and smooth muscle cells, which form the supportive network for the blood vessels (Le Lièvre and Le Douarin 1975; Foster, Sheridan et al. 2008). The NC–derived mesenchymal cells, along with cTECs, also express extracellular matrix which could be important for the thymocyte differentiation (Boyd, Tucek et al. 1993;

Savino, Villa-Verde et al. 1993).

1.2 Thymus organogenesis

1.2.1 Cellular basis of thymus organogenesis

The thymus is derived from the third pharyngeal pouches, which are bilateral outpocketings of pharyngeal endoderm and bud out from the endoderm at day 9 of embryonic development (E9.0) in the mouse (Figure 1.2a). Overt thymus organogenesis occurs from approximately E11 in the mouse, when the common thymus-parathyroid rudiments are growing out from the distal aspect of the third pharyngeal pouches (Figure 1.2b). At this stage, each rudiment is surrounded by a condensing population of mesenchymal cells derived from the NC. These cells support the growth and development of the primordium and will eventually form the capsule (Figure 1.2c). After further outgrowth, the common primordia finally separates from the pharynx by E12.5. The separated primordia migrate toward the anterior chest cavity (Figure 1.2d). By E13.5, the parathyroid and thymus domains resolve into physically separated organs. The thymus continues to migrate to the midline, whereas parathyroids migrate to the lateral margins of the thyroid gland (Blackburn and Manley 2004; Nowell, Farley et al. 2007) .

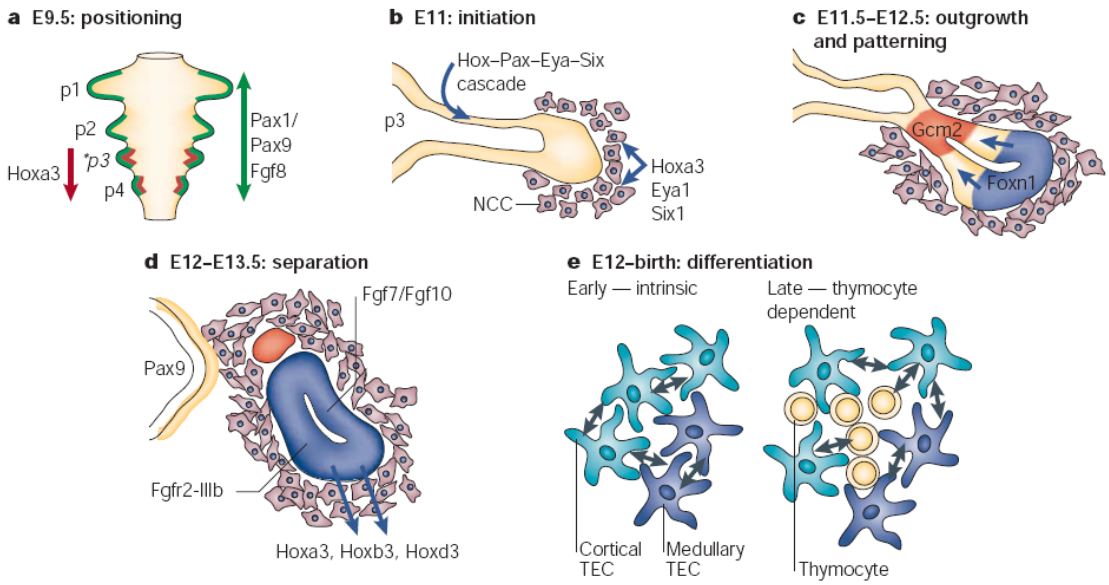

Figure 1.2 Thymus Organogenesis. See text for explanation. (from: Blackburn and Manley, 2004)

1.2.2 Cellular Interactions during thymus organogenesis

1.2.2.1 Lympho-Epithelial Cross-Talk

The first wave of haematopoietic progenitor cells seeds the thymus at about E11.5 (Owen and Ritter 1969; Fontaineperus, Calman et al. 1981), after formation of the thymus-parathyroid common primordium. The initial differentiation of TECs does not require inductive signals from lymphocytes (Klug, Carter et al. 2002); in the absence of lymphocytes, the differentiating thymus can give rise to cortical and medullary subsets which display normal gene expression profile and retain their functional capacity until E15.5 (Klug, Carter et al. 2002). However, the later stages of thymus epithelial cell maturation, expansion and maintenance require lympho-epithelial cross-talk (Ritter and Boyd 1993; Anderson and Jenkinson 2001). One example comes from research on Lymphotoxin ß receptor (LTßR) and its ligands lymphotoxin ß (LT ß) and LIGHT in the maintenance of the normal thymic 3-dimensional epithelial network. It has been shown that mature single-positive thymocytes are the main source of LTßR ligands, whereas LTßR is found on mTECs.

LTßR$^{-/-}$ mice display an abnormal mTEC network (Boehm, 2003).

1.2.2.2 Epithelial/mesenchymal interactions

The mesenchyme derived from neural crest cells (NCCs) is important for the thymus development. The first evidence came from Auerbach in 1960. At E12.5, the surrounding mesenchyme was removed from the thymus lobe; such lobes, when further cultured in fetal thymus organ conditions, could not give rise to a normal thymus (Auerbach, 1960). One possible way in which mesenchymal cells influence thymus organogenesis involves the provision of growth factors. *In situ* hybridization has show that Fibroblast growth factor 10 (Fgf10) is expressed in the mesenchymal cells of the thymic capsule, whereas fibroblast growth factor receptor 2 isoform IIIb (FgfR2IIIb), the receptor for Fgf7 and 10, is expressed in thymic epithelial cells at E12.5 (Revest, 2001). Furthermore, FgfR2-IIIb$^{-/-}$ mice demonstrate a block in the growth of the thymic epithelium from E12.5 (Revest, 2001). Although NCC-derived mesenchyme is necessary for generation of a normal thymus, initial pouch formation and thymus epithelial cell fate chosen do not appear to require epithelial/mesenchymal interactions, as mutant mice with a defect in NCCs develop an ectopic but properly patterned thymus (Griffith, Cardenas et al. 2009).

1.2.3 Molecular regulation of thymus development

The mechanisms that direct pharyngeal endoderm morphogenesis and patterning, and organogenesis of the various pharyngeal endoderm-derived organs are not completely understood. The following section describes several key genes which have been identified to have specific roles in thymus development based on genetic analyses.

1.2.3.1 *Tbx1*

Tbx1 is one of the T-box family genes. This family of genes is characterized by the

presence of a region of homology to the DNA-binding domain of the *T (Brachyury)* locus product (Bollag et al. 1994). The expression patterns of the T box genes, *Tbx1-Tbx5*, has been described during the early mouse development. Of these, Tbx1 was first detected in mesoderm within the E7.5 egg cylinder. At E9.5, Tbx1 was found in the pharyngeal region including the first to third pharyngeal pouch epithelium and the first to third pharyngeal arch mesenchyme cells. *Tbx1* expression was also found in the Otic vesicle at E9.5. Wholemount *in situ* hybridization also suggested *Tbx1* expression in non-pharyngeal region derived organs by E12, such as lung epithelium and spinal column (Chapman, Garvey et al. 1996).

Homozygosity for *Tbx-1* null mutation in the mouse results in failure of second and third pharyngeal arch and pouch formation during development. Interestingly, the adult phenotype of *Tbx1*$^{-/-}$ mice models the human DiGeorge/velocardiofacial syndrome (DGS/VCFS), including hypoplasia of the thymus and parathyroid (Jerome and Papaioannou 2001). Temporal-specific mutation of *Tbx1* established a crucial time interval for the requirement of *Tbx1* in thymus development, of between E7.5 to E11.5, as deletion of *Tbx1* before E8.5 led to athymia, deletion at E9.5 and E10.5 led to the thymus hypoplasia, and deletion after this time did not affect thymus formation. By lineage tracing, the *Tbx1* expressing cells at E8.5 contributed significantly to the thymus primodium in comparison with the limited contribution of E9.5 *Tbx1* expressing cells (Xu, Cerrato et al. 2005). In spite of the importance of *Tbx1* in thymus formation, these data indicate that *Tbx1* is not needed for thymus formation after E10.5. During the thymus/parathyroid primordium formation, *Tbx1* was found only expressed in the dorsal part of the 3rd pharyngeal pouch at E10.5, and was only expressed in the parathyroid-domain of the thymus/parathyroid common primordium at E11.5 (Liu, Yu et al. 2007). Manley and colleagues suggested a model for the *Tbx1* regulation of thymus and parathyroid organogenesis. Before E9.5,

deletion of *Tbx1* leads to failure of pouch formation and this leads to the subsequent failure of thymus formation. Deletion of *Tbx1* between E9.5 and E10.5 leads to the size reduction of the third pharyngeal pouch and thus leads to the thymic hypoplasia. *Tbx1* expression after E10.5 is needed only for parathyroid formation and the repression of *Tbx1* may be required for the thymus formation (Nowell, Farley et al. 2007; Manley and Condie 2010).

1.2.3.2 *Hoxa3*

Hox genes play an important role during vertebrate axial patterning during development, which includes regulation of the segmentation of hindbrain and axial skeleton (Krumlauf 1994; Alexander, Nolte et al. 2009). *Hoxa3*, a member of the *Hox* gene family, was found to be expressed in the third and fourth pharyngeal pouches, surrounding Neural Crest Cells (NCCs) and third and fourth pharyngeal arches. Its mutation leads to athymia and other pharyngeal organ defects (Manley and Capecchi 1995; Manley and Capecchi 1998). Unpublished data from the Manley lab suggested that third pharyngeal pouch formation does not require *Hoxa3*, but that later, patterning of the organ domains within third pharyngeal pouch, or the initial stage of organogenesis requires *Hoxa3*. It has also been demonstrated that *Hoxa3* expression in pharyngeal endoderm rather than in NCC is required for the third pharyngeal pouch patterning and initial organ development (unpublished data of Masuda *et al.*, summarized in Manley and Condie 2010), although deletion of *Hoxa3* expression in NCCs leads to failure of organ separation and migration.

1.2.3.3 *Pax1 and Pax9*

Pax genes are a family of transcription factors that act as developmental control genes during embryogenesis (Walther, Guenet et al. 1991; Buckingham and Relaix 2007). The Pax gene family members *Pax1* and *Pax9* are each expressed in the pharyngeal endoderm from E8.5. In *Pax9*-null mice, the invagination of the

endodermal cell layer of the developing thymus into the surrounding mesenchymal tissue is disturbed and an ectopic thymus forms located within the pharynx. Although the thymus primordium is colonized by T-cell precursors, failure of thymopoiesis is observed from E15.5 (Hetzer-Egger, Schorpp et al. 2002). *In situ* hybridizations detected *Pax1* expression in the endoderm of the foregut region as early as E8.5. At E9.5, transcripts were present in the first two pharyngeal pouches and by E10.5, clear expression was also observed in the third pharyngeal pouch. A large number of TECs are $Pax1^{+}$ and evenly distributed throughout the thymus primordium in day 12.5 embryos. With increasing age, the proportion of *Pax1*-expressing cells is reduced and in the adult mouse only a small fraction of cortical thymic epithelial cells retains strong *Pax1* expressoin. Mutations of the *Pax1* gene leads to thymus hypoplasia, also indirectly affects the maturation of thymocytes (Wallin, Eibel et al. 1996).

1.2.3.4 *Foxn1*

Foxn1 is the gene mutated in the nude mouse, which exhibits a phenotype of athymia and hairlessness (Nehls, Kyewski et al. 1996). Mutation of *Foxn1* in humans causes the same phenotype (Frank, Pignata et al. 1999). *Foxn1* is first detectable by RT-PCR at E9.5 (Nehls, Pfeifer et al. 1994) but is not detectable by in situ hybridization or reporter gene expression until E11.25, when it is specifically expressed in the third pharyngeal pouch (Gordon, Bennett et al. 2001). Although failure of *Foxn1* expression leads to athymia, *Foxn1* is not responsible for the initial thymus/parathyroid primordium formation or for thymic epithelial lineage specification. Rather, *Foxn1* is required in a cell-autonomous and dosage dependent manner for the further development of specified TECs (Blackburn, Augustine et al. 1996; Nehls, Kyewski et al. 1996; Nowell, Bredenkamp et al. 2011). In the absence of *Foxn1* expression, TECs undergo developmental arrest at an early progenitor cell stage, and clonal reactivation of expression leads to generation of a thymic lobule

containing both cortical and medullary TECs, that can support T-cell development (Bleul, Corbeaux et al. 2006). In addition, through affecting the TEC development, *Foxn1* is also required for the initial hematopoietic progenitor cell colonization of the thymic primordium and for seeding of the primordium with vascular endothelial progenitors (Itoi, Kawamoto et al. 2001; Mori, Itoi et al. 2010).

1.2.3.5 Regulatory network

Eyes absent gene 1 (Eya1) is expressed in third pharyngeal endoderm pouch, the mesenchyme surrounding it and the third pharyngeal ectoderm cleft at E9.5. Mutation of this gene results in failure of the thymus-parathyroid common primordium formation. Furthermore, the expression of *Six1*, mutation of which also leads to an absence of thymus, was found to be down-regulated within the pharyngeal region of *Eya1*$^{-/-}$ embryos, indicating *Eya1* acts upstream of *Six1* (Xu, Zheng et al. 2002).

Pax1 expression is reduced in the third pharyngeal pouches of *Hoxa3* null mutants, suggesting that *Hoxa3* acts upstream of *Pax1* (Manley and Capecchi 1995). The observation that the mutant phenotype of *Eya1* is similar to the mutant phenotype of *Hoxa3* (Manley and Capecchi 1995; Manley and Capecchi 1998; Xu, Zheng et al. 2002) and expression of *Hoxa3* in the third pharyngeal pouch was not altered in *Eya1* mutants, suggested that *Hoxa3* acts upstream of *Eya1*. A Pax-Eya–Six–Dach regulatory network was found during eye development of *Drosophila* (Wawersik and Maas, 2000), and expression of *Pax1* and *9* in third pharyngeal pouches is not altered in *Eya1* mutants. Thus, a Hox-Pax-Eya-Six network might exist in regulating thymus and parathyroid development. However, in more recent study, expression of *Eya1* and *Six1* were found independent of *Pax1* and *Pax9* expression. Moreover, expression of *Pax1* was shown to require *Eya1* and *Six1*, and *Tbx1* expression was

also reduced in mutant of *Eya1*. These data suggest that rather than acting in a classical ‘cascade’, these transcription factors may form a complex regulatory network, and that *Eya1* may act as early at the pharyngeal endoderm patterning stage (Zou, Silvius et al. 2006).

1.3 Thymic epithelial progenitor cells

1.3.1 Single origin for the cortical and medullary thymic epithelial compartments

A once prevailing hypothesis suggested that the cortex and the medulla are derived from the ectoderm and endoderm respectively, based on histological studies. Other studies, such as chick-quail chimera analysis, suggested that both cortical and medullary compartments are derived from isolated endoderm. This controversy was resolved by the work of Blackburn and colleagues (Blackburn, 2004; Gordon, 2004). First, the contact between the third pharyngeal pouch endoderm and third pharyngeal cleft ectoderm was confirmed as early as E10.5. However, a subsequent separation process between those two germ layers was found, based on analysis of apoptosis between E11.5 and E12.0. As the next step, the authors specifically marked the ectoderm using a cell-tracker dye, to trace the fate of the third pharyngeal ectoderm during embryo development *in vitro* for 30 hrs. The embryos used were isolated at E10.5 and analyzed at E11.5, the time window during thymus organogenesis in which the ectodermal contribution to the thymus had been argued to occur. No labelled ectoderm cells were found to contribute to the developing thymus in this experiment. Finally, the strongest evidence in this study was that the third pharyngeal pouch endoderm, isolated before contact with pharyngeal ectoderm (around E9.5), was shown to generate a functional thymus including both cortical and medullary

compartments after being ectopically transplanted under the kidney capsule of either nude or syngeneic wild type recipient mice. Interestingly, if the whole third pharyngeal compartment at the same stage was transplanted, the outcome was worse than transplanting third pharyngeal pouch alone, suggesting inhibition of thymic development by the ectoderm or other components of third pharyngeal pouch. Together, these data argued strongly in favor of a single-origin of the two compartments of the thymus and also suggested the existence of a common progenitor in the foregut endoderm for both cortical and medullary epithelial cells.

1.3.2 An MTS20^{+}24^{+} (Plet-1^{+}) phenotype identifies thymic epithelial progenitor cells

Identification and characterization of the progenitor cells for a particular somatic cell lineage *in vivo* is important for understanding how the tissue is generated and maintained, and is also required for investigation into generating cells of a particular lineage from ES cells differentiation *in vitro*. Thus a high fidelity marker, or markers, for identifying and isolating the progenitor cells is crucial. It has been established that mAbs MTS20 and MTS24, which recognize the orphan protein Plet-1, identify TEPCs within the fetal thymus until at least E15.5 (Bennett, Farley et al. 2002; Depreter, Blair et al. 2008). First, the MTS20 and MTS24 determinant expression profiles are consistent with those expected of TEPC markers (i.e. they mark a population in the third pharyngeal pouch and later thymus primordium, that initially represents the major epithelial cell type, and subsequently decrease with thymus maturation). Secondly, MTS20^{+}24^{+} cells purified from the thymus primordium at E12.5, followed by reaggregated fetal thymic organ cultures, can give rise to all thymic epithelial cell type based on expression of the adult cortical and medullary epithelial markers (Julie Sheridan and Clare Blackburn unpublished). Finally, ectopically transplanted MTS20^{+}MTS24^{+} cell reaggregates generated vascularized

thymi with both cortical and medullary structures, capable of attracting lymphocytes and supporting T-cell differentiation. This study did not determine whether the E12.5 thymic MTS20^{+}24^{+} population predominantly contained a common-progenitor for cortex and medulla, or contains distinct cortical and medullary progenitors already specified from earlier endoderm epithelial cells of wider potency.

1.3.3 Clonal evidence for a common progenitor for cortical and medullary TECs

It is well established that Plet-1 marks TEPCs, as described above. However, the possibility of generating both cTECs and mTECs from a single cell (common progenitor cell/bi-potent progenitor cell) was not demonstrated until recently. A single MTS24^{+} cell isolated at E12.5 from the thymus lobes of a genetically modified mouse that constitutively expressed eYFP, was injected into an E12.5 wild type thymus lobe. This lobe was grafted under the kidney capsule. Subsequent tracing of eYFP expressing cells demonstrated the ability of this single injected cell to generate cTECs and mTECs (Rossi, Jenkinson et al. 2006). Another clonal assay, conducted by Bleul and colleagues, demonstrated the presence of bi- and uni-potent progenitor cells for the cortical and medullary compartments in the neonatal mouse thymus, using short term lineage tracing. This analysis also showed that, in the absence of *Foxn1*, bi-potent progenitor cells persisted postnatally and indicated that these cells could give rise to a functional thymic microenvironment including both cortical and medullary compartments after reversion of the *Foxn1* allele (Bleul, Corbeaux et al. 2006). Collectively, the above work strongly suggested the existence of a common thymic epithelial progenitor cell, which can differentiate into all cortical and medullary epithelial cell types. Characterization of this common progenitor, understanding how it is generated and what controls its differentiation should facilitate generation of TECs from ES cells *in vitro*.

1.3.4 Foxn1 and TEPC

As described above, data on the neonatal clonal reactivation of the common TEPCs demonstrate that TEPCs form independently of *Foxn1*, but that *Foxn1* is required for their development into functionally mature cortical and medullary TECs (Bleul, Corbeaux et al. 2006). Interestingly, in the *Foxn1*$^{-/-}$ mouse, a Cldn4^{+} epithelial population could be observed in the E13.5 thymus primordium (Nowell, Bredenkamp et al. 2011). As it has been demonstrated that Cldn4^{+} cells appearing at the same stage in the wild type thymus primodium exclusively give rise to medullary TECs and thus represent the earliest medullary thymic epithelial progenitor cells (mTEPCs) (Hamazaki, Fujita et al. 2007), these data together indicate that the divergence of medullary progenitors is *Foxn1* independent.

It is not clear whether the divergence of cortical thymic epithelial progenitor cells (cTEPCs) from the common progenitor is *Foxn1* independent. However, the expression of CD205, which was recently identified as the earliest cortical epithelial lineage specific marker (Shakib, Desanti et al. 2009), can be detected within the thymus primordium only in the presence of *Foxn1* (Shakib, Desanti et al. 2009), (Nowell, Bredenkamp et al. 2011), thus suggesting a role for *Foxn1* in divergence of cortical progenitors.

The requirement for different *Foxn1* expression levels in regulating the lineage restricted progenitor cell differentiation and subsequent cortical and medullary epithelial cells maturation is carefully addressed in the recent published paper by Nowell and colleagues (Figure 1.3; Nowell, Bredenkamp et al. 2011). This shows that Foxn1 is required at multiple stages of TEC differentiation in the fetal and postnatal thymus, from exit from the earliest progenitor cell state to terminal

differentiation of cTEC and mTEC.

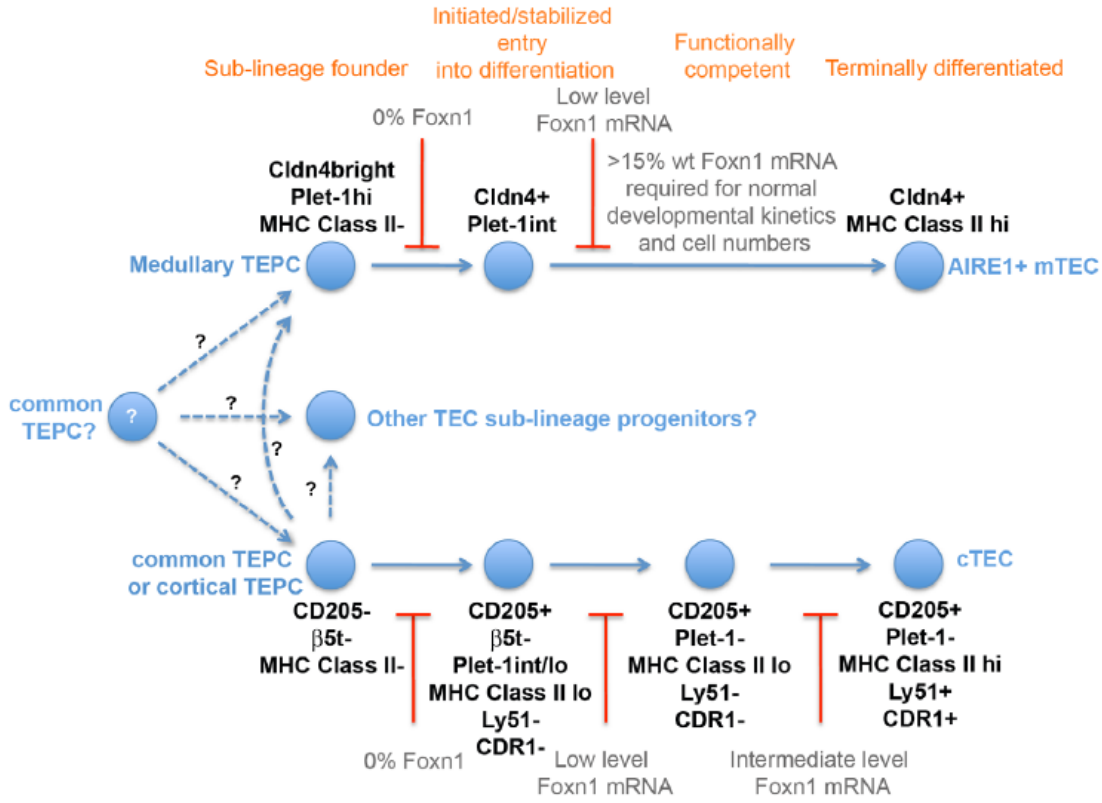

Figure 1.3 *Foxn1* regulation of TE lineage development (Nowell, Bredenkamp et al. 2011)

1.4 Potential to use embryonic stem cells to derive thymic epithelial progenitor cells

1.4.1 Embryonic stem cells

Both mouse (Evans and Kaufman 1981; Martin 1981) and human (Thomson 1998) embryonic stem (ES) cells are derived from the inner cell mass (ICM) of the embryo at the blastocyst stage. These cells can expand indefinitely in culture and remain pluripotent (Smith 2001). ES cells can be differentiated *in vitro* into endoderm, mesoderm, ectoderm and their derivatives, such as hepatocytes, hematopoietic cells, and neural cells. Therefore, ES cells are believed to hold a great promise as an unlimited source of cells for regenerative medicine (Murry and Keller 2008).

The initial derivation of mouse ES cells and their subsequent culture originally relied on feeder cells, which are mitotically inactivated mouse embryo fibroblast cells, and batch-selected fetal calf serum (Smith 2001). Later, the cytokine leukaemia inhibitory factor (LIF) was found to be able to activate STAT3, and together with bone morphogenetic protein (BMP) or serum was sufficient to support derivation and maintenance of mouse ES cells (Ying, Nichols et al. 2003). More recently, a chemically defined medium was derived. Through inhibition of glycogen synthase kinase-3 (Gsk3) by CHIRON99021 and mitogen-activated protein kinase (Mek) by PD0325901, mouse ES cells are shielded from differentiation stimuli, which act via the endogenous repressor activity of Tcf3 (Wray, Kalkan et al. 2011) and Fgf activated Mek-Erk signalling pathway (Kunath, Saba-El-Leil et al. 2007), respectively, and are thus maintained in a ground state of self-renewal (Ying, Wray et al. 2008). This “2 inhibitor” (2i) medium was also used to successfully to derive and maintain rat ES cells (Buehr, Meek et al. 2008).

In comparison with the serum containing culture method, mouse ES cells cultured in 2i medium are more homogeneous in morphology. The expression of the pluripotency markers Rex1, and key regulators, such as Nanog and Klf4, is also homogenous in 2i culture mouse ES cells, while mouse ES cells cultured in serum always have a considerable proportion of cells which have lost expression of these markers (Chambers, Silva et al. 2007; Toyooka, Shimosato et al. 2008; Niwa, Ogawa et al. 2009; Wray, Kalkan et al. 2010; Marks, Kalkan et al. 2012). Mouse ES cells cultured in 2i show a higher efficiency than mouse ES cells cultured in serum when differentiated to neuroectoderm (Marks, Kalkan et al. 2012). This approach, of growing mouse ES cells in a fully defined medium that maintains ground state pluripotency, is thought to offer an easier and more accurate way of studying regulation of pluripotency and of mouse ES cell differentiation.

1.4.2 Endoderm formation during embryo development

During the mouse embryo development, the ICM at the blastocyst stage will give rise to the epiblast and the primitive endoderm. The former gives rise to the whole fetus, and the latter to parietal endoderm and visceral endoderm. All three germ layers, endoderm, mesoderm and ectoderm, are generated through a process called gastrulation. The initiation of gastrulation in the epiblast is marked by formation of the primitive streak (PS) at the posterior part of the epiblast plate. Cells on the dorsal surface of the epiblast migrate to the PS in a posterior direction and, together with the cells surrounding the PS, transfer through the PS to the ventral part and then migrate in an anterior direction and form a new cell layer. Cells remaining on the epiblast surface will form the ectoderm. The new cell layer underneath will subsequently form the endoderm and mesoderm. The endoderm, or primitive gut tube, will first form at the two distal ends and these portals will migrate towards each other. In combination with the embryonic turning, this finally closes in the middle

and forms the entire primitive gut tube. The whole endoderm gut tube is regionalized from anterior to posterior into foregut, midgut and hindgut. The foregut endoderm gives rise to the pharyngeal endoderm and its derivatives, such as thymus and parathyroid. The respiratory system, including trachea and lung, together with the liver and pancreas are generally also considered as foregut endoderm derivatives, although they develop from a more caudal position. The mid-gut will give rise to the small intestine and the hind gut will give rise to large intestine and colon (Wells and Melton 1999; Zorn and Wells 2009).

1.4.3 Differentiation of embryonic stem cells into definitive endoderm cells

1.4.3.1 ES cell differentiation to definitive endoderm cells through embryoid body formation

ES cells can spontaneously form an aggregate, called an embyoid body (EB) when cultured in suspension. The precise interactions happening within an EB are still unclear, but it is believed that ES cells can re-initate the developmental program of the ICM and thus to some extent recapitulate embryonic development at this early stage (Smith 2001). For example, self-organization such as anterior-posterior polarization, formation of a primitive streak-like structure, and epithelial-to-mesenchymal transition have been observed during EB formation, and were demonstrated to be dependent on Wnt signalling (ten Berge, Koole et al. 2008)

The initial attempts to generate mature definitive endoderm (DE) derivatives relied on the spontaneous differentiation of EBs. Progenitor cells representing DE derivatives, such as hepatic or pancreatic cell lineage could then be isolated and further cultured in specific medium for their maturation. This type of method is relatively easy but has low efficiency (Smith 2001). However, an improved version

of this approach, with limited exposure to serum during EB formation, was found to enhance the efficiency of differentiating ES cells to definitive endoderm cells, based on the relative gene expression profile and functional assays. Activin A is a TGFβ family member which binds the same receptors as Nodal and thus triggering similar intracellular signaling events. It is widely used as an alternative of Nodal in cell culture due to its easier access through manufacture and lower cost. Administration of Activin A in serum-free medium during EB formation produced a similar result in terms of DE differentiation. In addition, a Brachyury-positive population was generated using this method, and its potential to generate both mesoderm and endoderm derivatives was tested via both gene expression profiling and kidney sub-capsule transplantation. This was the first demonstration of defined conditions for derivation of DE cells, and established the important role of Activin A in directing cell fate determination within the *in vitro* cell culture (Kubo, Shinozaki et al. 2004).

1.4.3.2 ES cell differentiation though a stepwise monolayer culture protocol

The most efficient method for generating definitive endoderm cells from ES cells published to date was established for human ES cells by D'Amour and colleagues, and is also based on manipulation of the Nodal signalling pathway (D'Amour, Agulnick et al. 2005). In D'Amour's study, medium with a series of different concentrations of serum supplemented with a high concentration of Activin A was tested for the DE induction efficiency based on the expression pattern of DE and non-DE markers. *SOX17* is expressed in DE and in primitive endoderm (PrE) and its derivatives visceral endoderm (VE) and parietal endoderm (PE). *FOXA2* is expressed in DE and also mesoderm, but not in PrE/VE/PE. Thus the combined expression of *SOX17* and *FOXA2* can be used to identify DE. It was found that the presence of Activin A (100ng/ml) and low serum concentrations produced cultures consisting of

up to eighty percent *SOX17*$^{+}$*FOXA2*$^{+}$ cells. During the differentiation process, NODAL and FGF8 expression, signifying the initial transition towards primitive streak-like cells, was first found, followed by the up-regulation of primitive streak markers such as brachyury, FGF4 and WNT3. Subsequently, with the rapid down-regulation of these primitive streak makers, the DE markers such as *SOX17* and *CER* exhibited rapid up-regulation. This temporal sequence of gene expression, characteristic of hES cell differentiation to DE is similar to the transitions that occur in the course of DE generation *in vivo*, suggesting a successful DE differentiation protocol. The potential of DE to give rise to its derivatives, such as liver and intestine, was verified through analysis of teratomas in the same study (D'Amour, Agulnick et al. 2005).

It has been reported that Activin A is present in the mouse embryo fibroblast-conditioned medium (MEF-CM), which is used for human ES cell maintenance (Beattie, Lopez et al. 2005). McLean and his colleagues demonstrated that suppression of phosphatidylinositol 3-kinase (PI3K) signalling alone could promote the human ES cells cultured in MEF-CM to differentiate into DE, and thus indicated a role of PI3K in blocking the differentiation of hES cells in response to Activin A (McLean, D'Amour et al. 2007). Further work indicated that insulin and insulin-like growth factor present in fetal calf serum (which is required at a concentration of twenty percent to promote self-renewal of hESCs), act through PI3K signalling to antagonize differentiation of hESCs, and thus further indicated why only in low concentrations of fetal calf serum (D'Amour, Agulnick et al. 2005) could Activin A promote DE differentiation (McLean, D'Amour et al. 2007). In summary, this research indicated that Activin A can efficiently specify DE from human embryonic stem cells only when PI3K is suppressed. In mouse ES cells, it has been demonstrated that the PI3K-Akt signalling pathway was activated by LIF signalling.

Through stimulation of transcription of *Tbx3*, the PI3K-Akt pathway can activate *Nanog* and *Sox2*, two transcription factors which together with Oct4 compose the key regulatory circuit for mouse ES cell pluripotency. Therefore, inhibition of PI3K may lead to the loss of pluripotency of mouse ES cells and thus promote differentiation (Niwa, Ogawa et al. 2009). However, whether PI3K plays the same role in human ES cells is unknown.

The thymus is derived from most anterior part of the endoderm. Therefore, knowledge of induction and monitoring the anterior-posterior patterning of the endoderm gut tube is important for directing ES cell differentiation to TEPC. Recently, Morrison and colleagues have developed a protocol for generating anterior definitive endoderm (ADE) cells from ES cells using the transcription factor Hex and the chemokine receptor Cxcr4 [1] as markers (Morrison, Oikonomopoulou et al. 2008). Previous studies suggested that Hex is expressed in both anterior visceral endoderm (AVE) and ADE (Thomas, Brown et al. 1998), while Cxcr4 is expressed in migrating mesoderm and definitive endoderm cells during gastrulation but not in the visceral endoderm (McGrath, Koniski et al. 1999; Yasunaga, Tada et al. 2005). Morrison and colleagues, therefore, used a combination of those two markers to identify the ADE population (and exclude visceral endoderm) in their ES differentiation system. A series of culture conditions were tested both in aggregation culture (through EB formation) and adherent monolayer culture. This modified protocol give rise to up to

[1]Cxcr4 is the receptor of chemokine ligand 12 (CXCL12). Analysis conducted on a lymphoma cell line demonstrated that CXCL12-Cxcr4 can activate multiple signal transduction pathways to modulate cell migration and proliferation (Ganju, Brubaker et al. 1998). In mice, CXCL12 and Cxcr4 are expressed in migratory cells during gastrulation and at later stages in developing neuronal, cardiac, vascular, hematopoietic and craniofacial tissues. At gastrulation, Cxcr4 expression is found within migrating mesoderm and definitive endoderm, whereas its ligand CXCL12 is found within the ectoderm (McGrath, Koniski et al. 1999). It, therefore, seems likely that Cxcr4 will have a role in activating signal transduction pathways required for migration of the anterior definitive endoderm cells to the anterior part of the embryo.

eighteen percent of $Hex^{+}Cxcr4^{+}$ cells in serum-containing aggregation culture, and thirteen percent in chemically defined adherent monolayer culture. The anterior definitive endoderm character of $Hex^{+}Cxcr4^{+}$ was confirmed through both gene expression pattern analysis and functional analysis. This population was also demonstrated to be able to be expanded for many passages while maintaining its DE derivative differentiation potential. Surprisingly, adding Fgf4 in from day 3 to day 7 to the chemically defined ADE induction monolayer culture significantly increased the $Hex^{+}Cxcr4^{+}$ percentage to twenty one percent. This finding is somewhat surprising, given the role of Fgf4 in promoting posterior and inhibiting anterior endoderm cell fate during mouse embryo development (Dessimoz, Opoka et al. 2006). Although the expression of Hex in the 3pp and thymus primordium has not been reported, Hex is initially expressed widely in the floor of the foregut endoderm. The restriction of Hex later to the thyroid and liver suggested distinct early and late functions (Thomas, Brown et al. 1998; Grapin-Botton and Melton 2000). Therefore, the findings of Morrison and her colleagues may also be useful for generation of TECs from ES cells.

1.4.3.3 ES cells differentiation to DE through genetic modification.

1.4.3.3.1 Genetic modification to integrate reporter genes

It is important to monitor the appearance of specific cell types during the course of ES cell differentiation in culture. Additionally, the ability to purify the desired cells, such as progenitors or precursors, may also be important for the final generation of mature cell types. Unless suitable specific cell surface markers and antibodies exist, cells can only be characterized by morphological changes, which is insufficient and sometimes misleading. To solve this problem, identification and purification of

specific ES cell-derivatives using stably integrated fluorescent reporter genes is widely used. For example, to monitor the pluripotency state of ES cells, plasmids containing enhanced green fluorescent protein (EGFP) reporter gene under control of the OCT4 promoter were transfected to the hES cells. Clonal cell lines were generated via transfection and showed normal pluripotent characteristics including the ability to produce all three gem cell lines (Gerrard, Zhao et al. 2005). In another example, to distinguish definitive and visceral endoderm, a mouse ES cell line that carries GFP and human IL2Rα marker genes in the goosecoid (Gsc) and *Sox17* loci, respectively, was generated for monitoring the gene expression during the ES cells to DE cells differentiation (Yasunaga, Tada et al. 2005).

1.4.3.3.2 Genetic modification to direct differentiation toward specific lineages

By ectopic expression or silencing of key developmental genes, genetically modified ES cells can be induced to differentiate toward specific lineages. In an excellent study recently published by Rossant and colleague, endodermal progenitors were generated by *SOX* transcription factor expression in human ES cells (Seguin, Draper et al. 2008). Expressing *SOX7* in human ES cell lines (one hundred and twenty fold increase over wild type) conferred on the cells an extraembryonic (ExEn) endoderm progenitor identity. Over-expression of *SOX17* (twenty five-fold increase) conferred DE progenitor identity on the human ES cells. Both the *SOX7* over-expressing line and *SOX17* over-expressing line were tested through teratoma and microarray assays, suggesting their ExEn and DE identity, respectively. Under the neural differentiation protocol, neither the *SOX7* over-expressing line nor *SOX17* over-expressing line could generate any neural lineage cells. ExEn inducing culture had no effect on the *SOX17* over-expressing line cells. However, in the absence of DE induction using

exogenous factors, seventy four percent of the *SOX17* over-expressing line cells already demonstrated a DE state based on co-expression of Cxcr4 and cKit. It was also shown that differentiation of the *SOX17* over-expressing line cell line to DE derivatives, such as hepatocytes and endocrine pancreatic cell was more efficient than differentiation initiated from wild-type ES cells. Most importantly, the *SOX17* over-expressing cell line directly differentiated to DE without the use of Activin A, and even showed more robust end-stage marker expression than the cells undergoing an activin A-dependent differentiation process. These “endodermal progenitor” cells were easily expanded and maintained all the above characteristics after up to 20 passages. Thus ectopic expression of *SOX17* may be a good way to generate the DE derivatives, including thymic epithelial cells, efficiently and homogeneously.

1.4.3.4 Efficient ES cells differentiation to DE cells directed by small molecules

A series of novel attempts to direct cell specification from both mouse and human ES cells based on the use of small molecules has been reported by Melton and colleagues (Borowiak, Maehr et al. 2009). In a screen of 4000 compounds, two small molecules were found to direct differentiation of ES cells into endodermal lineage. Nearly eighty percent of mouse ES cells appeared to form definitive endoderm after induction, and a high output of pancreatic progenitors was demonstrated. Although again the data did not really show whether the cells have the potential to give rise to any ADE derivatives, such as thymus, the microarray data showed a similar gene expression profile between the small molecule-induced ES cells and E7.75 $Sox17^{+}$ endoderm cells purified from embryos. The specific biochemical targets of these small molecules are unknown, but a high level of Smad2 phosphorylation and an increase of *Nodal* expression were detected after treatment with either of the two compounds, suggesting an interaction between the compounds and the components

of TGFß signalling pathway. A small molecular which can induce a substantial number of Pdx-1 positive pancreatic progenitor cells from definitive endoderm cells derived from human ES cells is also found within the same group. (Chen, Borowiak et al. 2009). The small molecular induction seems economical, convenient, and efficient. However, further work is required to demonstrate the reproducibility of these data and their suitability for generating ADE.

1.4.3.5 Towards embryonic stem cells to thymic epithelial cells differentiation

Definitive endoderm cells give rise not only to thymic epithelial cells but also other derivatives, such as liver and pancreas. So it is important to impose foregut endoderm, or more accurately, the pharyngeal endoderm fate on cells generated during ES cell differentiation, in order to specifically derive thymic epithelial cells. It has been demonstrated that during EB formation, several pharyngeal-endoderm related genes can be detected (Hidaka, Nitta et al. 2010, and previous work in this lab, see Figure 5.1). This raised the question of how to enrich for a cell population expressing these genes. Hidaka and his colleague found that during EB formation based on the hanging drop method, if serum was withdrawn on day 4 and the cells were then cultured as attached EBs, the expression of pharyngeal endoderm and pharyngeal pouch formation related genes was enhanced on day 7. Expression of *Tbx1, Pax1, Pax9, Vgll2, Six1,* and *Eya1* were detected in this study. Later, on day 12 and day 13, *Hoxa3* and *Foxn1* expression was also found to be enhanced in comparison with the serum and flow-cultured EBs. Interestingly, this method was originally designed for enhancing the output of cardiomyocyte derivation. Moreover, a transient small population of $Nkx2.5^{+}E\text{-}cadherin^{+}$ cells was observed and found to be further enriched for pharyngeal endoderm genes. This is interesting, as Nkx2.5 was originally identified as an highly specific marker for deriving cardiomyocytes (Kasahara 1998; Hidaka, Lee et al. 2003).

Green and his colleagues have recently demonstrated a stepwise induction method for deriving ADE and subsequently the pharyngeal endoderm from human ES (hES) cells (Green, Chen et al. 2011). First, hES cells acquired the differentiation stimuli through EB formation. The EBs were then dissociated and cultured in a monolayer. Activin A was introduced first to induce the expression of primitive streak-genes and, later on, definitive endoderm specification. To acquire foregut endoderm identity, dozens of combinations of inhibitors or inducers were tested, assaying expression of foregut endoderm marker genes. Inhibition of Activin A after initial endoderm induction, together with addition of Noggin (the antagonist of BMP4), was found to be most beneficial for more specific foregut endoderm induction. Finally, a combination of different growth factors and cytokines was shown to induce lung and pharyngeal pouch-specific marker expression. However, differentiation markers for thymus were not found. In summary, this paper indicated a complex role for Activin A in specification of pharyngeal endoderm, and points to the possibility of deriving more anterior endoderm cell types than liver and pancreas.

There are several papers published regarding directing ES cells differentiation to thymic epithelial cells, but none of them demonstrates reliable evidence for the success of TEC induction (Lai and Jin 2009; Inami, Yoshikai et al. 2011).

Work from Lai and Jin (Lai and Jin 2009) suggests that TEPCs can be derived by directly adding FGF-7, FGF-10, BMP4 and EGF to undifferentiated monolayer ES cells or to EBs 2 days after formation. After 10 days, they found up to twenty percent (in monolayer culture) and nine percent (3D culture) $EpCAM^+$ cells, which had significantly higher expression of *Pax1*, *Pax9*, *Foxn1* and Plet-1 than the $EpCAM^-$ cells. Eighty percent of the $EpCAM^+$ cells were K5 and K8 double positive. Further functional testing demonstrated that these $EpCAM^+$ cells, when reaggregated with T

cell progenitors, could form a thymus structure and support T-cells differentiation 6 weeks after grafting under the kidney capsule, while $EpCAM^+$ cells alone or $EpCAM^-$ cells reaggregated with T progenitor cells could not form thymus structure. It is surprising that a method that omitted the definitive endoderm induction step proved so efficient. The reasons for adding of FGF-7 and FGF-10 are based on the finding that NCC-derived mesenchymal cells support thymus organogenesis by secreting these growth factors. However, neither the initial 3pp endoderm identity or the thymic epithelial fate require these induction signals from the NCC-derived mesenchyme. They are required for expansion of TEPCs once formed. Similarly, FGF signalling, BMP4 and EGF play different roles in different temporal and spatial stages during the embryogenesis (Zorn and Wells 2009). So it is surprising that this combination of different factors could give the desired outcome.

However, this is not the first report suggesting that ES cells can be induced to produce differentiated cells types without recapitulating the developmental steps that occur in vivo. Functional hepatocytes can be induced from human ES cells in vitro culture in the presence of dimethyl sulfoxide (DMSO), hepatocyte growth factor (HGF) and other growth factors and cytokines without understanding the exact mechanism (Hay, Zhao et al. 2007). However, the subsequent study suggested that forcing cells to differentiate to definitive endoderm cells (an intermediate step which occurs in vivo) at the beginning of cell culture can increase the efficiency of hepatocyte differentiation from human ES cells (Hay, Zhao et al. 2008). Interestingly, during T-cell development, exogenous delivery of OncostainM (OSM) or transgenic expression of this cytokine can induce efficient T-cell differentiation without the need for a thymus, the organ normally required for T-cell differentiation (Clegg, Rulffes et al. 1996). This further suggested that it is possible to produce a terminally differentiated cell type without mimicking the exact process that occurs in vivo. This

is understandable, as signals (e.g. positional signal from 3D organization) that might induce and maintain certain precursor states or terminal differentiated cell types are likely to be absent in vitro and thus extra or different types of manipulation may be required. This may explain why the approach used by Lai and Jin (2009) proved successful in generating TEPCs. Another thing that needs to be considered is the suitability of EpCAM as the marker for TEPCs during ES cell differentiation. EpCAM is expressed by many proliferating epithelial cell types and is not a specific TEPC marker. A more specific TEPC marker, such as Plet-1, should have been used in this study. Of note is that mouse ES cells express low levels of EpCAM, without induction of differentiation, in both serum-containing (Gonzalez, Denzel et al. 2009) and chemically-defined medium, as shown later in this thesis (Figure 6.2 B and Figure 6.11 B) This means that cells sorted only on the basis of EpCAM expression may include undifferentiated ES cells, which could lead to teratoma formation after transplanting under the kidney capsule, as reported for an experiment described later in this thesis (Figure 6.10). Similarly, K5 and K8 co-expression is a characteristic of, but does not define, TEPCs. The claim that a thymus structure had been formed from sorted “TEPCs” in this paper was based only on the K5 and K8 expression pattern. None of the different subtypes that a thymus should contain, such as UEA-1^{+} medullary TECs or $Ly51^{+}$ cortex TECs were demonstrated, and nor were any functional characteristics of TECs, such as MHC Class II expression, demonstrated. Therefore, further work is required to better characterize the putative TECs produced by the system reported by Lai and Jin (2009).

Inami and colleagues have also recently reported an induced pluripotent stem cell (iPSCs) to TECs protocol with a detailed stepwise induction procedure (Inami, Yoshikai et al. 2011). First, iPSCs were induced to differentiate to mesoendoderm and subsequently to definitive endoderm cells by using Activin A and the GSK3

inhibitor LiCl. The growth factors FGF-8, FGF-7, FGF-10 and BMP4 were added 4 days later, based on the literature that these growth factors and morphogens are needed during thymus organogenesis. Gene expression patterns including for some key transcription factors required during thymus organogenesis, such as *Hoxa3*, *Pax1*, *Pax9*, *Eya1*, *Six1* and *Foxn1*, were tested, and expression of these markers during differentiation was confirmed. A small population of $EpCAM^{+}MTS24^{+}$ cells was also found. However, no functional evidence was provided and the TEPC character was only confirmed by phenotype.

1.5 Aims

The overall aim of this PhD project was to differentiate mouse ES cells to TEPCs. To approach this, it was important and necessary to define the TEPC clearly *in vivo* before the *in vitro* induction work. Therefore, the initial aim of this work was to determine whether a functional TEPC could persist from the fetal thymus development stage to the postnatal mouse, if the cells ability to express *Foxn1* was limited genetically (Figure 1.4; Chapter 3), and to determine for how long this population could persist *in vivo* (Chapter 4).

To achieve the aim of differentiating mouse ES cells to TEPCs, an appropriate induction protocol for ES cells to ADE is required. Therefore, I next tested a series of existing and modified ADE differentiation protocols, with the aim of determining in which condition genes related to thymus development were most strongly induced and of testing the capacity of cells induced by these protocols to contribute to mature TECs networks *in vivo* (Chapter 5 and 6). The final aim was to build on these findings to develop an optimized protocol for generation of TEPCs from ES cells.

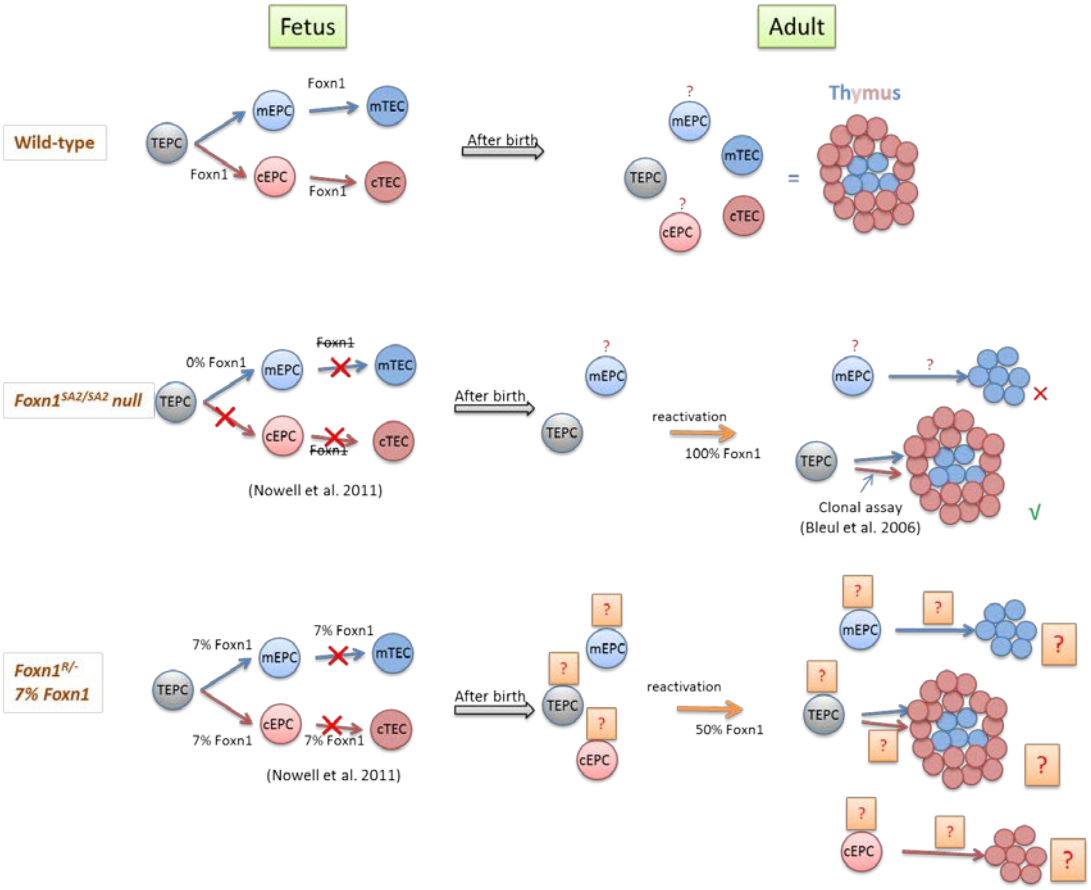

Figure 1.4 Early thymic epithelial lineage specification and persistence of common or lineage restricted progenitor cells at postnatal stage - Known and unknown. "×" on arrows: a particular lineage specification is blocked; "?": persistence of such a cell type needs to be confirmed; "?" in square: questions that can be possibly addressed in this thesis; " √ " : tissue structure observed; "×": tissue structure not observed.

Chapter 2 Material and Methods

2.1 Mice

All animal work was conducted according to UK Home Office guidelines, as established in the ANIMALS (SCIENTIFIC PROCEDURES) ACT 1986.

2.1.1 Mice strains

Foxn1$^{R/R}$ (Nowell, Bredenkamp et al. 2011) and *Rosa26*$^{CreERt2/+}$ (Hameyer, Loonstra et al. 2007) mice were maintained as homozygotes. *Foxn1*$^{-/-}$ (Nehls, Kyewski et al. 1996) mice were maintained as heterozygotes on a C57BL/6 background. *Foxn1*$^{R/R}$ mice were crossed with *Foxn1*$^{+/-}$ to generate *Foxn1*$^{R/-}$ mice, which were then crossed with *Rosa26*$^{CreERt2/+}$ mice, as decribed. Genotyping was performed on ear biopsy samples at 4 weeks of age.

2.1.2 Tamoxifen treatment

4-hydroxy-tamoxifen (4OHT) (Sigma-Aldrich) was dissolved in ethanol (20mg/ml) and stored at -80℃ until required. When needed, 4OHT was further diluted in a cremophor (Sigma-Aldrich)/PBS carrier and was delivered to the mice by a single intraperitoneal (IP) injection. Injection volumes varied from 200µl to 400µl, depending on the 4OHT dose required (250µg, 500µg, 1mg, 1.5mg and 2mg as described in Result Chapter 3). Mice were analyzed 7 weeks after injection.

To treat reaggregates in CoROC culture, pre-dissolved 4OHT in ethanol (20mg/ml) was diluted in culture medium to final concentration as 1µM.

Tamoxifen citrate salt (Sigma-Aldrich) was used to deliver Tamoxifen through the drinking water. Tamoxifen citrate salt was dissolved in ethanol (10mg/ml) and stored

in aliquots at -80℃. When needed, tamoxifen citrate salt was diluted in the drinking water to 0.1mg/ml. Tamoxifen-treated water was changed on a weekly basis.

2.2 Immunohistochemistry

2.2.1 Tissue preparation

Dissected thymic tissue was washed in PBS, embedded in OCT compound (Sakura), frozen on dry ice and then stored at -80℃. Frozen tissue blocks were cryo-sectioned to 6-8 μm sections and collected on Poly-L-Lysine coated slides that were either fixed immediately or stored at -80℃.

2.2.2 Tissue Staining

Slides were removed from -80℃ and left to reach room temperature before fixation in -20℃ acetone for 2 minutes. Sections were air dried, circled with a hydrophobic marker pen and further air dried for 15 minutes. Sections were then rinsed in PBS, and blocked using 5% serum (secondary antibody host species) in PBS-T (0.1% Tween 20 (Sigma)) for 15 minutes at room temperature. Primary antibodies were prepared in PBS at the appropriate concentration and incubated on each section for either 1 hour at room temperature or at 4℃ over-night (O/N). Sections were then washed in PBS-T for 3x 5 minutes. Secondary antibodies were applied in the same manner for 1 hour and then washed in PBS-T for 3x 5 minutes. Sections were rinsed in dH2O after the final wash and air dried at room temperature. Sections were either mounted in 50% glycerol and analyzed immediately, or in Vectshield (Vector Laboratories) and allowed to set at 4℃ O/N before analysis. A Leica AOBS confocol microscope was used for fluorescent imaging.

2.2.3 Antibodies

The antibodies used for immunohistochemistry are listed below:

Antibody Name	Clone	Isotype	Source	Working Conc.
MTS24	n/a	Rat IgG2a	R.L Boyd, Monash University, Melbourne	1 in 3
Anti-Pan-keratin	Polyclonal	Rabbit IgG	DAKO	17μg/ml
Anti-Keratin 5	AF138	Rabbit IgG	Covance	2.5μg/ml
Anti-Keratin 8	Troma 1	Rat IgG2a	DSHB	Hybridoma Stock (1:5)
Anti-Keratin 14	AF64	Rabbit IgG	Covance	2.5μg/ml
UEA-1	n/a	Lectin	Vector Laboratories	5μg/ml
Anti-MHCIIB	M5/114.15.2	Rat IgG2b	BD Bioscience	2.5μg/ml
CDR1	CDR1	Rat IgG2a	Gift from B Kyewski	Hybridoma Stock (1:10)
CD45	30-F11	Rat IgG2b	eBioscience	10μg/ml
Ly51	6C3	Rat IgG2a	BioLegend	10μg/ml
Cldn4	Polyclonal	Rabbit IgG	Invitrogen	0.5μg/ml
H-2K^{b}	AF6-88.5	IgG2a,k	BD Pharmingin	1.25μg/ml

Secondary antibodies used:goat anti-rabbit IgG-Alexa488, goat anti-rat IgG2a-Alexa647, streptavidin-Alexa647 and streptavidin-Alex488 (1:1000).

Isotype controls: rat IgG2a and IgG2b, rabbit IgG (BD Pharmingen or eBioscience).

2.3 Flow cytometry

2.3.1 Cell preparation

2.3.1.1 Lymphocytes

Dissected thymi, trimmed of connecting tissue and fat, or whole thymic rudiment tissue regions were collected in Hanks Balanced Salt Solution (HBSS) (Sigma). The tissue was then cut into several pieces and mechanically disaggregated between two glass slides; dissociated lymphocytes were collected in a petri dish in HBSS. The remaining tissue fragments and cell suspension were then filted through a 70μm cell strainer into a fresh 50ml centrifuge tube. The petri dish was then rinsed with 10ml HBSS and this was transferred into the same 50ml tube through the cell strainer. Cells were collected by centrifugation at 1500rpm (284rcf) for 10 minutes at 4^{o}C, the

supernatant was discarded and the cell pellet was resuspended in 1 - 10ml FACS wash (PBS with 5% FCS), depending on cell number. Red blood cell lysis was performed if there was significant red blood cell contamination, as was the case following thymic rudiment tissue dissaggregation. If required, collected cells were resuspended in 1ml 1x Red cell lysis buffer (Biolegend) and incubated at room temperature for 5 minutes. The lysis reaction was inactivated by the addition of 4ml FACS wash (5% FCS in PBS), the cells were collected by centrifugation at 1500rpm for 5min, and then resuspended in 1-10ml FACS wash. Cell number was determined by counting cells in a Neubauer hemocytometer. For cell staining, $5x10^6$ cells were transferred to a 5ml FACS tube, and the volume was adjusted to 100µl with FACS wash.

2.3.1.2 Thymic epithelial cells

Freshly dissected thymi were transferred into RPMI medium in a petri dish, and the blood vessels and fat were removed. Thymi were minced up as finely as possible using scissors and then 5ml of pre-warmed dissociation buffer (RPMI containing 1.25mg/ml Collagenase D (Roche), and 140-220U/ml DNase I) was added. The cells were incubated at 37^{o}C for 15 minutes, with gentle pipetting every 5 minutes. After incubation, the undissociated tissue fragments were allowed to collect at the bottom of the tube before the dissociated cells in suspension were transferred to a new 50ml tube on ice through a 70µl cell strainer. A further 5ml of pre-warmed dissociation buffer was added to the tube and same dissociation procedure was repeated twice. Finally, the remaining tissue fragments were treated with another dissociation buffer (5ml RPMI containing 1.25mg/ml Collagenase/Dispase (Roche) and 140-220U/ml DNase1) for 30min at 37^{o}C, with gentle pipetting every 15 minutes. Dissociated cells were transferred to the same tube through a cell strainer. Cells were collected by centrifugation at 1500rpm (284rcf) for 10min at 4℃. Cell number was then determined and an appropriate amount of cells was transferred to FACS tube for cell

staining.

2.3.1.3 TECs enrichment

Thymic epithelial cells were enriched, prior to flow cytometric analysis or isolation, by depletion of lymphocytes (Gray, Fletcher et al. 2008). Anti-CD45 labelled microbeads (Miltenyi Biotech) were incubated with the dissociated postnatal thymic cell preparations (5μl of microbeads per 10^7 cells). Cells were then run through the AutoMACS (Miltenyi Biotech) using the DepleteS programme and then collected by centrifugation.

2.3.2 Cell staining

For lymphocyte analysis, Fc receptors were blocked prior to staining by a 15min incubation with a CD16/32 antibody (BioLegend). 100ul of FACS wash containing the primary antibody or directly-conjugated antibody was then added to each tube and incubated for 20min on ice. Cells were then washed once in 1ml FACS wash and collected by centrifucgation at 1500rpm (284rcf) for 5min at 4℃. Cells were incubated with secondary antibody (if applicable) for a further 15min and then washed again. Cells were then re-suspended in 200μl FACS wash and either 7AAD (1:40) or Dapi (1:20,000) were added prior to analysis to gate out dead cells.

2.3.3 Flow cytometry procedure

Single stain, isotype and fluorescent minus one (FMO) controls were prepared for each flow cytometry experiment. Cells were analyzed on a FACSCalibor or a LSR Fortessa (Becton Dickinson). Cells sorting was conducted by Simon Monard or Olivia Rodrigues on FACS Aria II or FACS Jazz cell sorters (Becton Dickingson). Flow cytometric data obtained were analyzed using FlowJo.

2.3.4 Antibodies

The antibodies used for flow cytometry are listed below:

Antibody Name	Clone	Isotype	Conjugate	Source	Working Conc.
CD45	30-F11	Rat IgG2b	APC, PerCP/Cy5.5	BD Pharmingen	2.5μg/ml
CD4	H129.19	Rat IgG2a	FITC, PE	BD Pharmingen	2.5μg/ml
CD8	53-6.7	Rat IgG2a	FITC, PE	BD Pharmingen	2.5μg/ml
CD25	3C7	Rat IgG2b	PE	eBioscience	1μg/ml
CD44	1M7	RatIgG2b	APC	eBioscience	2μg/ml
CD3	145-2C11	Hamster IgG1	FITC	BD Pharmingen	2.5μg/ml
CD31	390	RatIgG2a	FITC, APC	BD Pharmingen	2.5μg/ml
Ter119	Ter119	Rat IgG2b	APC, FITC	BD Pharmingen	1μg/ml
NK1.1	PK136	Mouse IgG2a	FITC	BD Pharmingen	2.5μg/ml
CD11b	M1/70	RatIgG2b	FITC	BD Pharmingen	2.5μg/ml
CD19	1D3	RatIgG2a	FITC	BD Pharmingen	2.5μg/ml
EpCAM	G8.8	RatIgG2a	FITC,PE	Biolegend	2μg/ml
Cxcr4-APC	2B11/CXCR4	RatIgG2b,k	APC	BD Pharmingen	2.5μg/ml

MTS20/24 antibodies were kind gifts from by R.L Boyd at Monash University, Melbourne, Australia. The isotype of the MTS20 antibody is RatIgM, and of MTS24 is RatIgG2a. The working concentration for these antibodies is neat. The secondary antibody chosen for MTS20 is PE labled mouse anti RatIgM, for MTS24 is goat anti Rat IgG-Alex488.

2.4 Intrathymic cell count

Dissected thymus or thymic rudiment tissue was processed as described in 2.3.1.1. The total number of cells ($\mathbf{N_t}$) were counted before cells were processed for cell staining. Cells were then stained with CD45, CD4 and CD8 and analysed by flow cytometry. For analysis in FlowJo, non-viable cells were gated out, and the percentage for $CD45^+$ cells was recorded ($\mathbf{P_{45}}$). Cells were further analysed with CD4 and CD8 and the percentage of double positive $CD4^+CD8^+$ cells was recorded ($\mathbf{P_{dp}}$). The total intrathymic DP cell number was determined as follows, $\mathbf{N_t} \times \mathbf{P_{45}}\% \times \mathbf{P_{dp}}\%$.

For statistics analysis of sample groups, t-tests were calculated using Microsoft Excel, Fisher's Exact test was calculated online (http://vassarstats.net/index.html) and that analyses of variance, Kruskal-Wallis tests and regression analyses were calculated using GraphPad Prism software.

2.5 Reaggregate organ culture

Compact reaggregate organ culture (CoROC) was previously developed in the Blackburn laboratory (Sheridan, Taoudi et al. 2009). This technique, as described in Figure 2.1, was used in this thesis. Unless otherwise stated, the medium used for reaggregated culture was GMEM/FCS medium (described in section 2.8.1) with 50U/ml penicillin and 50µg/ml streptomycin.

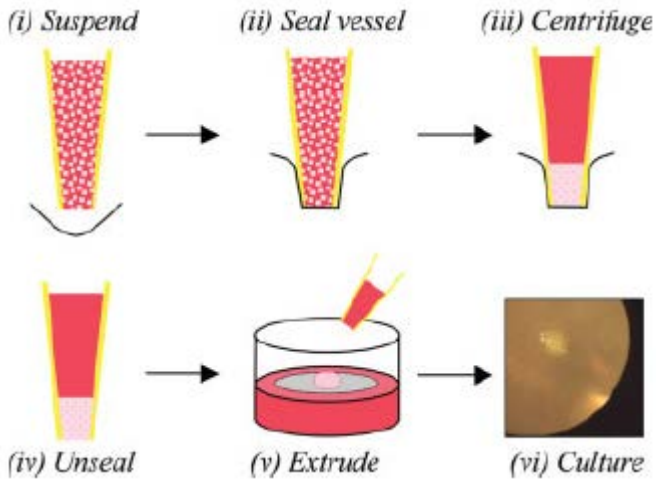

Figure 2.1 Overview of the CoROC technique. A single cell suspension is drawn into a nonbevelled pipette tip, which is then sealed with folded Parafilm. During centrifugation, a compacted cell mass forms. On removal of Parafilm, the compacted mass is extruded onto a membrane at the gas-liquid interface for reaggregation and subsequent culture (Sheridan, Taoudi et al. 2009).

2.6 Cell culture

2.6.1 ES cell maintainence

2.6.1.1 Serum conditions

Mouse E14tg2a ES cells at early passage (p14-p30) were cultured in gelatin-coated flasks or plates (Iwaki). The medium used was GMEM/FCS with 1× leukaemia inhibitory factor (LIF) (see below). The medium was changed every two days, cells were passaged 1 in 10 (or 0.5×10^6 per 25 cm^2 flask) every 3 or 4 days.

GMEM/FCS medium:

Glasgow minimum essential medium (GMEM) (Invitrogen), with:

10% foetal calf serum (FCS),

1 × nonessential amino acids,

4mM glutamine,

2mM modium pyruvate,

0.1mM 2-mercaptoethanol,.

2.6.1.2 Serum-free conditions

A vial of early passage E14tg2a mouse ES cells, that had previously been cultured in the serum containing medium (GMEM/FCS+Lif)(Ying, Nichols et al. 2003) were thawed and cultured in the same medium for expansion. One week later, the cells were passaged and transferred to 2i medium (Ying, Wray et al. 2008) (see below). ES cells were maintained in 2i medium for at least 1 week using standard techniques before differentiation protocals were conducted. Cells were passaged every 3 or 4 days, at a ratio of 1 in 8 (or 0.5×10^6 cells per 25cm^2 flask).

2i Medium:

N2B27 Base medium (Stem Cell Sciences Inc or prepared in-house) with the

following inhibitors:

CHIRON99021: 3μM (Stemgent)

PD0325901: 1μM (Stemgent)

2.6.2 Cell differentiation

2.6.2.1 Anterior definitive endoderm differentiation protocol

An unpublished, confidential protocol from Dr. Gillian Morrison (University of Cambridge), which is based on a previously published protocol from *Morrison et al*. (Morrison, Oikonomopoulou et al. 2008), was used to generate definitive endoderm cells from E14tg2a ES cells. Briefly, ES cells were cultured in 2i medium and differentiation was initiated at day 2 after the most recent passage of the cells. Cells were dissociated with Accutase to single cells and replated on gelatin coated culture plates. For a 6 well culture plate (Iwaki), $3x10^4$ cells were plated into one well in 3 ml of medium. No passaging was needed during the 7 day DE differentiation protocol. This protocol has two main stages with a medium change at day 2 (medium 1 to medium 2) and a further change into medium 2 on day 4. The protocol is described below.

DE differentiation protocol summary:

Day 0 – plate out in media 1

Day 2 – change to media 2

Day4 – replace media 2

Media 1: N2B27 base

3uM CHIRON99021

20ng/ml Activin A

10ng/ml FGF4

1ug/ml Heparin

50nM PI-103

Media 2: SF5 Base*

3uM CHIRON99021

20ng/ml Activin A

10ng/ml FGF4

1ug/ml Heparin

50nM PI-103

20ng/ml EGF

***SF5 Base medium:**

DMEM/F12(- L-glutamine)	500ml
Beta-mercaptoethanol	0.55ml
L-glutamine 2mM	5.0ml
N2(Gibco)	2.5ml
B27(Gibco)	5.0ml

N2B27 was prepared in house or purchased from Stem Cell Sciences Inc.

2.6.2.2 Embryoid body formation

E14tg2a cells, previously cultured in GMEM/FCS+Lif medium, were trypsinised and collected by centrifugation. Cells were resuspended in GMEM/FCS without LIF at a density of 10^5 cells/ml . 10µl drops of this cell suspension were pipetted onto the inside of a lid of a 140 mm petri dish (Sterlin Ltd). A repeat pipettor was used to achieve consistent results. The lid was then placed back on its base which contained 20ml PBS for a humid environment. Cells were incubated for 2 days to allow spontaneous EB formation to occur. Aggregates were then flooded from the lid with media into 90 mm petri dish (Sterlin Ltd.). Aggregates were then cultured in

suspension for 5 days in 15ml GMEM/FCS. Media was not changed or changed once depending on the EBs density. To change media, suspension EBs were transferred to a conical bottomed tube and allowed to settle by gravity before media was replaced.

2.6.2.3 EB differentiation with Activin A

ES cells previously cultured in 2i medium were dissociated to single cells with Accutase and then plated in a 90 mm petri dish (Sterlin Ltd) for spontaneous EB formation. 10ml medium with $5x10^4$ cells were used for each 90mm petri dish. Medium conditions used are described below:

Serum containing culture:

Day 0 - Day 2: GMEM/FCS

Day 2 - Day 7: N2B27 plus 20ng/ml Activin A, 20ng/ml EGF

Chemically defined medium:

Day 0 – Day 2: N2B27 plus 10ng/ml BMP, 20ng/ml Activin A

Day 2 – Day 7: SF5 plus 20ng/ml EGF, 10ng/ml FGF4

2.6.3 Growth factors, cytokines and inhibitors

The growth factors, cytokines and inhibitors used for cell culture are listed below:

Name	Cat No.	Supplier
Activin A	PHG9014	Invitrorgen
FGF4	PHG0154	Invitrogen
CHIRON 99021	04-0004	Stemgent
PD0325901	04-0006	Stemgent
Heparin	H3149-10KU	Sigma
PI-103	528100	Calbiochem
Mouse EGF	2028-EG	R&D System
FGF-7	251-KG	R&D System

2.7 X-gal staining

2.7.1 X-gal staining on co-cultured EBs or ES cells

Cultured EBs or cells were washed in PBS, and then washed in X-gal wash for 3 x 5min at 4℃. Samples were then fixed in X-gal fix for 20min at 4℃, and washed in X-gal wash for 3x 20min at room temperature. X-gal stain solution was then added to cover the sample surface, and staining process was performed at 37℃ in dark for 18 hours. X-gal stain solution was removed and X-gal fix solution was added to prevent leaching of the X-gal reaction product. Samples were stored at 4℃ or immediately imaged under the microscope.

2.7.2 Solutions

X-gal wash:

0.1 M phosphate buffer (pH 7.3)
2 mM MgCl2
0.1% sodium desoxycholate
0.02% NP-40
0.05% BSA

X-gal stain:

Made up in X-gal wash mixed with:
0.024% spermidine
5 mM K3FE(CN)6
5 mM K4FE(CN)6
0.0014% NaCl
2.5 mM X-gal
0.1% DMF

X-gal fix:

0.1 M phosphate buffer (pH 7.3)

0.2% glutaraldehyde

2 mM MgCl2

5 mM EGTA

2.7.3 FDG staining

FDG staining was conducted using *FluoReporter* ® lacZ *Flow Cytometry Kits*, according to the manufactures instructions.

2.8 Q-PCR

Cells were collected and lyzed in QiaZol (Qiagen). RNA was extracted according to the manufacturers instructions (QIAzol Handbook, Qiagen). RNA quality and quantity was analysed using the Nanodrop. cDNA was synthesized from total RNA using SuperScript First-Strand Synthesis System for RT-PCR (Invitrogen), according to the manufactures instructions. cDNA was diluted three or five-fold with PCR grade water and 2.5µl was added to the following reaction: 5µl of 2× Lightcycler 480 Probes Master, 0.05µl of each 10 µM primer, 0.1µl of 100× UPL probe, PCR grade water to 10µl. Reactions were performed on a Roche LightCycler 480 instrument (384 System) using the standard run protocol. At least 3 technical repeats were performed per sample and data were analysed using the LightCycler 480 software (v1.5). Standard curves were established for each gene analysed using E14.5 $EpCAM^+$ TECs cDNA or E12.5 whole thymic lobe cDNA. Dilutions series was set as 1, 10^{-1}, 10^{-2}, 10^{-3}, 10^{-4} (where 1 represents the 1/2.5 diluted cDNA sample).

2.8.1 Primer and probe

The following primers[2] were used for QRT-PCR analysis:

Primer	Sequence (5'-3')	UPL probe
α-tubulin F	CGGACCACTTCAAGGACTAAA	58
α-tubulin R	ATTGCCGATCTGGACACC	
Oct-4 F	GTTGGAGAAGGTGGAACCAA	95
Oct-4 R	CTCCTTCTGCAGGGCTTTC	
Nanog F	CCTCCAGCAGATGCAAGAA	25
Nanog R	GCTTGCACTTCATCCTTTGG	
Rex1 F	GCACACTCACTCTATTGAGAGA AGAA	16
Rex1 R	CAGCTCCTGCACACAGAAGA	
Sox17 F	CACAACGCAGAGCTAAGCAA	97
Sox17 R	CGCTTCTCTGCCAAGGTC	
Hex F	TCAGAATCGCCGAGCTAAAT	2
Hex R	CTGTCCAACGCATCCTTTTT	
Plet-1 F	CATCCGTGAAAATGGAACAA	20
Plet-1 R	TCACAGTTGGAGTCGTGTTTATG	
Tbx1 F	GCTGTGGGACGAGTTCAATC	104
Tbx1 R	ACGTGGGGAACATTCGTCT	
Hoxa3 F	CAAGGCAGAACACTAAGCAGAA	78
Hoxa3 R	GTCACCAGCGCAGCTCTC	
Pax1 F	CTCCGCACATTCAGTCAGC	105
Pax1 R	TCTTCCATCTTGGGGGAGTA	
Pax9 F	AGCAGGAAGCCAAGTACGG	33
Pax9 R	TGGATGCTGAGACGAAACTG	
Foxn1 F	TGACGGAGCACTTCCCTTAC	42
Foxn1 R	GACAGGTTATGGCGAACAGAA	
IL-7 F	CTGCTGCAGTCCCAGTCAT	10
IL-7 R	TCAGTGGAGGAATTCCAAAGAT	

[2] All primers were designed on line by Universal ProbeLibrary System (Roche).

Chapter 3 Investigation of the capacity of thymic epithelial progenitor cells to persist *in vivo*.

3.1 Introduction

The existence of a common progenitor cell that can generate both cortical and medullary TEC compartments has been demonstrated within both fetal thymic primordium and the neonatal mouse (Bleul, Corbeaux et al. 2006; Rossi, Jenkinson et al. 2006). Using a revertible *Foxn1* null allele, bi-potent progenitor cells were shown to persist until the neonatal period (postnatal day 14) in *Foxn1* null mice. When the *Foxn1* allele was reverted, a single progenitor cell could give rise to both cortex and medulla and subsequently support T-cell development (Bleul, Corbeaux et al. 2006).

A hypomorphic *Foxn1* allele, $Foxn1^{R}$, was previously generated in our lab (Figure 3.1). Due to the splicing around the inserted sequence, this allele can express only 15% of wild type (WT) *Foxn1* expression levels. Further analysis demonstrated that, as in $Foxn1^{-/-}$ mice, the development of the $Foxn1^{R/-}$ thymus was arrested at the early primordium stage and remained non-functional throughout life with respect to supporting T cell development. However, $Foxn1^{R/-}$ mice expressed CD205, the earliest marker known so far for cortical specific epithelial progenitor cells (Shakib, Desanti et al. 2009), in the thymus primordium at E15.5. Moreover, while the Plet-1^{-} :Plet-1^{+} epithelial cell ratio was maintained from E13.5-E15.5 in $Foxn1^{-/-}$ mice, this ratio increased within $Foxn1^{R/-}$. Plet-1 is the earliest TEPC marker and the loss of its expression accompanies thymic epithelial lineage differentiation (Bennett, Farley et al. 2002). A low level of MHC Class II expression was also detected on TECs from

Foxn1$^{R/-}$ mice at this stage. It was also been demonstrated that even in the *Foxn1*$^{-/-}$ mice, K5^{hi}Cldn4^{hi} cells could be detected at E13.5. Cldn4^{hi} cells at this stage in the wild type thymus have been demonstrated to be medulla-specific thymic epithelial progenitor cells (Hamazaki, Fujita et al. 2007). This suggested that at low *Foxn1* expression levels, at least some TEPCs become committed to the cortical and medullary TEC lineages (Nowell, Bredenkamp et al. 2011). Therefore, it was important to determine whether at low levels of *Foxn1* expression, the common TEPCs, or cortical and medullary sub-lineage restricted TEPCs persisted, and also to determine how long these cells could persist for *in vivo*.

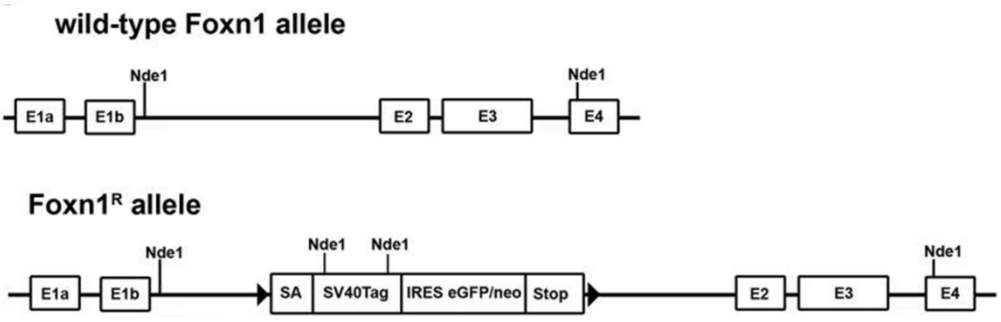

Figure 3.1. Wild-type *Foxn1* allele and *Foxn1*^{R} allele. A LoxP flanked cassette containing the 5' engrailed 2 splice acceptor site (SA), the SV40TAg coding region, an internal ribosome entry site coupled to an enhanced green fluorescent protein/neomycin resistance fusion protein (IRES-EGFPneo), and the CMAZ transcriptional pause was inserted into intron 1b of the *Foxn1* locus of mouse ES cells. E, exon. The SV40 T antigen was originally introduced to allow TEPC cells derived from these mice to be immortalized in vitro and was demonstrated to not affect TEC differentiation and function in this model, and the revertibility of the *Foxn1*^{R} allele was also demonstrated (Figure adapted from Nowell, Bredenkamp et al. 2011).

A *Foxn1* reversion model was subsequently created by crossing the *Foxn1*$^{R/-}$ mouse

with *Rosa26*^{CreERt2} (Hameyer, Loonstra et al. 2007) to generate *Foxn1*$^{R/nu}$*;Rosa26*^{CreERt2} mice (*R/-;CreERt2*). Unlike the *Foxn1*$^{SA2/SA2}$ strain (Bleul et al 2006), the *R/-;CreERt2* mice expresses a low level of *Foxn1* (7% of WT *Foxn1* expression). Adult *R/-;CreERt2* mice had a normal skin phenotype but were athymic (Dr. Craig Nowell's previously unpublished data in Blackburn's Lab), as expected from studies of *Foxn1*$^{R/-}$ mice (Nowell, Bredenkamp et al. 2011) and carrier injected *R/-;CreERt2* mouse (Figure 3.2). Using this model, I investigated whether the common thymic epithelial progenitor cells or the sub-lineage specified medullary thymic epithelial progenitor cells (mEPC) and cortical thymic epithelial progenitor cells (cEPC) could persist in postnatal mice.

3.2 Results

3.2.1 Reversion of the *Foxn1*^{R} allele leads to thymus development in *R/-;CreERt2* mice

To test whether functionally competent thymic epithelial progenitor cells were still present in adult *R/-;CreERt2* mice, 2-4 month old *R/-;CreERt2* mice were injected intraperitoneally (IP) with 4-hydroxytamoxifen (4OHT). This allowed me to determine whether, by recovering the capacity of TECs to express wild-type levels of *Foxn1*, the structure and function of the thymus could also be recovered. I first tested 5 different doses of 4OHT; 250μg, 500μg, 1mg, 1.5mg and 2mg. Carrier only injection was used as a control. Mice were analyzed after 7 weeks for structural and functional changes.

For histological and immunohistochemical analysis, 8 μm cryosections were cut for each thymus / thymic rudiment (see Materials and Methods). Every 30th section was stained with α-pan-cytokeratin (PanK) and 4'6-diamidino-2-phenylindole (Dapi) in order to determine the position of the potential thymus / thymic rudiment within the

whole block (Figure 3.2 and Figure 3.14). The general outcome, and the age and dose of 4OHT for each mouse processed for immunohistochemical analysis were summarized in Table 3.1.

Dose of 4OHT	Age	Outcome	No. of Mice
Carrier	2-4 months	No reactivation	>3
250µg	2-4 months	No reactivation	>3
500µg	2-4 months	Reactivated	>3
1mg	4 months	Reactivated	1
1.5mg	4 months	Reactivated	1
2mg	4 months	Reactivated	1

Table 3.1 Mice processed for immunohistochemical analysis

The *R/-;CreERt2* mice injected with carrier-only contained a small thymic rudiment, and histologically showed a cystic epithelial structure (Figure.3.3). No cortex and medulla organization could be observed. Most epithelial cells ($PanK^{+}$) co-expressed Keratin 5 (K5) and Keratin 8 (K8), two markers widely used to identify the medulla and cortex in the mature WT thymus, respectively, (Klug, Carter et al. 1998) and co-expressed on the progenitor cells during ontogeny (Bennett, Farley et al. 2002). More than 50% of epithelial cells were positive for Plet-1, which marks the earliest progenitor cells present during thymus organogenesis (Bennett, Farley et al. 2002) and also marks the thymic remnant within an adult *nu/nu* mouse (Blackburn, Augustine et al. 1996). Therefore, the epithelial cells detected here were indistinguishable from the $Foxn1^{R/-}$ thymus, which is composed of undifferentiated TECs (Nowell, Bredenkamp et al. 2011).

MHC Class II is considered to be a marker of mature functional TECs (Bonfanti, Claudinot et al. 2010). It is also expressed in macrophages, monocytes, dendritic cells and B cells (Ting and Trowsdale 2002). The carrier injected *R/-;CreERt2* mice

are athymic, have no functional thymic epithelial cells and so cannot support T-cell development. It is, therefore, interesting that MHC Class II staining was present in most of the epithelial area of carrier-only injected mice, as previously observed in *Foxn1*$^{R/-}$ mice (Nowell, Bredenkamp et al. 2011).

The 250μg4OHT injected mouse showed the same cystic epithelial structure and immunostaining profile as carrier-only injected and *R/-* mice (Figure 3.2), indicating the absence of any reversion of the *Foxn1*^{R} allele at this dose.

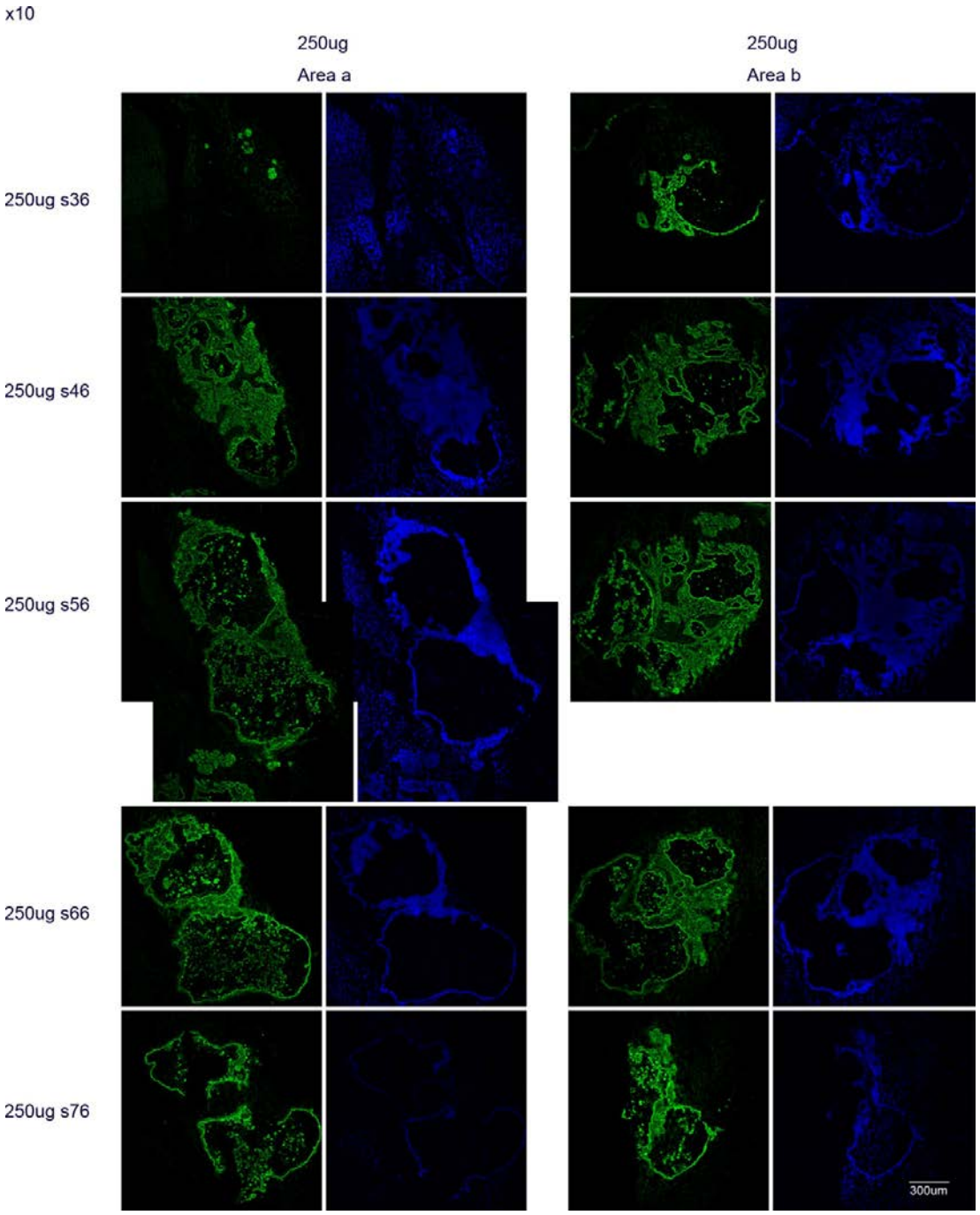
x10
250ug
Area a
250ug
Area b
250ug s36
250ug s46
250ug s56
250ug s66
250ug s76
300um

Figure 3.2

Figure 3.2 *R/-;CreERt2* mice were injected intraperitoneally with 250µg 4OHT. After 7 weeks, the thymus or thymic rudiment was microdissected and processed for cryosectioning. 8µm sections were cut, and groups of 3 adjacent sections were placed on a single Poly-L-Lysine coated slide. The slides numbers (s36 etc) are listed in the left panel of the figure. So that 40 slides here have 120 sections and thus covers 960µm. Images show pancytokeratin (PanK, green) and DAPI (blue) staining of every 30th section from a block containing one thymus/thymic rudiment. PanK was used to identify the epithelial cells. Dapi (Blue) was used to marker the cell position. There are two main epithelial cell area (Area A and Area B) detected within most of the sections. Sections were localized in the actual histological order. Area A in slide 56 is shown in two images due to the size of the section. All pictures are at the same magnification (x10). Scale bar: 300µm.

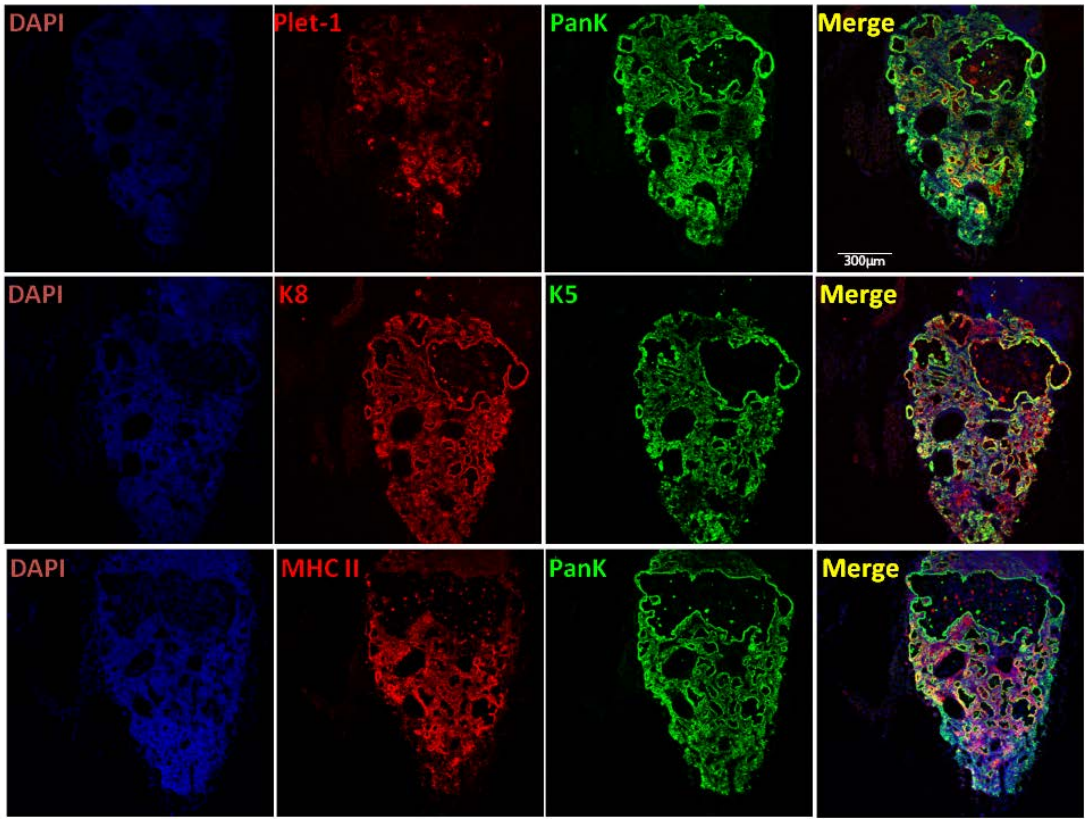

Figure 3.3 Immunohistochemical analysis of carrier-only injected *R/-;CreERt2* mice. At least two 2-4 month old R/-;CreERt2 mice were injected with carrier only. 7 weeks later, the mice were examined for the presence of an overt thymus, and the region containing the thymic rudiment was microdissected and processed for cryosectioning. No overt thymus-like organs were found.. 8 μm cryosecions were cut and stained for the markers indicated on the photographs. Carrier-only injected *R/-;CreERt2* mice contained a thymic rudiment which showed a cystic epithelial morphology, with most of the PanK^{+} epithelial cells co-expressing K5, K8 and Plet-1. Scale bars: 300 μm, images shown are representative of at least two individual mice. (Data in graph is from the one conducted by Dr. Craig Nowell.

At all doses above 500 μg of 4OHT injection, a thymic structure with both cTECs and mTECs was clearly observed based on K5, K8 and DAPI staining (Figure 3.5). UEA-1, which marks medullary TECs (Figure 3.6), and Ly51, which marks mature cortical TECs (Figure 3.7) were detected within the two compartments, respectively. Notably, UEA-1 staining was also detected, although in fewer cells, in the carrier-only and 250ug-4OHT injected thymi. This is consistent with the staining profile in nu/nu mice (Figure 3.3, 3.4) (Nowell, Bredenkamp et al. 2011). In thymi from mice that received 1mg, 1.5mg and 2.0mg 4OHT, MHC Class II, a marker of mature TECs, also showed staining profile indistinguishable from that seen in WT thymi (Figure 3.8).

For all of the reactivated thymi, i.e. all the doses above 500 μg 4OHT, Plet-1^+ areas of undifferentiated tissue could be seen adjacent to the thymus structure. These were histologically similar to the undifferentiated tissue within the carrier-only injected *R/-;CreERt2* mice (Figure 3.3) and *nude* mice (Blackburn, Augustine et al. 1996), suggesting that these cells were non-reactivated TEPCs. These regions were clearly different from the scattered Plet-1^+ areas normally observed within a WT thymus, and detected within the medulla formed following Foxn1 reactivation (Figure 3.4).

These data established that in the postnatal *R/-;CreERt2* mice, reversion of the *Foxn1*^{R} allele lead to thymus generation, suggesting the presence of persisting thymic epithelial progenitor cells. The amount of thymus tissue appeared to be proportional to the dose of tamoxifen, indicating that the number of TEPCs reactivated was higher at higher doses. The presence of a well-organized structure containing most major cortical and medullary TEC sub-types, especially within the high-dose injected mice, further indicated the full functional capacity of these progenitors.

A

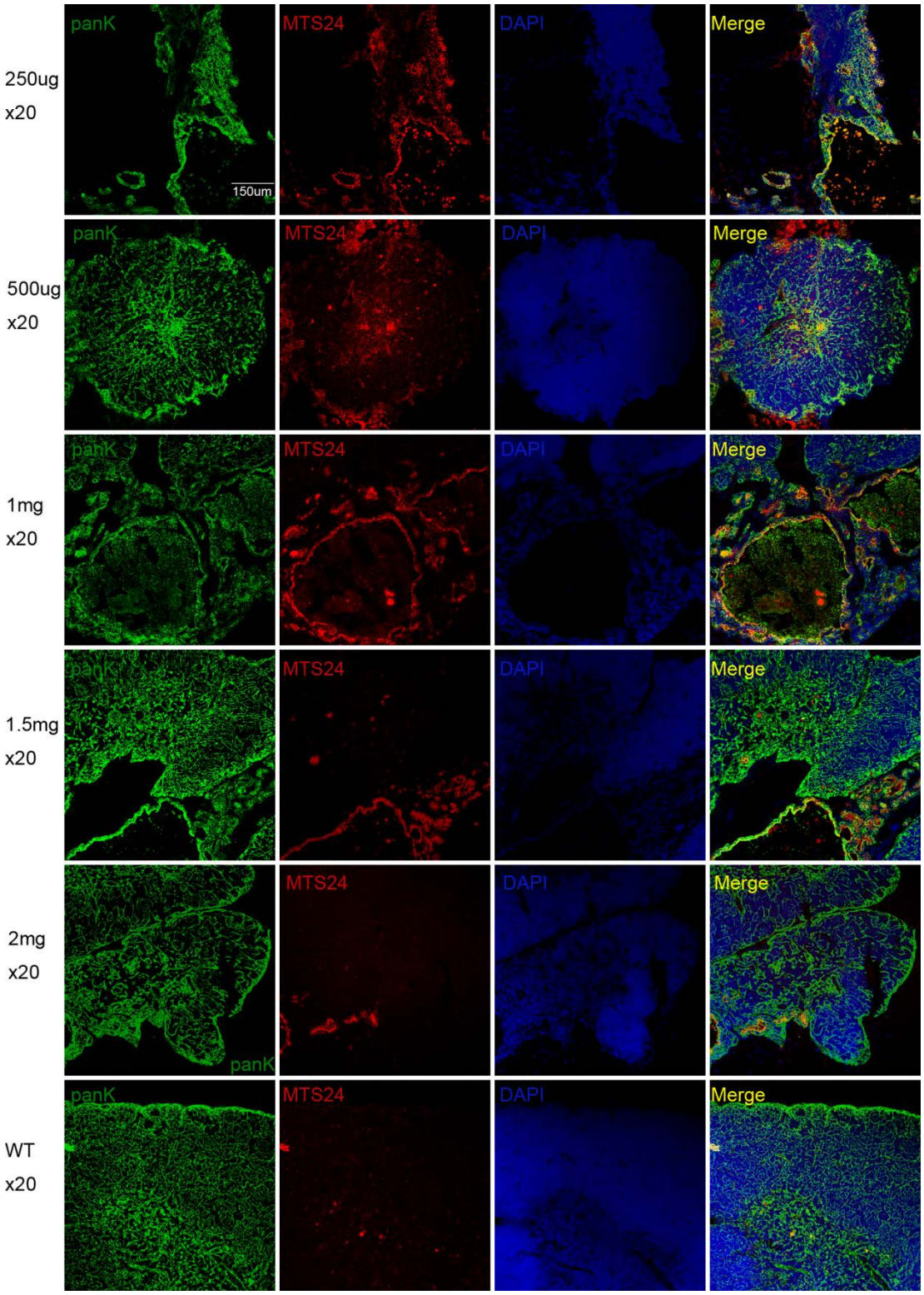

Figure 3.4 (Part 1)

B

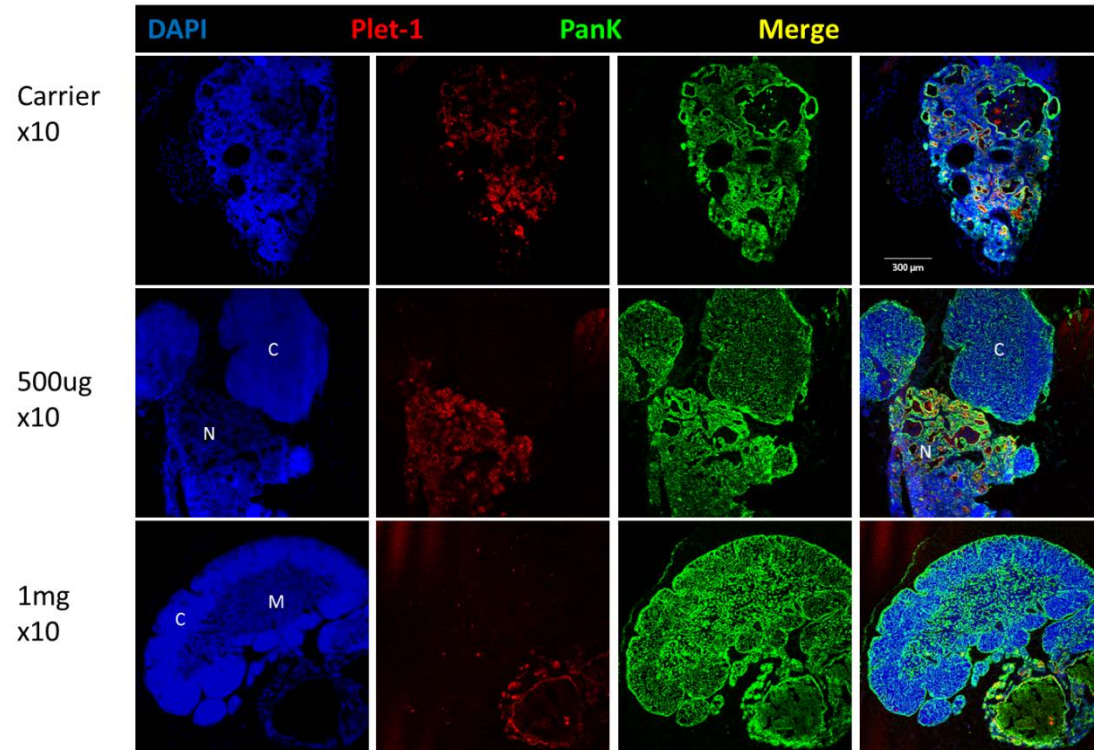

Figure 3.4 Immunohistochemistry staining profile of Plet-1 on all doses of 4OHT injected *R/-;CreERt2* mice. 2-4 month old *R/-;CreERt2* were injected with 4OHT or carrier only. 7 weeks later, the thymi or thymic rudiments were dissected and processed for cryosectioning. 8 µm cryosections were cut and stained with MTS24 (mAb for Plet-1) and PanK. 250µg 4OHT injected mouse showed the same cystic epithelial morphology and Plet-1 staining profile as the carrier-only injected mice did (**A 250µg** and **B Carrier**). Plet-1^{+} non-reactivated epithelial cells were evident adjacent to the thymic tissue (shown in **A 1mg**, **A 1.5mg** and **B 500µg**, **B 1mg**) and Plet-1+ cells within medullary area as normal WT thymus did (as shown in **A 1.5mg**, **A 2mg**, **A WT**) could be observed in all doses above 500 µg 4OHT injected mice. Images shown are representative of mice receiving the different doses. **C**: cortex, **M**: medullar, **N**: non-reactivated area. n=2 for carrier-only, 250µg and 500µg 4OHT injected mice. n=1 for 1 mg, 1.5mg and 2mg 4OHT injected mice. (Dr. Craig Nowell performed the staining work for carrier-only and 500µg 4OHT injected mice in part **B**.)

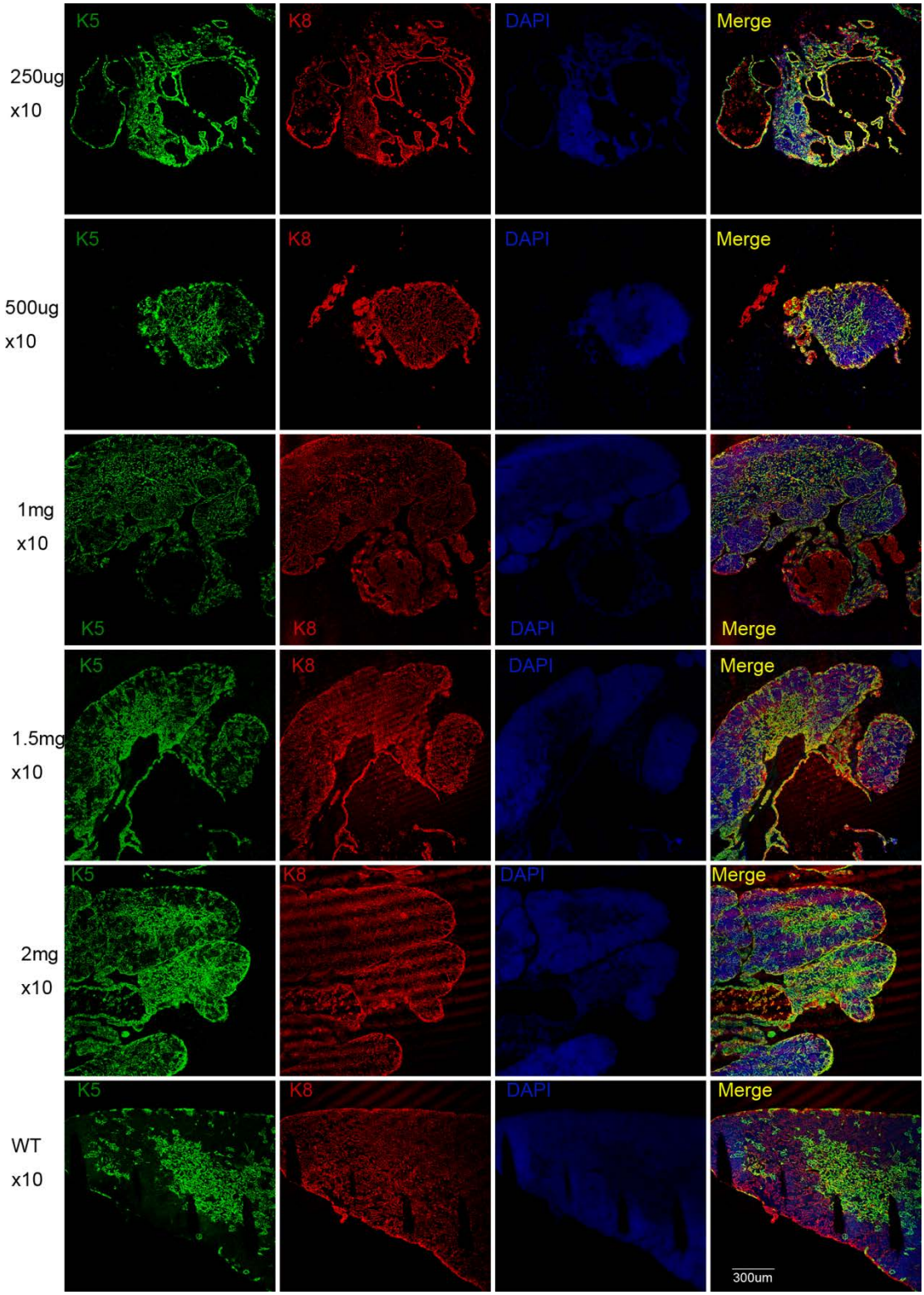
K5
K8
DAPI
Merge
250ug
x10
500ug
x10
1mg
x10
1.5mg
x10
2mg
x10
WT
x10
300um

Figure 3.5

Figure 3.5 Immunohistochemical staining profile of K5 and K8 on 4OHT injected *R/-;CreERt2* mice. 2-4 months old *R/-;CreERt2* were injected with 4OHT or carrier only. 7 weeks later, thymi or thymic rudiments were dissected and processed for cryosectioning. 8 µm cryosections were cut and stained with K5 (green) and K8 (red). The 250µg 4OHT injected mouse shows a cystic epithelial structure co-expressing K5 and K8. Individual $K5^{-/low}K8^{+}DAPI^{dense}$ cortical and $K5^{+}/K8^{low}DAPI^{dim}$ medullary compartments can be observed within all mice that received 500µg or higher doses of 4OHT. n=2 for carrier-only, 250µg and 500µg 4OHT injected mice. n=1 for 1 mg, 1.5mg and 2mg 4OHT injected mice.

A

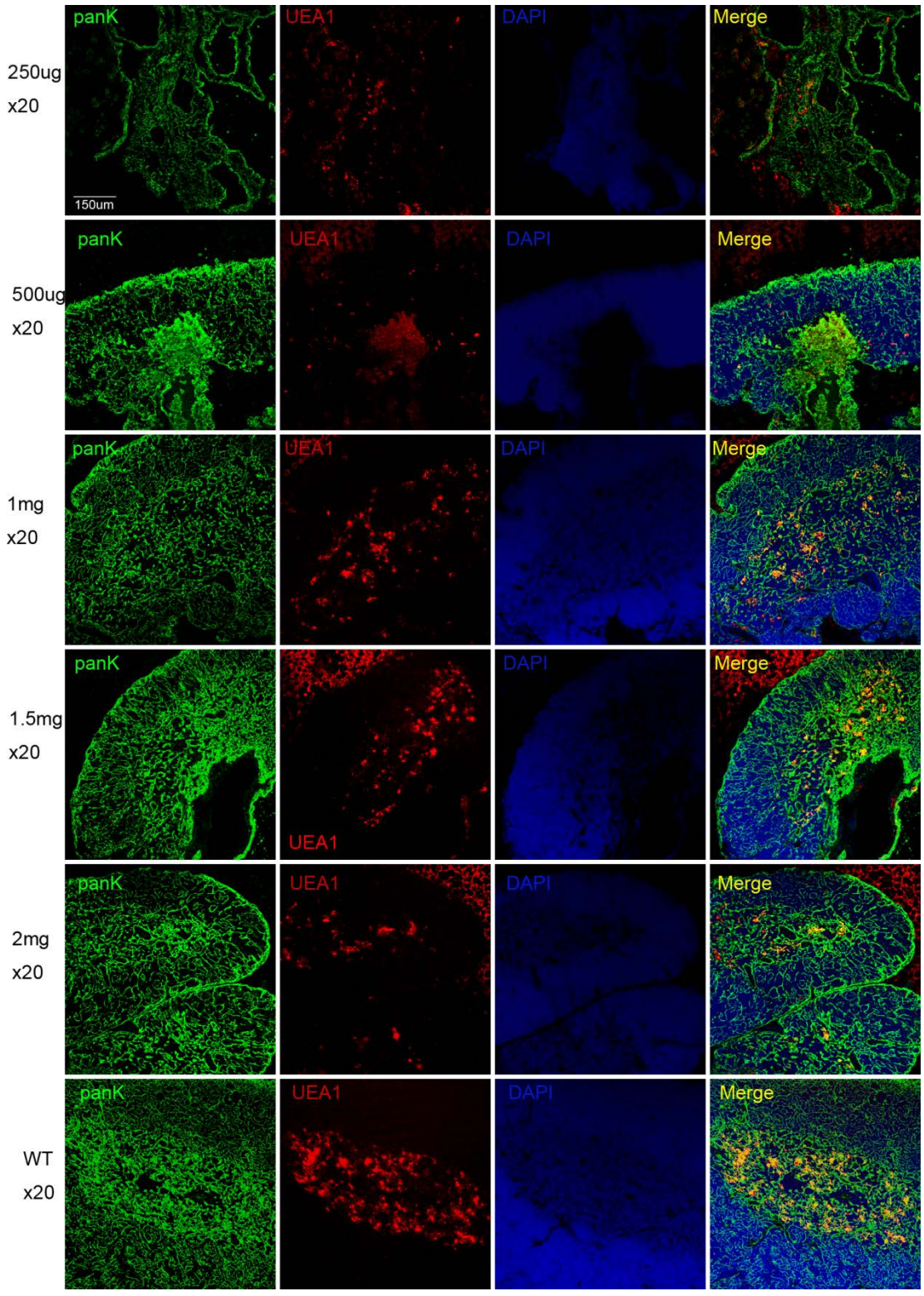

Figure 3.6 (Part 1)

B

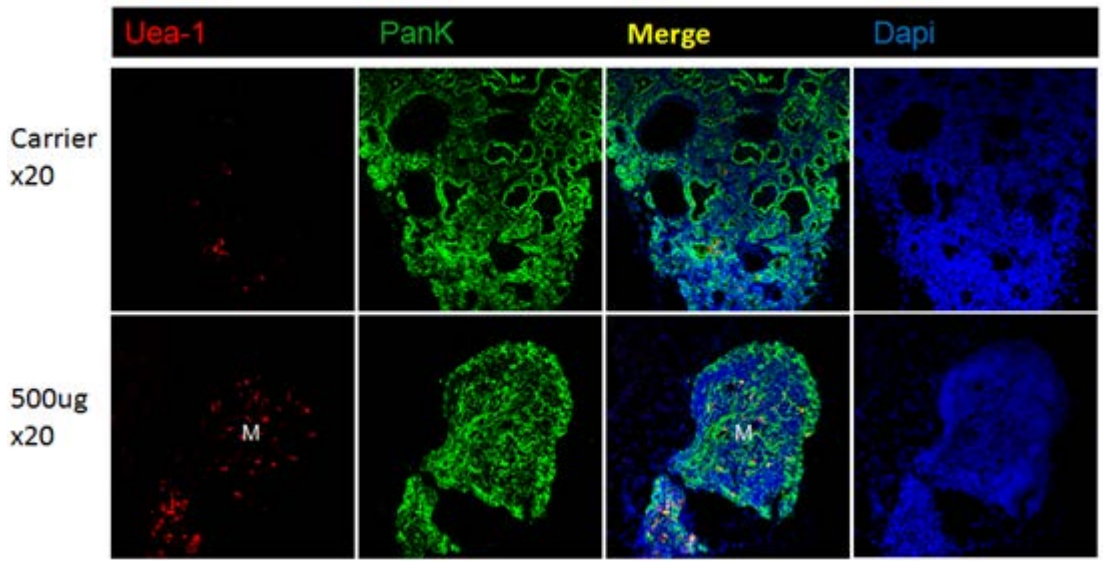

Figure 3.6 Immunohistochemical staining profile of UEA-1 and PanK on 4OHT and carrier-only injected *R/-;CreERt2* mice. 2-4 months old *R/-;CreERt2* were injected with 4OHT or carrier only. 7 weeks later, thymi or thymic rudiments were dissected and processed for cryosectioning. 8 µm cryosections were cut and stained with PanK (green) and UEA-1 (red). Carrier-only and 250µg4OHT injected mice showed a epithelial structure and UEA-1 expression could be detected only occasionally and without clear boundary of expression area (**A 205g** and **B Carrier**). UEA-1-marked medullary areas can be detected in all mice receiving 500µg or higher doses of 4OHT (**A** and **B**). n=2 for carrier-only, 250µg and 500µg 4OHT injected mice. n=1 for 1 mg, 1.5mg and 2mg 4OHT injected mice. Dr. Craig Nowell performed the staining work for part **B**.

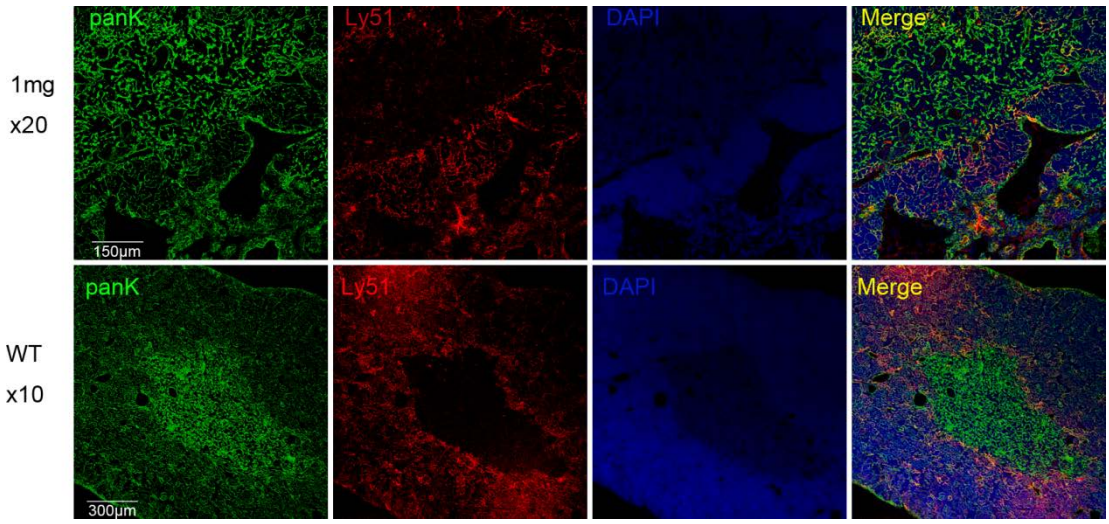

Figure 3.7 Immunohistochemical staining profile of Ly-51 and PanK on 4OHT injected *R/-;CreERt2* mice. 2-4 months old *R/-;CreERt2* were injected with 4OHT or carrier only. 7 weeks later, thymi or thymic rudiments were dissected and processed for cryosectioning. 8µm cryosections were cut and stained with Ly-51 (red) and PanK (green). Ly-51 a marker of mature cortical epithelial cells, exclusively marked the cortex area in both 1mg 4OHT injected *R/-;CreERt2* mouse and the WT C57BL/6 control. n=1.

A

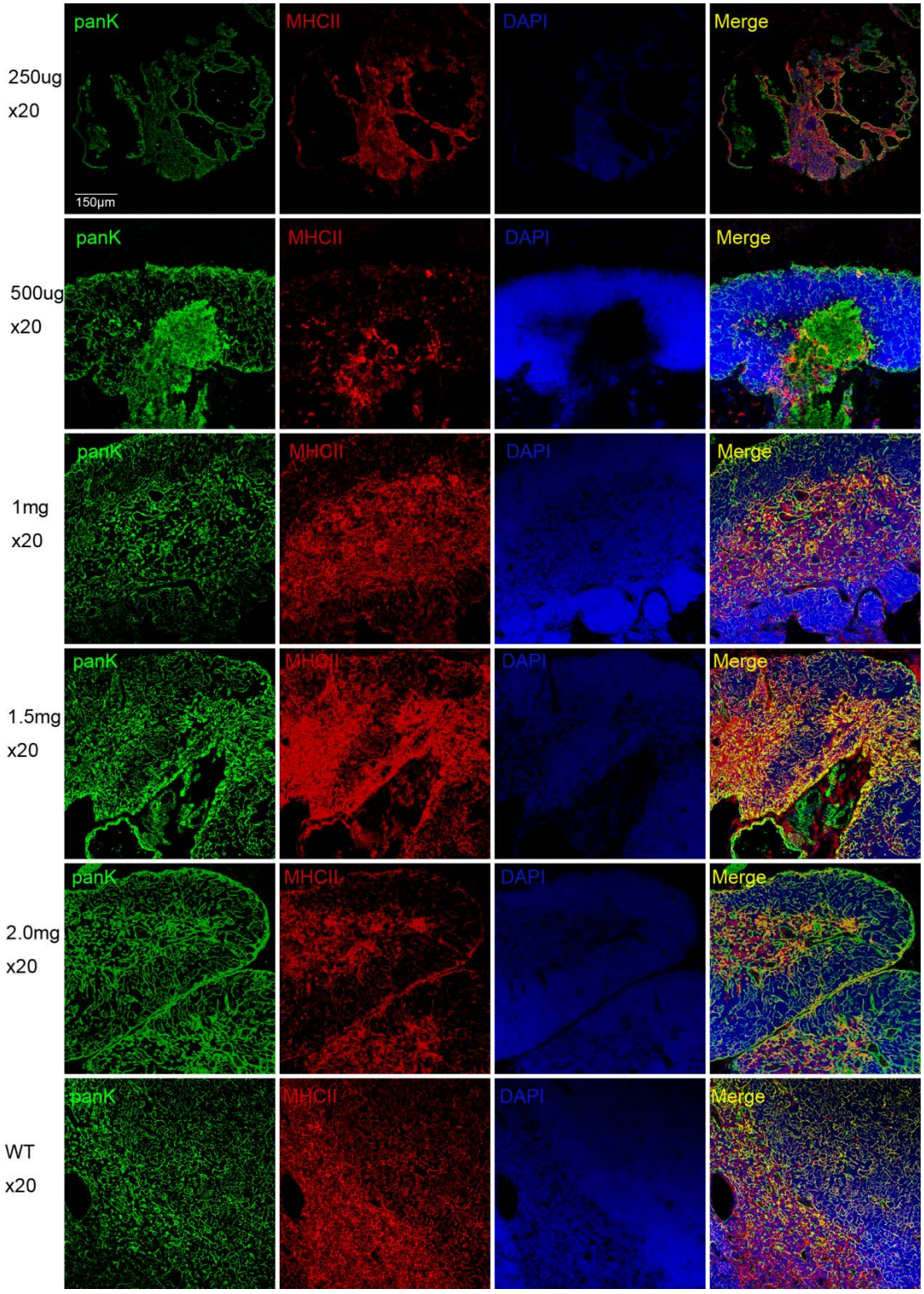

Figure 3.8 Immunohistochemical staining profile of MHC Class II and PanK on 4OHT and carrier-only injected *R/-;CreERt2* mice.(Part-1)

B

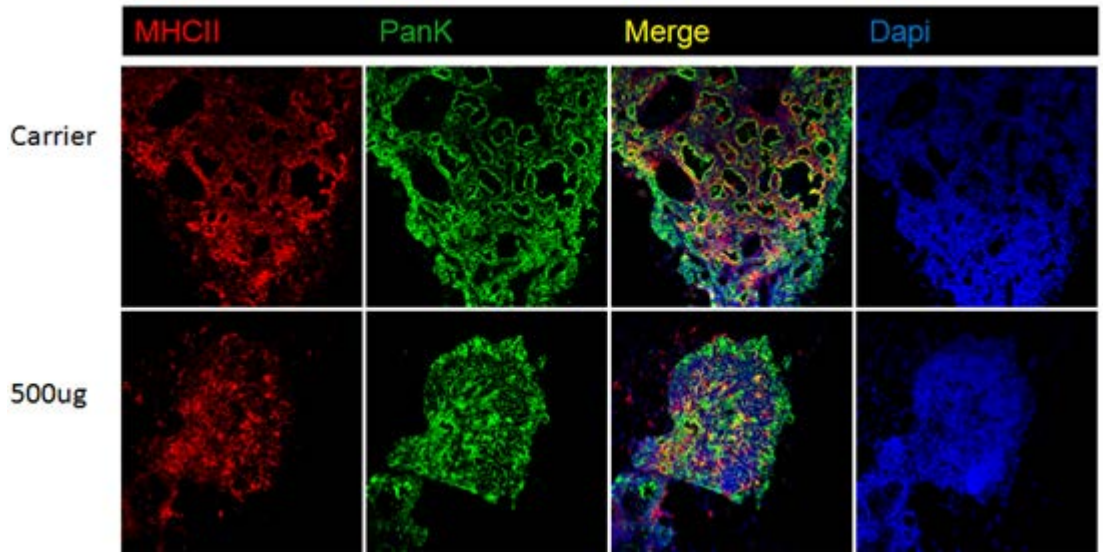

Figure 3.8 Immunohistochemical staining profile of MHC Class II and PanK on 4OHT and carrier-only injected *R/-;CreERt2* mice. 2-4 months old R/-;CreERt2 were injected with 4OHT or carrier only. 7 weeks later, thymi or thymic rudiments were dissected and processed for cryosectioning. 8μm cryosections were cut and stained with PanK (green) and MHC Class II (red). Carrier-only and 250μg4OHT injected mice showed a cystic epithelial structure and expressed MHC Class II in the majority of the epithelial cells (**A 250g** and **B Carrier**). MHC Class II positive cells could be detected in both cortical and medullary regions in all mice that received 500μg or higher doses of 4OHT (**A** and **B**), and the expression patterns were same as the WT C57BL/6. n=2 for carrier-only, 250μg and 500μg 4OHT injected mice. n=1 for 1 mg, 1.5mg and 2mg 4OHT injected mice.

3.2.2 Functional analysis of the thymi generated upon reactivation of *Foxn1*^{R} allele.

Thymopoiesis, the process by which haematopoietic progenitor cells become mature T-cells, occurs as thymocytes migrate through the thymus and requires interaction with a variety of thymic stroma cell types. The process of T-cell development can be monitored using a series of cell surface markers. In the earliest stages of development, thymocytes lack expression of CD4 and CD8, and are called double negative cells (DN, $CD4^{-}CD8^{-}$). As the developing thymocytes migrate through the cortex to the sub-capsular area, they become committed to the T-cell fate and eventually start to express both CD4 and CD8, becoming double positive thymocytes (DP, $CD4^{+}CD8^{+}$). DP thymocytes migrate through the cortex back to the medulla, just before entering the cortex, they become single positive immature T cells ($CD4^{+}CD8^{-}$ or $CD4^{-}CD8^{+}$), and subsequently mature in medulla (Petrie and Zuniga-Pflucker 2007).

I used flow cytometry analysis to test the different population of intrathymic lymphocytes. No DP cells were detected in carrier-only injected mice (Figure 3.9), consistent with the athymic phenotype observed by immunohistochemistry (IHC) analysis (Figure 3.3). The thymus from 1mg 4OHT injected mice contained DP cells, as well as the later stage single positive (SP) cell types, although more than half of the cells were still double negative (DN). With the increasing 4OHT dosage, the DP proportion increased, consistent with reactivation of *Foxn1* having occurred in more progenitor cells within the higher dose 4OHT injected mice, as suggested by IHC (Figure 3.9). The total number of DP cells within each thymus was determined for each dose of tamoxifen. While the carrier-only injected mice contained no intrathymic DP cells, at doses of 4OHT above 500µg, the injected mice contained DP

cells. With increasing doses of 4OHT, more DP cells were detected (Figures 3.9 and 3.10), suggesting a higher number of mature TECs.

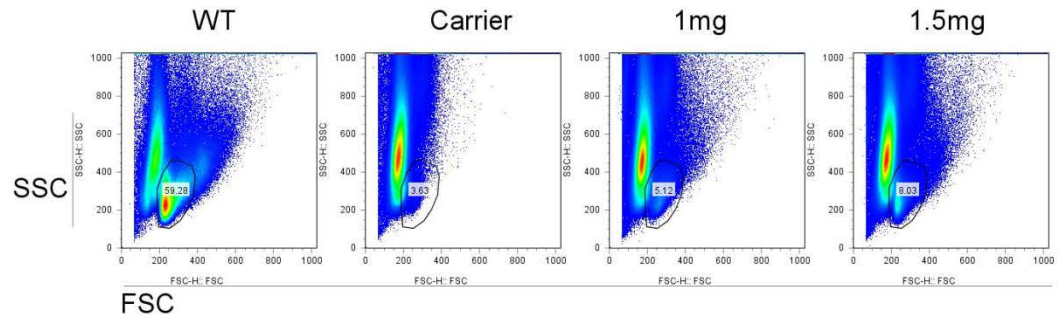
WT
Carrier
1mg
1.5mg
SSC
FSC
59.28
3.63
5.12
8.03

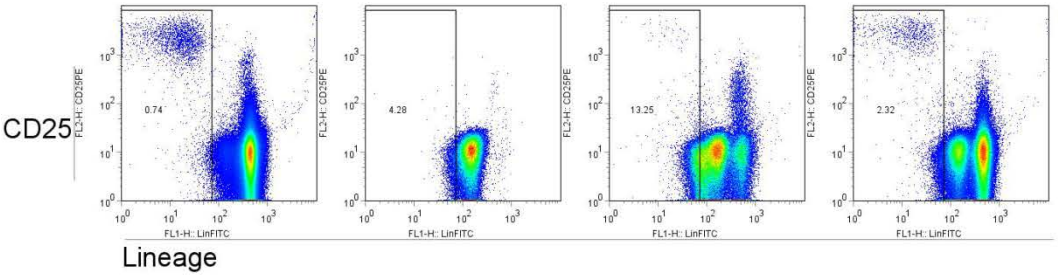
CD25
Lineage
0.74
4.28
13.25
2.32

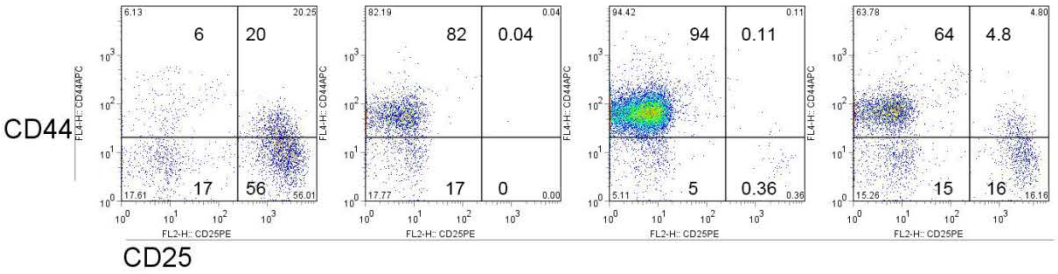
CD44
CD25
6
20
17
56
82
0.04
17
0
94
0.11
5
0.36
64
4.8
15
16

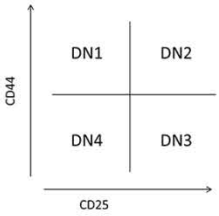
DN1
DN2
DN4
DN3
CD44
CD25

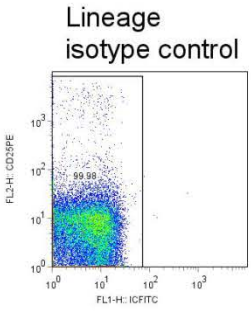
Lineage
isotype control
99.99

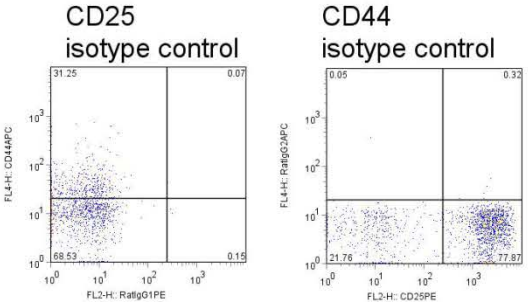
CD25
isotype control
CD44
isotype control
31.25
0.07
68.53
0.15
0.05
0.32
21.76
77.87

Figure 3.9 CD4 and CD8 intrathymic lymphocyte staining profile in carrier-only and 4OHT injected *R/-;CreERt2* mice. The thymus from a 6 week old C57BL/6 wild type mouse, and thymi from carrier-only or 4OHT injected *R/-;CreERt2* mice were dissected and thymocytes were collected by mechanically homogenizing the thymic tissue. Cells were stained with antibodies specific for CD45, CD4 and CD8, or appropriate isotype controls, and were first analyzed by flow cytometry on the base of forward and side scatter (FSC/SSC). Then, 7AAD or DAPI was used to gate out the dead cells, and CD45 was used to identify intrathymic haematopoietic cells before further analysis of developing T-cell subsets. Carrier-only injected mice contained no $CD4^+$ $CD8^+$ DP cells. 1mg and 1.5mg 4OHT injected mice contained DP and SP cells, indicating functionality of the thymi. n>3 for **WT** and **Carrier**; n=1 for **1mg** and **1.5mg**.

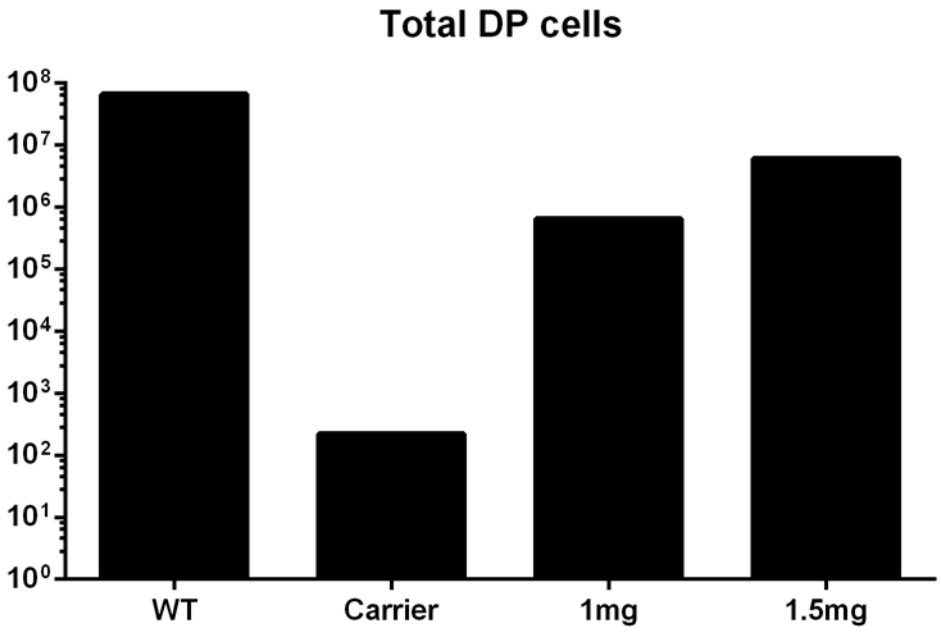

Figure 3.10 Number of DP cells within carrier-only or 4OHT injected *R/-;CreERt2* mice. Thymus from a 6 week old C57BL/6 wild type mouse, and thymi from carrier-only or 4OHT injected *R/-;CreERt2* mice were dissected and thymocytes were collected by mechanically homogenizing the thymic tissue. Before staining, red blood cells were lysed, and the total live cell numbers were counted. Cells were processed and analyzed as in Figure 3.9. Total DP cell numbers were determined from the total cell number, percentage of $CD45^+$ cells and the percentage of DP cells as shown in Figure 3.9. Y axis is displayed in logarithmic scale. Samples presented here were processed at the same time. At least two more samples within the same age for WT (Chapter 4 Figure 4.3) and Carrier (previous work by Dr. Craig Nowell), respectively, were conducted and showed the same number as here. n=1 for 1mg and 1.5mg.

The DN population can be further divided based on CD25/CD44 staining (Godfrey, Kennedy et al. 1993). These stages are called DN1-4. Cells mature in a sequence from $CD44^{+}CD25^{-}lin^{-}$ (DN1) to $CD44^{+}CD25^{+}$ lin^{-} (DN2) to $CD44^{-}CD25^{+}$ lin^{-} (DN3) to $CD44^{-}CD25^{-}$ lin^{-} (DN4), where lin is a cocktail of antibodies for lineages containing CD3, CD4 and CD8 for lymphocytes , NK1.1 for nature killer cells, Ter119 for red blood cells, CD19 for B cells and Mac1 for Macrophage.

In the carrier-only injected mice, most Lin^{-} cells fell within the DN1 quadrant (Figure 3.11). The small number of cells within the DN4 proportion was eliminated by CD45 staining in later experiments, using 16-channel flow cytometry. The absence of DN2, DN3 and DN4 suggested either a block of T-cell maturation from DN1 to DN2 or that the thymus rudiment failed to attract any lymphocytes. The absence of $CD45^{+}$ cells in thymic rudiments from 250µg 4OHT injected mice supported the latter possibility (Figure 3.12).

DN2 and DN3 cells were detected in 1mg 4OHT injected mice, and the proportion and number of cells in each of these populations both increased when the 4OHT dose was increased to 1.5mg. These data provided a further demonstration of T-cell development at the DN stage within the thymus generated upon reversion of the $Foxn1^{R}$ allele in $Foxn1^{R/-}$ mice.

R/-;CreERt2 mice injected with 250µg 4OHT failed to attract lymphocytes, consistent with the non-reactivated status described above. $CD45^{+}$ lymphocytes were detected within the rebuilt thymic tissue of 500µg 4OHT-injected *R/-;CreERt2* mice (Figure 3.12), and both DP and SP cells were also detected (data in Figure 3.13 from Dr. Craig Nowell). consistent with the presence of thymic tissue demonstrated by immunohistochemistry (Figure 3.4-3.6 and Figure 3.8).

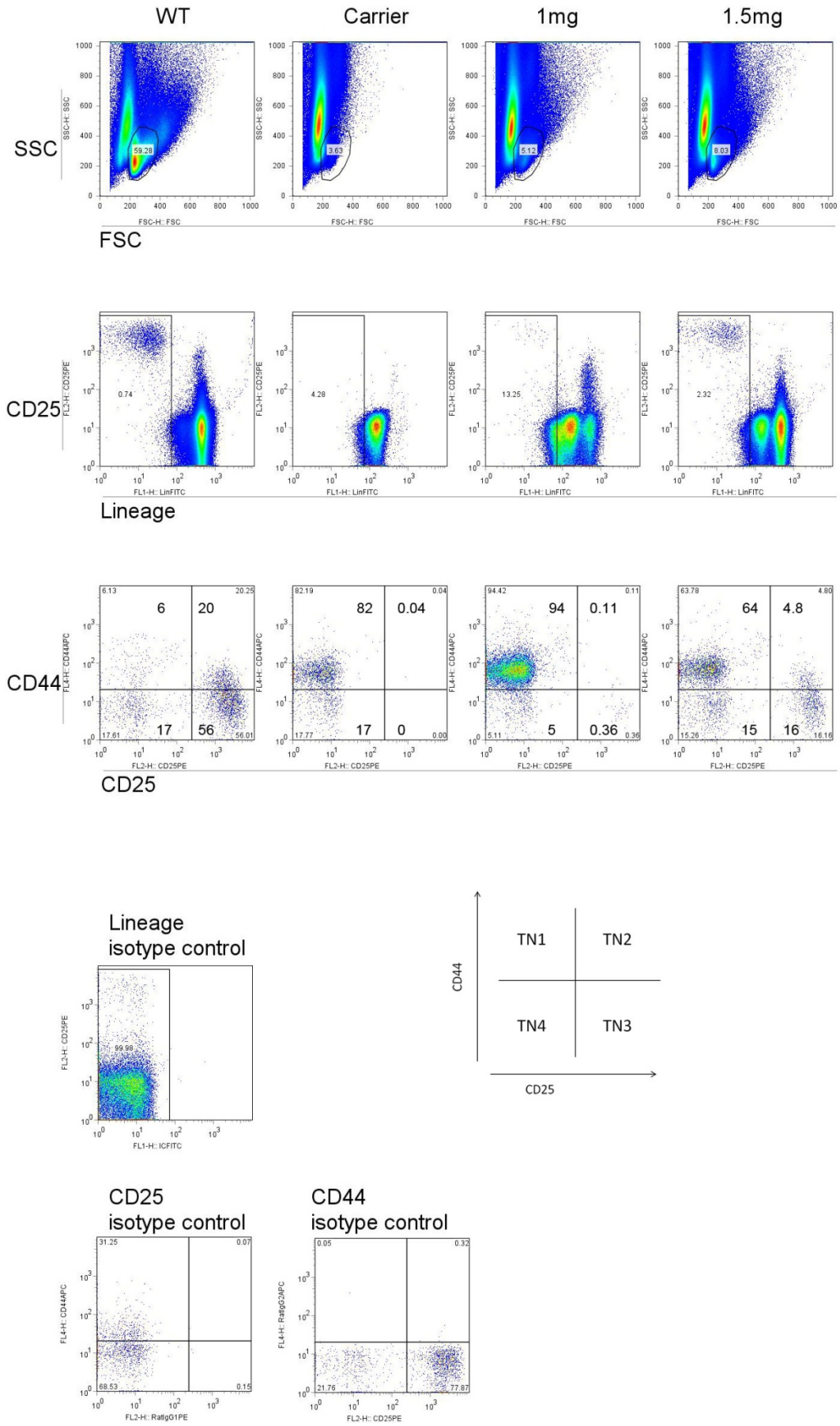
WT
Carrier
1mg
1.5mg
SSC
FSC
CD25
Lineage
CD44
CD25
Lineage
isotype control
TN1
TN2
TN4
TN3
CD44
CD25
CD25
isotype control
CD44
isotype control

Figure 3.11 DN1-4 subset profile within Carrier-only and 4OHT injected *R/-;CreERt2* mice. Thymus from a 6 week old C57BL/6 wild type mouse, and thymi from carrier-only or 4OHT injected *R/-;CreERt2* mice were dissected and thymocytes were collected by mechanically homogenizing the thymic tissue. Stained cells were first analyzed on the base of forward and side scatter (FSC/SSC). Then, 7AAD or DAPI was used to gate out the dead cells. To avoid contamination with other lymphocytes,, samples were stained with a lineage cocktail of FITC conjugated antibodies (lineage – FITC) to gate out all the DP and SP T-cells (CD3, CD4, CD8) and other lymphocytes lineages (NK1.1 for Nature Killer cells, Ter119 for red blood cells, CD19 for B cells, Mac1 for Macrophages). Thymic rudiments from carrier-only injected *R/-;CreERt2* mice contained no DN2 and DN3. Thymi from 4OHT injected *R/-;CreERt2* mice contained DN1, DN2 and DN3 populations, and the proportion increased with increasing 4OHT dose. n>3 for WT and Carrier, n=1 for 1mg and 1.5mg.

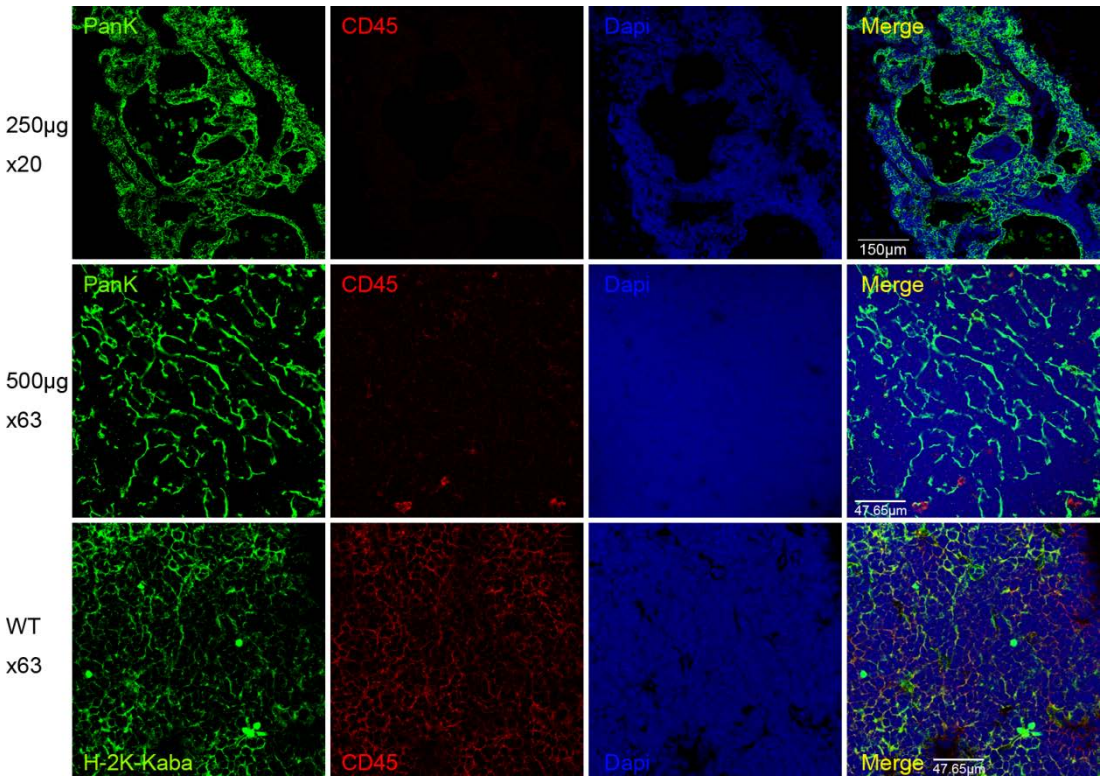

Figure 3.12 CD45 positive cells can be detected within thymic tissue from mice receiving 500µg 4OHT but not within the thymic rudiment of mice receiving 250µg 4OHT. Samples were prepared as for other immunohistochemical staining described. There were no $CD45^{+}$ cells within 250µg 4OHT injected *R/-;CreERt2* thymic rudiment, consistent with lack of Foxn1 reactivation. There were, although much fewer than the WT control, CD45 positive cells detected within thymic area of 500µg 4OHT-injected *R/-;CreERt2* mice. WT is a 6 week old CBA adult thymus. Green channel for WT shows MHC H2-K positive cells. Green channel for 250µg and 500µg 4OHT injected mice shows PanK positive cells. Scale bars x20, 150µm; x63, 47.65µm. (n>2)

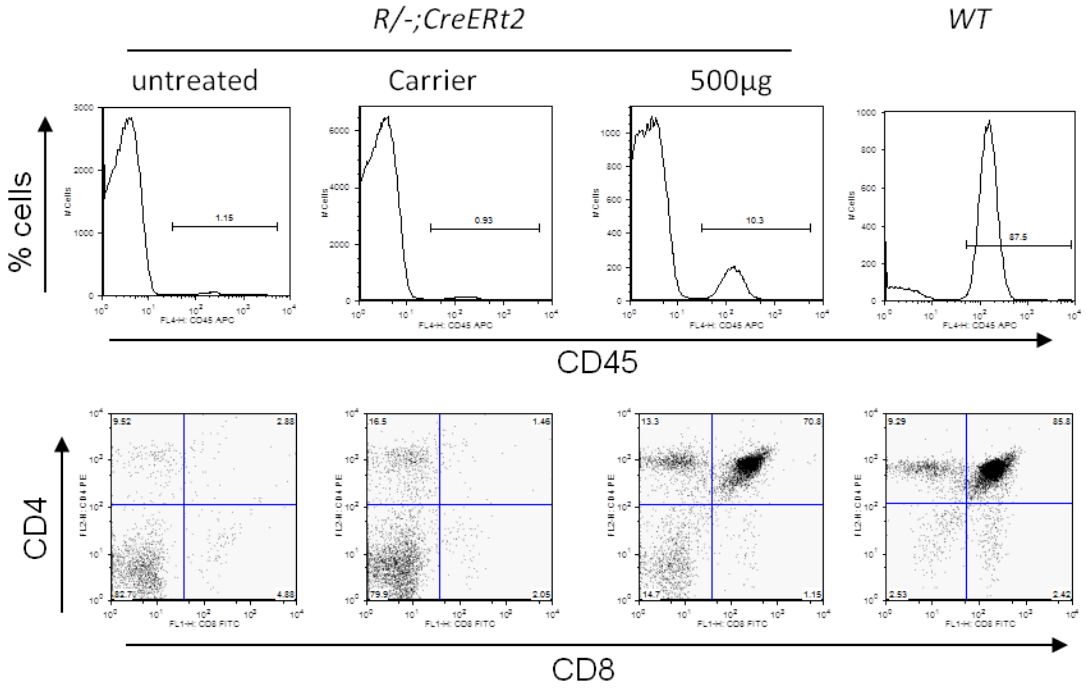

Figure 3.13 CD4 and CD8 intrathymic lymphocyte staining profile in untreated, carrier-only and 500µg 4OHT injected *R/-;CreERt2* mice. Sample prepared and stained as Figure 3.9 described. ***R/-;CreERt2***: 2-4 month-old; ***WT***: C57BL/6 6 week old. (Data from Dr. Craig Nowell)

In summary, the presence of all thymocyte subsets defined by CD44, CD25, CD4 and CD8 in *R/-;CreERt2* mice receiving 500µg or higher doses of 4OHT confirmed the functionality of the thymi generated upon Cre-mediated reversion of *Foxn1*^{R} allele.

3.2.3 A Single injection of high dose of 4OHT led to multiple independent reactivations each gave rise to a thymic lobe with both cortical and medullary compartments.

Within the high dose (1mg, 1.5mg and 2mg)-4OHT injected *R/-;CreERt2* mice, there were always several separate lobes (at least 3 for 1mg, 5 for 1.5mg and 2mg, Figure 3.14) within each thymus, indicating that a series of independent reactivation events

had occurred after injection. All these lobes contained both cortical and medullary compartments. There were clear boundaries between each lobe, and they all surrounded a cystic epithelial cells region which was histologically the same as the carrier-only injected thymi. This suggested that all these lobes originated and budded from these un-differentiated thymic epithelial cells.

The accurate size of each independent thymic lobe was not determined precisely, however, the regenerated lobes resulting from treatment with different doses of 4OHT all appeared to be in the same size range (diameter: 0.3mm-1.2mm).

A

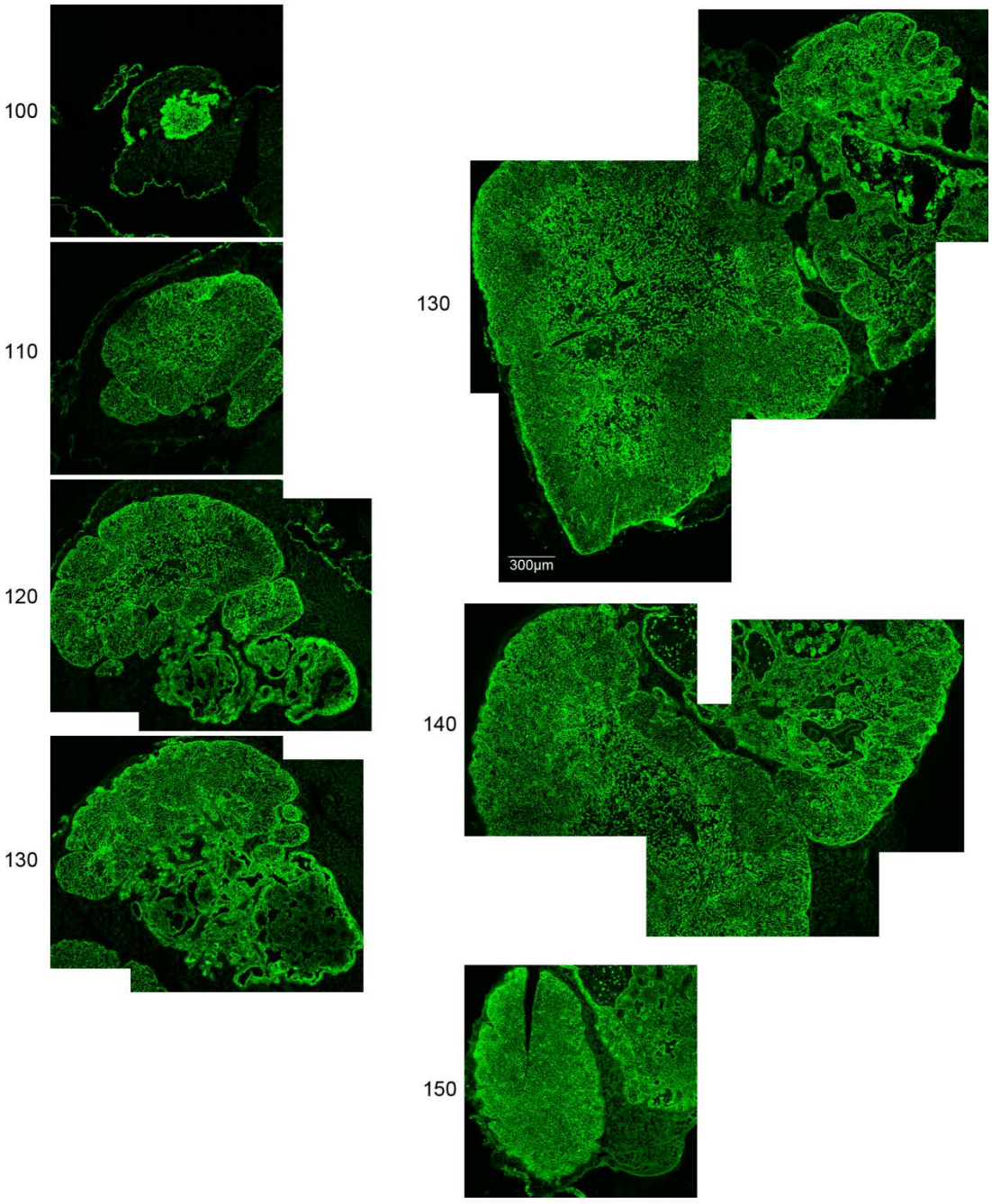

B

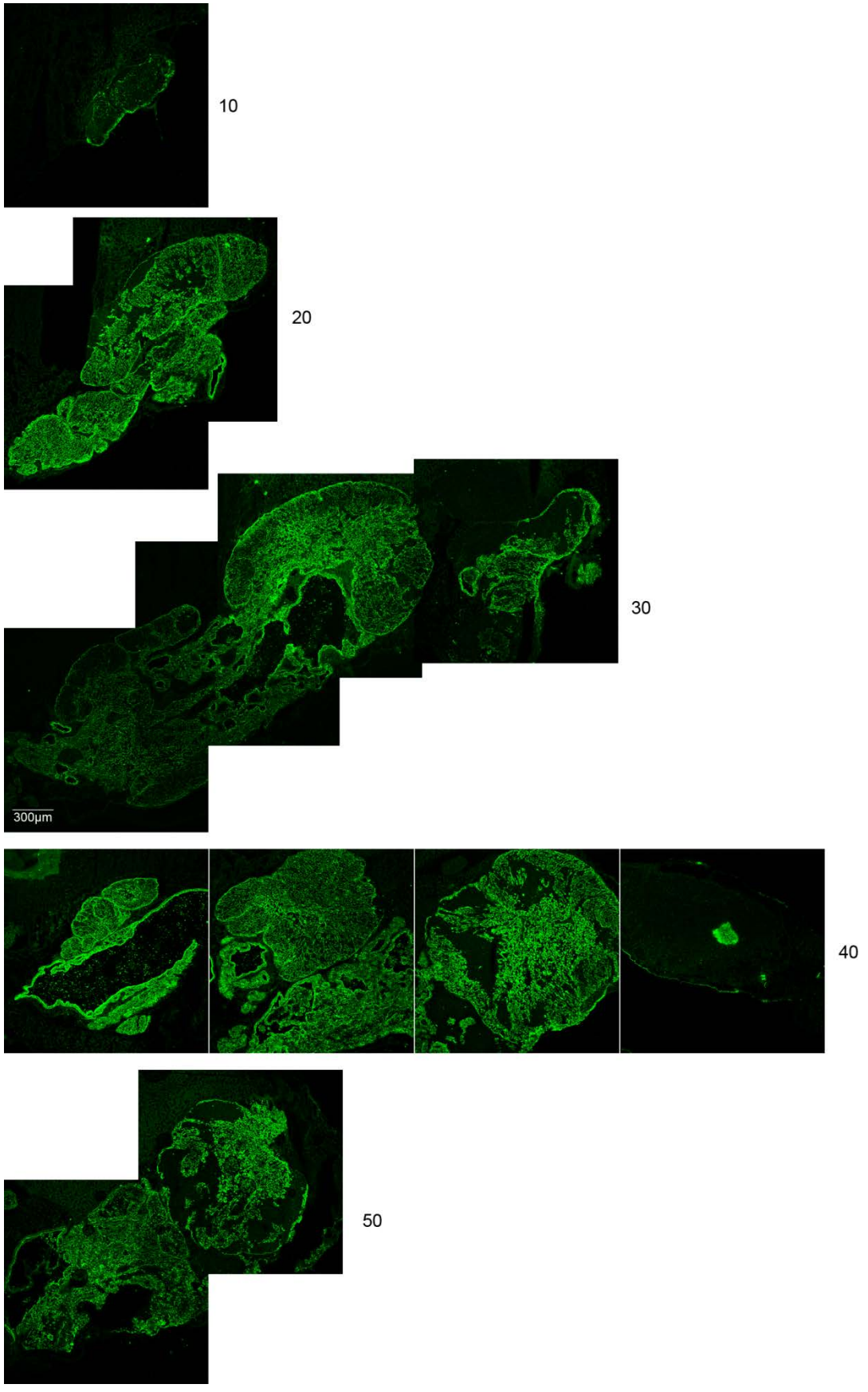

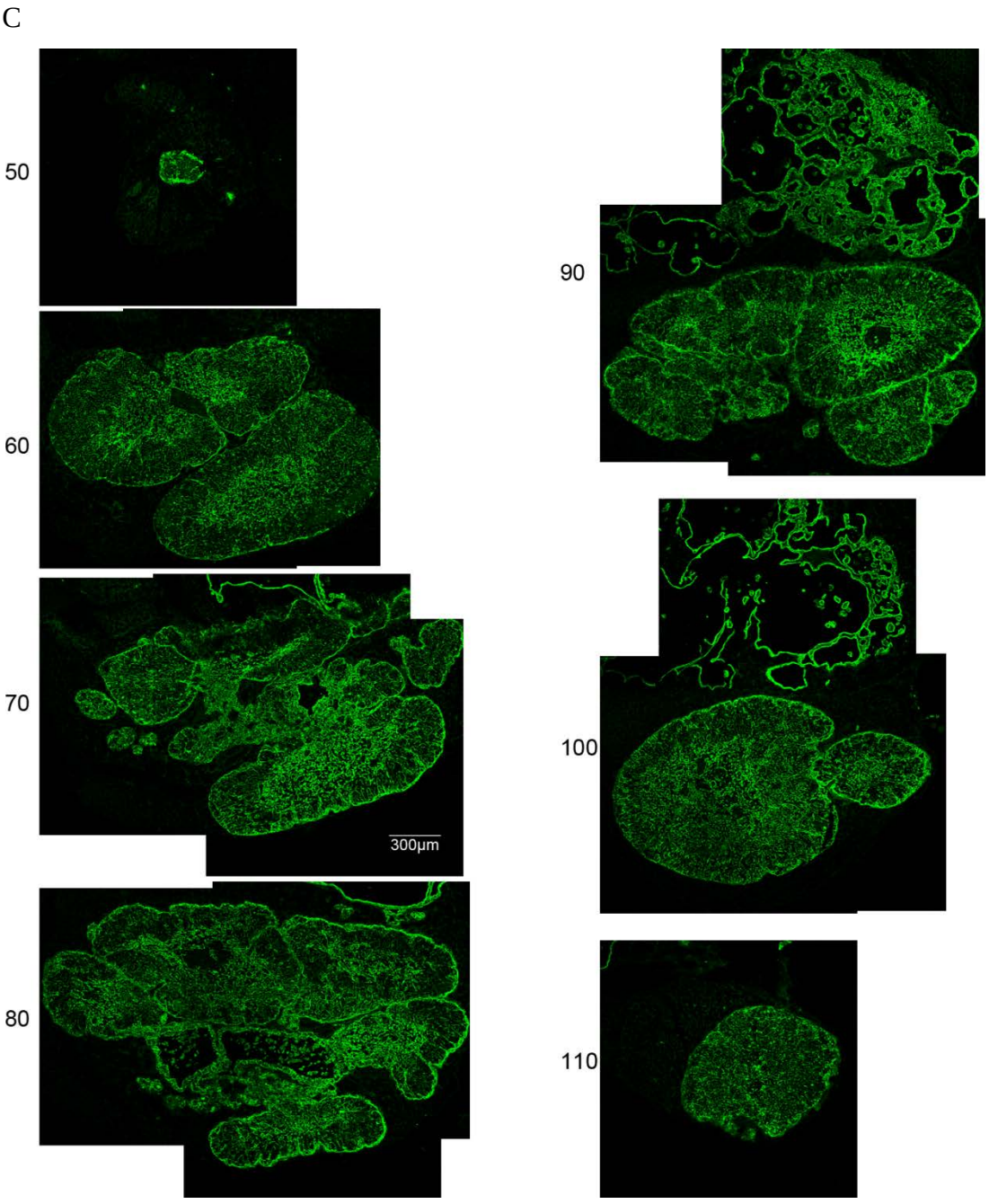

Figure 3.14 Histological structure of thymic tissue blocks resulting from administration of high dose 4OHT to *R/-;CreERt2* mice. Images show sections through the thymus recovered from a (**A**) 1mg 4OHT injected mouse. (**B)** 1.5mg 4OHT injected thymus. **(C)** 2.0mg 4OHT injected thymus. Every 30th section was stained with PanK and DAPI. The sections presented here are annotated with their numerical position in the series of sections (numbers are shown beside the images). Where the tissue region was large, several images are combined. Scale bar: 300um.

3.3 Discussion

In this chapter, I have demonstrated that administration of 4OHT to 2-4 months old *R/-;CreERt2* mice, in order to activate Cre recombinase and therefore to cause reversion of the $Foxn1^{R}$ allele, resulted in generation of functional thymi with a organized thymic structure. These data contributed to a recent paper investigating the function of Foxn1 in TECs (Nowell, Bredenkamp et al. 2011). Previous work in this lab has shown that *R/-;CreERt2* mice express *Foxn1* at 7% of the WT level (Nowell, Bredenkamp et al. 2011). Therefore, data presented here suggest that at this level of *Foxn1* expression, thymus development was arrested and un-differentiated TECs persisted postnatally, as in the $Foxn1^{-/-}$ thymus (Bleul, Corbeaux et al. 2006). When *Foxn1* expression was restored, a functional thymus with both cortical and medullary TECs was generated, indicating that a thymic epithelial progenitor cell population persisted postnatally in *R/-;CreERt2* mice. Since the data presented in this chapter were obtained from 2-4 month-old mice (4 month-old for 1mg, 1.5mg and 2mg 4OHT injected mice. Table 3.1), they extend the findings of Bleul et al (2006) who demonstrate that clonal reactivation of a Foxn1 null allele in neonatal mice resulted in generation of an intact thymus.

This lab has recently shown Foxn1 is not required for medullary thymic epithelial cell sub-lineage specification. Furthermore, specification of both cortical and medullary thymic epithelial progenitor cells was observed in $Foxn1^{R/-}$ mice (Nowell, Bredenkamp et al. 2011). This suggested that sub-lineage specified thymic epithelial progenitor cells might exist within the postnatal *R/-;CreERt2* thymic rudiment. We especially carefully looked at the 500µg 4OHT injected *R/-;CreERt2* mice, since this was the lowest dose of 4OHT at which reactivation was seen. We found no cortical-only or medullary-only regions in any thymic tissue generated by reactivation of Foxn1. Thus, we could not find direct evidence for the existence of cortical or

medullary sub-lineage specified progenitor cells in the *R/-;CreERt2* thymic rudiment. This suggested that, although at least medullary sub-lineage specific TEPCs arise independent of Foxn1 expression, in the absence of Foxn1 or in the low level of Foxn1 expression, only the common TEPCs can persist to the postnatal stage.

It could also be possible that mTEPCs can persist, but can only generate mTECs in the presence of differentiating cTECs (or thymocytes). Similarly, if cTEPCs persist, they might only be able to generate cTECs in the presence of differentiating mTECs (or thymocytes). The immunohistochemical staining profile of the *R/-;CreERt2* thymic rudiment with Plet-1, UEA-1 and MHC Class II indicated the heterogeneous character of the un-differentiated cystic epithelial cells within both carrier-injected and 4OHT injected mice. This suggested that the common thymic epithelial progenitor cells do not represent all of the cells, within these thymic rudiments. To further address the questions about which progenitor cell types could exist within the postnatal thymic rudiment, different cell population could be separated based on different staining profiles and tested through ectopic transplantation. Also, chimaeric mice could be made to look at the distribution of cells from different source in contributing to the same rebuilt thymus (Rodewald, Paul et al. 2001).

Chapter 4: Investigation of the persistence of thymic epithelial progenitor cells in aged mice

4.1 Introduction

In Chapter 3, I demonstrated that a functional thymic epithelial progenitor cell pool exists in *R/-;CreERt2* mice up to 4 months of age. Therefore, I next set out to determine how long these progenitor cells could persist *in vivo*.

This work was started one year after the initial work on the younger *R/-;CreERt2* mice. Surprisingly, in contrast to my previous findings, tamoxifen-independent reversion of the R allele was observed in *R/-;CreERt2* mice without 4OHT induction (see 4.2.1). In this chapter, I determine whether this tamoxifen-independent reversion can be used to assay the persistence of thymic epithelial progenitor cells in *R/-;CreERt2* mice.

4.2 Results

4.2.1 Detection of spontaneous (ligand-independent) CreERt2-mediated recombination in *R/-;CreERt2* mice

The initial evidence for the occurrence of spontaneous recombination came from histological analysis of a carrier-only injected 6 month old *R/-;CreERt2* mouse. A thymus structure containing both cortical ($PanK^+CDR1^+$) and medullary ($PanK^+K14^+$) thymic epithelial tissue was observed in this mouse. The wild type-like MHC Class II profile on the thymic tissue suggested that the thymic tissue was functional (Figure 4.1 A). A series of small lobes containing both cortex and medulla was observed adjacent to the un-differentiated cystic epithelial cells (Figure 4.1 B), suggesting that a series of recombination events had occurred. DP thymocytes were subsequently also found, in some *R/-;CreERt2* mice of other ages that were either

carrier-only injected or untreated (Table 4.2). Together, these data demonstrated the occurrence of spontaneous recombination of the R allele in *R/-;CreERt2* in the absence of 4OHT induction.

To determine the cause of this spontaneous recombination, I compared the intrathymic CD4 and CD8 staining profile of *R/-;CreERt2* mice and *R/-* mice. While DP cells could be easily detected within untreated aged *R/-;CreERt2* mice, there were no DP cells within the aged *R/-* mice. It indicate that the spontaneous recombination was CreERt2-dependent (Figure 4.2).

This demonstrated that the tamoxifen-independent reversion of the Foxn1R allele observed in *R/-;CreERt2* mice was caused by this spontaneous activity of the CreERt2 recombinase. A low-level of spontaneous recombination in the *Rosa26CreERt2* mouse strain was previously reported in un-induced *Rosa26CreERT2;EGFP* mice (Hameyer, Loonstra et al. 2007). Low-level spontaneous recombination in other CreERt2 transgenic mice strains in the absence of Tamoxifen has also been reported (Bleul, Corbeaux et al. 2006).

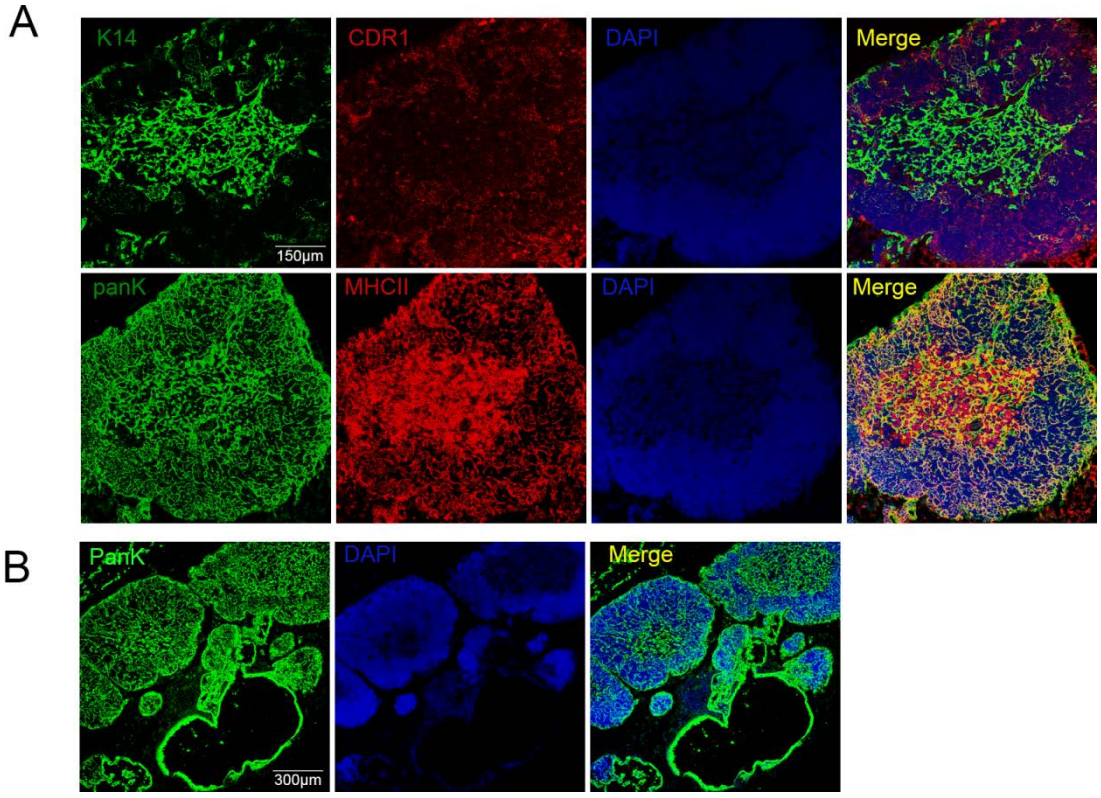

Fig 4.1 Detection of spontaneous reversion of the R allele in aged *R/-;CreERt2* mice. A representative sample of carrier-only injected 6 months old *R/-;CreERt2* mice. One month after injection, the thymus was dissected and analyzed through immunohistochemistry. **(A)** The carrier-only injected mice contained a thymus structure which contained both cortex and medulla, marked by CDR1 and K14, respectively. The presence of $PanK^{+}MHCII^{+}$ cells suggested that the TECs in this thymus were functional. Scale bar: 150um. **(B)** shows a series of small thymic lobes found in a carrier-only injected mouse, suggesting the occurrence of multiple spontaneous recombination events. Scale bar: 300um.

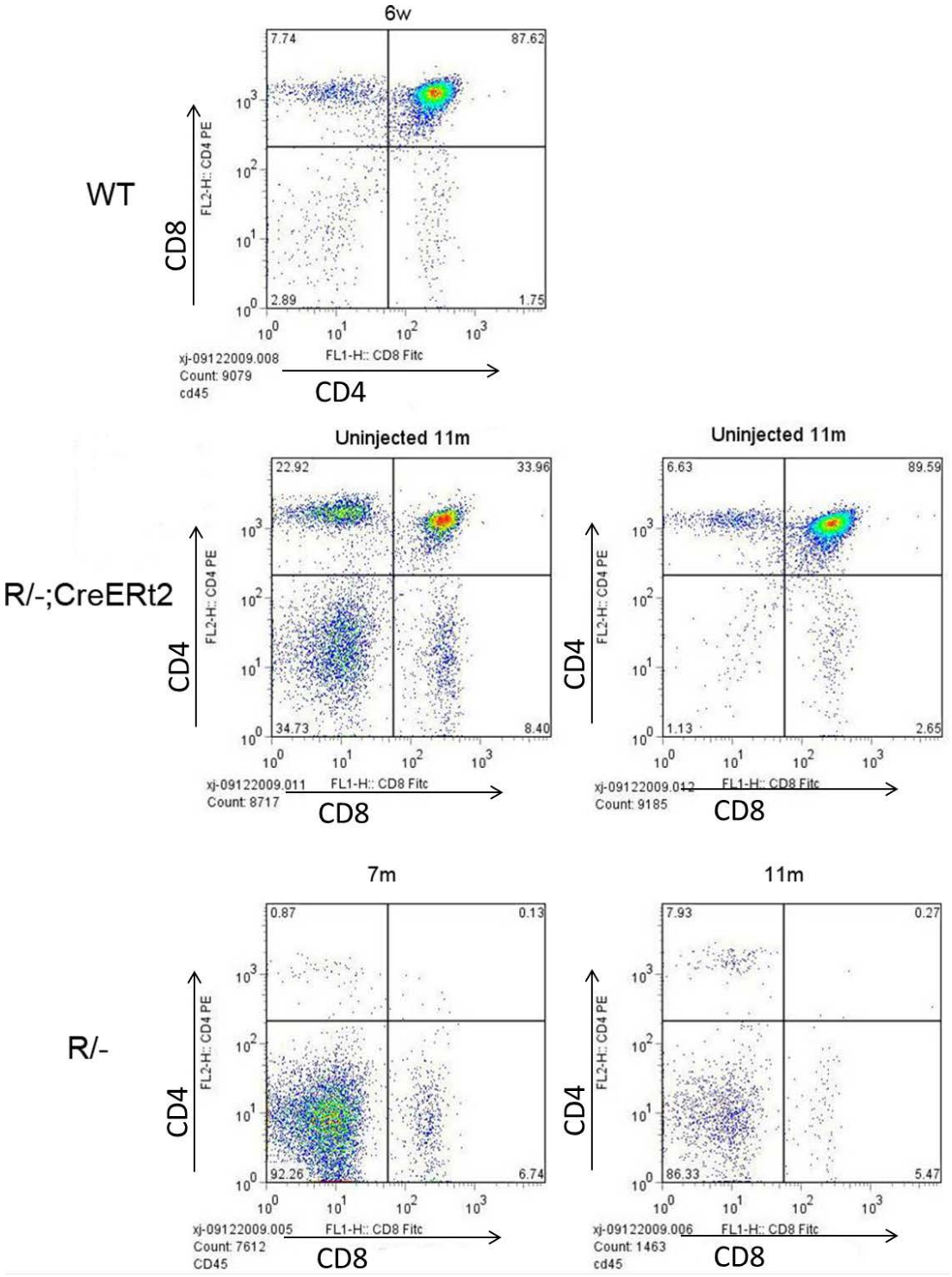
6w
WT
7.74
87.62
2.89
1.75
CD8
CD4
FL2-H:: CD4 PE
FL1-H:: CD8 Fitc
xj-09122009.008
Count: 9079
cd45
Uninjected 11m
R/-;CreERt2
22.92
33.96
34.73
8.40
xj-09122009.011
Count: 8717
Uninjected 11m
6.63
89.59
1.13
2.65
xj-09122009.012
Count: 9185
7m
R/-
0.87
0.13
92.26
6.74
xj-09122009.005
Count: 7612
CD45
11m
7.93
0.27
86.33
5.47
xj-09122009.006
Count: 1463
cd45

Figure 4.2 Comparison of *R/-;CreERt2* and *R/-* mice. Thymic rudiments, or thymic tissue, was microdissected from two randomly selected, untreated 11 month old ***R/-;CreERt2*** mice and two untreated ***R/-*** mice (7m and 11m old, respectively) and processed through flow cytometry analysis to determine the CD4 and CD8 staining profile. The *R/-;CreERt2* mice showed a significant proportion of DP cells within the $CD45^+$ population (33.9% and 85.6%, respectively) while the *R/-* mice contained few if any DP cells (0.13% and 0.27%). A WT of C57BL/6 was used as a positive control, and contained 88% DP cells.

4.2.2 Investigation of the frequency of spontaneous recombination with age in *R/-;CreERt2* mice.

As it appeared from my initial experiments that the proportion of *R/-;CreERt2* mice in which a spontaneous recombination event had occurred increased with age, I next tested whether analysis of untreated *R/-;CreERt2* mice could be informative regarding the length of time for which thymic epithelial progenitor cells could persist *in vivo* in this mouse strain.

The rationale used in these experiments was as follows. If un-recombined functional progenitor cells persist in aged *R/-;CreERt2* mice, and spontaneous recombination occurs throughout the lifespan, we might expect to see a continuous increase in TEC number (and thus thymus size) with age. Proliferation of pre-existing TECs generated by spontaneous recombination that occurred at a previous time point is unlikely to contribute to the increase in total TEC number, because all mature TECs undergo an age-related involution which starts to occur from 6 week old within wild type thymus and eventually leads to a decrease of functional TEC number with age (Chinn, Blackburn et al. 2012; Griffith, Fallahi et al. 2012) (Section 4.2.3 & 4.2.4).To test whether spontaneous recombination continued to occur even in aged mice, and thus whether a pool of un-reactivated cells persisting as the *R/-;CreERt2* mice aged could still give rise to mature TECs, I therefore next set up a series of *R/-;CreERt2* mice of different ages and different treatments, and determined thymus size in each of these mice. The number of DP thymocytes is proportional to the number of functional mature TECs, unless TECs are functionally compromised (Klug, Crouch et al. 2000; Jenkinson, Rossi et al. 2007; Nowell, Bredenkamp et al. 2011) and therefore, the number of DP cells was used to assay relative thymus size. As age-related thymic involution causes a decrease in thymocyte number with age (Section 4.2.3), this effect was also considered when interpreting the results.

A total of seventy six *R/-;CreERt2* mice were analyzed in these experiments. These were separated into 4 different groups on the basis of age: 2 months, 4 months, 6 months and 10 months old. Each age group was further divided into 3 subgroups: uninjected, carrier injected and 2mg 4OHT injected. Males and Females were equally distributed within the different treatments (Table 4.1).

The uninjected or carrier injected *R/-;CreERt2* mice were sacrificed at the age shown, and the total number of DP T-cells within the thymus/thymus rudiment were counted. The total number of DP cells in *R/-* mice (male: 440, and female: 608) was used as control to set the background level of the DP cells in the absence of reversion of the *R* allele. *R/-;CreERt2* thymi which had the same or fewer DP cells in the thymus than the *R/-* mouse were categorized as not containing a spontaneous recombination event. Table 4.2 summarizes the data from the uninjected and carrier injected *R/-;CreERt2* mice.

Although evidence of spontaneous recombination was found in all four age groups, the frequency varied with age (Table 4.2A and 4.2B), with a trend to more recombination in older mice. This showed that the occurrence of spontaneous CreERt2–mediated reversion of the R allele accumulated over time. These results showed that a pool of progenitor cells must still exist and be able to be reactivated until at least 6 months old in males, and at least 4 month old in females, because mice lacking a tamoxifen-independent recombination event were present until these ages.

Therefore, we can conclude that the TEPCs in low Foxn1 expression *R/-;CreERt2* mice are stable, retaining the capacity to differentiate into functional TECs, for at

least 6 months *in vivo*.

	Male				Female			
Age (months)	2	4	6	10	2	4	6	10
Uninjected	0	3	9	4	0	7	4	1
Carrier	1	4	2	2	2	7	4	0
Tamoxifen	2	3	6	3	1	5	5	1

Table 4.1. Summary of the total number of *R/-;CreERt2* mice analyzed in each age treatment group.

Age		2 months			4 months			6 months			10 months		
		Total	**NoR**	**% NoR**	**Total**	**NoR**	**% NoR**	**Total**	**NoR**	**% NoR**	**Total**	**NoR**	**% NoR**
Male	Un-injected	0	n/a	***n/a***	3	0	***0***	9	1	***11.1%***	4	0	***0***
	Carrier	1	1	***100%***	4	1	***25%***	2	0	***0***	2	0	***0***
	Combined	1	1	***100%***	7	1	***14.3%***	11	1	***9.1%***	6	0	***0***
Female	Un-injected	0	n/a	***n/a***	7	2	***28.6%***	4	0	***0***	1	0	***0***
	Carrier	2	1	***50%***	7	0	***0***	4	0	***0***	0	n/a	***n/a***
	Combined	2	1	***50%***	14	2	***14.3%***	8	0	***0***	1	0	***0***

Table 4.2A. Evidence for continued tamoxifen-independent recombination with age in *R/-;CreERt2* mice.

Age (months)	2 months	4 months	6 months	10 months
No recombination	2	3	1	0
Recombination	1	18	18	7
Total	**3**	**21**	**19**	**7**
% Recombination	**33.3%**	**85.7%**	**94.7%**	**100%**

Table 4.2B: Comparison of Recombination Frequency with Age.

Table 4.2. Evidence for continued tamoxifen-independent recombination with age in *R/-;CreERt2* mice. Table 4.2A shows the total number of uninjected (**Uninj**) and carrier-only injected (**Carrier**) *R/-;CreERt2* mice analysed within each age group, and the gender of each mouse (**Total No.** column). Mice which had almost the same or fewer intrathymic DP thymocytes as *R/-* mice were regarded as showing no evidence of tamoxifen-independent recombination (no recombination; **NoR)** column. In both males and females the proportion of mice showing no evidence of tamoxifen-independent recombination decreased with age. In females, all mice showed evidence of tamoxifen-independent recombination by 6 months old, while males this status at 10 months old. Table 4.2B shows pooled results for males and females which demonstrated a significant difference in recombination frequency among ages (p = 0.0499 by 2x4 Fisher's Exact Test).

4.2.3 Analysis of the effect of ageing on DP cell numbers in WT thymi.

In both mouse and human, the thymus undergoes a stereotypical degeneration with age, known as involution. This involves a decrease in thymus size and cellularity, with decreased numbers of thymic epithelial cells (TECs), structural changes, and decreased thymopoiesis (Linton and Dorshkind 2004; Gray, Seach et al. 2006).

To interpret the data on the number of total DP cells over the life span in *R/-;CreERt2* mice, we also needed to consider the potential impact of age-related involution on TECs that had arisen from tamoxifen-independent reversion of the *Foxn1R* allele. Therefore, to understand how thymus involution affects the total DP cell number, I first counted the total DP cells with age in C57BL/6 WT mice. As expected, age-related involution was observed within C57BL/6 mice. This was represented by a decrease in the total number of DP thymocytes with age (Figure 4.3). The overall decrease in DP cells was was significant by 1-way ANOVA and the differences between 1.4 and 6 months and between 1.4 and 10 months were significant by post-hoc tests (Figure 4.3). Pairwise differences were also compared by Student's t-tests (Figure 4.3). After 4.5 to 6 months, the rate of decrease slowed. The observed decline in DP cell numbers is consistent with previous reports showing a decline of thymus size (Gray, Seach et al. 2006) and total DP cell numbers (Min, Montecino-Rodriguez et al. 2006) with age.

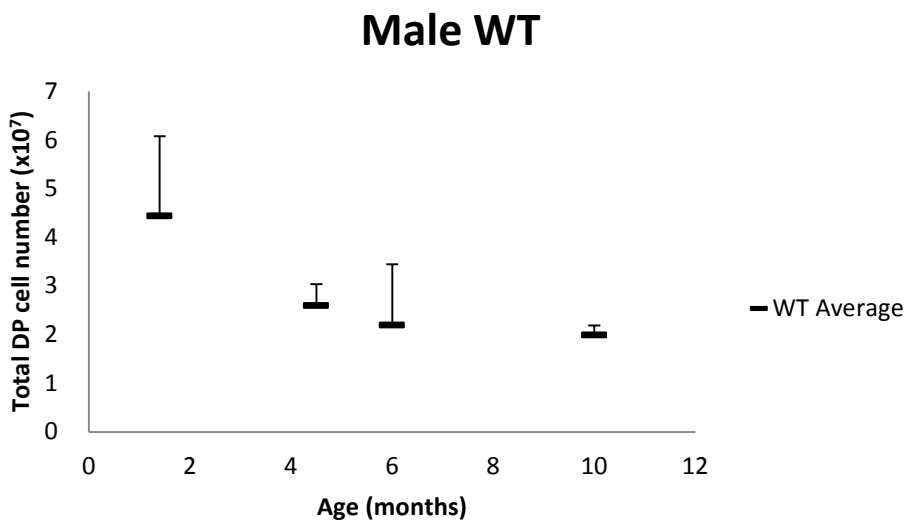

Age (n)		Age in month (n)	P value
1.4 (7)	v	4.5 (3)	0.05
1.4 (7)	v.	6 (4)	0.02
1.4 (7)	v.	10 (3)	0.02
4.5 (3)	v.	6 (4)	0.47
4.5 (3)	v.	10 (3)	0.05
6 (4)	v.	10 (3)	0.40

Figure 4.3. DP cell number within the WT thymus decreases with age. At least three WT C57BL/6 males for each age group were used to count the total DP cell number within the thymus. The average value and standard deviation are shown in the graph. The Y axis is displayed in linear scale. The p value was generated using Student's t test and is listed in the table, together with the sample number analyzed for each age group. DP cell numbers also differed significantly among ages overall by 1-way analysis of variance ($p = 0.0290$). Comparison of individual ages to the initial 1.4-month values by Bonferroni post-hoc tests showed cell numbers had declined significantly at 6 months ($p < 0.05$) and 10 months ($p < 0.05$) but not at 4.5 weeks.

4.2.4 Analysis of DP cell numbers in uninjected, carrier-only and 4OHT injected *R/-;CreERt2* mice thymus with age

The absolute number of DP cells in the un-injected, carrier-only injected and 2.0mg 4OHT injected *R/-;CreERt2* mice was then analyzed. Again, background numbers of DP cell numbers was determined from the *R/-* mouse.

There were no significant differences among ages in the number of DP cells in *R/-;CreERt2* mice (Figure 4.4). Unlike the wild-type control mice (Figure 4.3), there was no decline with age and, if anything, there was some evidence of a trend for an increase with age. An increase in DP cells could be due either to the growth of TECs generated by tamoxifen-independent recombination in young mice, or to an increase in the tamoxifen-independent recombination events and thus activation of additional thymic epithelial progenitor cells with age. As WT C57BL/6 mice undergo age-related thymus involution from 6 weeks after birth, we assume that any TECs generated by tamoxifen-independent recombination before this age, would undergo the same process – and indeed that age-related thymic involution would affect TECs generated at any age after 6 weeks (Griffith, Fallahi et al. 2012). As there was no evidence for a decline in DP cell numbers with age in *R/-;CreERt2* mice over 10 months (Figure 4.4), we conclude that un-reactivated TEPCs may persist until at least between 6 and 10 month old and that, throughout this period, TEPCs continue to undergo reactivation events to generate new mature TECs. Importantly, although the *Foxn1R* allele expresses SV40 T antigen under the control of the Foxn1 promoter, the SV40 T antigen cDNA is excised upon reversion of the allele, so T antigen is no longer expressed in TECs and does not complicate interpretation of these data.

The female *R/-;CreERt2* mice showed a similar picture to the males (Figure 4.5) and there were no significant differences among ages. There was a non-significant trend for an increase in DP cell numbers with age in carrier-injected females but not uninjected females. These data suggest, in female mice, that a TEPC pool persists until at least between 4 months to 6 months old (Figure 4.5) and can generate new mature TECs upon reactivation of the Foxn1 R allele.

Both male and female 4OHT-injected mice showed a slight increase of total DP cells

with age too. Initial multiple pairwise comparisons using t-tests suggested a significant increase in DP cells between 2 and 4 months for tamoxifen-treated males (Figure 4.6). However, further investigation using a 1-way analysis of variance (ANOVA), to reduce the risk of false-positive significant differences, revealed no overall significant differences among ages for tamoxifen-treated males ($p = 0.1642$). As there were only one 2-week and one 10-week sample for tamoxifen-treated females, a 1-way ANOVA was not appropriate. If recombination occurs only in some mice, the distribution of cell numbers may not be normal so the 1-way ANOVA was repeated with a non-parametric Kruskal-Wallis test. There were no significant differences overall among ages for either tamoxifen-treated males ($p = 0.2564$) or tamoxifen-treated females ($p = 0.9615$). (Kruskal-Wallis test results are included in the legends for Figures 4.4-4.7.)

Results for tamoxifen-treated males were pooled to increase the number of samples per age but again there were no significant differences overall among ages by either 1-way ANOVA ($p = 0.7656$) or non-parametric Kruskal-Wallis test ($p = 0.4441$). Linear regression analysis was used in an attempt to test whether age-related changes in DP cell numbers in tamoxifen-treated *R/-;CreERt2* mice differed significantly from those in wild-type mice. Linear regression lines were fitted to data shown for wild-type males in Figure 4.3 and the combined male and female data for tamoxifen-treated *R/-;CreERt2* mice. The results, shown in (Figure 4.7), showed that the slope of the change in DP cell numbers differed significantly from zero for wild-type males ($p = 0.0061$) but not for tamoxifen-treated *R/-;CreERt2* mice ($p = 0.3822$) and that the two slopes differed significantly from one another ($p = 0.0014$). Although a linear regression may not be a realistic model for these age-related changes, the significant difference between the two slopes suggests that cell numbers do not decline in tamoxifen-treated *R/-;CreERt2* mice and may actually increase with age. This further suggested a TEPC pool persists as mice aged (Figure 4.6).

Table 4.2A,B shows that young mice have a lower incidence of tamoxifen-independent recombination than older mice. As this alone would explain the observed increase in average DP cell number with age in the uninjected and carrier-only injected mice, I also analyzed the data separately for only the *R/-; CreERt2* mice that were classified as having ‘reactivated’ cells (more DP cells than control *R/-* mice) in

the three treatment groups (uninjected, carrier-injected and 4OHT-injected). This analysis showed a similar pattern, confirming that reactivation of long-term persisting progenitor cells within *R/-;CreERt2* thymus occurred until at least 6 months of age. (Figure 4.8-4.10)

In summary, as *Foxn1*^{R} allele reversion was confirmed in Chapter 3 to cause generation of functional mature TECs, I conclude that a functional progenitor cell pool can persist within the *R/-;CreERt2* mice until they are at least 6 months old.

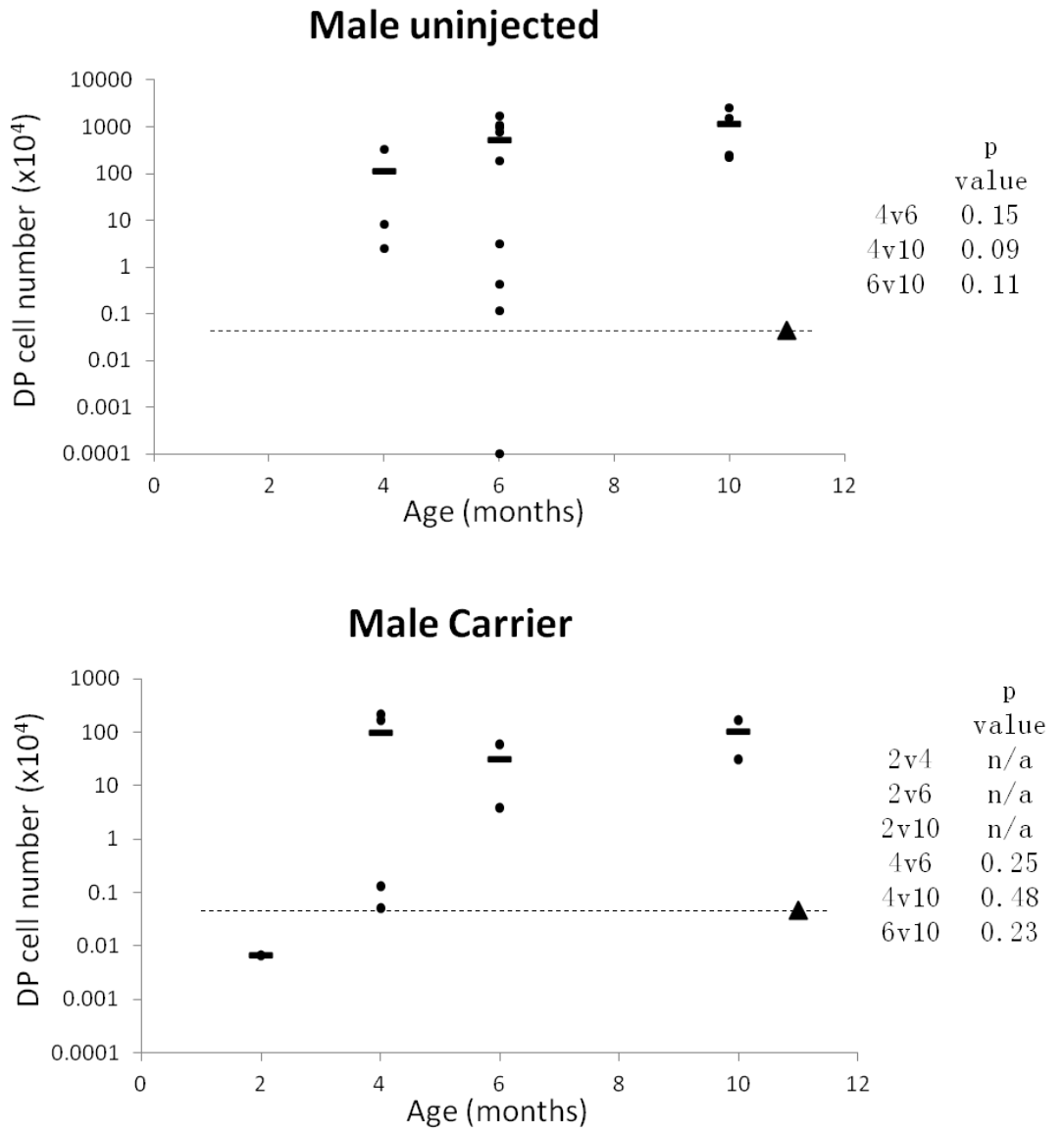

Figure 4.4 Quantification of DP cell number in uninjected and carrier-only injected Male *R/-;CreERt2* mice with age. *R/-;CreERt2* mice of untreated (**Uninjected**) and carrier-injected mice of the age groups shown, were analysed to determine the total number of DP cells. For the injected mice, analysis was 5 weeks after the injection(**Carrier**). Data points shown each represent an individual mouse. The mean number of total DP cells (horizontal bar), and the p value determined by Student's T test result are also shown. One male *R/-* mouse (solid triangle) was used to determine the background (dashed line) of total DP cells in the absence of reversion of the *Foxn1*^{R} allele. Y axis is displayed in logarithmic scale. If cell numbers change in some mice but not others the distribution of cell numbers may not be normal at each time point. For this reason, the analysis was repeated using the non-parametric Kruskal-Wallis test. In agreement with the individual t-tests, this showed no overall significant differences among the three ages for either uninjected males ($p = 0.2746$) or carrier-injected males ($p = 0.4290$).

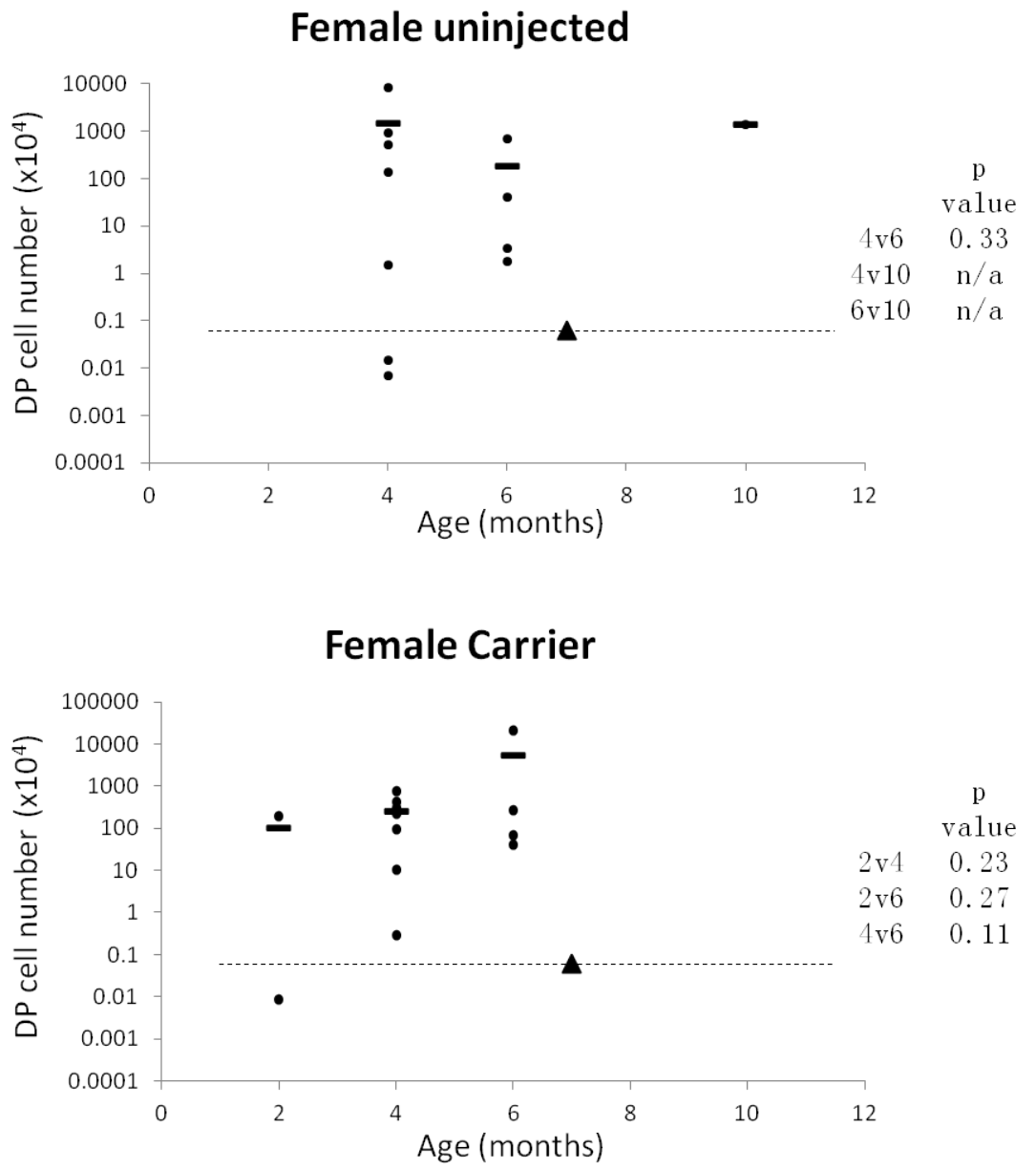

Figure 4.5 Quantification of DP cell number in uninjected and carrier-only injected Female *R/-;CreERt2* mice with age. Female *R/-;CreERt2* mice of untreated (**Uninjected**) and carrier-injected mice of the age groups shown, were analysed to determine the total number of DP cells. For the injected mice, analysis was 5 weeks after the injection(**Carrier**). Data points shown each represent an individual mouse. The mean number of total DP cells (horizontal bar), and the p value determined by Student's T test result are also shown. One female *R/-* mouse (solid triangle) was used to determine the background (dashed line) of total DP cells in the absence of reversion of the *Foxn1*^{R} allele. Y axis is displayed in logarithmic scale. In agreement with the individual t-tests, the non-parametric Kruskal-Wallis test also showed no overall significant differences among the three ages for either uninjected females (p = 0.4267) or carrier-injected females (p = 0.4917).

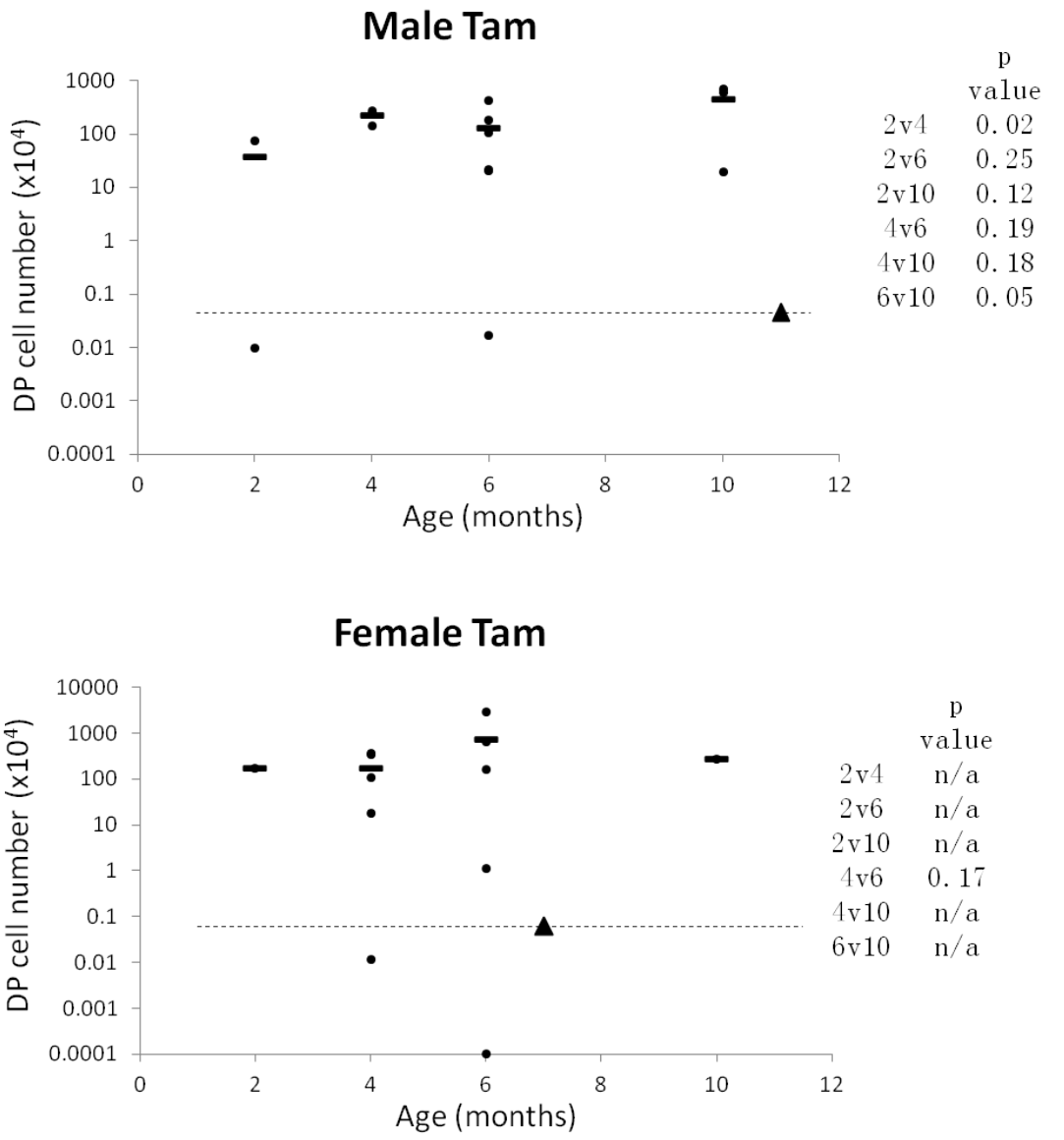

Figure 4.6 Quantification of DP cell number in 4OHT injected *R/-;CreERt2* mice with age. 4OHT-injected *R/-;CreERt2* mice of the age groups shown, were analysed to determine the total number of DP cells. Analysis was 5 weeks after the injection. Data points shown each represent an individual mouse. The mean number of total DP cells (horizontal bar), and the p value determined by Student's T test result are also shown. One male and one female *R/-* mouse (solid triangle) were used to determine the background (dashed line) of total DP cells in the absence of reversion of the *Foxn1*^{R} allele. The top panel shows data collected from males, and the bottom panel shows data collected from females. Y axis is displayed in logarithmic scale. Despite one significant t-test for males (2 vs. 4 months), the non-parametric Kruskal-Wallis test showed no overall significant differences among the three ages after tamoxifen treatment for either males ($p = 0.2564$) or females ($p = 0.9615$).

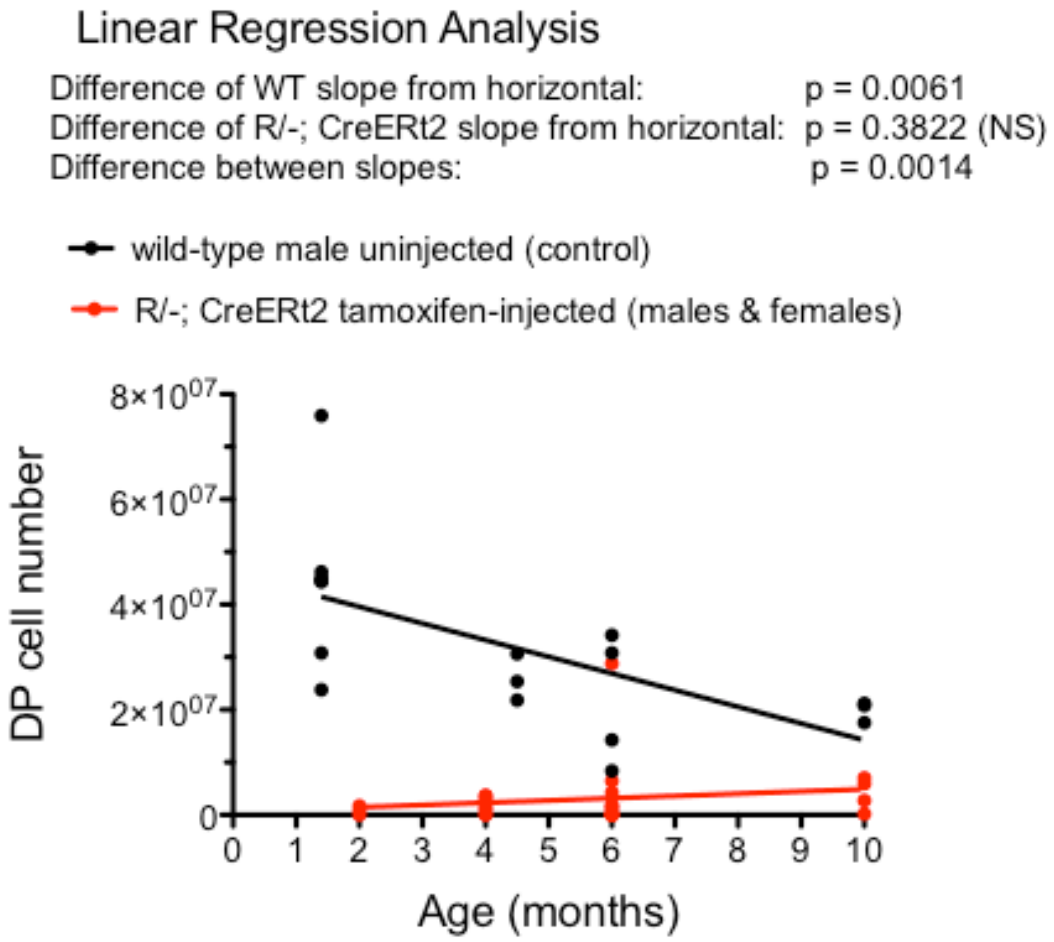

Figure 4.7 Linear regression lines for decline in DP cell numbers in wild-type males (data from Figure 4.3) and changes in DP numbers for combined data for tamoxifen-treated *R/-;CreERt2* males and females (Figure 4.6). The p-values for differences in the slopes of the lines from one another and from a horizontal line (indicating no change with age) are shown.

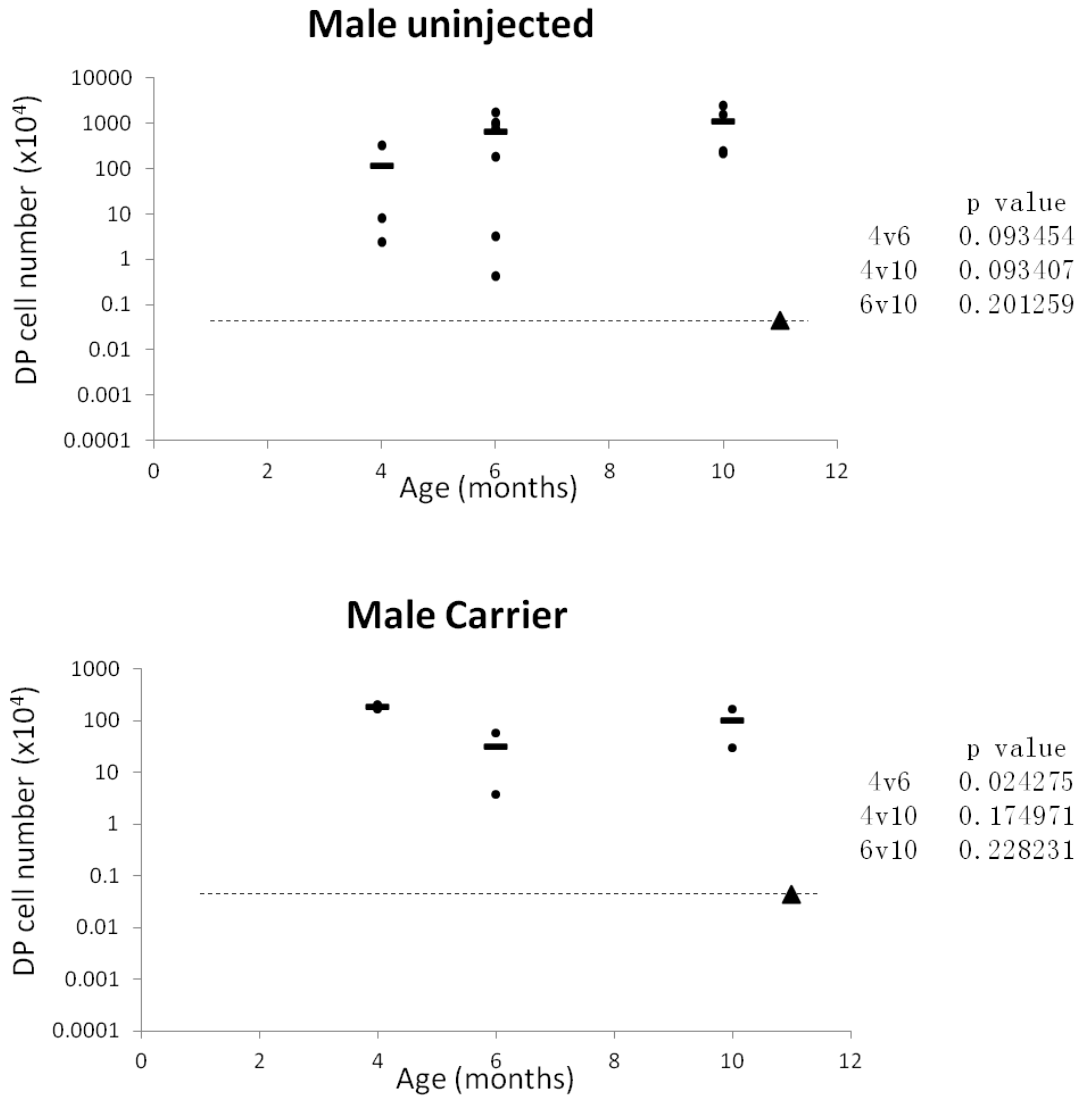

Figure 4.8 Total DP cells within the uninjected and carrier-only injected Male *R/-;CreERt2* mice with age (sample carrying DP cells below the background level were excluded). Data demonstrated same as Figure 4.4 except the mice showing no evidence of recombination of the Foxn1R allele have been excluded from the analysis.

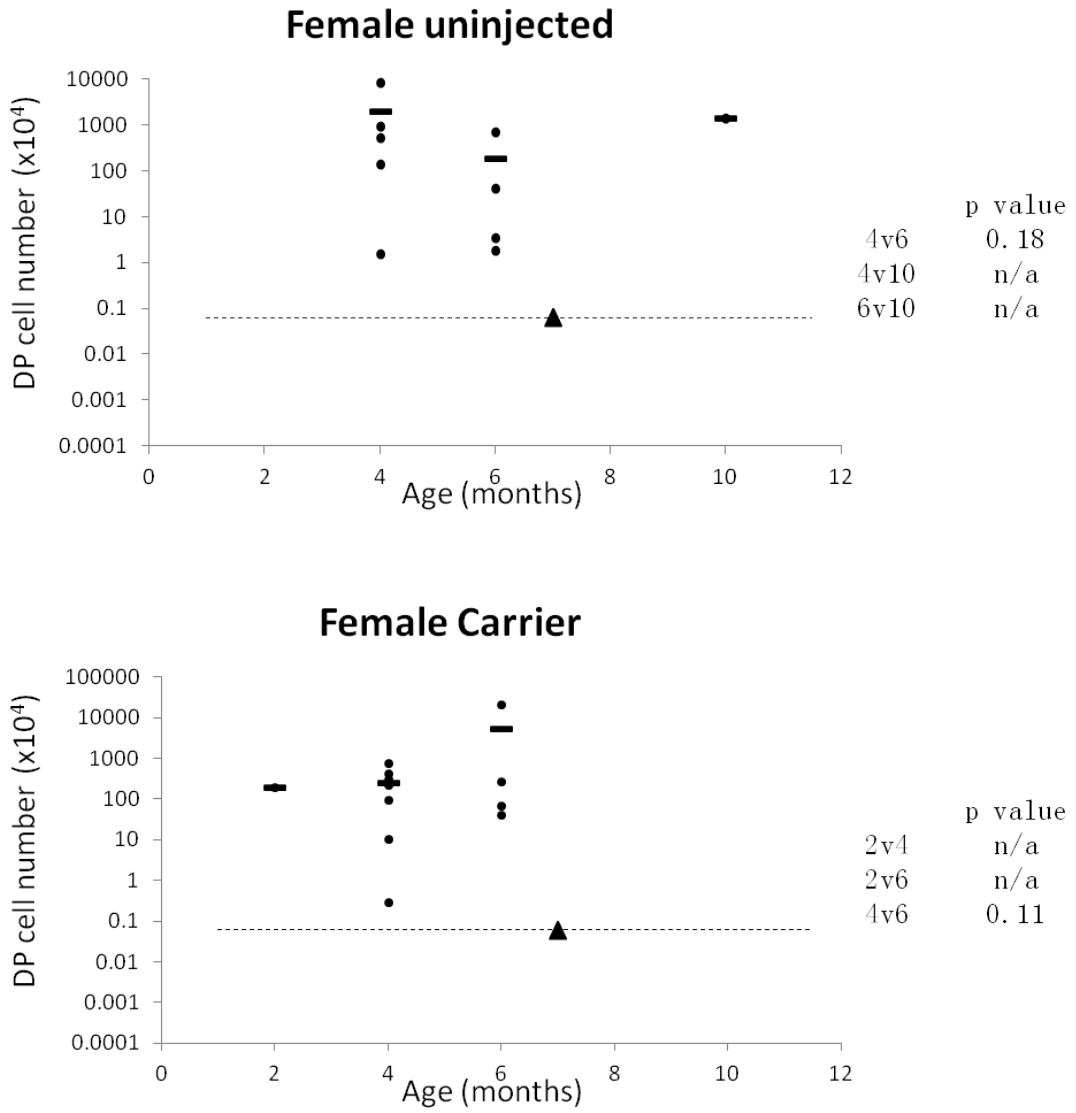

Figure 4.9 Total DP cells within the uninjected and carrier-only injected Female *R/-;CreERt2* mice with age (sample carrying DP cells below the background level were excluded). Data demonstrated same as Figure 4.5 except the mice showing no evidence of recombination of the Foxn1R allele have been excluded from the analysis.

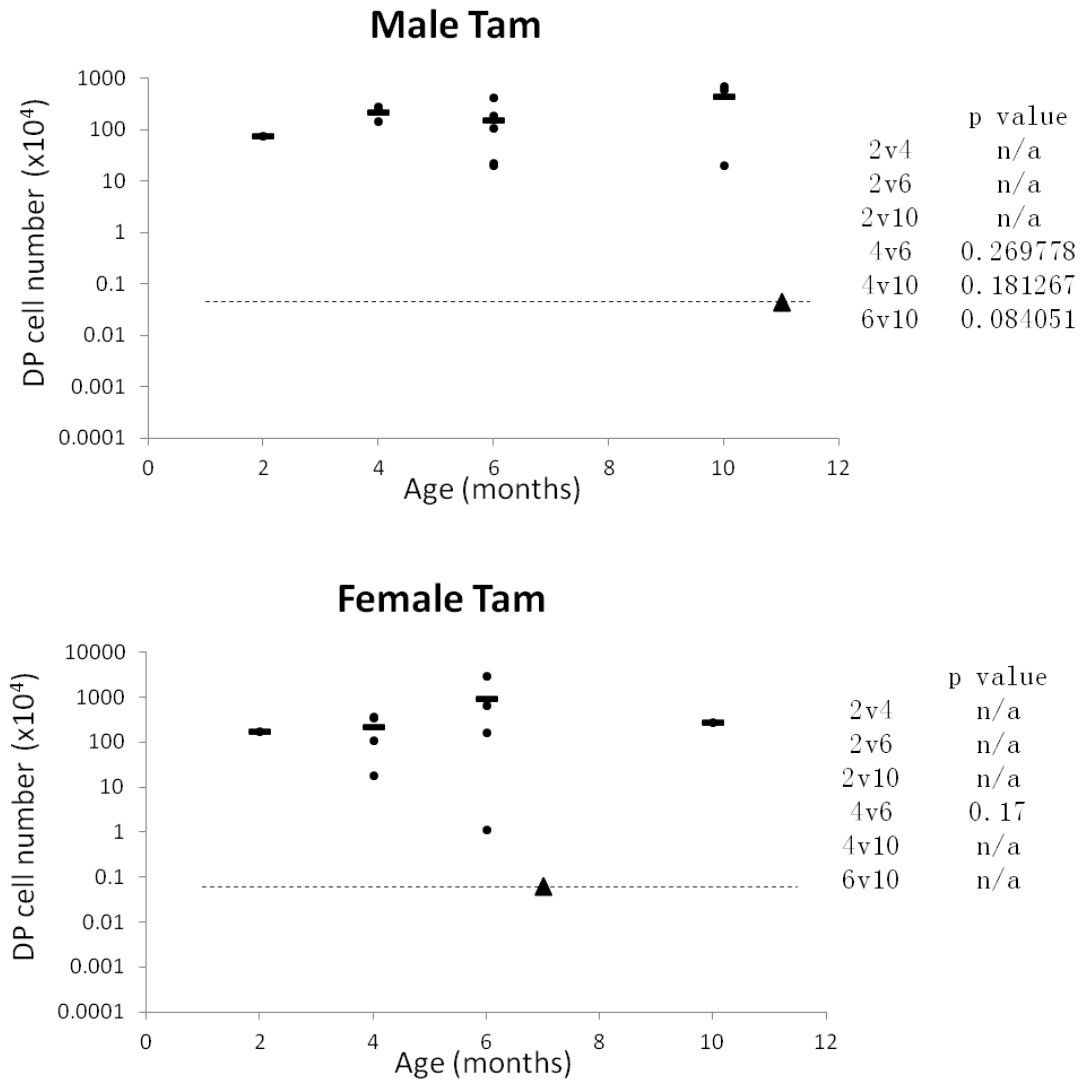

Figure 4.10 Total DP cells within the 4OHT injected *R/-;CreERt2* mice with age. (sample carrying DP cells below the background level were excluded). Data demonstrated same as Figure 4.6 except the mice showing no evidence of recombination of the Foxn1R allele have been excluded from the analysis.

4.2.5 Establishment of a transplantation-based assay for testing progenitor cell persistence within *Foxn1R/-; Rosa26CreERt2* mice

The data presented before suggested that a TEPC pool persisted in aged *R/-;CreERt2* mice. However, we wished to provide direct evidence confirming this conclusion. We also wished to determine the potential of these cells to give rise to both mature cTECs and mTECs. As tamoxifen-independent CreERt2 activity was observed in most if not all *R/-;CreERt2* mice by 6 months old, use of tamoxifen to induce recombination could not be used to unequivocally show that new TECs could be generated from persisting progenitors. Therefore, we chose to establish an assay system to address this issue. This required that un-reactivated progenitor cells could be isolated by flow cytometric cell sorting, allowing the reversion of R allele of these cells to be induced by subsequent 4OHT treatment.

In this section, I first explain the strategy used for development of this assay system. I then validate the assay using a series of control experiments. Finally, I test putative thymic epithelial progenitor cells isolated from *R/-;CreERt2* mice.

4.2.5.1 Experimental Strategy:

4.2.5.1.1 Isolation of putative thymic epithelial progenitor cells from *R/-;CreERt2* mice.

Plet1 marks undifferentiated thymic epithelial progenitor cells in fetal wild type thymi (Bennett, Farley et al. 2002). In the $Foxn1^{R/-}$;$Rosa26^{CreERt2}$ mouse line, in the absence of tamoxifen-mediated recombination, more than fifty percent of TECs were Plet-1 positive (Chapter 3). Furthermore, following 4OHT-induced Cre-mediated recombination, a Plet-1^{+} area was always found adjacent to the area of Plet-1 negative thymus tissue. We therefore hypothesised that, in this model, persisting thymic epithelial progenitor cells would be marked by Plet-1 and thus that Plet-1 could be

used to isolate un-reactivated progenitor cells from *Foxn1*$^{R/nu}$; *Rosa26*^{CreERt2} thymi. A caveat for this approach was that Plet-1 positive cells are also found in the thymic medulla, and these cells if present in a reactivated area would also be purified with the un-reactivated cells. Therefore, the presence of the *R* allele in the sorted cells was used to determine whether and to what extent this occurred.

4.2.5.1.2 Reaggregated Organ Culture combined with Kidney capsule grafting can be used to test thymic epithelial progenitor cell function.

In previous work, our lab has established a protocol for using reaggregate fetal thymic organ culture to test the potency of thymic epithelial progenitor cell (Bennett, Farley et al. 2002; Gordon, Wilson et al. 2004; Sheridan, Taoudi et al. 2009). Briefly, E12.5 – E14.5 thymic lobes from WT embryos are dissected and the whole thymic lobes are then dissociated and used as carrier cells. A defined number of "test" cells are then mixed with these carrier cells and this cell mixture is reaggregated, cultured *in vitro* overnight, and then transplanted under the kidney capsule. As the carrier cell population contains all the developing TECs and naïve T-cells, they offer a strong inductive environment for TEC differentiation.

To develop this system to assay the presence, and potency, of thymic epithelial progenitor cells in aged *Foxn1*$^{R/-}$;*Rosa26*^{CreERt2} mice, the 'test' cell population also required induction with 4OHT. If the test cells have thymic epithelial progenitor cell identity, they should be able to give rise to mature TECs after induction.

4.2.5.1.3 MHC Class II haplotype can be used to identify the test cells within a graft

In order to use this system to test the functional properties of Plet1^{+} TECs from aged *Foxn1*$^{R/-}$;*Rosa26*^{CreERt2} mice, it was also necessary to identify cells of different origins within a mixed graft. The *Foxn1*$^{R/R}$ line was original generated from 129 ES cells and

was then backcrossed onto a C57BL/6 background. This strain was later crossed first with *Foxn1*$^{+/-}$ mice, and then with *Rosa26*^{CreERt2}, both also on a C57BL/6 background, to generate *Foxn1*$^{R/-}$; *Rosa26*^{CreERt2} (*R/-;CreERt2*) mice (Nowell, Bredenkamp et al. 2011)(Chapter 2). The MHC haplotype of both 129 and C57BL/6 mice is b (H-2^{b}). So, in order to be able to distinguish the putative progenitor cells isolated from *R/-;CreERt2* mice from the carrier cells, carrier cells of another haplotype were required. CBA fetal thymus cells were therefore used as carrier cells, as CBA mice are MHC haplotype k (H-2^{k}).

4.2.5.2 Identification of optimized conditions for 4OHT administration to test cells.

Tamoxifen has been used as an oestrogen antagonist to treat the breast cancer for decades. However, adverse effects of tamoxifen, including increasing the risk of endometrial cancer, was also observed (Jordan 2003). CreERt2 activity was also reported to be able to cause direct hematological toxicity and illegitimate chromosomal recombination (Higashi, Ikawa et al. 2009).

My initial data from flow cytometric cell sorting of Plet-1 positive cells from the *R/-;CreERt2* mice suggested that a maximum of 250 Plet-1^{+} cells could be collected from a single *R/;CreERt2* mouse (data not shown). Therefore, given the low cell numbers available, it was important to minimize the possible adverse affects of 4OHT treatment by determining the optimum dose and most appropriate delivery method for 4OHT treatment. The aim was to maximise both cell viability and the efficiency of reactivation of the *Foxn1*^{R} allele in *R/-;CreERt2* thymic epithelial progenitor cells.

I initially tested 2 different methods (named as *Method B* and *Method C*) for delivering tamoxifen. In *Method B* I first made a mixed reaggregate containing both sample cells and carrier cells, then cultured the reaggregate culture in 1uM 4OHT to overnight (O/N), before grafting it under the kidney capsule of CBAxC57BL/6 recipients. In *Method C*, I first grafted the mixed reaggregates containing the test

cells, then treated the grafted mice with tamoxifen in the drinking water continually for 3 weeks, starting at day 2 after grafting. Both methods had previously been used to induce Cre mediated recombination in laboratories in CRM. However, the efficiency of recombination and toxicity effects on low number of cells had not previously been tested.

To determine which of these treatments had the best outcome, I compared them using $EpCAM^{+}$ fetal thymic cells from E12.5 *CBA;C57BL/6* embryos as test cells, as these were not limited in number. In these experiments, the carrier cells used were E13.5 CBA thymus cells. To make the reaggregates, a ratio of 1,000 test cells : 200,000 carrier cells was used. One reaggregate for *Method B*, two for *Method C* and one control reaggregate were analyzed. All of these were successfully grafted into CBAxC57BL/6 F1 recipient mice but after three weeks, grafts were recovered only from the *Method C* graft recipients (c1 and c2).

$H\text{-}2K^{b}$-positive cells were observed on 3 out of 6 slides analysed in graft c1 and 4 out of 11 slides analysed in graft c2 (every 10 slides were checked, 3 sections on each slide). On each slide, several $H\text{-}2K^{b}$ positive area were observed and these co-expressed the epithelial marker PanK (Figure 4.11). Positive and isotype controls were conducted at the same time (Figure 4.14).

Method B was tested using TECs obtained from E12.5 *sGFP;Rosa26*^{CreERt2} embryos (*sGFP;CreERt2*) (Gilchrist, Ure et al. 2003). One small $H\text{-}2K^{b+}$ area was found in each of the resulting grafts (Gb1 and Gb2). These cells also co-expressed PanK, and appeared to contribute well to the $H\text{-}2K^{b}$ TEC network in the grafts on morphological grounds (Figure 4.12).

To determine whether expression of CreERt2 had any toxic effects on the cells, I also tested TECs obtained from E12.5 *sGFP;Rosa26*^{CreERt2} embryos (*sGFP;CreERt2*) using *Method C* (graft Gc1) Consistent with the high viability of cells treated with

Method C, demonstrated via analysis of grafts c1 and c2 (Fiure 4.10), graft Gc1 demonstrated a strong contribution from H-2K^{b+} cells. However, none of these co-expressed PanK. Additionally, they did not appear to contribute to TEC-like structures (Figure 4.13).

The data described above suggested that the test TECs survived within both the *Method B* and *Method C* grafts. However, when *sGFP;Rosa26*^{CreERt2} test TECs were used, the TEC-derived cells in the grafts retained their TEC character and were able to contribute to TEC networks only when *Method B* was used. I therefore chose to use *Method B* for testing of the un-reactivated progenitor cells within aged *R/-;CreERt2* mice.

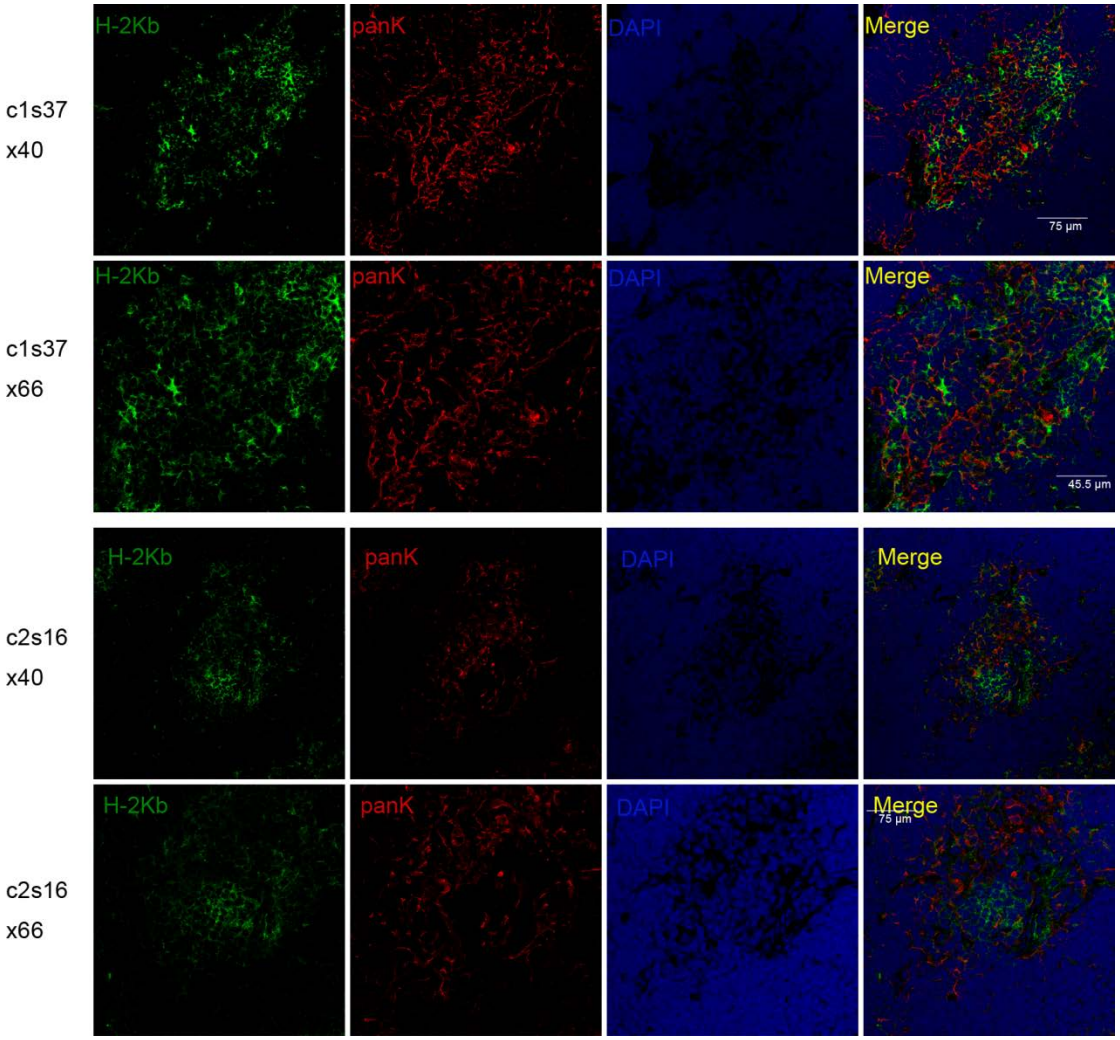

Figure 4.11 H-2K^{b} Staining suggested a contribution of E12.5 *CBA;C57BL/6* thymic epithelial cells to the grafts by using Method C. 1,000 EpCAM^{+} cells from E12.5 *CBA;C57BL/6* fetal thymi (test TECs) were reaggregated with 200,000 dissociated E12.5 CBA fetal thymus cells. Reaggregates were cultured overnight and subsequently transplanted under the kidney capsule of F1 (*CBAxC57BL/6*) mice. 2 days after transplantation, recipient mice were fed with 4OHT water for 3 weeks until grafts were collected. The upper and lower panels are representative of the two grafts recovered after tamoxifen treatment. H-2Kb (green) marks the cells derived from the test TECs. PanK (red) was used as a general epithelial cell marker. Both grafts showed a good contribution of test TECs to the grafts, but these cells did not co-express the epithelial marker panK. Scale bar for x40 is 75 µm; for x66 is 45.5µm.

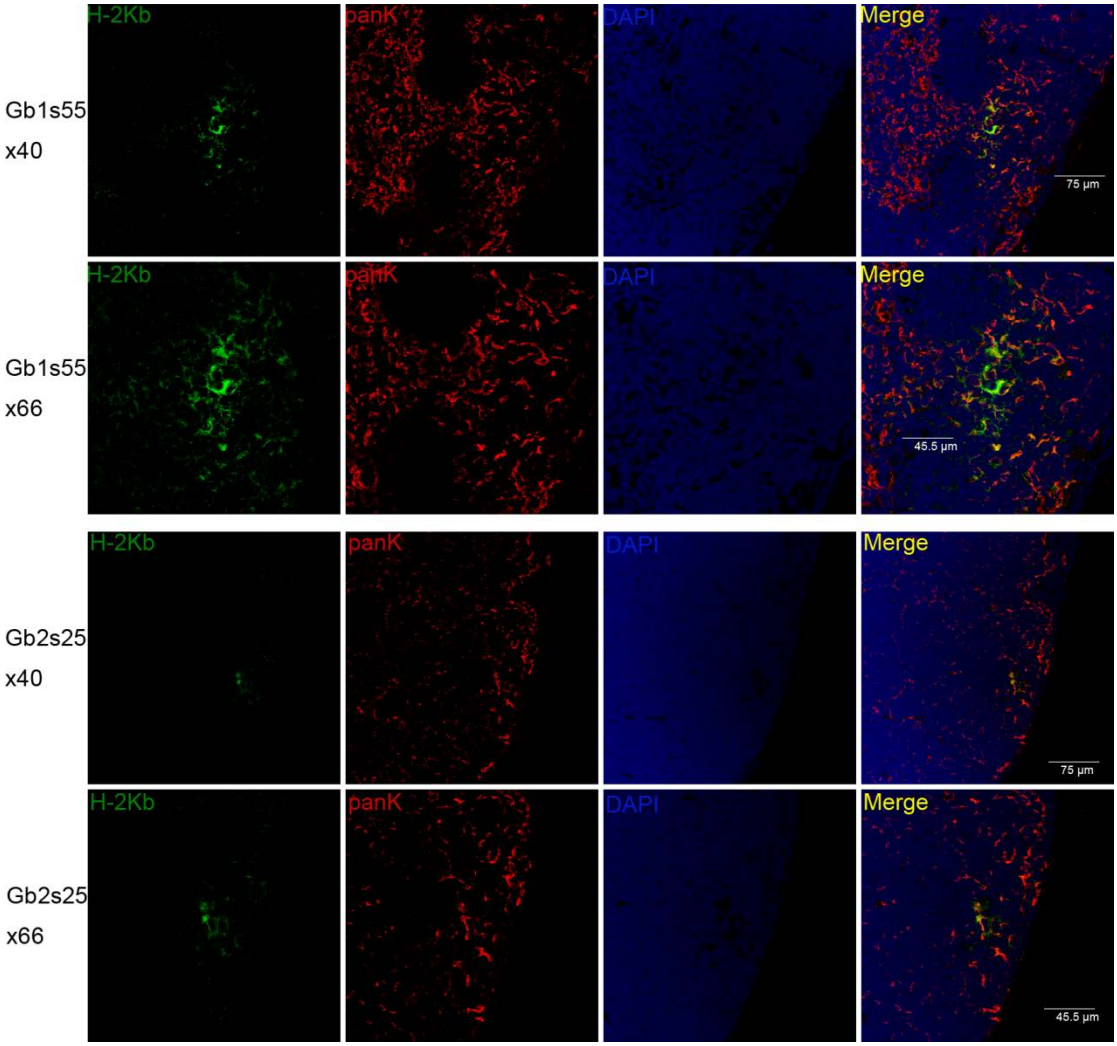

Figure 4.12 H-2K^b Staining demonstrating contribution of E12.5 *sGFP;CreERt2* thymic epithelial cells to grafts generated by *Method B*. 1,000 EpCAM$^+$ cells from the E12.5 *sGFP;CreERt2* fetal thymus (test TECs) were reaggregated with 200,000 dissociated E12.5 CBA fetal thymus cells. Reaggregates were cultured over-night in 1µM 4OHT in reaggregate medium and were then transplanted under the kidney capsule of F1 (*CBAxC57BL/6*) mice. Grafts were recovered and analyzed 3 weeks later. One green area was found in each of the two grafts analysed. Sections were stained for H-2K^b to localize the contribution of the *sGFP;CreERt2* cells. As the silent GFP should be reactivated by 4OHT-induced Cre-mediated recombination, the green signal indicated either a contribution of un-reactivated cells (no GFP) or of reactivated cells (with GFP). Both cases indicated the viability of the test TECs in the grafts generated by *Method B*. Note that all green cells co-express the epithelial cell marker panK (red). Scale bar for x40 is 75 µm; for x66 is 45.5µm.

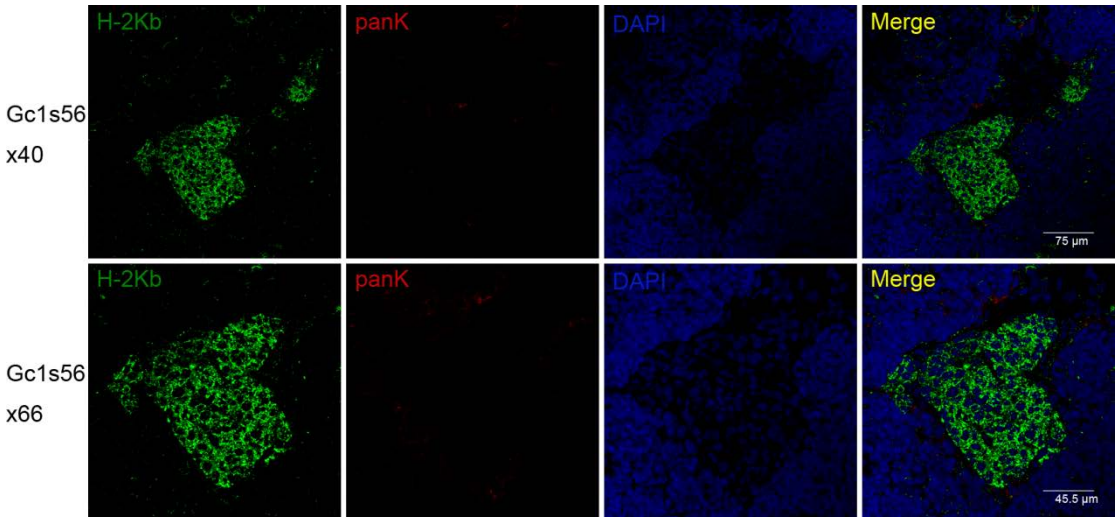

Figure 4.13 H-2K^{b} Staining suggested a contribution of E12.5 *sGFP;CreERt2* thymic epithelial cells to the grafts after treatment with Method C. Samples were prepared as Figure 4.11 described. H-2K^{b+} cells could be detected and indicating the presence of cells derived from the test TECs, but these cells failed to show any epithelial structure. PanK staining was largely absent from the whole graft. Scale bar for x40 is 75 µm; for x66 is 45.5µm.

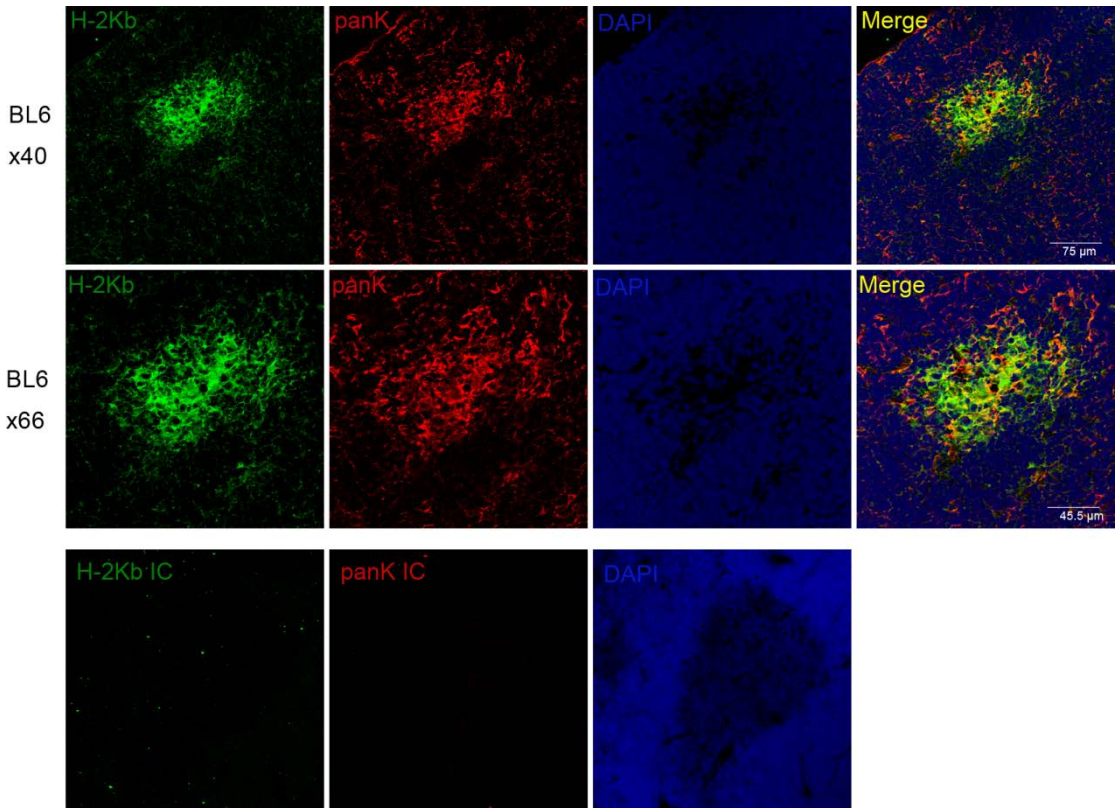

Figure 4.14 Wild type C57B/6 thymus staining profile of H-2K^b and PanK and their isotype controls. A 6 week old male C57BL/6 thymus was used as a positive control for H-2K^b and PanK staining. Staining was conducted at the same time as the samples showed in Figures 4.11-4.13. Isotype controls for both H-2K^b and PanK are shown in the bottom panel. Note the difference in H-2K^b positive signal strength difference between cortical and medullary compartments.

4.2.5.3 Purification of Plet-1^{+}EpCAM^{+} cells from aged *R/-;CreERt2* mice

In order to directly assess whether TEPCs were present in the thymi of aged *R/-;CreERt2* mice, I next isolated putative TEPCs by flow cytometric sorting using Plet1. Thymi were dissected from twelve *R/-;CreERt2* mice, aged from 6 months to 12 months. There were obvious differences in the size and morphology of the thymic rudiments among these mice, even between those of the same age, consistent with spontaneous reversion of the R allele having occurred to different extents in different mice (see sections 4.2.2 and 4.2.4).

The thymi from these mice were independently dissociated, stained and sorted to obtain Plet-1^{+}EpCAM^{+} cells. The number of cells obtained varied widely between the different samples, as described in Table 1. At least 60 cells from each sample were used for genotyping, to determine the presence or absence of cells carrying a reverted *Foxn1*^{R} allele.

To determine whether or not the individual pools of purified cells included cells that had undergone tamoxifen-independent reversion of the *R* allele, PCR analysis of genomic DNA was performed using two primer pairs. The first pair (called T) was designed to detect the SV40Tag cassette in the *Foxn1*^{R} allele (Nowell, Bredenkamp et al. 2011) and was used to detect the unrecombined R allele within the *R/-;CreERt2* cells. The second pair (called GF/GR; Nowell et al 2011) detects the wild-type *Foxn1* allele. Since these primers flank the LoxP site that remains after recombination of the *R* allele, they were used to determine whether cells in which spontaneous reversion had occurred were present in the sample. As GF anneals to the region of Foxn1 65bp upstream of the point of insertion of the R allele, and the GR anneals to the region of Foxn1 225 bp down-stream of the point of insertion of the R allele, if there is no deletion of the loxP-flanked cassette, no product will be generated due to the length (8kb) of the inserted cassette. If cells in which spontaneous reversion had occurred were present, a PCR product of about 470bp would be generated. The null allele in

the *R/-;CreERt2* mice was generated by insertion of a stop cassette into the 3 exon of *Foxn1*(Nehls, Kyewski et al. 1996), down-stream of the GR annealing point. So we would also expect to see a 290bp product corresponding to the null allele in all *R/-;CreERt2* mice. In summary, for the non-recombined *R* allele, we would expect to generate a 611bp T product and a 290bp GF/GR product, but not a 470bp GF/GR product, using these two primer pairs.

The PCR results are shown in Figure 4.15 and Table 4.3. Of the twelve samples of sorted cells, three contained only cells that had not undergone any spontaneous reversion. To achieve a reasonable cell number for making a cellular reaggregate, these samples were pooled and reaggregated with 200,000 dissociated E13.5 CBA fetal thymus cells. A carrier cell-only reaggregate was also made. As described above for *Method B*, these reaggregates were cultured overnight at the present of 1μM 4OHT, and then grafted into two CBAxC57BL/6 recipient male mice.

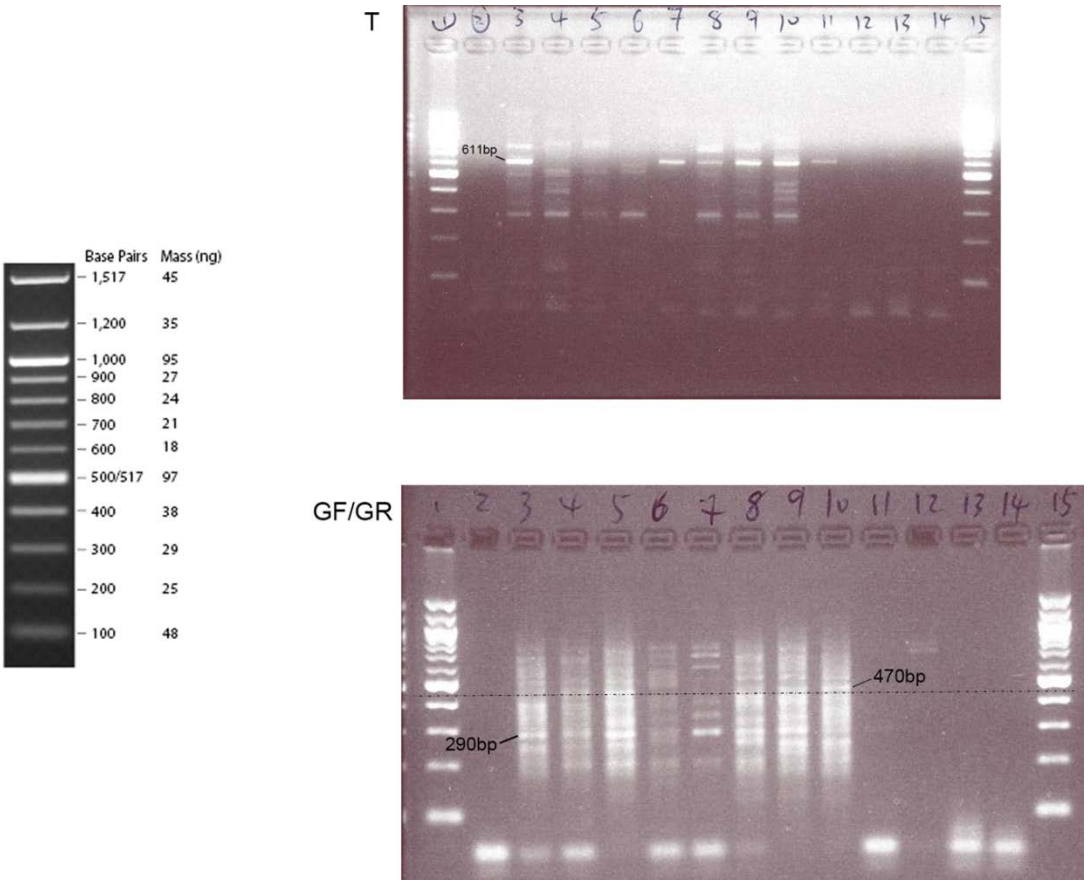

Figure 4.15. **Genotyping result of sorted Plet-1^{+}EpCAM^{+} cells.** 60 cells from each sorted Plet-1^{+}EpCAM^{+} sample were used for genotyping. The left image shows the 100 bp DNA Ladder (BioLabs) used for electrophoresis. The sample numbers match those in Table 4.3. The presence of a 611bp product using the T primers (top right image) indicates the presence of an unrecombined R allele (samples 3, 7, 8, 9, 10 and 11), as does the presence of a 290bp (bottom right image; samples 3, 4, 5, 6, 7, 8, 9, 10 and 11) but not a 470bp GF/GR product (bottom right image; samples 2, 3, 6, 7, 11, 12 and 13).

Lane No.	Sample	Age months	Number of Plet1^{+}EpCAM^{+} cells isolated	Cells taken for genotyping	Sv40Tag (T)	GF/GR (290bp)	GF/GR(470bp) or similar	Chosen for making reaggregate	Cells left after genotyping
1	Ladder								
2	RL3	8	30	All	n	n	n		
3	SQ30	7.5	525	60	++++	y	n	Y	465
4	SQ40	7.5	206	60	n	y	y		
5	UR11	5.5	355	60	n	y	y		
6	UR40	5.8	120	60	n	y	n		
7	UR44	5.8	139	60	++	y	n	Y	79
8	UR31	5.8	269	60	+	y	y		
9	PN10	10	337	60	++	y	y		
10	PN3	10	139	60	+++	y	y		
11	MQ3	12	22	All	+	y	n	Y*	0
12	RL30	8	33	All	n	n	n		
13	UR41	5.8	20	All	n	n	n		
14	H2O								

Table 4.3. Summary of cell numbers and genotyping results for Plet-1^{+}EpCAM^{+} cells isolated from aged *R/-;CreERt* mice.
Sample numbers matche those in the two gel photographs in Figure 4.15. The presence of a 611bp product (samples 3,7,8,9,10 and 11) using the T primers indicates the presence of an unrecombined R allele, as does the presence of a 290bp but not a 470bp GF/GR product (samples 3, 7 and 11).
*: All cells had been used for genotyping, so no cells left for making reaggregates.

4.2.5.4 Graft result

The two recipient mice were sacrificed 1 month after grafting. No grafts were found on the kidneys of either mouse. The entire kidneys were sectioned and analysed, but, no TEC-like tissue was observed (not shown). It seems likely that this experiment failed for technical reasons. (For example, dissociated cells were exposed to sub-optimal conditions (on ice) for too long because the experiment procedures took a long time and reaggregates were only grown for 6 hours before transplanting them to the kidney and this was probably insufficient time).

4.4 Discussion

The work described in this chapter first demonstrates the occurrence of tamoxifen-independent Cre-mediated recombination in *R/-;CreERt2* mice. Within an individual mouse, the detection of multiple 'reactivated' regions containing different sized foci of thymus tissue suggested the occurrence of multiple tamoxifen-independent recombination events over time. Analysis of groups of *R/-;CreERt2* of different ages then provided evidence for accumulation of tamoxifen-independent recombination events with age, and suggested that a thymic epithelial progenitor cell pool existed until at least 6 months old. I analyzed the effect of age-related thymic involution phenomenon on the number of intrathymic DP cells. Interestingly, I found no decrease in DP cell numbers over the life span within the *R/-;CreERt2* thymi generated by tamoxifen-independent recombination, further suggesting the existence of a functional thymic epithelial progenitor cell pool.

Due to technical limitations, I was not able to monitor the changes occurring within the thymus of each individual mouse over time. Therefore, our analyses relied on statistical analysis of a sample group; the accuracy of the data would be improved if the size of the sample group was increased.

It is not clear why no tamoxifen-independent Cre-mediated recombination was observed in our initial experiments (Chapter 3), but this was observed at in later experiments. It is possible that we inadvertently selected a sub-strain of Rosa26CreERt2 mice in which tamoxifen-independent Cre-mediated recombination occurred more frequently than in the original strains. However, an important issue that should also be addressed is whether the dosage of the *Rosa*^{CreERt2} allele affects the rate of tamoxifen-independent Cre-mediated recombination. The method used in our lab for genotyping this strain did not distinguish heterozygotes and homozygotes for*Rosa*^{CreERt2}, and thus our sample group may contained both zygosities. This may explain why a range of phenotypes was seen within each age-group (see e.g. male uninjected, Figure 4.5). To address this issue, further analysis using mice in which homozygotes and heterozygotes at Rosa26CreERt2 were identified would be necessary; this was not performed due to cost and time considerations. Despite this, samples analyzed here still suggested that a thymic epithelial progenitor cell pool existed until between 6 and 10 months old.

The data presented in 4.2.5 *"Establishment of a transplantation-based assay for testing progenitor cell persistence within Foxn1R/-; Rosa26CreERt2 mice"* section demonstrate that through an overnight 4OHT treatment, TEPCs could survive in such low cell number (1000 per reaggregate).

They also demonstrate that Plet-1^{+} cells that show no evidence of tamoxifen-independent recombination were present within *R/-;CreERt2* thymi up to 12 months old. This is consistent with data presented in 4.2.2 and 4.2.4, which suggest generation of new thymic epithelial cells following tamoxifen-independent recombination of the R allele in aged *R/-;CreERt2* mice. Unfortunately, however, the attempt to provide direct evidence to support the presence of functional TEPCs in aged *R/-;CreERt2* mice, and to determine the progenitor-progeny relationships, failed

for technical reasons.

Due to the relatively low number of collected Plet-1^+ cells within the aged *R/-;CreERt2* mice, an *in vivo* assay method would be preferable, as this would minimize the loss of cells during the *in vitro* procedures. For example, BrdU injection could be used after 4OHT injection. If there is a progenitor cell pool persisting within the aged *R/-;CreERt2* mice, that can give rise to new TECs when the *Foxn1*^{R} allele is reverted, we would expect to see cluster of $BrdU^+$ mature TECs, distinct from pre-generated mature TECs, which are likely to be BrdU-negative. It is possible that the pre-generated TECs might continue to proliferate and cells generated by these TECs would also be BrdU positive. However, we expect this proliferation to be at a much lower level compared to the proliferation of progenitor cells when they give rise to mature TECs, especially within an old thymus. A series of control experiments should be conducted to investigate this. The proliferation marker Ki-67 could also be used here, but again an appropriate control group is needed to distinguish the different origins of newly generated TECs.

Chapter 5: Investigation of the potential for deriving TEPCs/TECs from Embryonic Stem Cells.

5.1 Introduction

A major aim of this work was to derive thymic epithelial cells from mouse embryonic stem (ES) cells. ES cells are derived from the inner cell mass of the preimplantion embryo at the blastocyst stage of development and hold the potential to differentiate into all three primary germ layers and all subsequent cell types derived from them. The epithelial component of the thymus has a single origin in development, and is derived from the third pharyngeal pouch endoderm (Chapter 1). Therefore, to obtain thymic epithelial cells or thymic epithelial progenitor cells from ES cells, the first step should be to differentiate the ES cells into definitive endoderm cells, specifically into foregut endoderm cells from which the third pharyngeal pouch is derived.

Definitive endoderm (DE) induction can be achieved through formation of 3-dimensional embryoid bodies (EB) in the presence of an appropriate exogenous stimulus, such as Activin A. The use of this approach for giving rise to DE derivative cell-types, such as hepatic cells, has been demonstrated (Kubo, Shinozaki et al. 2004; Gouon-Evans, Boussemart et al. 2006) (also see Chapter 1). However, the potential for using ES cells through EB formation for deriving TEC related cells from ES cells has been rarely reported.

Previous work in this laboratory showed that genes related to primitive streak formation and definitive endoderm formation can be detected by RT-PCR in EBs formed spontaneously by the hanging-drop method (Chapter 2) for hanging drop

method (T. Gaskell and C. Blackburn, unpublished). *Foxn1*, a TEC and skin lineage specific gene (Nehls, Pfeifer et al. 1994) was also detected although at low-level and at later stage (Figure 5.1 IIE). Further co-culturing of EBs with E12.5 thymic lobes was demonstrated to increase Foxn1 expression to levels detectable by reporter assay (A. Farley and C. Blackburn, unpublished). A Foxn1-LacZ reporter ES cell line (Nehls, Kyewski et al. 1996) was used in these experiments. When Foxn1-LacZ EBs at day 7 after EB formation were co-cultured with E12.5 fetal thymic lobes, β-galactosidase^{+} cells could be found on day 11, while EB-only or fetal thymic lobe-only controls showed very few or no β-galactosidase^{+} cells (A. Farley and C. Blackburn, unpublished). Further *in situ* staining showed that most of the cells expressing *Foxn1* also expressed *Pax1* (A. Farley and C. Blackburn, unpublished), therefore suggesting a primary TEC lineage character rather than a skin lineage character (Figure 5.1). This study provided the first evidence to show that spontaneously formed EBs can be induced to form TEC-like cells, and thus demonstrated the possibility for using ES cells to generate the TEC lineage.

In this chapter, I will first demonstrate that Foxn1-expressing cells can be generated in EBs made from Foxn1-LacZ reporter ES cells through two different co-culture methods, and that a method has been established for sorting LacZ expressing cells. Second, through testing of existing and modified protocols for generating anterior definitive endoderm in EBs, I will demonstrate that the TEPC-related genes and cell surface markers can be induced, thus establishing the possibility of using ES cells to derive TEPCs/TECs.

I.

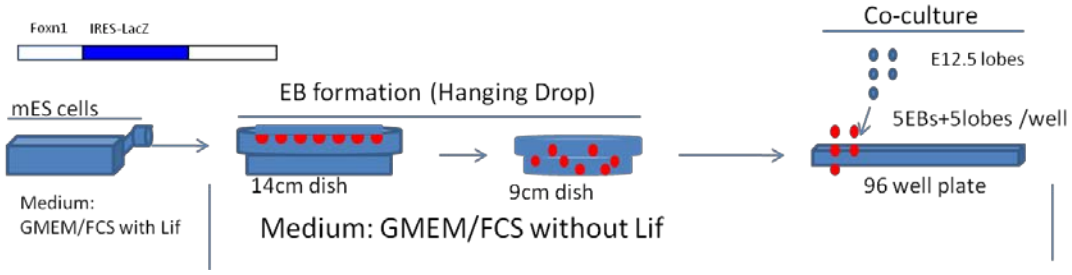

II.

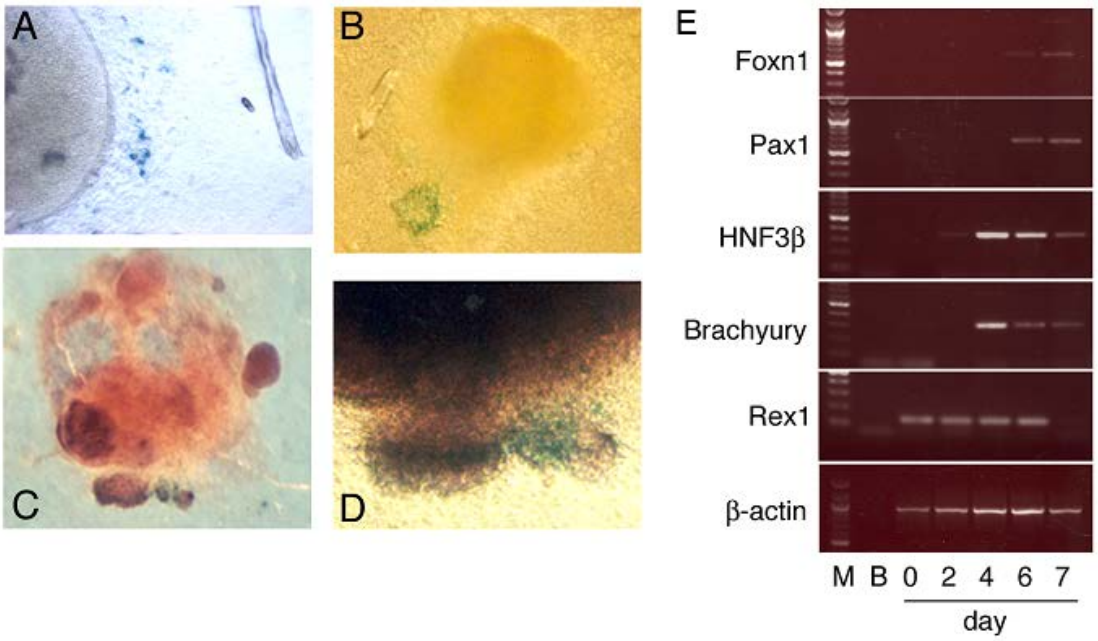

Figure 5.1. ES cells give rise to Foxn1+/Pax1+ cells when co-cultured with fetal thymic lobes. I. Diagram showing co-culture protocol. **II.** After 7 days of EB formation culture, EBs derived from the Foxn1-LacZ ES cells were co-cultured with the E12.5 fetal thymic lobes for a further 3 days. β-galactosidase^{+} activity was tested through X-gal staining (A-D). EBs were then hybridised with a DIG-labelled antisense Pax1 probe followed by an alkaline phosphatase-coupled anti-DIG antibody. Pax1 expression is revealed by BM-purple staining (C-D). D) shows detail from box in C); blue cells are present throughout this Pax1-positive outgrowth. In all EBs examined, most β-galactosidase^{+} cells were also Pax1-positive. (n>=3) E) Gene expression profile during 7 days EB formation culture (n>=3). (A. Farley and T. Gaskell and C. Blackburn, Centre for Regenerative Medicine, University of Edinburgh, unpublished).

5.2 Results

5.2.1 Foxn1 positive cells can be induced using an embryoid body plus fetal thymic lobe co-culture system.

I first repeated the EB plus fetal thymic lobe (FTL) co-culture experiments described in the introduction, using the same Foxn1-LacZ reporter cell line. Thus, EBs formed through a hanging drop method on day 7 were co-cultured with dissected C57BL/6 x CBA E12.5 thymic lobes at a ratio of 5 to 5 per well of a 96 well-plate. EBs only (5 per well) and thymic lobes only (5 per well) were also cultured as controls. EB culture medium (GMEM/FCS without LIF) was used for both EB formation and co-culture (as in Figure 5.1 I). After 8 days, cells were fixed and stained with X-gal. Undifferentiated OKO ES cells, an Oct-4-LacZ reporter ES cell line derived from E14 (Mountford, Zevnik et al. 1994) were used as a positive control for X-gal staining. As expected, OKO cells were β-galactosidase^{+}, but with a variety of levels of staining intensity. That was consistent with Oct4 expression by all ES cells (Chambers, Silva et al. 2007) (Figure 3.2). Almost no blue cells were observed within the fetal thymic lobes only wells or the wild type E14tg2a EBs only wells. A considerable number of blue cells were observed in the Foxn1-LacZ EBs plus fetal thymic lobes co-cultures (Figure 5.2B), suggesting that these ES cells were expressing Foxn1. Surprisingly, there were also some β-galactosidase^{+} cells within the Foxn1-LacZ EBs only samples (Figure 5.2B). This suggested that the Foxn1 expression detected here might due to the spontaneous differentiation of EBs.

These data, together with the data shown in Figure 5.1 established that β-galactosidase, reporting Foxn1 expression, could be detected both in the presence or absence of fetal thymic lobes, thus indicated the possibility of deriving TECs from ES cells using this and other protocols. *In vivo*, X-gal staining in the Foxn1-LacZ reporter mouse is only detected when Foxn1 is expressed at functionally relevant

levels, suggesting that such levels were also achieved here.

5.2.2 Isolation of viable β-galactosidase^{+} cells by flow cytometry.

In order to establish a protocol for analysis of the putative TECs derived from Foxn1-LacZ ES cells, we tested the whether a *fluorescein-di-β-D-galactopyranoside* (FDG) staining protocol could be used to collect the *Foxn1* expressing cells. FDG is a fluorogenic substrate of β-galactosidase and that permits vital staining of cells with LacZ expression.

More than 93% of undifferentiated OKO cells were positive for FDG staining (Figure 5.3), consistent with the known Oct-4 expression profile and the X-gal staining shown in Figure 5.2.A. Few cells within the undifferentiated E14tg2a and Foxn1LacZ ES cells were FDG positive, indicated a background for FDG staining (Figure 5.3). PI staining indicated a high viability (>90%) within all test samples (Figure 5.3). Collectively, this suggested that FDG staining could be used to isolate the β-galactosidase^{+} cells while maintaining cell viability.

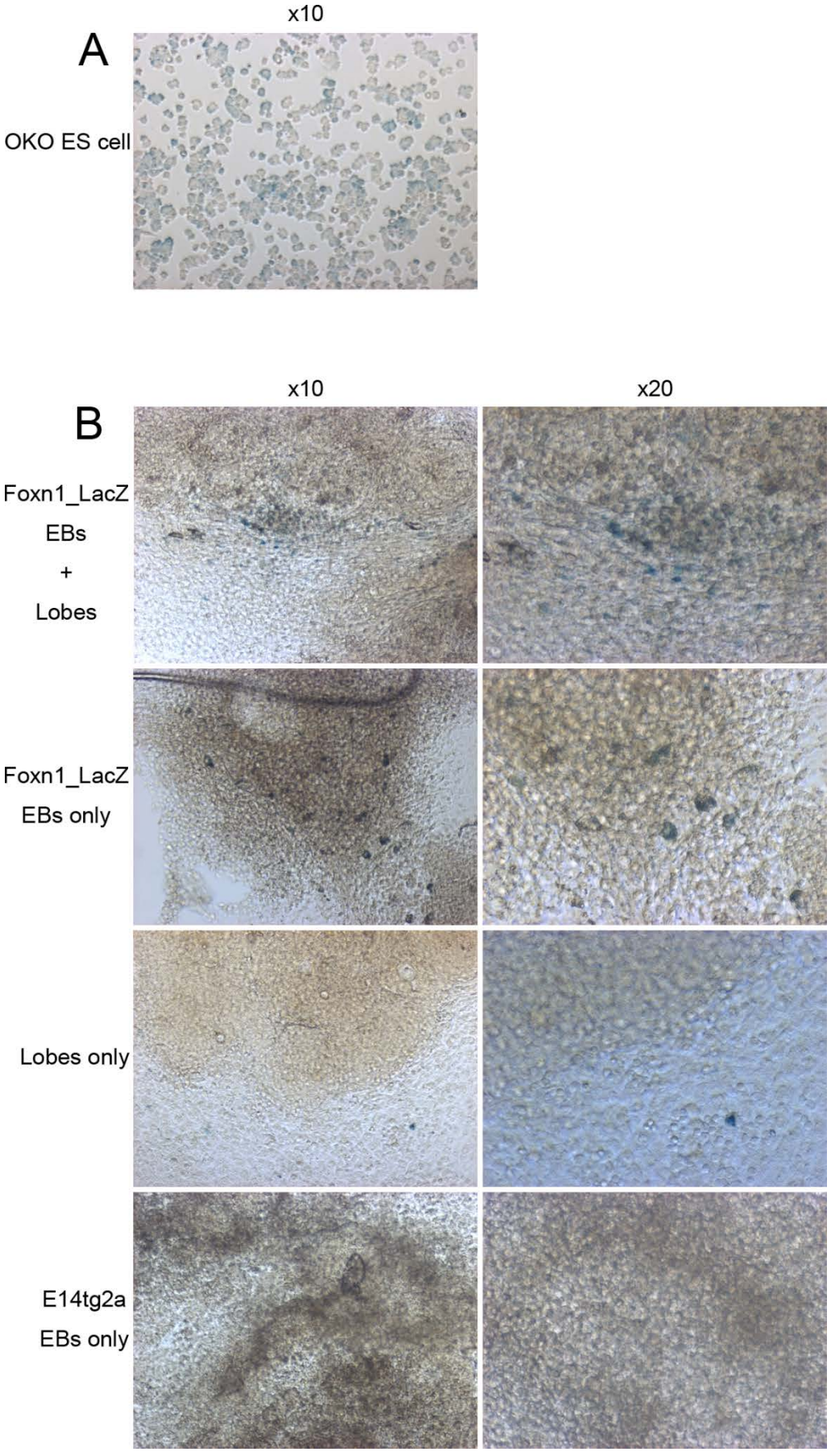
x10
A
OKO ES cell
x10
x20
B
Foxn1_LacZ
EBs
+
Lobes
Foxn1_LacZ
EBs only
Lobes only
E14tg2a
EBs only

Figure 5.2. LacZ expression can be detected in Foxn1-LacZ EBs. (A) Undifferentiated OKO ES cells. (B) Foxn1LacZ ES cell-derived EBs were co-cultured with E12.5 CBA x C57B/6 fetal thymic lobes. Controls were Foxn1LacZ EBs only, Lobes-only and E14tg2a EBs only. Blue cells were found within Foxn1LacZ-derived EBs plus lobes co-cultures and were also present in Foxn1LacZ-derived EBs-only cultures, but not in E124tg2a-derived EBs-only cultures. The single blue cell in lobes-only cultures might be a non-specific signal generated by endogenous lysosomal β-galactosidase.

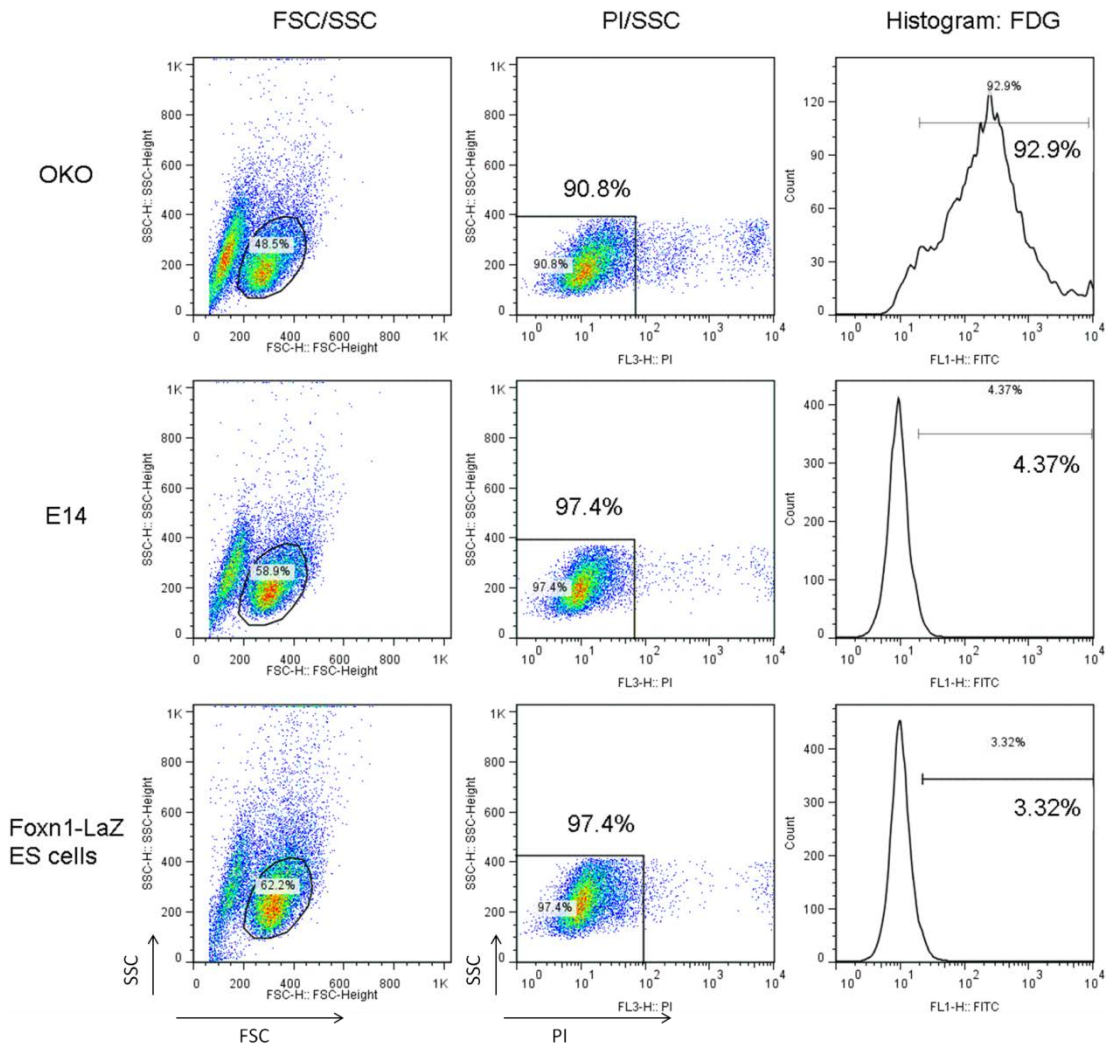

Figure 5.3: ß-galactosidase expression in live, undifferentiated ES cells can be detected by flow cytometry using FDG staining. FDG staining was conducted on the undifferentiated wild type mouse ES cell line **E14tg2a**, and two undifferentiated ß-galactosidase reporter ES cell lines: **OKO** (reporting Oct4 expression) and **Foxn1-LacZ** (reporting Foxn1 expression). An inhibition of lysosomal β-galactosidase using a chloroquine procedure was conducted prior to FDG staining, to exclude non-specific staining. The profiles shown here were first gated for cells (**FSC/SSC**), and then gated on live cells by excluding PI^+ cells (**PI/SSC**). The FDG positive regions were established using untreated/unstained cells for each individual cell line (**Histogram: FDG)**. Data represent at least 3 repeats.

5.2.3 Induction of Foxn1 positive cells in compact reaggregate organ culture of dissociated EB and fetal thymic lobe cells.

As described above, Foxn1^{+} cells can be generated via EB formation and EB plus FTL co-culture. However, based on the frequency of cells observed upon X-gal staining, the efficiency of inducing Foxn1^{+} cells is very low. In the co-culture system, the fetal thymic lobes and EBs were cultured in 96 well-plates, as the limited culture media volume used was thought to increase the induction efficiency of fetal thymic lobes, either through secreted factors or through direct cell to cell contact. Unpublished data from this laboratory also suggested that the Foxn1^{+} cells were most likely to appear at the confluence of the EBs and fetal thymic lobes. However, the capsule surrounding the fetal thymic lobes, and the compact structure of EBs, may significantly block cell:cell communication.

Cellular reaggregation was used to identify the Plet-1^{+} epithelial cells in E12.5 third pharyngeal pouch as thymic epithelial progenitor cells (Bennett, Farley et al. 2002). The fetal thymic cells reaggregated with the progenitor cell candidates were believed to offer important stimuli for thymic epithelial progenitor cell differentiation and TEC maturation. Recently, a compaction reaggregation organ culture (CoROC) has been devised in this lab (Sheridan, Taoudi et al. 2009), in which the reaggregated cells can be cultured on filter paper raft floating on the surface of culture medium. Such reaggregates can be cultured in vitro and tested directly without need for in vivo grafting.

Therefore I next used the compact reaggregate organ culture method described above to test whether Foxn1 expression could be induced more efficiently in comparison with the previous co-culture system. Foxn1-LacZ EBs were cultured until day 7 and

then dissociated whole E12.5 fetal thymic lobes (which contain epithelial, mesencymal and haematopoietic cells) were also dissociated. 40,000 Foxn1-LacZ EB cells and 400,000 FTL cells were used to make each reaggregate. Reaggregates were subsequently cultured on a floating polycarbonate filter paper raft (Millipore) on GMEM/FCS medium without LIF for 9 days. Flow cytometry analysis after FDG staining indicated that although there was substantial cell death, a small subpopulation of viable cells (1.36%) was FDG positive, suggesting that Foxn1 expression had been induced.

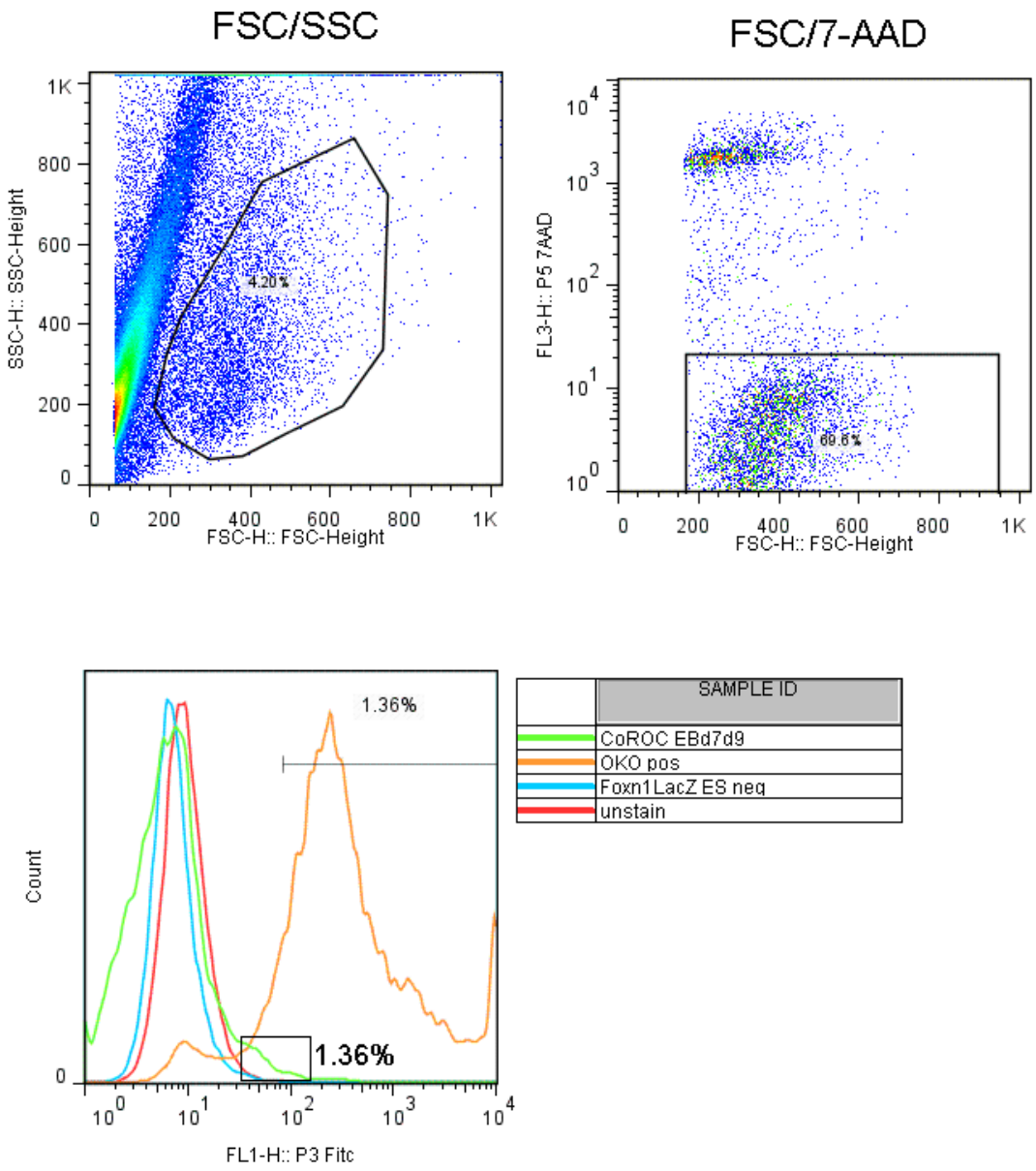

Figure 5.4 Detection of Foxn1 expression within CoROC system through FDG vital staining of Foxn1-LacZ cells. Reaggregates were generated as described in the text were dissociated and stained by FDG. Cells were first gated for cells (**FSC/SSC**) and dead cells were then gated out through on the basis of 7-AAD staining (**7-AAD/SSC**). Unstained E14tg2a ES cells (red line) provided the negative control. Undifferentiated OKO ES cells (orange line) and undifferentiated Foxn1-LacZ ES cells (blue line) provided the positive control and background control, respectively. A small population of FDG^{lo} cells was present specifically in the Foxn1-LacZ CoROC cells, indicating induction of Foxn1 expression. n=1.

5.2.4 Expression of TEPC related genes and cell surface markers during Activin A induced EB differentiation to anterior definitive endoderm.

Both of the two FTL-co-culture methods described above led to generation of Foxn1 expressing cells at a low efficiency. This might largely due to heterogeneity within the spontaneously formed EBs. Therefore, I investigated whether generation of EBS under conditions that enrich for induction of anterior definitive endoderm (ADE) cells might improve the outcome of the co-culture experiments.

Two different EB to ADE differentiation cultures were tested using wild-type E14tg2a ES cells and a novel reporter line “Plet1-GFP” in which GFP is knocked in to the Plet-1 locus (T. Gaskell and C. Blackburn, unpublished). On day 7 in both protocols, the differentiated EBs were very large. These EBS were partially dissociated using Collagenase/Dispase and the cells released by this treatment were collected. These cells are marked as “outer cells” in Q-RT-PCR result and “outer” in FACS profile. The EBs were then further treated with trypsin to complete the dissociated and these remaining cells were collected. These cells are marked as “inner cells” for Q-PCR and “inner” for FACS.

I first tested a previously published protocol for ADE induction in EBs (Morrison, Oikonomopoulou et al. 2008). ES cells were cultured on un-coated dishes in GMEM/FCS media, to allow spontaneous EB formation for two days. From day 2 to day 7, they were cultured in N2B27, Activin A and EGF. As GMEM were used for the first two days, this protocol was named “G”. Cells on day 4 and day 7 were collected and analyzed by Q-RT-PCR and flow cytometry. In both cell lines tested, the pluripotency marker *Oct4* (Ying, Nichols et al. 2003)was down-regulated and almost undetectable on day 7. *Sox17*, the definitive endoderm (DE) and anterior

visceral endoderm (AVE) marker (Yasunaga, Tada et al. 2005), was induced by day 4 and decreased at later stages. *Hex*, a marker for anterior character during ES to ADE differentiation (Morrison, Oikonomopoulou et al. 2008), was also expressed, and, in contrast to *Sox17*, its expression increased at later stages of culture. *Plet-1* expression was detectable in the ES cells by Q-RT-PCR. An obvious increase in expression was detected during the EBs differentiation. Plet-1 expression on day 7 was also confirmed by flow cytometric analysis (Figure 5.5 and 5.6).

The second protocol used was a modified, serum-free, medium defined culture system developed for these experiments (see Chapter 2). Here, dissociated ES cells were cultured on un-coated dishes in N2B27, BMP4 and Activin A to allow EB formation. From day 2 to day 7, they were cultured in SF5 base medium (see Chapter 2), EGF, Activin A and FGF4. As N2B27 was used for the first two days, this protocol was named "N". Cells on day 4 and day 7 were analyzed as above. *Oct4* and *Sox17* showed a similar profile to that observed for the "G" protocol, while *Hex* was first up-regulated earlier and then down-regulated at later stage. Plet-1 expression was also detected at day 7 by Q-RT-PCR and flow cytometric analysis (Figure 5.5 and 5.6).

This confirmed that the Activin A based induction led to ADE differentiation in EBs, as expected, and that the TEPC related marker, such as *Plet-1* could be detected in cells generated via this protocol.

Figure 5.5

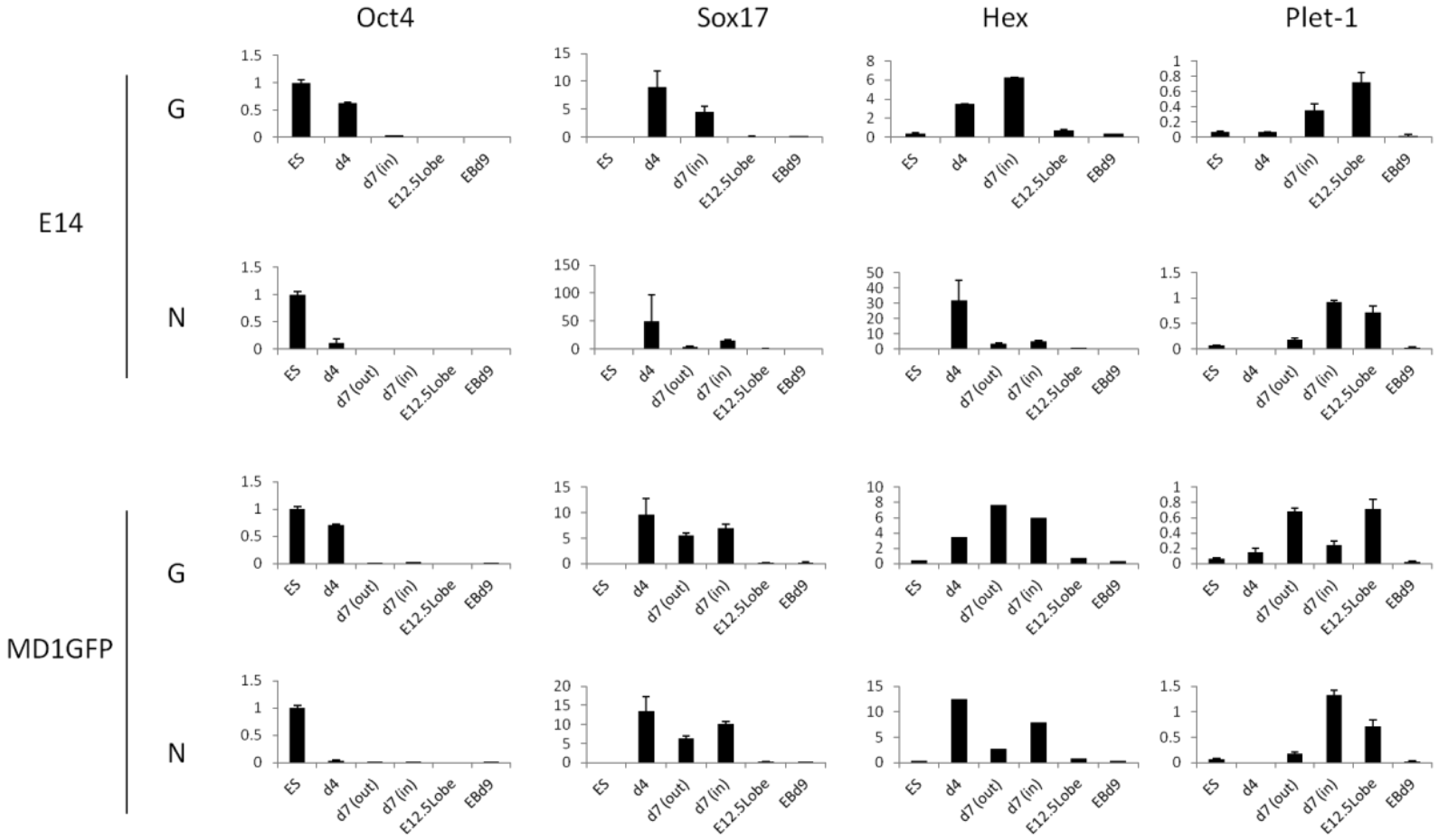
Oct4
Sox17
Hex
Plet-1
E14
MD1GFP
G
N
ES
d4
d7 (out)
d7 (in)
E12.5Lobe
EBd9

Figure 5.5 Gene expression profile in cells generated via two different EBs to ADE differentiation protocols for two independent ES cell lines. E14 and Plet-1-GFP reporter (**MD1GFP)** ES cell lines were used to test two different EBs to ADE differentiation protocols: protocol **G** and protocol **N**, as described in Chapter 2. Undifferentiated ES cells (first column in each data set), E12.5 thymic lobes, and classical day 9 spontaneously differentiated EBs (as used in the co-cultures) (last two columns in each graph) were used as controls. On day 7, cells first dissociated from EBs by Collagenase/Dispase are marked as “day 7 (out)”, cells dissociated from EBs in the following trypsin treatment are marked as “day 7 (in)”. Error bars are based on technical repeats. n=1 biological repeat for each cell line.

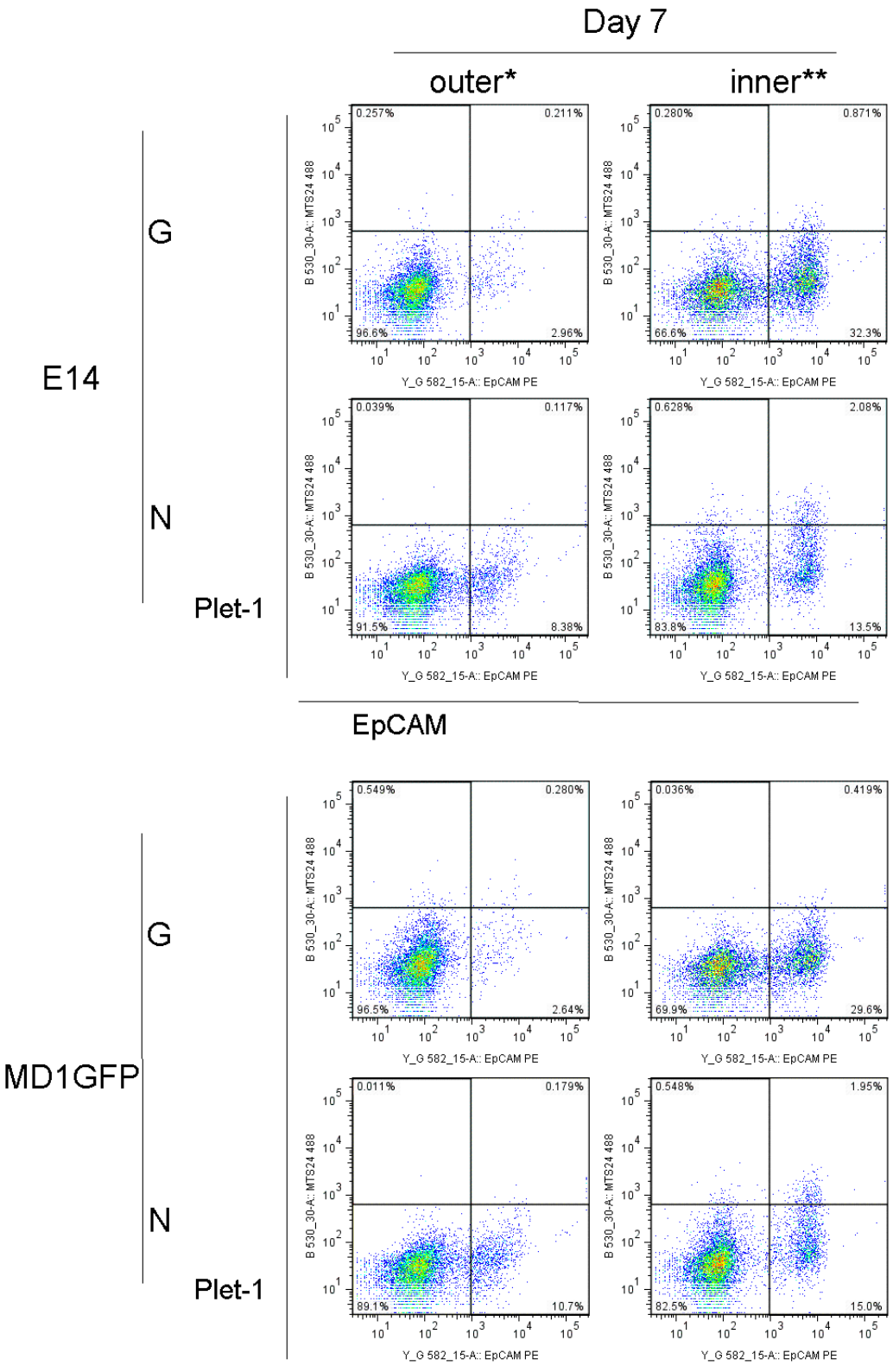

*: Cells dissociated after Collagenase/Dispase
**: Cells need further Typsin treatment to be dissociated after the Collagenase/Dispase treatment

Figure 5.6 Plet-1 can be detected at day 7 in cells generated using both EBs to

ADE differentiation protocols. E14 and Plet-1-GFP reporter (**MD1GFP**) ES cell lines were used to test two different EBs to ADE differentiation protocols, **G** and **N**. Expression of the epithelial marker EpCAM and TEPC marker Plet-1 was analysed on day 7 by flow cytometry. Cells first dissociated from EBs by Collagenase/Dispase are marked as “outer”, cells dissociated from EBs in the following trypsin treatment are marked as “inner”. Quadrants are set based on FMO controls. n=1 for each cell line.

5.3 Discussion:

Both the previous work in this laboratory and that presented here demonstrates that Foxn1 expression can be induced in ES cell-derived cells, through co-culture of EBs and FTLs. Furthermore, using 2 different EBs to ADE protocols, Plet-1 was found to be induced. Collectively, this suggested the possibility for using ES cells to derive TEPCs/TECs through induced EBs formation. The next step would be more detailed characterization of gene expression, modification of existing protocols to increase the TEPC related genes expression, such as *Plet-1*, and linking of FTL induction affect on final *Foxn1* expression.

However, due to the time limitations and the heterogeneous character of EBs, I moved to a more specific step-wise monolayer differentiation method which is described in Chapter 6. Issues that are relevant to both chapters 5 and 6 are included in the Discussion of chapter 6 (section 6.3).

Chapter 6 Investigation of the use of a monolayer protocol for anterior definitive endoderm induction from ES cells for generating TEPCs

6.1 Introduction

The EBs plus FTLs co-culture strategy to induce ES cells to TEPCs described in Chapter 5 resulted in generation of TE lineage cells at low efficiency. EB formation leads to generation of cells from all three germ layers at the beginning of ES cell differentiation (Smith 2001), which may lower the efficiency for generating the derivatives of a specific germ layer, and furthermore, the three-dimensional interactions within EBs make this approach hard to control. Therefore, we wished to attempt to generate TEPCs under more defined conditions.

Our collaborators Gillian Morrison and Austin Smith (University of Cambridge) have derived a new monolayer method for efficiently differentiating ES cells that have previously been cultured in 2i medium (Ying, Wray et al. 2008) into anterior definitive endoderm cells. 2i medium-cultured ES cells are anticipated to give a higher output of a particular target cell population due to their homogeneity compared to ES cells grown in GMEM/FCS plus LIF (Chapter 1). Use of completely defined conditions should also improve consistency between experiments. I therefore tested this new anterior definitive endoderm differentiation protocol (2i ADE), with the expectation of using it as the first step for deriving TEPCs/TECs from ES cells.

6.2 Results

6.2.1 Morphological changes during 2i ADE differentiation

To differentiate ES cells to ADE, cells grown in 2i medium (Ying, Wray et al. 2008)were first taken into N2B27 medium supplemented with CHIRON 99021 (inhibitor of glycogen synthase kinase-3), Activin A, FGF4, Heparin and PI-103 (inhibitor of Phosphatidylinositol 3-Kinase) and cultured for 2 days. From day 2 to day 7, they were cultured in SF5 base medium with the same factors plus EGF (see Chapter 2 for details). The cells were examined every day for morphological changes, and samples were also collected every day to determine the gene expression pattern within the culture, by Q-RT-PCR and flow cytometry.

The morphology of cells varied slightly between each culture and between each individual well within the same culture, but was generally as shown in Figure 6.1. Small compact colonies appeared on day 1 and grew continually until day 2. Considerable cell death was also observed, which might suggest a selection progress due to the specific cell culture conditions. On day 2, the medium was changed. Starting from day 3, the cells piled up and formed larger more compact colonies. Flat elongated cells also started to appear surrounding the compact colonies and these finally linked the colonies between day 5 and day 7. Cell death dramatically dropped after the first medium change, but cells again started to lose adhesion to the culture plate and die on day 8.

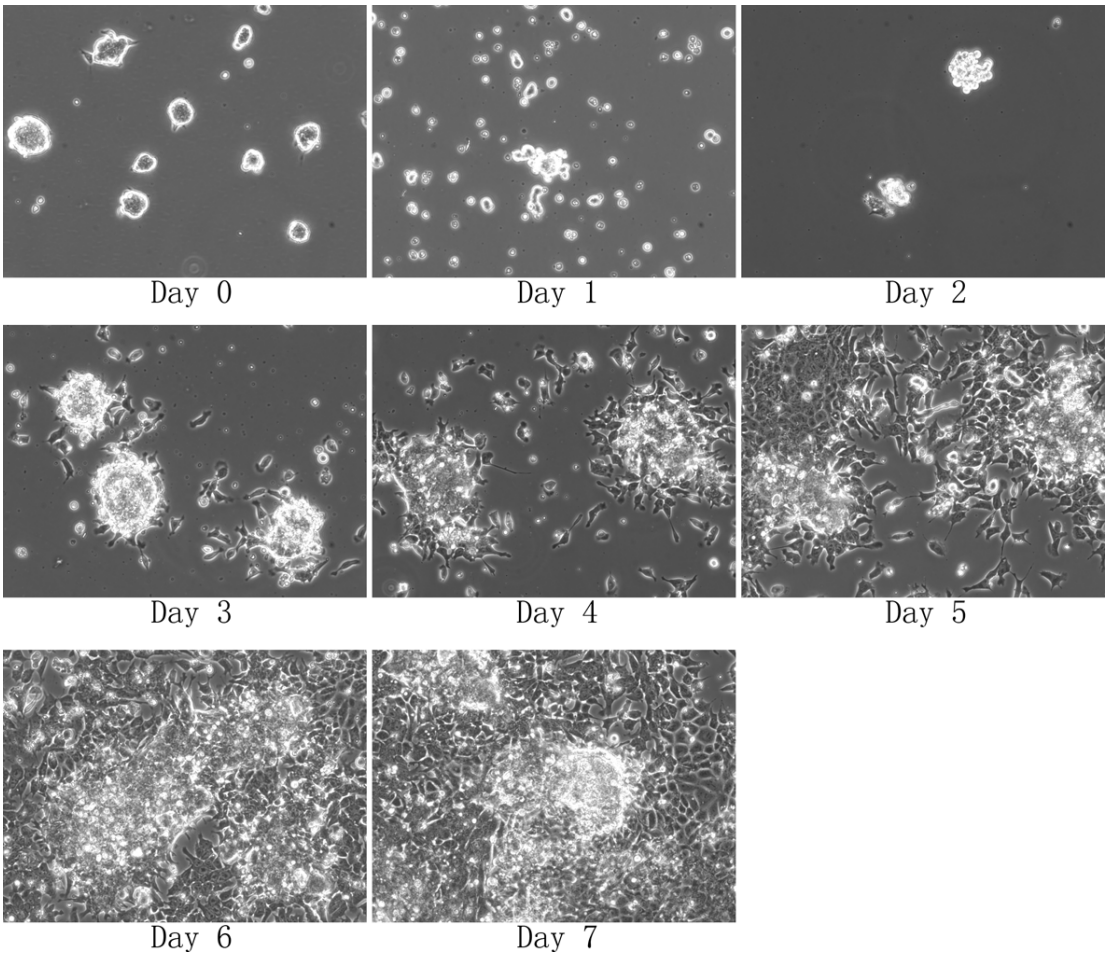

Figure 6.1. Morphological changes occurring during a typical 7 day differentiation culture using the 2i ADE protocol. E14tg2a were cultured in 2i Medium (Day 0) then were differentiated to DE cells using the protocol described in the text (Day 1 – 7). Cells were cultured on gelatin coated 6 well plates. Cells were checked and images of representative cell morphologies collected every 24 hrs (Magnification x 20).

6.2.2 Characterisation of cells generated via 2i ADE differentiation.

To determine whether the protocol outlined above generated ADE cells, I analyzed expression of markers associated with ADE in the differentiated cells.

Cxcr4 stains developing definitive endoderm (DE) but not visceral endoderm *in vivo* (McGrath, Koniski et al. 1999). It has also been previously identified as a mesoderm and definitive endoderm cell surface marker and shown to mark DE cells during ES cell differentiation (Yasunaga, Tada et al. 2005). In the 2i ADE differentiation protocol used here, $Cxcr4^+$ cells started to emerge from day 1 and encompassed about 90 percent of cells at around day 4 - day 5. The percentage of cells expressing very high levels of Cxcr4 dropped afterwards, but most cells in the population continued to express this marker (Figure 6.2).

The transcription factor *Sox17* is used as a marker for both definitive endoderm and visceral endoderm (Yasunaga, Tada et al. 2005) and *Hex* is used to demonstrate anterior positional identity in endodermal cells (Morrison, Oikonomopoulou et al. 2008). In the 2i ADE differentiation, both *Sox17* and *Hex* were induced. The peak values for both genes expression were reached at the time at which the percentage of $Cxcr4^+$ cells was highest, suggesting the anterior definitive endoderm character of the $Cxcr4^+$ cells rather than anterior visceral endoderm or mesoderm (Figure 6.3). In contrast, the pluripotency markers *Oct4*, *Nanog*, and *Rex1* were lost during differentiation (Figure 6.3). From these data, we conclude that 2i ADE protocol induced differentiation of ES cells to ADE.

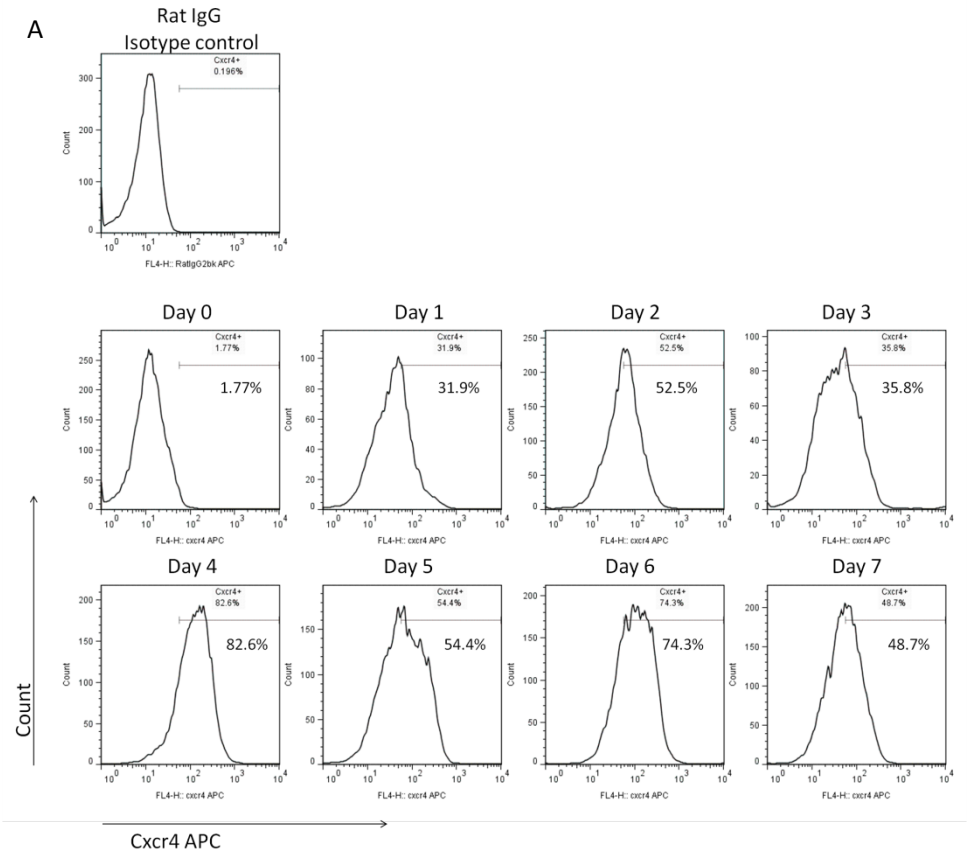
A
Rat IgG
Isotype control
Day 0
Day 1
Day 2
Day 3
Day 4
Day 5
Day 6
Day 7
1.77%
31.9%
52.5%
35.8%
82.6%
54.4%
74.3%
48.7%
Count
Cxcr4 APC

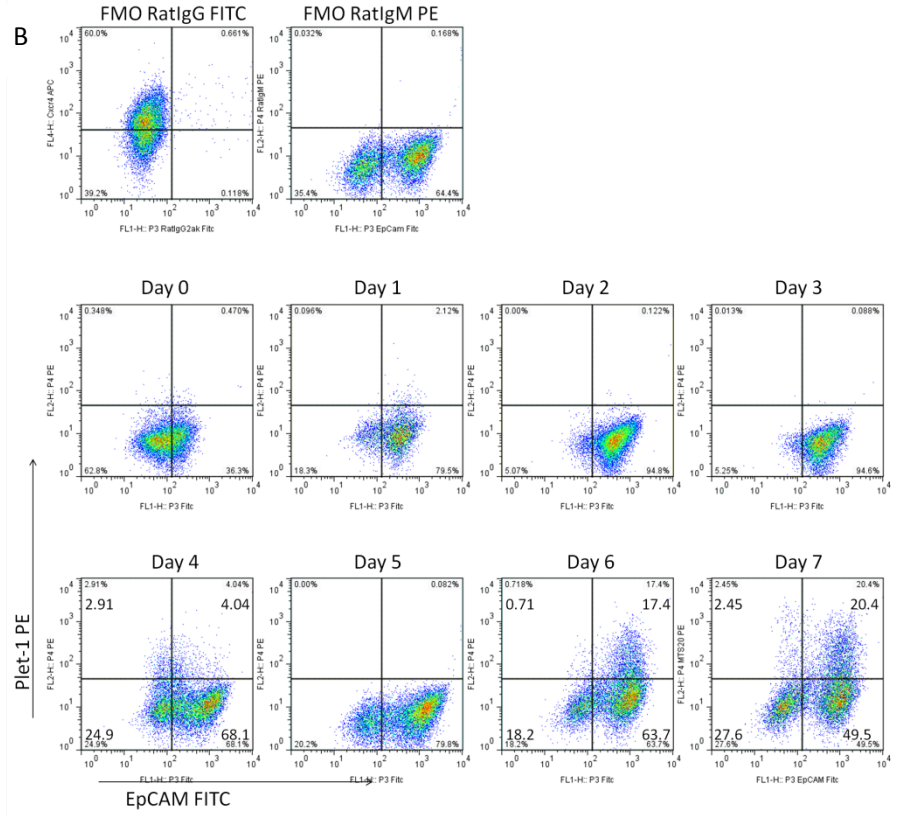
B
FMO RatIgG FITC
FMO RatIgM PE
Day 0
Day 1
Day 2
Day 3
Day 4
Day 5
Day 6
Day 7
2.91
4.04
24.9
68.1
0.71
17.4
18.2
63.7
2.45
20.4
27.6
49.5
Plet-1 PE
EpCAM FITC

Figure 6.2 Cell surface marker expression during 2i ADE differentiation. E14tg2a ES cells previously maintained in 2i medium were differentiated using the 2i ADE differentiation protocol. A) Cxcr4 expression during the 7 days differentiation culture. B) Plet-1 and EpCAM expression profiles during the 7 days differentiation culture. Data are representative of at least 3 individual cultures.

6.2.3 Expression of known regulators of thymus development during 2i ADE differentiation.

I next investigated whether any genes associated with thymus development were expressed.

Tbx1 is important for the pharyngeal segmentation and structure formation and thus for thymus development, but is not expressed in thymus primordium after E10.5 (Manley and Condie 2010). In the 2i ADE cultures, *Tbx1* expression, although very low, was first detected on day 4 and remained expressed until at least day 7, which suggested the presence of pharyngeal endoderm cells. The detection of *Tbx1* in control sample E12.5 thymic lobes, may be due to the presence of unseparated parathyroid dissected together with the thymic lobes (Figure 6.3).

Hoxa3, a transcription factor required for early pharyngeal pouch patterning and thymus-parathyroid primordium formation (Su, Ellis et al. 2001), was found to be induced on day 4 and increased until day 6. As expected, *Hoxa3* was detected in E12.5 thymic lobe controls (Figure 6.3). Of note is that the anterior boundary of *Hoxa3* expression is the 3pp.

Pax1 and *Pax9* are expressed in the pharyngeal endoderm from E9.0 and the third pharyngeal pouch (3pp) from E9.5. Furthermore, our unpublished data shows these factors are required together for induction of *Foxn1* expression in thymic primordium. Mutation of either or both of these two genes caused impaired thymus formation (wallin; Hetzer-Egger; Zhou; Kelly and Blackburn unpublished). Like *Tbx1* and *Hoxa3*, *Pax9* expression was detected from day 4 during 2i ADE differentiation, with expression slightly increasing until day 7. *Pax1* expression was almost undetectable (1 out of 6 samples) (Figure 6.3).

IL-7 is expressed in third pharyngeal pouch independently of Foxn1 expression. Very low level *IL-7* expression (n>5), was detected during 2i ADE differentiation including in undifferentiated ES cells, but it was unclear whether this represented expression above background (Figure 6.3 B).

A very low level of *Foxn1* expression can be detected within 3pp from E9 (Nehls, Pfeifer et al. 1994). Similarly, very low but reproducible *Foxn1* expression was detected during the 2i ADE differentiation (Figure 6.3 B).

Plet-1, a marker of the founder cells for thymic epithelial cell lineage (Depreter, Blair et al. 2008), was also up-regulated during 2i ADE differentiation. Very low-level *Plet-1* expression was detected in ES cells, while *Plet-1* expression in E12.5 lobes was around half of the expression level of differentiated ES cells on day 7 (n>5) (Figure 6.3).

In summary, *Tbx1*, *Hoxa3* and *Pax9* are all genes related to the third pharyngeal pouch formation and affect the thymus organogenesis *in vivo*. Their expression, together with the confirmed ADE markers, further indicated the presence of cells with foregut endoderm characteristics within the 2i ADE differentiation culture.

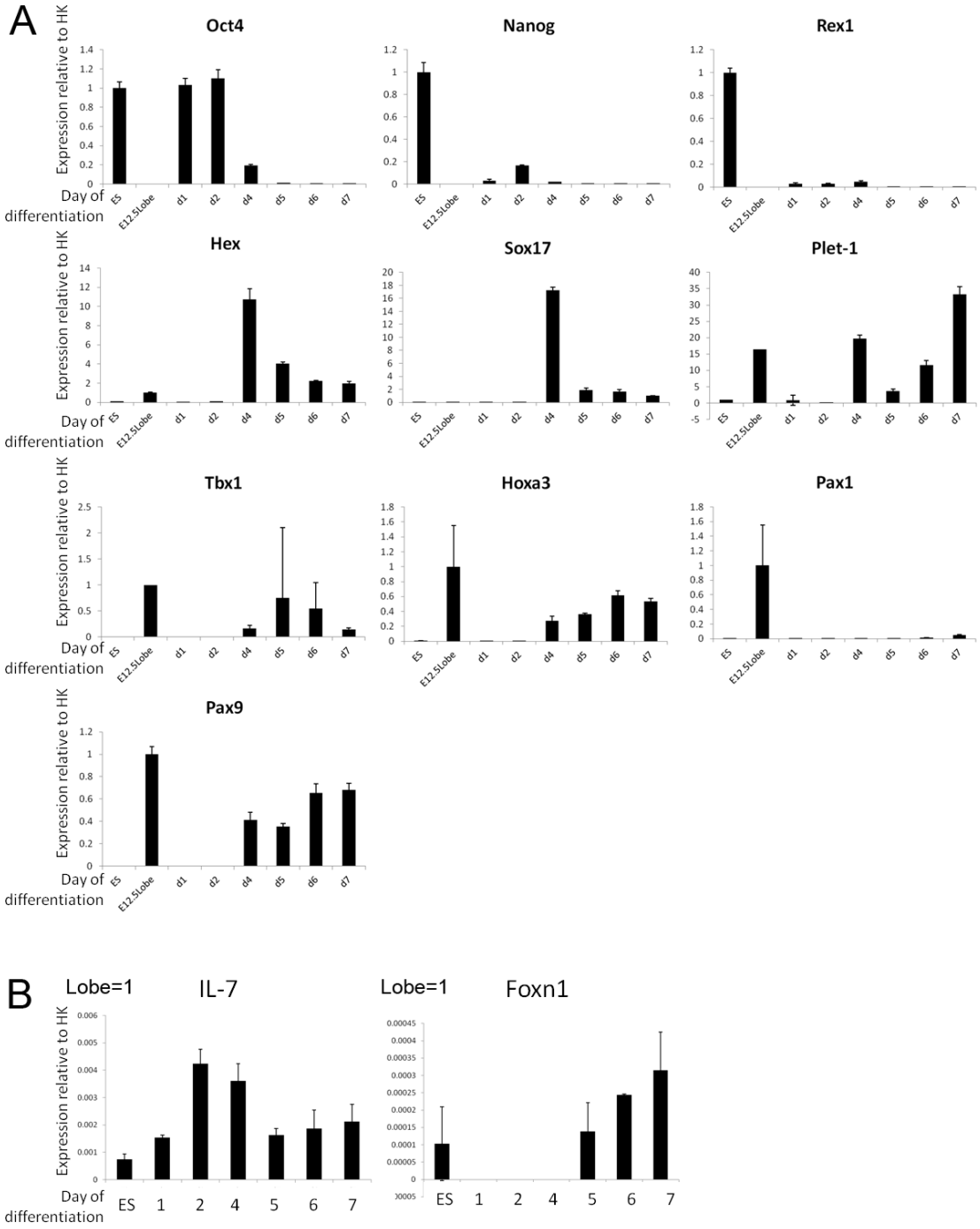

Figure 6.3 Gene expression pattern during 2i ADE differentiation.

Figure 6.3 Gene expression pattern during 2i ADE differentiation. E14tg2a ES cells previously maintained in 2i medium were differentiated using the 2i ADE differentiation protocol. **A)** Data show gene expression relative to α–Tubulin in undifferentiated ES cells (ES), E12.5 fetal thymic lobes (L) and after 1, 2, 4, 5, 6 and 7 days of 2i ADE differentiation (the expression level detected in ES cells is taken as 1 for *Oct4*, *Nanog*, *Rex1* and *Plet-1*; the expression level detected in E12.5 thymic lobes is taken as 1 for *Hex*, *Tbx1*, *Hoxa3*, *Pax1*, *Pax9*, *IL-7* and *Foxn1*; the expression level detected at day 7 of 2i ADE culture was taken as 1 for *Sox17*). Expression of the pluripotency markers *Oct4*, *Nanog*, *Rex1* was lost during differentiation. The definitive endoderm marker *Sox17* and the ADE marker *Hex* were up-reguated by day 4, as were the pharyngeal endoderm markers *Plet-1*, *Tbx1*, *Hoxa3* and *Pax9*. **B)** *IL-7* and *Foxn1* were detectable at extremely low expression levels in comparison with E12.5 thymic lobes, which was set to 1. The data shown in **A** and **B** above are from a single representative experiment as biological repeats (n>5) showed very similar trends but differences in relative expression levels.

6.2.4 Emergence and characterisation of Plet-1^{+}EpCAM^{+} cells during 2i ADE differentiation.

Plet-1 marks the founder cells for the thymic epithelial lineage from E9.5 (Depreter, Blair et al. 2008). Purified Plet-1^{+} epithelial cells from the thymus primordium at E12.5 were found to be able to generate functional thymus upon ectopic transplantation. The clonal level progenitor cell characteristic of Plet-1^{+} cells at E12.5 was also demonstrated (Rossi, Jenkinson et al. 2006). The expression of *Plet-1* in other tissues, such as postnatal kidney tissue, epithelial region of the pancreas from E11.5 and postnatal keratinocyte progenitor cells, has also been reported (Nijhof, Braun et al. 2006; Depreter, Blair et al. 2008).

During 2i ADE differentiation, Plet-1^{+} cells were detected by flow cytometry on day 4, 6 and 7. Epithelial cell adhesion molecule (EpCAM) staining confirmed the Plet1^{+} cells detected on day 6 and day 7 were epithelial, but Plet1 was not co-expressed with EpCAM on day 4 (Figure 6.2 B).

As Cxcr4 indicates a DE identity, we hypothesized that the Cxcr4^{+}EpCAM^{+}Plet-1^{+} cells on day 6 and day 7 should be foregut endoderm progenitors and/or TEPCs. Therefore, these cells were purified by flow cytometric cell sorting and further analyzed for gene expression profile. The Cxcr4^{+}EpCAM^{+}Plet-1^{-} cells on day 6 and day 7 were also sorted as controls.

Both Plet-1^{+}EpCAM^{+} and Plet-1^{-}EpCAM^{+} cells on day 6 and day 7 showed an extremely low level of *Nanog* and *Rex1* expression compared to ES cells. However, *Oct4* was expressed within Plet-1^{-}EpCAM^{+} population on day 6. Although *Oct4* expression, together with *Nanog* and *Rex1*, fell on day 7, its expression in Plet-1^{-} cells was still higher than in the Plet-1^{+} counterparts. This might suggest the existence of undifferentiated pluripotent stem cells in the Plet1^{-} population (Figure

6.4).

Expression of endoderm markers was detected in both the Plet-1^{+} and Plet-1^{-} populations within the day 6 and day7 EpCAM^{+} cells, with *Hex* expression being slightly higher in the Plet-1^{+} population. The high expression level of *Plet-1* within Plet-1^{+}EpCAM^{+} population, but low expression level within Plet-1^{-}EpCAM^{+}, as detected by QRT--PCR confirmed the fidelity of the MTS20 antibody in the sorting process. *Hoxa3* and *Pax9* were not enriched in any population but showed even lower profile than in unsorted cells. Thus suggested that the contribution of these genes expression on day 6 and 7 before sorting were mainly from EpCAM^{-} cells (Figure 6.4).

Interestingly, *Foxn1* expression, although low, was found within the Plet-1^{-}EpCAM^{+} population on day 6 and day 7 (Figure 6.4). This is consistent with the observation that epithelial cells within developing thymus lose Plet-1 and gain Foxn1 expression as they begin to differentiate (Nowell 2011). Thus the Plet-1^{-}EpCAM^{+} population might contain cells with maturing or mature TECs identity.

Plet-1^{+} cells on day 4 were EpCAM low, which could indicate that they have mesoderm identity; Plet-1 is expressed in the mesonephros from E9.5 – E11.5 and therefore, it was possible that these Plet-1^{+} could represent early kidney progenitor cells. Thus the Plet-1^{+}EpCAM^{low} and Plet-1^{-}EpCAM^{+} cells were isolated for further analysis (Figure 6.4). No expression of *Pax2*, an important gene associated with kidney development (Walther, Guenet et al. 1991; Torres, Gomez-Pardo et al. 1995), was detected however, and therefore we could not support this hypothesis (Data not shown).

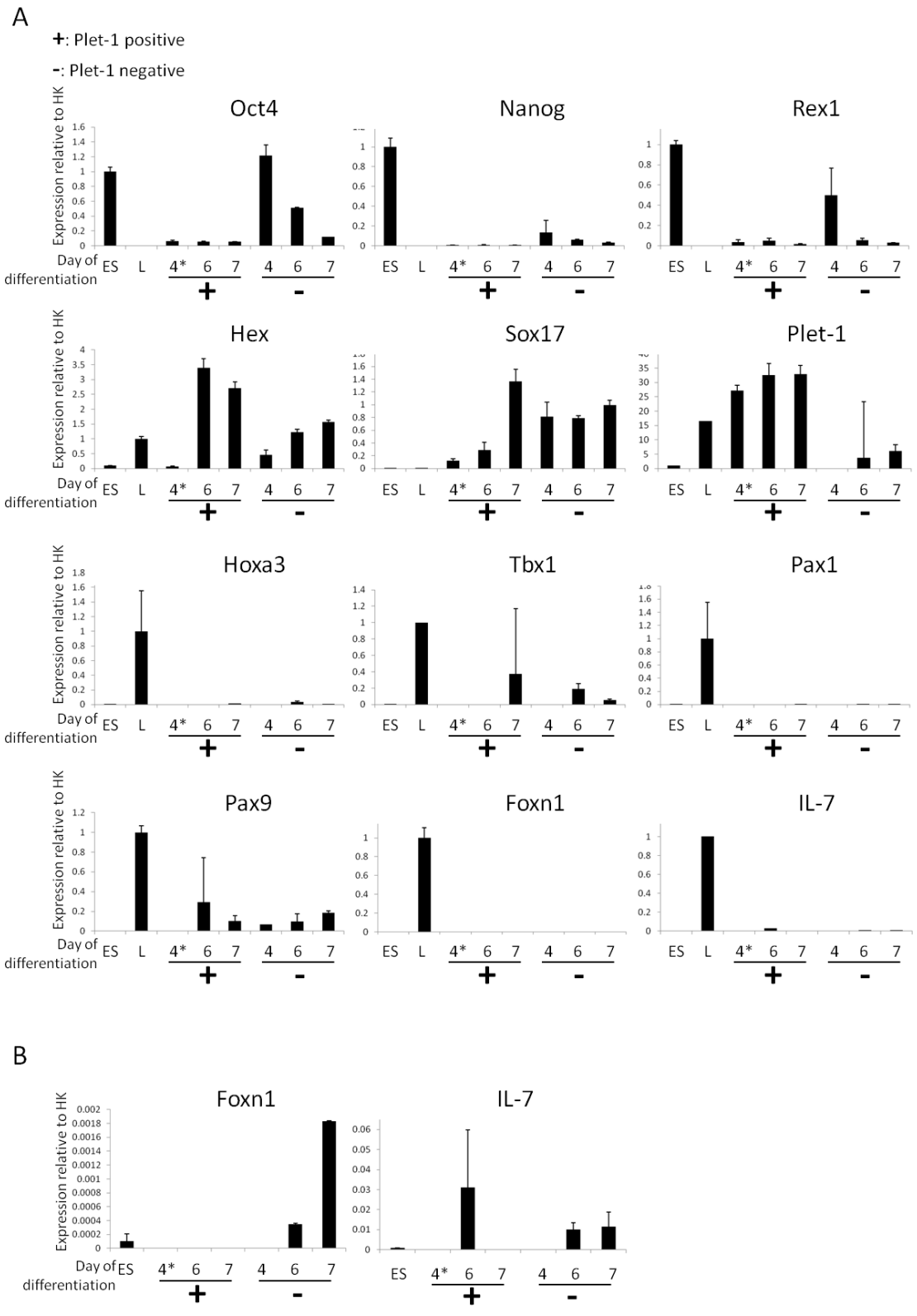

Figure 6.4 Gene expression pattern within sorted Plet-1^{-} and Plet-1^{+} cells.

Figure 6.4 Gene expression pattern within sorted Plet-1$^-$ and Plet-1$^+$ cells. ES cells previously cultured in 2i medium was differentiated through 2i ADE differentiation protocol. Cells were first gated for Cxcr4, then Plet-1 positive ("**+**") cells and Plet-1 negative ("**-**") cells were sorted for gene expression pattern analysis (**A** and **B**). All sorted cells were gated for Cxcr4 and EpCAM expression, except for the samples marked "*****", which were Cxcr4 positive and EpCAM negative. **B** shows the same data as **A** but excluding the E12.5 fetal thymic lobes, whose expression level was set as 1 (n=2 for *Oct4*, *Sox17*, *Hex* and *Plet-1*; n=1 for the other genes).

6.2.5 Functional testing of Plet-1+ cells generated during 2i ADE differentiation.

The results described above show that expression of some TEPC-related genes was induced in cells generated during the 2i ADE protocol. Therefore, I wished to test the potential for these cell populations to give rise to TEPCs or even mature TECs.

To achieve this, I made use of the RFTOC assay described in Chapter 4 to test the potency of the ES-derived cells when differentiated within an actively differentiating fetal thymic microenvironment. As summarized in Table 6.1 for experiments C, D and E, wild type E14tg2a ES cells were first differentiated through 2i ADE differentiation, and at a specified stage, Plet-1^{+}EpCAM^{+} cells were sorted and reaggregated with dissociated CBA fetal thymic lobes (and MEFs in experiment E). In these experiments, the cells were not gated for Cxcr4. The reaggregates were cultured for 1 or 2 days, then transplanted under the kidney capsule of the NOD.Cg-*Prkdc*^{scid} *Il2rg*^{tm1Wjl}/SzJ (NOD/SCID) immunodeficient recipient mice. As the MHCII haplotype of E14tg2a ES cells is H-2b, and MHCII haplotype of CBA mouse is H-2k, the contribution of the ES cell-derivatives to the grafts could be distinguished from the carrier cells using haplotype-specific antibodies.

As expected, the carrier cells in the graft formed an organized and functional thymus structure (Figure 6.5, and 6.7-6.9). There was no H-2K^{b} staining within the carrier cells-only graft (Figure 6.5). The haplotype of NOD/SCID mice is *g7* (Jax Mice database). Surprisingly, the kidney tissue from the NOD/SCID mice also stained H-2k^{b} positive. However, this could be easily distinguished from the grafted tissue by position, the extremely bright H-2k^{b} positive signal, and large cell size (Figure 6.6)

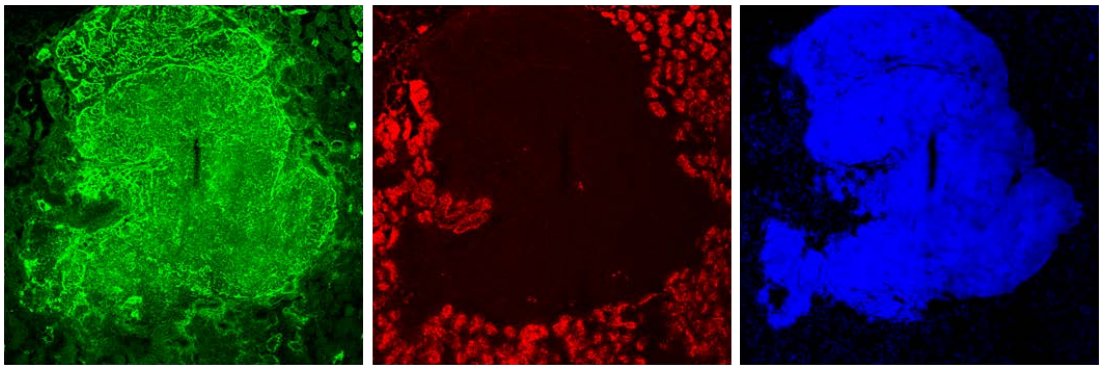

Figure 6.5 CBA fetal thymus cells graft shows no H-2K^{b} staining. E13.5 fetal thymic lobes were dissociated. 400,000 cells were reaggregated, cultured for 18 hours and subsequently transplanted under the kidney capsule of NOD/SCID mouse. 3 weeks later, the graft was recovered, cryosectioned and processed for IHC analysis. PanK (Green) was expressed in all cells in carrier cells-only grafts, while H-2K^{b} (Red) was not detected except in host kidney tissue. n=1

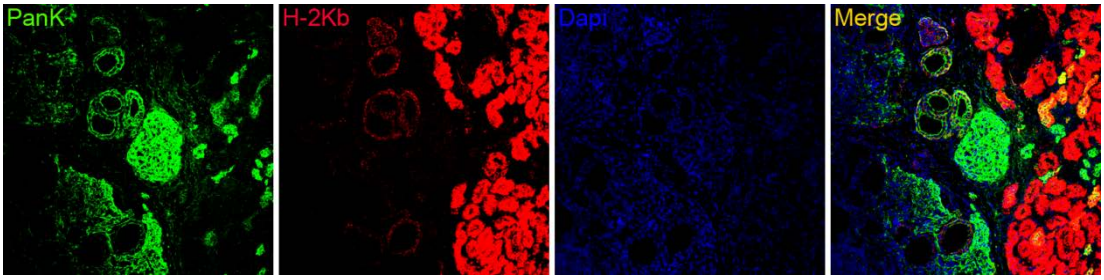

Figure 6.6. Non-specific staining of H-2k^{b} on kidney tissue. Image shows example from experiment E illustrating the different signal intensity of H-2K^{b} staining between the ES cell-derivatives and the recipient mouse kidney.

Experiment	Test Cells	Carrier cells	Recipient mice	Culture time before grafting	Results
A	AGFP97 d7 EpCAM$^+$ (Plet-1$^-$)	CBA E12.5	NOD/SCID	Tiny reaggregate, grown for 1 week before grafting.	Teratoma (Fig. 6.10)
B	AGFP97 d7 EpCAM$^+$ (Plet-1$^-$)	CBA E12.5 CBAxBL6 E13.5	NOD/SCID	42 hours	Teratoma (Fig. 6.10)
C	E14 d7 Plet-1$^+$EpCAM$^+$	CBA E13.5 &E12.5	NOD/SCID	18 hours	Good graft. ES contribution detected but no thymus like tissue (Fig. 6.7)
D	E14 d7 Plet-1$^+$EpCAM$^+$	CBA E13.5 &E12.5	NOD/SCID	18 hours	Hollow graft. ES contribution detected but few and no thymus like tissue (Fig. 6.8)
E	E14 d6 Plet-1$^+$EpCAM$^+$	CBA E13.5 MEFs	NOD/SCID	42 hours	Good graft. ES contribution detected, most tube-like, few thymus-like (Fig. 6.9)
F	E14 d6 Plet-1$^-$ EpCAM$^+$	CBA E13.5 MEFs	NOD/SCID	42 hours	Good graft. No detection of ES, may be due to staining failure (Data not shown)

Table 6.1. Summary of graft analysis.

For experiments C, D and E (Figures 6.7-6.9). Plet-1^{+}EpCAM^{+} cells on day 7 were sorted and their differentiation potential was tested as described in Table 6.1. The ES-derived cells marked by H-2K^{b} (red) mainly formed tube-like structures. Some of them were also PanK positive (green), and thus were not likely to be endothelial cells. Also, as no folds were detected within the tubes, they were unlikely to represent mature intestinal epithelium (Figure 6.7-6.9). Notably, a thymic epithelial cell-like region contributed by ES cell-derivatives was found in Experiment E. As shown in Figure 6.9, cells morphologically TEC-like and positive for both H-2K^{b} and PanK were localized within a thymus like area (PanK positive and densely packed “Cortex” area and PanK positive less densely packed “Medulla” area. Cell density was indicated by Dapi staining). The less dense of Dapi staining suggested a possible medullary lineage character for these cells.

I also used AGFP 97 ES cells (Experiments A and B in Table 6.1), with the aim of distinguishing the ES cells-contributed regions within grafts. As no Plet-1 positive cells were found in these experiments, I purified all the EpCAM^{+} cells on day 7 of 2i ADE differentiation and used these cells to generate RFTOCs for grafting. Teratoma formed from both of these grafts (Figure 6.10) suggesting the existence of undifferentiated ES cells within this population on day 7 of two 2i ADE differentiation. This is consistent with the Q-RT-PCR analysis of the Plet-1^{-}EpCAM^{+} population, where the pluripotency marker expression was maintained (Figure 6.4).

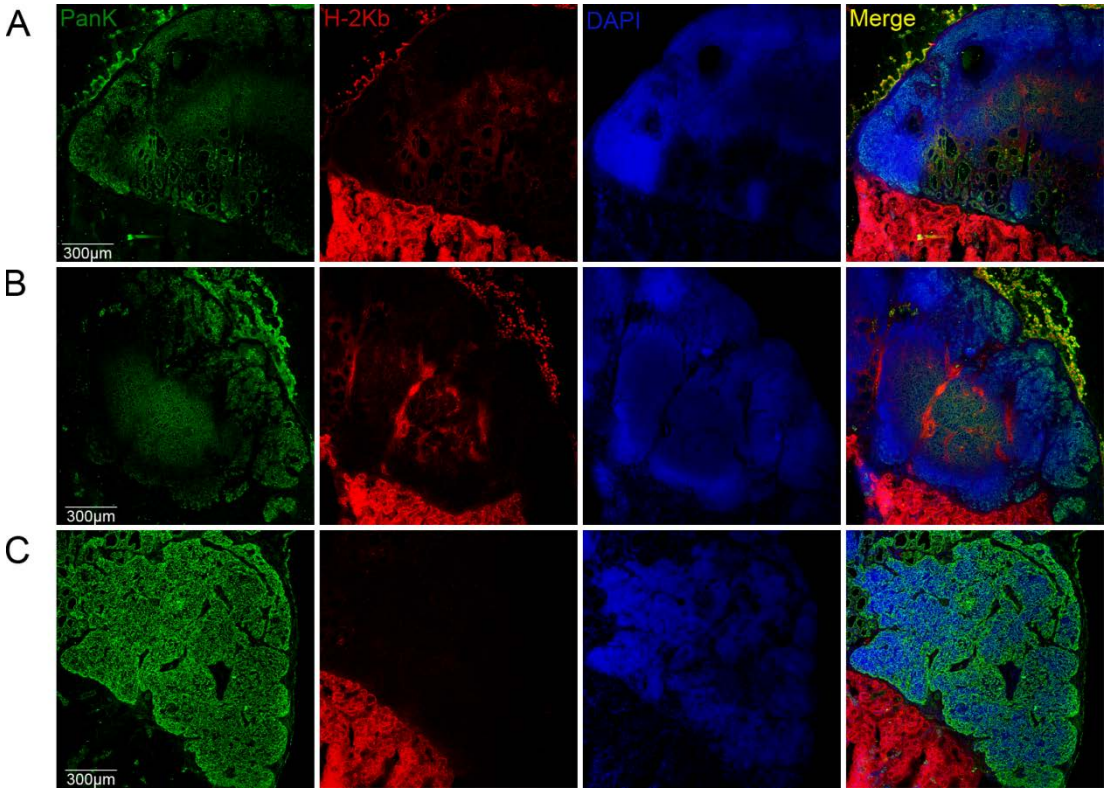

Figure 6.7 Contribution of ES cell-derivatives to grafts in experiment C. 6,200 Plet-1^{+}EpCAM^{+} cells from day 7 2i ADE differentiation culture were reaggregated with 220,000 carrier cells. The reaggregate was cultured 18 hours and then transplanted under the kidney capsule of a NOD/SCID recipient mouse. 3 weeks later, the graft was collected, cryosectioned and processed for PanK (Green), H-2K^{b} (Red) and DAPI (Blue) staining. **A** and **B** shows that the differentiated ES cell-derivatives (H-2K^{b} positive and red on image) mainly contributed to non-thymus-like structures in graft. **C** shows the carrier cells (H-2K^{b} negative) generated a thymus-like structure. Scale bar: 300μm.

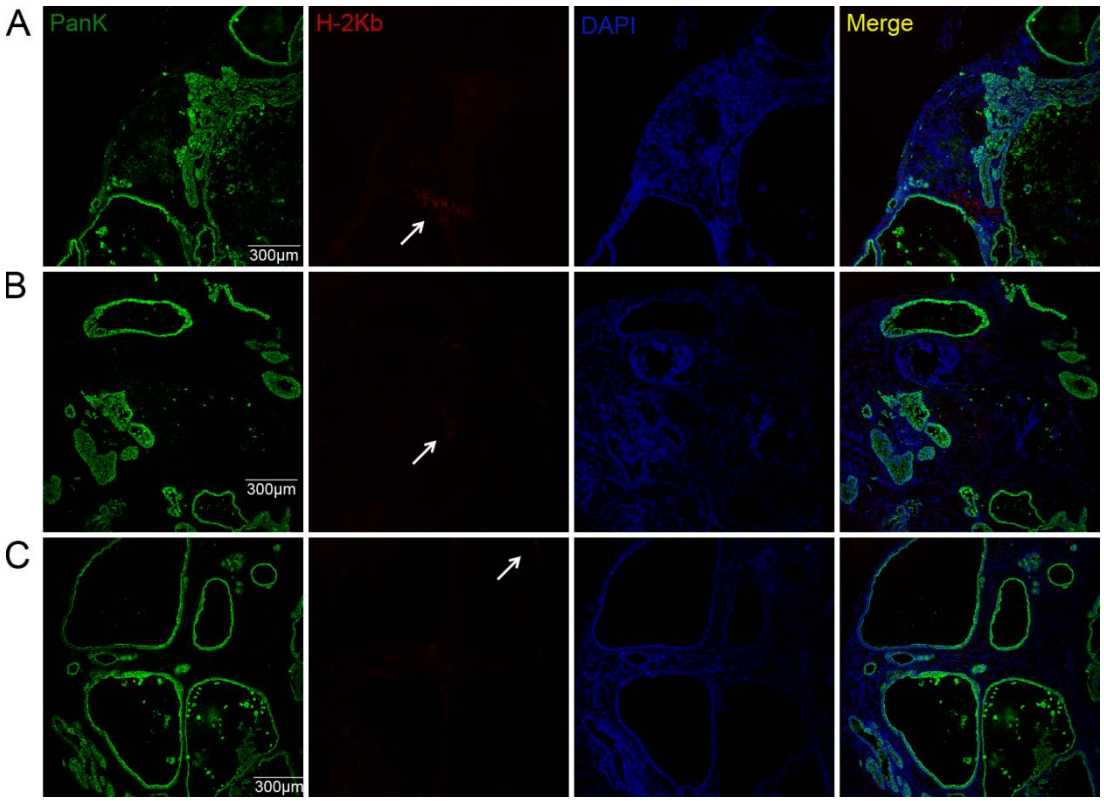

Figure 6.8 Contribution of ES cell-derivatives to the graft in experiment D. 3,800 Plet-1^{+}EpCAM^{+} cells from day 7 2i ADE differentiation culture were reaggregated with 200,000 carrier cells. The reaggregate was cultured for 18 hours and then transplanted under the kidney capsule of a NOD/SCID recipient mouse. Three weeks later, the graft was recovered, cryosectioned and processed for PanK (Green), H-2K^{b} (Red) and DAPI (Blue) staining. **A**, **B** and **C** show the cystic structure of graft. A low level contribution from ES cell-derivatives was detected (arrows). Scale bar: 300μm.

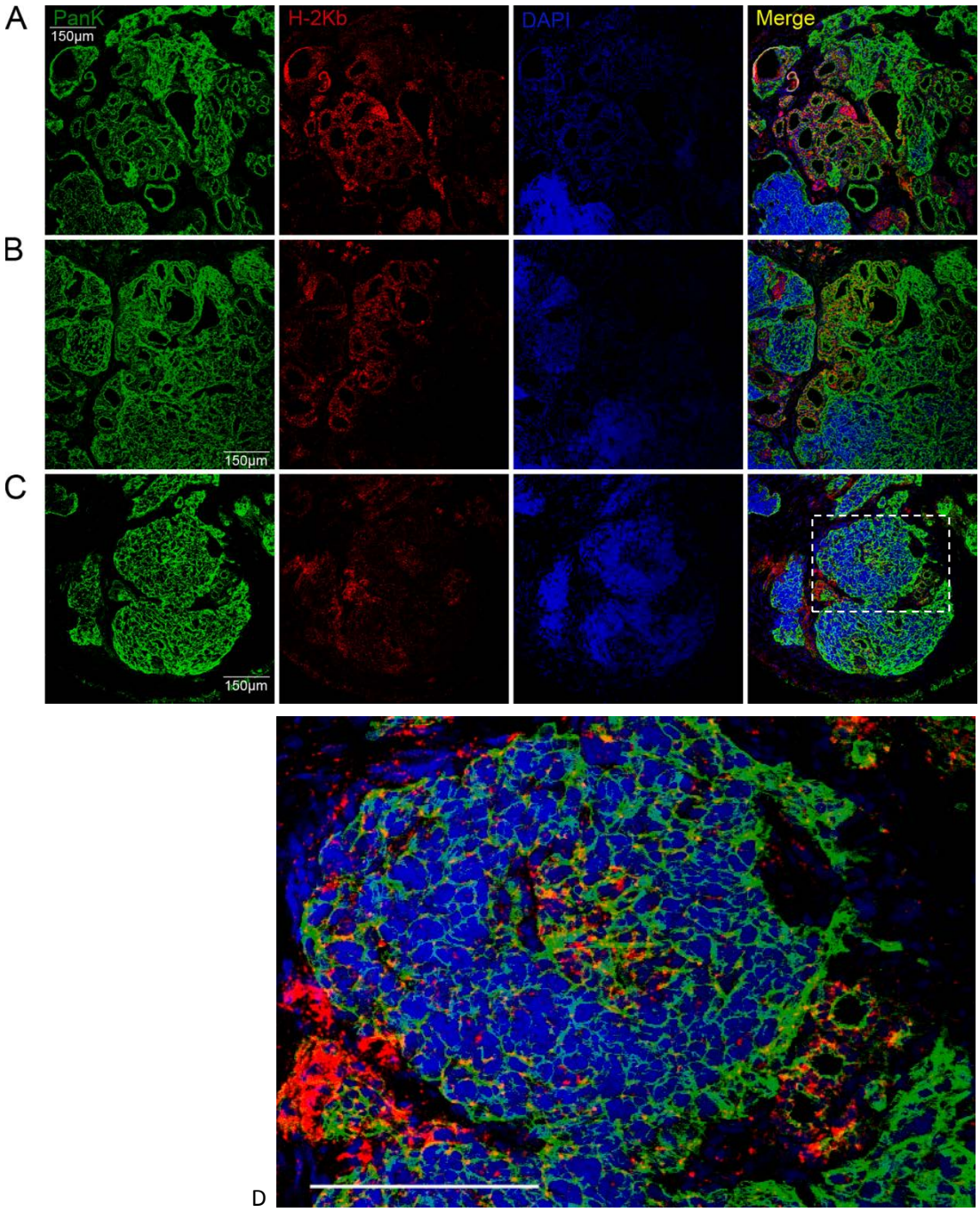

Figure 6.9 Contribution of ES cell-derivatives to graft in experiment E.

Figure 6.9 Contribution of ES cell-derivatives to graft in experiment E. 13,000 Plet-1^{+}EpCAM^{+} cells from day 6 2i ADE differentiation culture were reaggregated with 300,000 carrier cells (Table 6.1). The reaggregate was cultured for 42 hours and then transplanted under the kidney capsule of a NOD/SCID recipient mouse. Three weeks later, the graft was recovered, cryosctioned and processed for PanK (Green), H-2K^{b} (Red) and DAPI (Blue) staining. Panels **A** and **B** show that the differentiated ES cell-derivatives (H-2K^{b} positive and red on image) mainly contributed to non-thymus-like structures in graft. **C** shows the carrier cells (H-2K^{b} negative) generated a thymus-like structure. **D** Magnified image shows the possible contribution of ES cell-derivatives to a TEC network in a thymus region of the graft. Scale bar: 150μm.

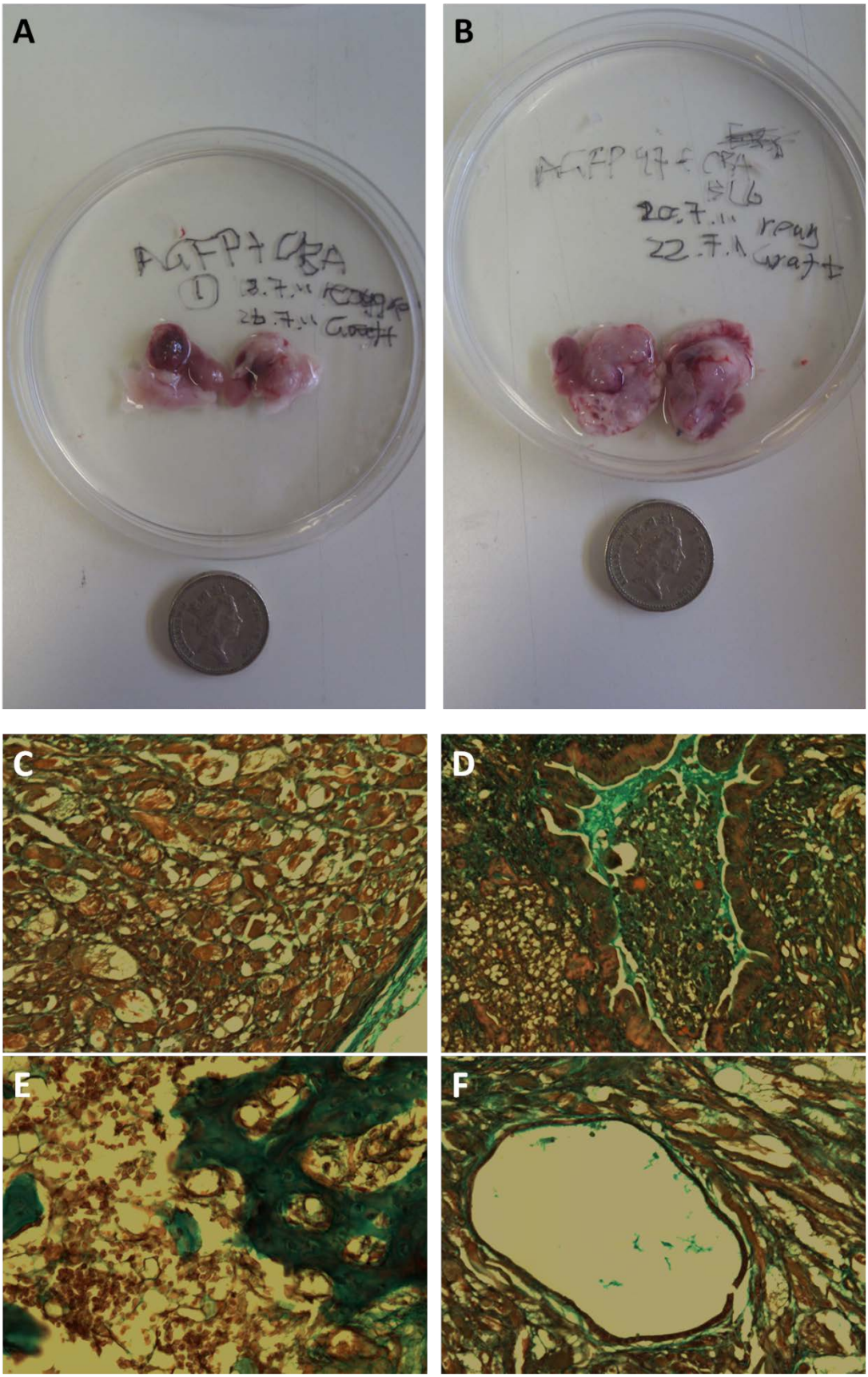
A
B
C
D
E
F

Figure 6.10 EpCAM+ cells on day 7 of AGFP 97 2i ADE differentiation, when reaggregated with carrier cells and grafted under the kidney capsule, formed teratomas. A-B) shows the dissected grafts from experiment A and B described in Table 3, respectively. **C-F)** are selected Masson's trichrome staining slides from the experiment **B** graft. Tissue were provisionally identified as probably **C)** muscle or respiratory epithelium. **D)** gut epithelium. **E)** nervous tissue. **F)** respiratory epithelium.

In summary, sorted Plet-1^{+}EpCAM^{+} cells on either day 6 or day 7 contributed to the thymus grafts but mainly formed tube-like rather than thymus-like structures, and thus suggested that most Plet-1^{+}EpCAM^{+} cells might be committed to different endodermal cell lineages rather than being thymus lineage progenitor cells or a mutlipotent endodermal progenitor cell type. This is consistent with the lack of *Hoxa3* and very low *Pax9* expression within the sorted Plet-1^{+}EpCAM^{+} population on day 6 and day 7 compared with the whole 2i ADE differentiation culture. Cells sorted on the basis of EpCAM expression alone on day 7 gave rise to teratomas after grafting. Therefore, I concluded that to generate TEPCs from ES, a more specific induction protocol would be required.

6.2.6 Withdrawal of FGF4 leads to down-regulation of ADE markers and loss of Plet-1 expression

It has been reported that Fgf4 promotes the posterior identity of endoderm cells during the anterior-posterior patterning of the primitive gut tube (reviewed in Zorn, Wells 2009; Dessimoz, Opoka et al. 2006). It's also been demonstrated that FGF4 promotes the outcome of ADE cells from the differentiating mouse ES cells (Morrison, Oikonomopoulou et al. 2008). Therefore I tested whether withdrawal of Fgf4 from the 2i ADE differentiation culture could lead to development of cells with a more anterior, 3pp/TEPC-like identity.

Ffg4 is present throughout the original 2i ADE induction protocol. I tested the effect of withdrawing of Fgf4 from the first day of ADE induction. This led to no significant difference in expression of pluripotency markers (Figure 6.12). No difference in Cxcr4 expression was observed in the presence or absence of Fgf4 (Figure 6.13 A). However, *Sox17* and *Hex* induction was much lower in the "no Fgf4" condition. Plet-1 expression was not detectable by flow cytometry at any point in the "no Fgf4" condition (Figure 6.13 B); its absence was further confirmed by Q-RT-PCR (Figure 6.12). The pharyngeal marker *Hoxa3* was expressed at higher levels

in the absence of Fgf4, but there was a lack of *Tbx1* expression and less *Pax9* induction. FgfR2IIIb, the receptor for Fgf7 and Fgf10 (Ornitz, Xu et al. 1996), is required for the proliferation of TEPCs after formation of the common thymus-parathyroid primordium (Revest, Suniara et al. 2001). *FgfR2IIIb* expression was observed in both conditions, but was higher in cells cultured in the presence of Fgf4. Both *Foxn1* and *IL-7* were detected in cells generated under both conditions, but at extremely low expression levels compared to whole E12.5 fetal thymic lobes (Figure 6.12).

Collectively, these data suggested that the presence of Fgf4 was beneficial for generation of ADE cells from ES cells in this protocol.

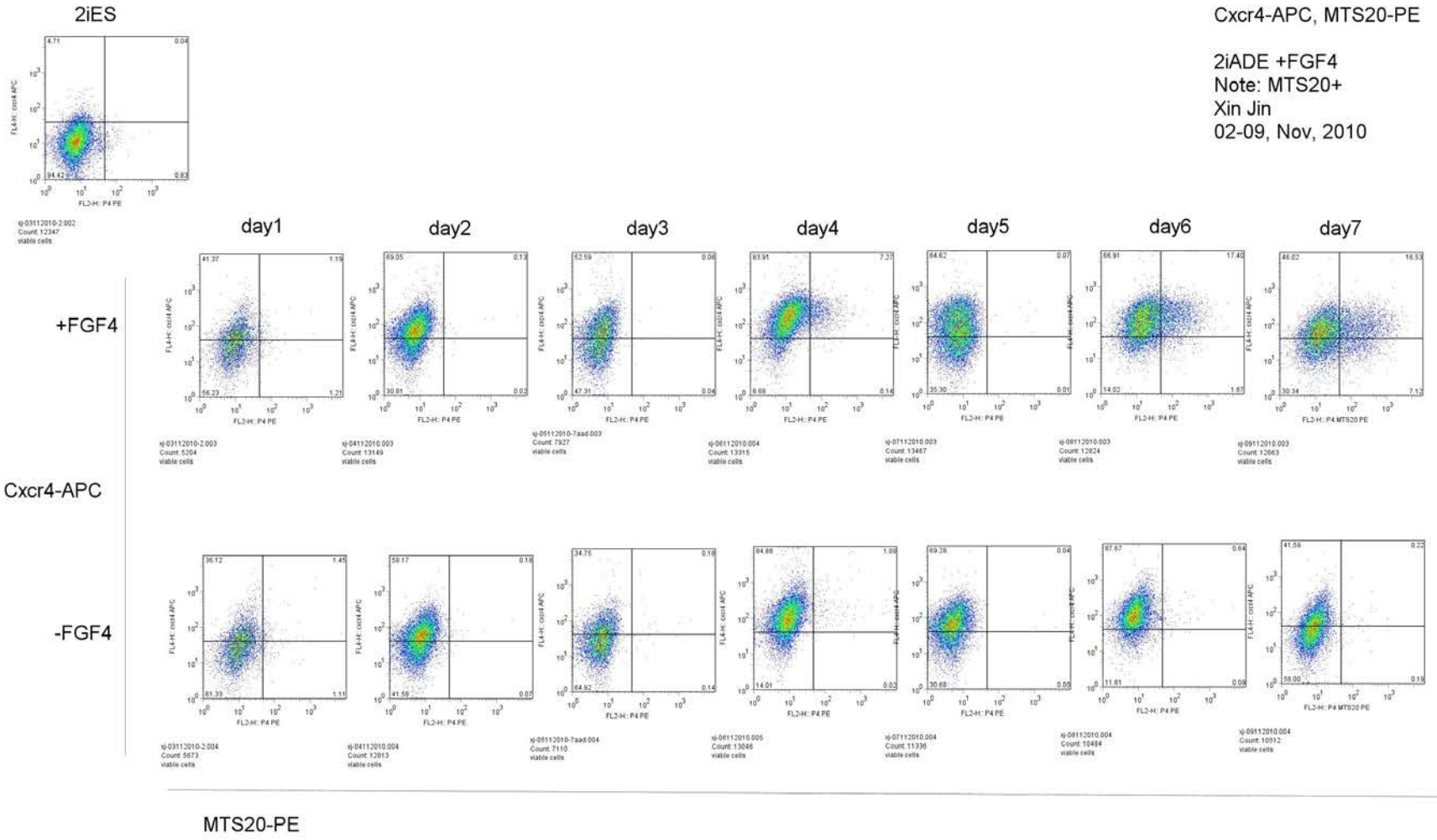
2iES
Cxcr4-APC, MTS20-PE
2iADE +FGF4
Note: MTS20+
Xin Jin
02-09, Nov, 2010
day1
day2
day3
day4
day5
day6
day7
+FGF4
-FGF4
Cxcr4-APC
MTS20-PE

Figure 6.11 A

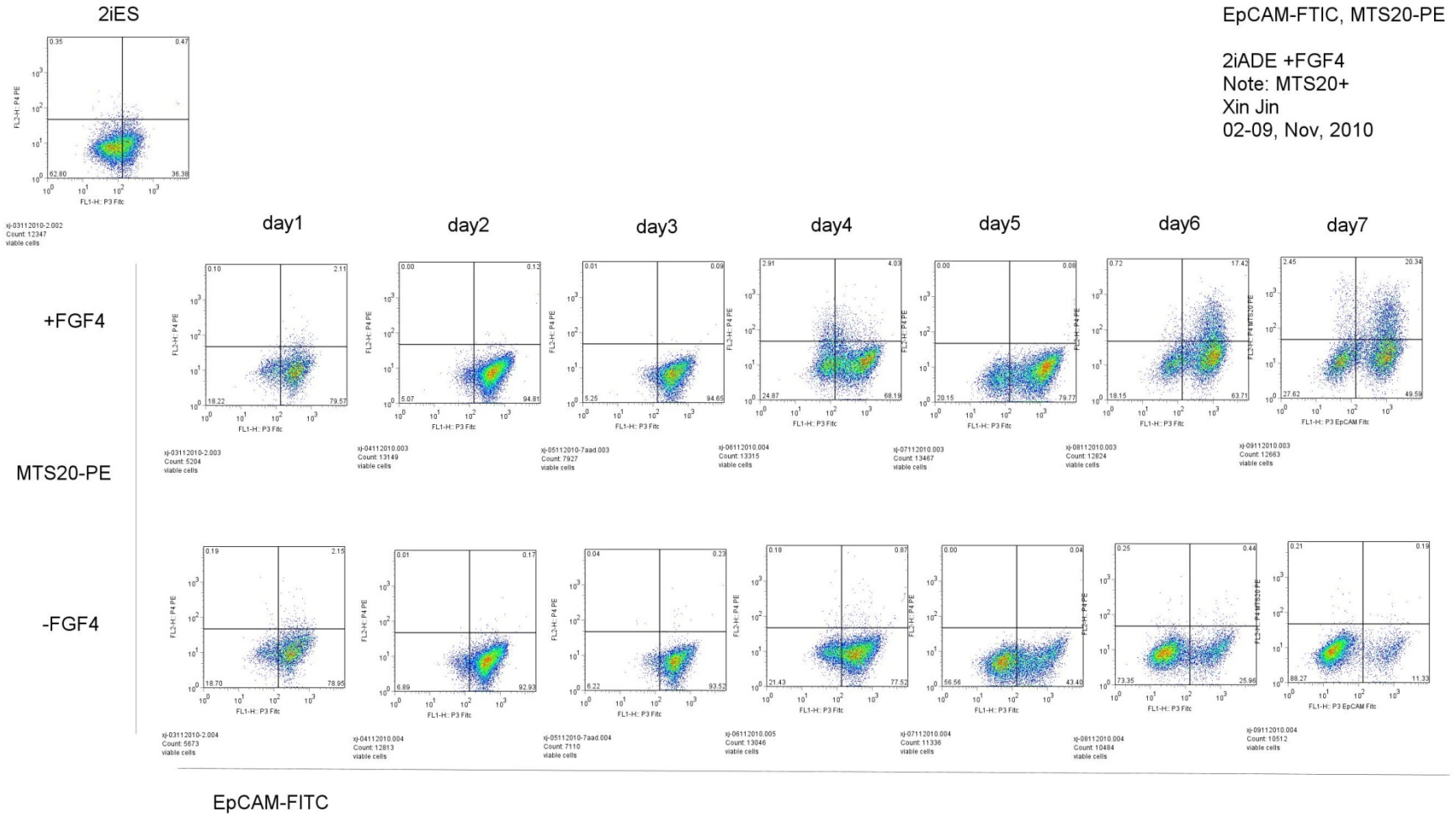
2iES
EpCAM-FTIC, MTS20-PE
2iADE +FGF4
Note: MTS20+
Xin Jin
02-09, Nov, 2010
day1
day2
day3
day4
day5
day6
day7
+FGF4
MTS20-PE
-FGF4
EpCAM-FITC

Figure 6.11 B

Figure 6.11 Comparison of cell surface marker expression pattern following ADE differentiation in the presence and absence of Fgf4. ES cells previously cultured in 2i medium were differentiated through 2i ADE differentiation protocol. In parallel cultures, conditions were identical except that Fgf4 was withdrawn from day 1 ("–FGF4" treatment). **A** The Cxcr4 expression pattern was identical between the +FGF4 and –FGF4 treatments. **B** Plet-1 expression was undetectable in cells differentiated in the absence of Fgf4. There were also fewer EpCAM+ cells in cells differentiated in the absence of Fgf4. An undifferentiated ES cell culture in 2i medium was used as a control. MTS-20 was used here to mark Plet-1 expression (Depreter, Blair et al. 2008). Quadrants were set based on FMO controls for each antibody. n=1.

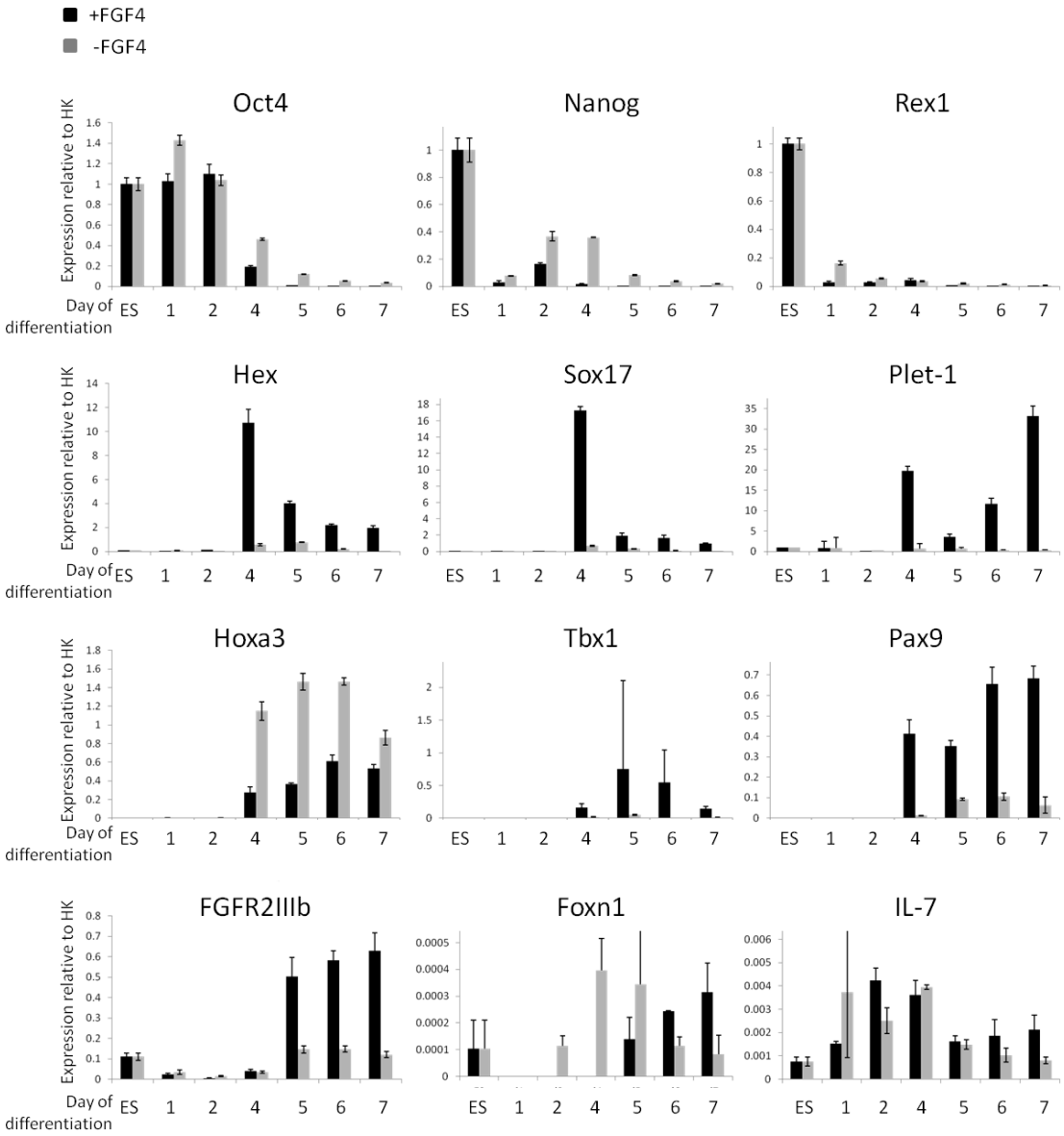

Figure 6.12. Comparison of gene expression patterns in cells generated by ADE differentiation in the presence and absence of Fgf4. ES cells previously cultured in 2i medium were differentiated through 2i ADE differentiation protocol. Fgf4 was withdrawn from day 1 ("–FGF4" treatment). Undifferentiated ES cells and cells at 1, 2, 4, 5, 6 and 7 days after differentiation were analyzed by Q-RT-PCR. In the absence of Fgf4, the endoderm makers *Sox17* and *Hex* were induced less strongly; No induction of *Tbx1* or *Plet-1* was observed; *Pax9* induction was maintained at a low level. *Hoxa3* could be detected and showed a higher level induction than in the presence of Fgf4. Both *Foxn1* and *IL-7* could be detected but at an extremely low level. Data are shown normalized to α-tubulin. (the expression level detected in ES cells is taken as 1 for *Oct4*, *Nanog*, *Rex1* and *Plet-1*; the expression level detected in E12.5 thymic lobes is taken as 1 for *Hex*, *Tbx1*, *Hoxa3*, *Pax1*, *Pax9*, *IL-7* and *Foxn1*; the expression level detected at day 7 of 2i ADE culture was taken as 1 for *Sox17*) (n=1)

6.2.7 Investigation of the potential for induction of TEPCs through co-culturing of 2i ADE differentiated ES cells with fetal thymic lobes.

Previous data have shown that the third pharyngeal pouch related genes *Tbx1*, *Pax9*, *Hoxa3* and *Plet-1* are induced in some cells during the 7 day 2i ADE differentiation. Meanwhile, the mature TEC markers *Foxn1* and *IL-7* were not strongly induced. These data also revealed that expression of the DE and pharyngeal endoderm markers arose at around day 4. Therefore, I hypothesised that if a specific stimulus could be given at that time point, more TEPC-like cells might be generated. To test this hypothesis, I therefore further induced the cells by co-culturing the differentiating ES cells with dissociated cells from fetal thymic lobes. Cell morphology changes and gene expression pattern were closely monitored.

I used the AGFP97 ES cell line (Gilchrist, Ure et al. 2003) in this co-culture system. GFP is ubiquitously expressed in transgenic mice derived from this line, and is anchored to the cell membrane (Figure 6.14). The same differentiation response of this cell line to the 2i ADE differentiation induction was first confirmed by comparing several key gene markers expression to the wild type E14 ES cells including Cxcr4 by FACS and *Sox17* by QRT-PCR. Plet-1 within AGFP97 2i ADE differentiation was induced but at a lower level than in E14Tg2a cells (Figure 6.13).

AGFP97 ES cells were then induced to ADE using the 2i ADE differentiation protocol and differentiated cells on days 4, 5 and 6 were each co-cultured with intact E12.5 CBAxC57BL/6 fetal thymic lobes (FTLs) for a further period (2, 4 and 7 days). ES cell-derivatives only and fetal thymic lobes only were also cultured as controls.

The co-cultured ES cell derivatives were purified from the co-cultures based on GFP expression and the purity was confirmed after sorting. From the gene expression patterns summarized in Figure 6.15 and 6.16, it is evident that in two different co-culture conditions (Table 6.2), although to different extents, *Sox17*, *Plet-1* and *Pax9* expression was higher in the co-cultured ES cell-derivatives compared with the ES-derivatives only. *Hoxa3* was up-regulated in condition B, *Pax1* was up-regulated in condition A. This suggested that both fetal thymic lobes and the culture conditions could affect the outcome of ES cell differentiation.

Moreover, the up-regulation of *Foxn1* and *IL-7* expression observed in co-culture was specific to condition B, strongly suggesting that TEPC/TEC-like cells might exist within the population of differentiating ES cell-derivatives generated under these conditions (Figure 6.16).

Collectively, these data suggested that the induction of the differentiating ES cells by co-culturing with FTLs induced generation of cells with characteristics of TEPCs, and therefore that optimization of culture conditions should further improve this process.

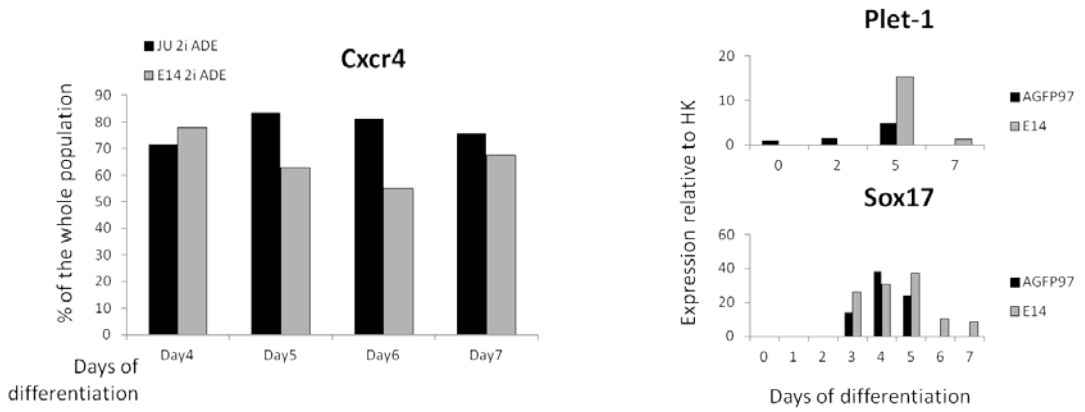

Figure 6.13 Comparison of cell surface marker and gene expression between the AGFP97 and wild type E14 ES cell lines. AGFP97 and E14 were cultured and induced to ADE using 2i ADE differentiation protocol. Both cell lines showed a similar profile for Cxcr4 staining over the differentiation period. The *Sox17* expression pattern was also similar between the two cell lines. *Plet-1* was induced in both cell lines in 2i ADE differentiation, but at much lower levels in AGFP97 compared with wild type E14. QRT-PCR data are shown normalized to α-tublin and relative to the expression levels in E12.5 fetal thymic lobes, which is set as 1.n=1

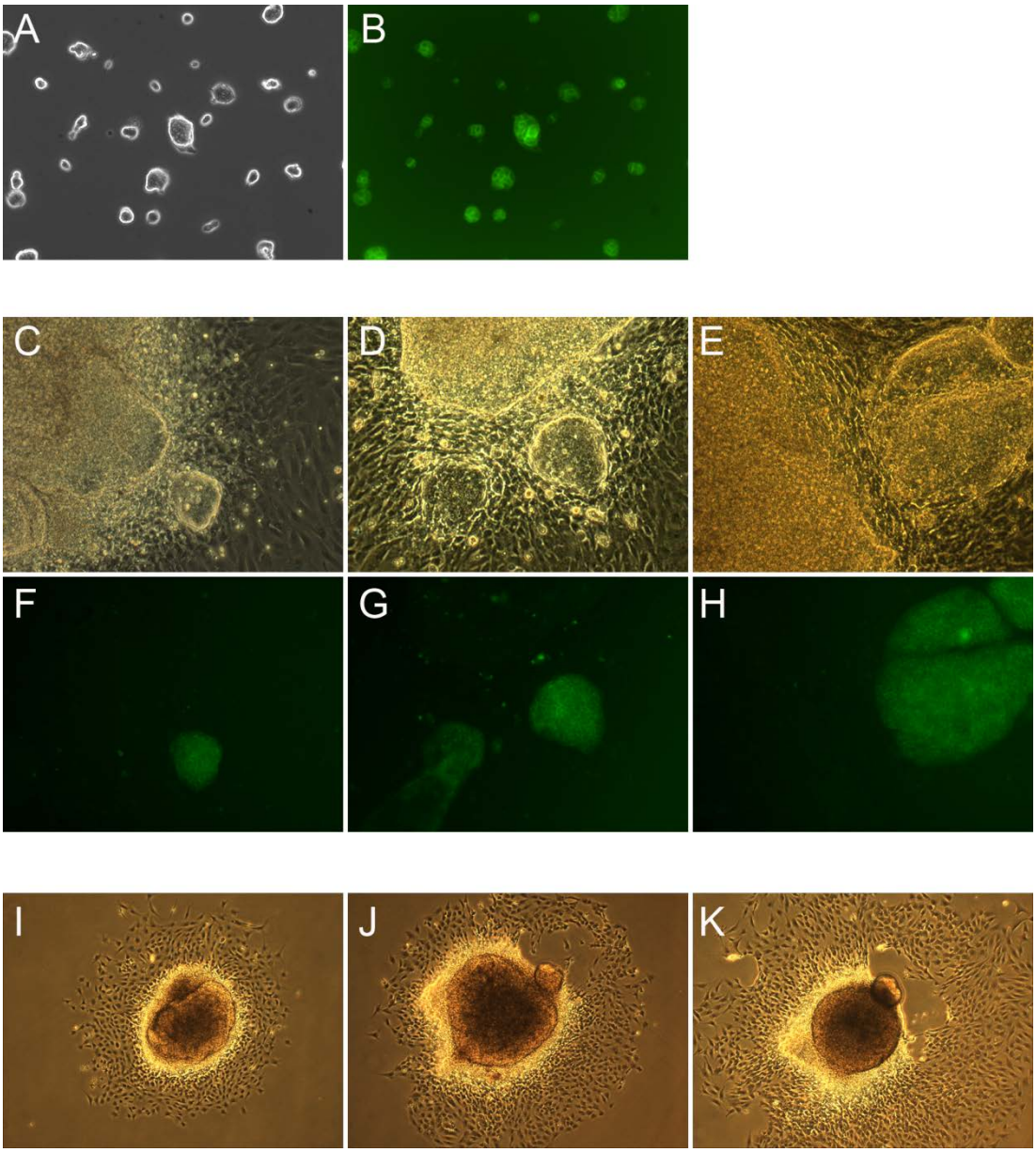

Figure 6.14 GFP distinguishes the AGFP97 ES cell-derivatives from the fetal thymic lobe cells in co-culture. Images are representative of co-culture Condition A. **(A)** AGFP97 ES cells maintained in 2i medium. GFP expression can be detected in all cells. (**B**) Cells were differentiated using 2i ADE differentiation protocol and cells at days 4, 5 or 6 were further co-cultured with E12.5 fetal thymic lobes. (**C-H)** shows day 6 differentiated AGFP97 cells after 2, 4 and 7 days of co-culture with FTLs. Cell morphology was assessed on day 2 (**C, F**), 4 (**D, G**) and 7 (**E, H**) of co-culture. **F-H** shows that GFP expression was exclusively contributed by the AGFP97 ES cell-derived cells rather than the FTLs and FTLs-derived cells. Lobes only samples were also monitored and imaged on day 2 (**I**), 4 (**J**) and 7 (**K**). Magnification: A-B x20, C-H x10, I-K

x4.

	Condition A	Condition B
Medium:		
2i ADE stage (d0-d2)	N2B27+ CHIRON 3µM, Activin A 20ng/ml FGF-4 10ng/ml Heparin 1µg/ml PI-103 50nM	Same as Condition A
2i ADE stage (before co-culture)	SF5 Base+ All factors added during d0-d2 plus EGF 20ng/ml	Same as Condition A
co-culture stage	N2B27+ CHIRON 3µM Heparin 1µg/ml PI-103 50nM P/S 1/100	N2B27+ FGF-7 50ng/ml EGF 10ng/ml P/S 1/100
Observations:		
Cells (both co- and not co-cultured)	Survived, proliferated strongly (by eyes) (Figure 6.12)	Massive cell death, no obvious proliferation of remaining cells (by eyes)
FTLs	Survived, and grew well (Figure 6.12)	Survived, and grew well
Q-RT-PCR		
Genes up-regulated in +lobe co-culture compared with –lobe control	*Sox17 Plet-1 Tbx1 Pax1 Pax9 Foxn1*	*Sox17 Plet-1 Hoxa3 Pax9 Fgf7 Foxn1 IL-7*

Table 6.2 Summary of the results from the two conditions used for co-culturing ES cells with E12.5 fetal thymic lobes.

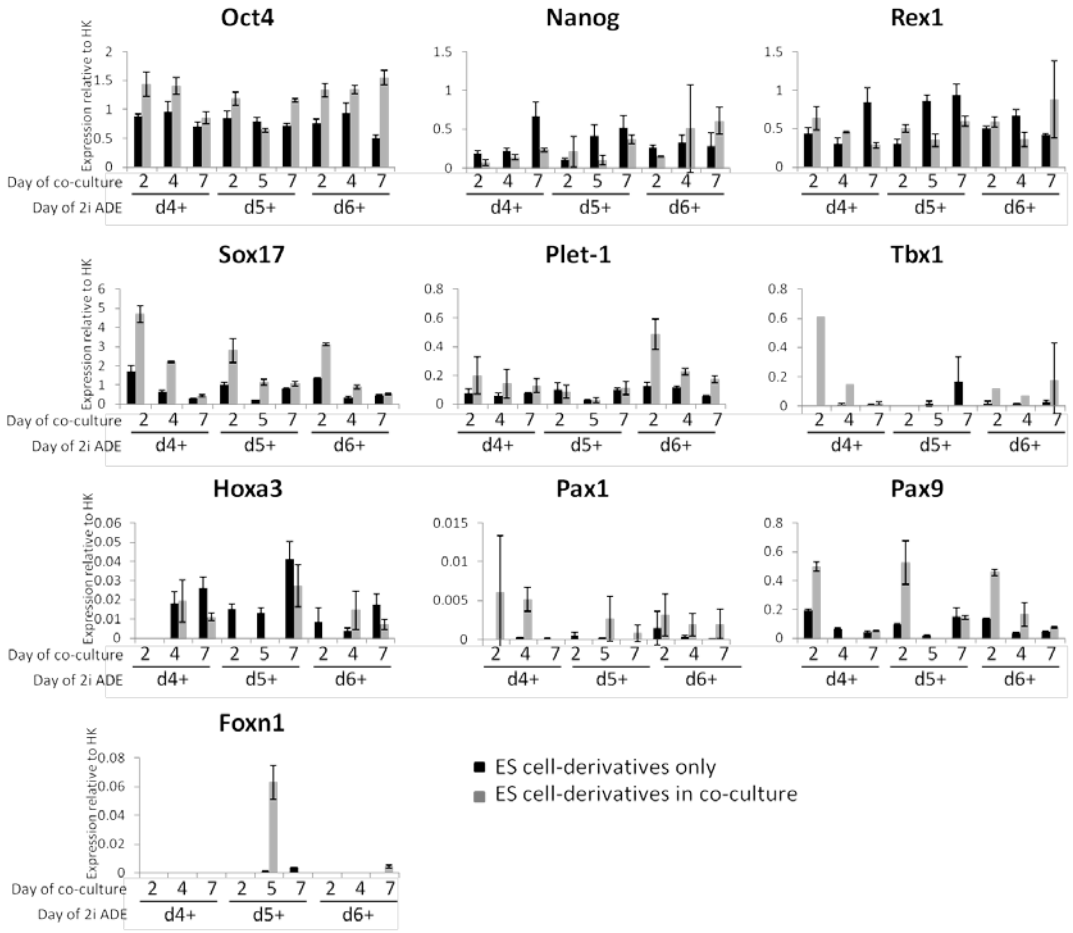

Figure 6.15 Gene expression pattern of ES cell-derivatives in co-culture condition A. AGFP 97 ES cells were differentiated using the 2i ADE method and cells were then placed into co-culture with E12.5 CBAxC57BL/6 fetal thymic lobes (FTLs) at day 4 (**d4+**), day 5 (**d5+**) and day 6 (**d6+**) of ADE differentiation, with 10 FTLs per well of a 6-well-plate. Medium was changed as described for condition A in Table 6.2. ES cell-derivatives were co-cultured with FTLs for a further 2, 4 and 7 days, then purified based on GFP expression (grey bars). "ES Cell-derivatives only" (black bars) were cultured under identical conditions as controls. Data show Q-RT-PCR analysis of cells for the markers shown. Y axis represents the expression level relative to α-tubulin. For *Oct4*, *Nanog* and *Rex1*, the expression level in ES cells was set as 1. For the other genes, the expression level in E12.5 thymic lobes was set as 1. Technical repeats n = 3, Biological repeats n = 1.

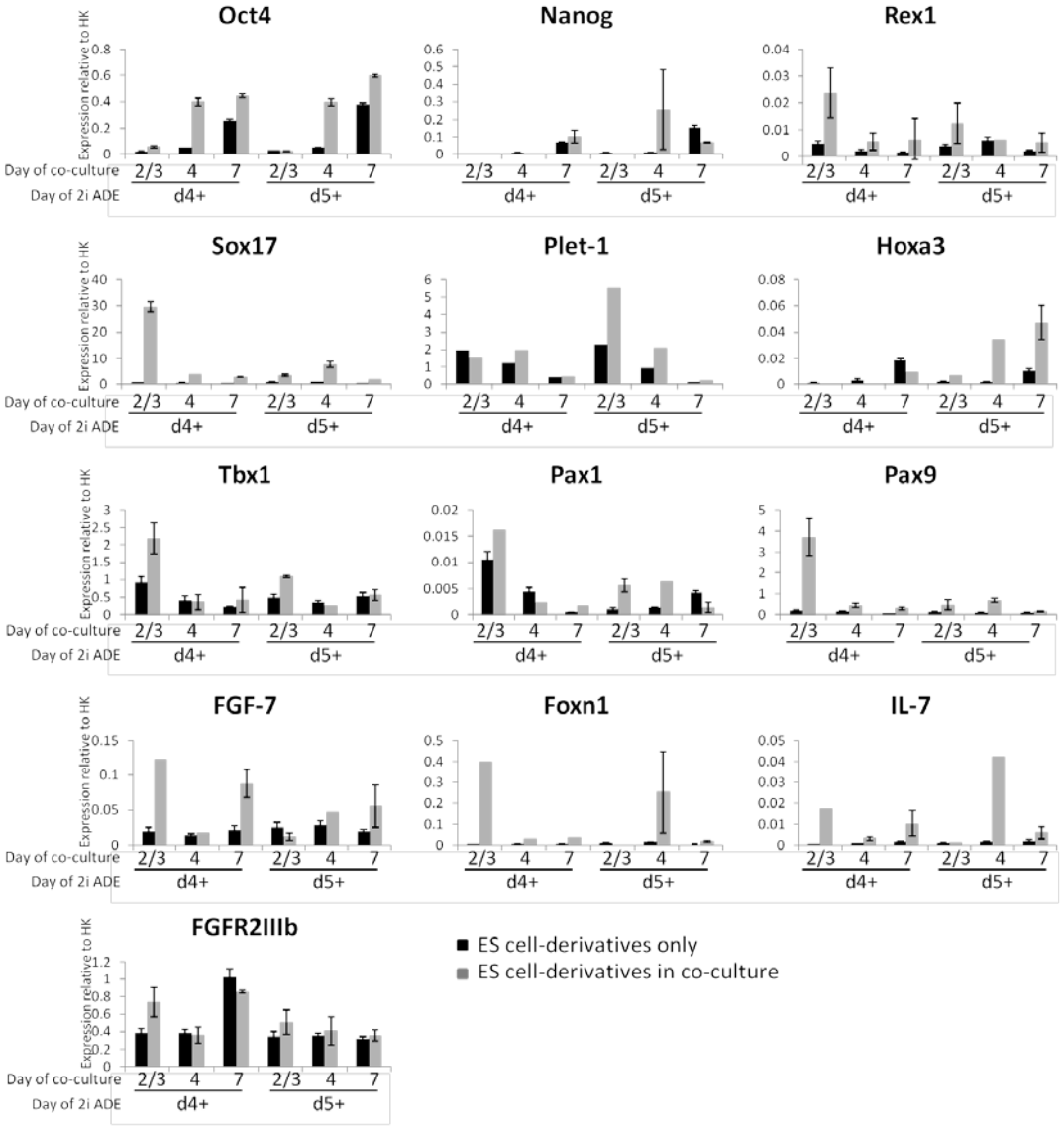

Figure 6.16 Gene expression pattern of ES cell-derivatives generated in co-culture Condition B. AGFP 97 ES cells were differentiated using the 2i ADE method and cells were then placed into co-culture with E12.5 CBAxC57BL/6 fetal thymic lobes (FTLs) at day 4 (**d4+**) and day 5 (**d5+**) of ADE differentiation. (10 FTLs were placed in one well of a 6-well-plate). Medium was changed as described for Condition B in Table 6.2. ES cell-derivatives were co-cultured with FTLs for further 2 to 3, 4 or 7 days, then purified based on GFP expression (grey bars). “ES Cell-derivatives only” (black bars) were cultured under identical conditions as controls. Data show Q-RT-PCR analysis of cells for the markers shown. Y axis represents the expression level relative to *α-tubulin*. For *Oct4*, *Nanog* and *Rex1*, expression in ES cells was set as 1. For the other genes expression in E12.5 thymic lobes was set as 1. Technical repeats n = 3, Biological repeats n = 1.

6.3 Discussion

In this chapter, I first confirmed that the 2i ADE differentiation protocol developed by our collaborators G. Morrison and A.G. Smith, can be used to generate anterior definitive endoderm marker. I further demonstrated the expression in the cell population generated via this protocol of pharyngeal endoderm markers and of genes with known roles in thymus development. Additionally, I showed that Plet-1^{+} epithelial cells were also present within the culture. Using a functional assay, I detected a possible contribution of cells generated via this protocol to TEC networks, but most cells contributed to non-thymus structures in this assay. This suggested that a more specific induction protocol was required. I therefore tested the outcome of co-culturing the differentiating cells in 2i ADE cultures with fetal thymic lobes. In these conditions, genes with known roles in thymus development were specifically induced, which strongly suggested the possibility of inducing TEPCs/TECs from ES cells by using optimised differentiation protocols.

6.3.1 ES cells to anterior definitive endoderm differentiation

The 2i ADE differentiation protocol developed by Morrison and Smith relies on TGFbeta signalling, by Activin A, to induce ADE cells from ES cells, which mimics the mechanism of endoderm formation during the normal embryonic development and also has been demonstrated to be the first step to induce the DE cells from both human and mouse ES cells (Kubo, Shinozaki et al. 2004; D'Amour, Agulnick et al. 2005). A putative mesendoderm intermediate cell population was found during Activin A-mediated endoderm induction from mouse ES cells in vitro (Tada, Era et al. 2005) and Cxcr4 was demonstrated to mark this cell population and its derivatives: mesoderm and definitive endoderm (Yasunaga, Tada et al. 2005). Recently, through a novel lineage tracing method, this intermediate ‘mesendoderm’ cell population was shown not to exist in the early mouse embryo during gastrulation (Tzouanacou, Wegener et al. 2009). Therefore, the ‘mesendoderm’ observed in vitro

in definitive endoderm induction mediated by Activin A may be a mixed cell population containing both mesoderm and definitive endoderm cells. Most cells within our 2i ADE differentiation expressed Cxcr4. Two distinct populations, Cxcr4+EpCAM+ and Cxcr4+EpCAM-, were observed as early as day 4; these may represent the epithelial cell property of DE cells and mesenchymal cell property of mesoderm cells, respectively. This would be consistent with the dual role of Activin A in induction of both mesoderm and definitive endoderm (Zorn and Wells 2009) and with the existence of both germ layers in other endoderm induction protocols (Kubo, Shinozaki et al. 2004; Yasunaga, Tada et al. 2005; Morrison, Oikonomopoulou et al. 2008). In summary, the 2i ADE differentiation protocol generated a heterogeneous population, and thus either an optimized protocol for more specific induction of ADE, or a protocol for purification of ADE cells from the mixed population is required for future work. For the former, use of a high dose of Activin A might give an improved outcome, as it has been demonstrated that high doses of Activin A lead to an enrichment of endoderm cells in the differentiating population while lower doses lead to an enrichment of mesoderm (Green and Smith 1990). For the latter, the *Hex* reporter cell line (HexRedStar) was constructed and used for test ADE specific induction protocol (Morrison, Oikonomopoulou et al. 2008), could be useful for these purposes.

6.3.2 Role of Activin A in defining anterior-posterior identity during definitive endoderm differentiation.

The time period for Activin A in inducing ADE is crucial. In human ES cells, short (3 days) Activin A treatment induces both foregut and hindgut endoderm lineage cells, while 4-5 days of Activin A treatment mainly gives rise to anterior endoderm lineage cells (Spence, Mayhew et al. 2011). However, a prolonged exposure to Activin A is not good for the very anterior foregut endoderm, such as pharyngeal endoderm derivatives. Evidence comes from a recent report that an inhibition of

TGF-beta signalling, together with the inhibition of BMP signalling, after the initial Activin A induction most efficiently induced the pharyngeal endoderm lineage from human ES cells (Green, Chen et al. 2011). In our culture conditions, Activin A was present from the beginning to the end. Although there are several other differences in our culture system, such as the presence of Fgf4, identification of the optimum time window for Activin A addition and withdraw could be crucial for future work aiming to generate TEPCs from ES cells.

6.3.3 Combination of markers for identifying ADE cells.

None of genes used here to mark the ADE can exclusively mark this lineage. *Sox17* marks both definitive endoderm and visceral endoderm (Yasunaga, Tada et al. 2005). Cxcr4 marks both definitive endoderm and mesoderm during ES cell differentiation (Yasunaga, Tada et al. 2005). Endogeneous *Hex* can be detected within mesoderm derived hematopoietic/endothelial precursors in addition to ADE derivatives (Morrison, Oikonomopoulou et al. 2008). Therefore, we tested all the three markers within the culture and believed that it would be enough to confirm the presence of ADE cells. However, a recent report suggested that *Sox17* was also expressed in some hematopoietic cells after E9.5 during mouse embryo development (Choi, Kraus et al. 2012), and Cxcr4 was expressed in both primitive endoderm (including parietal endoderm and visceral endoderm) and definitive endoderm in mouse embryo and thus was suggested as a pan-endoderm marker (Drukker, Tang et al. 2012). Therefore, the additional markers may be required to accurately distinguish the ADE cell identity. Thus, more detailed, step by step, monitoring of changes in phenotype during differentiation, and a careful selection of more gene and cell surface markers are required to better describe the differentiation process and the cell outcome.

6.3.4 The missing step in definitive endoderm induction *in vitro*.

In this 2i ADE protocol, mouse ES cells (ESCs) were initially cultured in 2i medium, a culture condition that maintains ES cells in the so called “ground state” pluripotency. This state is equated to inner cell mass (ICM) cells from 3.5 dpc mouse blastocysts (Nichols and Smith 2009; Nichols and Smith 2011). Between the ICM-stage and the occurrence of gastrulation at around 5.0 dpc, cells in the embryo pass through a state called epiblast, as described before in gastrulation section. So, to differentiate the ESCs to definitive endoderm, it may be beneficial to mimic this progression. It has been demonstrated that a new pluripotent cell type can be derived from postimplantion epiblast and, also from the preimplanted embryo. These are called epiblast stem cells (EpiSCs). It has been demonstrated that the EpiSCs represent a different pluripotency state to ESCs. EpiSCs require Activin A and FGF2 to maintain their pluripotent state, similar to human ES cells (hESCs), while ESCs require LIF-STAT3 signalling. EpiSCs also share the similar epigenetic status as hESCs, such as DNA methylation and female X choromosome inactivation, while ESCs are different (Brons, Smithers et al. 2007; Tesar, Chenoweth et al. 2007; Najm, Chenoweth et al. 2011). In consideration of the differences in cell source origins, genetic and epigenetic status, the EpiSCs are believed to represent a “primed” state which is about to differentiate, while ESCs are believed to represent a more naïve and primitive pluripotent state (Nichols and Smith 2009; Marks, Kalkan et al. 2012). So, to differentiate ESCs to definitive endoderm, the ES cells may need to pass through an EpiSCs state first, as it is these epiblast cells that are ready for gastrulation to occur. Many successful endoderm derivation protocols are based in human ES cells (D'Amour, Agulnick et al. 2005; D'Amour, Bang et al. 2006; Seguin, Draper et al. 2008; Green, Chen et al. 2011), a cell type sharing a similar genetic and epigenetic state to mouse EpiSCs (Tesar, Chenoweth et al. 2007). So, a link between ESCs and EpiSCs should be constructed, as well as applying the knowledge from human ESCs in differentiating definitive endoderm cells to mouse ESCs. It has been demonstrated that ESCs can readily differentiate to EpiSCs when cultured in Activin

A and FGF2 medium for several passages (Guo, Yang et al. 2009). However, this is apparently a low efficiency method, as the transition *in vivo* from ICM to Epiblast, is transient. To improve the efficiency of the ESCs to EpiESCs transition in terms of definitive endoderm generation, application of FGF2 may be needed in combination with Activin A. Also the "epiblast" genes, such as *Fgf5*, and "primitive streak" genes, such as *Mid1* and *Brachyury*, should be monitored during the differentiation process. Spontaneous EB formation may also be a solution as it mimics the 3D embryo structure, and may thus offer important cell-to-cell adhesion stimulus. However, it may remain a low efficiency approach, as all three germ layers would be generated. The successful derivation of EpiSCs from preimplantion 129 mouse embryos, a strain which has been previously demonstrated to be biased for ESCs derivation, relies on a different experimental procedure, such as medium formula and embryo manipulation method (Najm, Chenoweth et al. 2011). This may point to a new direction to identify key factors, especially from the extraembryonic cells, in directing the ESCs to EpiSCs transition.

6.3.5 Expression pattern of genes with known roles in thymus development.

During 2i ADE differentiation, *Tbx1*, if detectable, was found to be on from about day 4 and maintained at a low levels thereafter. This low expression in the ADE culture is not surprising, as *Tbx1* is not restricted to a particular germ layer or anterior: posterior axis position. For example, *Tbx1* expression is expressed in the mesoderm and its derivatives, such as the mesoderm core of pharyngeal arches and secondary heart field. It is also expressed the lung epithelium and the posterior sclerotome (Chapman, Garvey et al. 1996; Hu, Yamagishi et al. 2004; Xu, Morishima et al. 2004). Also, *Tbx1* has been shown to be expressed exclusively in the parathyroid domain before and after thymus/parathyroid primordium formation and is likely to regulate GCM2 expression and thus specify the parathyroid rather

than thymus fate (Liu, Yu et al. 2007). Therefore, during an optimum TEPC induction protocol, we would expect to detect Tbx1 expression in cells upstream of 3rd pharyngeal pouch cells in the differentiation hierarchy, and would then identify cells that had down-regulated Tbx1 as this is a characteristic of cells that acquire thymic epithelial cell fate *in vivo*.

It was disappointing to find only a very low level of *Pax1* expression in the differentiating cultures, as Pax1 is highly expressed in the 3rd pharyngeal pouches prior to thymus/parathyroid formation. However, *Pax1* and *Pax9* have been show to be at least partly redundant in skeleton development (Peters, Wilm et al. 1999) and more recently, in developing TECs (M. Kelly and C. Blackburn, unpublished). So the strong expression of *Pax9* may still indicate (or lead to) the presence of cells with pharyngeal pouch identity within the induced anterior definitive endoderm population.

Foxn1 is exclusively expressed within thymus and skin. Its expression was detected both in the original 2i ADE differentiation culture conditions and in the the co-cultured ES cell-derivatives, strongly suggesting the existence of TEPCs/TECs like cells. Single cell analysis, such as immunocytochemistry, would help to tell whether the Foxn1 expression reflected a general transcriptional state within the whole cell population or the high expression from certain individual cells.

As each genes described above may have a multiple expression location during embryo development, analysis of phenotype of cells at single cell level is crucial and will improve the conducted work. This will give information on what proportion of each cell expressing each marker, and which markers are expressed together. Therefore, It will be important to identify possible TEPC population.

6.3.6 Plet-1 expression during 2i ADE differentiation

The data presented here demonstrate for the first time that an epithelial cell population with Plet-1 expression can be detected during ES cell differentiation to definitive endoderm culture. Inami and colleagues reported that a small population of Plet-1^{+} cells could be found on day 14 of an induced pluripotent stem cells to thymic epithelial cells differentiation protocol (Inami, Yoshikai et al. 2011). However, my interpretation of the forward and side scatter characteristics of this population is they are not viable cells.

Although Plet-1 was found to be expressed by differentiating AGFP97 cells in 2i ADE differentiation by Q-RT-PCR, I failed to detect its expression by flow cytometry in this cell line. This may suggest that this line responds differently to the protocol in expressing this protein. Also, as the wild type E14 used here had been cultured in 2i medium for many passages (>10), but the AGFP97 ES cells had only recently been transferred from GMEM/FCS+LIF to 2i (<3 passages), the failure to detect Plet-1 in AGFP97 2i ADE differentiation through flow cytometry might reflect a difference in transcriptional and epigenetic states between these two cell lines (Marks, Kalkan et al. 2012). And thus long-term in 2i medium culture probably increase the response of cells to the inductions.

We were excited that a viable epithelial cell population with Plet-1 expression could be observed during the 2i ADE differentiation. However, Plet-1 expression is found in a variety of cell types, such as early developing kidney and pancreatic duct. It is also expressed in 1^{st} and 2^{nd} pharyngeal pouch endoderm, which gives rise to different organs. Given the heterogeneity within 2i ADE cell culture described in the result, this might explain why we found that these cells mainly contributed to structures other than the thymus regions in the functional assay. In this respect, the loss of *Hoxa3* expression within this cell population may be significant, since Hoxa3

may play a role in specifying 3pp identity (Manley and Condie 2010).

It is also important to note that Plet-1 is not expressed in the human thymus either during embryonic development or in the adult (Depreter, Blair et al. 2008). So a combination of markers, other than Plet-1, would help for isolating TEPCs from human ES cell differentiation cultures.

6.3.7 Further development of the co-culture system.

Co-culture within condition A led to cell proliferation, and maintenance of pluripotency marker expression. This was probably due to expansion of remaining undifferentiated ES cells, or reprogramming of the differentiated cells back to ES cells in response to the withdrawal of differentiation stimulus, such as Fgf4 and Activin A. CHIRON, as one of the two inhibitors which can maintain the ES cells in ground state pluripotency (Ying, Wray et al. 2008), was maintained in the co-culture medium, might have promoted the maintenance or reprogramming processes. Therefore, to exclude the interference of these cell populations, cell surface markers of pluripotency , such as Tra-1-81 and SSEA4, could be used to gate out pluripotent cells before analysis.

Co-culture within condition B led to massive cell death, but some viable cells survived. FTLs-only grew well within the same medium and thus excluded the possibility of contamination. This suggests that this condition imposes a stringent selection for growth of particular cell types. Cells co-cultured in this condition expressed relatively high levels of *Foxn1* and *IL-7*, suggesting induction or expansion of TEPCs and/or TECs by this protocol. Function testing of cells cultured in this condition is therefore a priority for future work.

Chapter 7 Concluding remarks

The overall aim of my PhD project was to generate TEPCs from ES cells. Therefore, it was very useful to understand the characteristics of TEPCs *in vivo*. In particular, it was of interest understand how stable the TEPC cell type is *in vivo* in the absence or at low levels of expression of Foxn1, a specific regulator of TEC differentiation .

Using a conditionally revertible Foxn1 mouse model, I have clearly demonstrated that a fully functional TEPC population persist postnatally up to 4 months old in the presence of low Foxn1 expression (seven percent of wild type Foxn1 mRNA levels). When *Foxn1* expression was restored to fifty percent of wild type mRNA expression levels, these persisting progenitor cells gave rise to a mature thymus structure containing both cTECs and mTECs, that was functional in terms of supporting T cell development. Further, statistically-based analysis of tamoxifen-independent reversion of the $Foxn1^{R}$ allele in *R/-;CreERt2* mice indicated that in this model, TEPCs could persist until between 6 months and 10 months old *in vivo*.

To my knowledge, this is the first report demonstrating that a functional TEPC population can persist long-term *in vivo* in the presence of low-level Foxn1 expression. Bleul and colleagues previously demonstrated that clonal reactivation of a Foxn1 null allele in neonatal mice up to 14 days old resulted in generation of an intact thymus (Bleul, Corbeaux et al. 2006). My data considerably extend this finding, demonstrating that at low levels of Foxn1-expression, at least some cells in the TEPC population that arises during fetal development maintain a stable and functional TEPC identity until at least 6 months old. These findings provided important *in vivo* information relevant to the induction and/or expansion of stable TEPCs from ES cells *in vitro*.

In the fetal thymus, analysis of *Foxn1*$^{R/-}$ mice has demonstrated that, although the differentiation of TEC was blocked so that the thymus was never able to support T cell development, the earliest cortical and medullary cell lineage specification events occurred (Nowell et al 2011). Furthermore, medullary lineage-specific markers were expressed in a regionally restricted manner in the complete absence of Foxn1 expression (Nowell et al 2011). Thus it was also important to know whether these committed cTEPCs and mTEPCs could persist, and if so, for how long. Using our conditional revertible *Foxn1* mouse model, I failed to detect generation of structures containing only cTECs or only mTECs upon reversion of the *Foxn1*^{R} allele. This suggested that either only the common TEPCs could persist *in vivo* until the postnatal stage, or that generation of the cortical or medullary compartments depend on each other (Figure 7.1). Further work is required to judge which of these possibilities is true; the outcome of this analysis would be very important for projects aiming to direct ES cells differentiation to thymic epithelial lineage-specified progenitor cells.

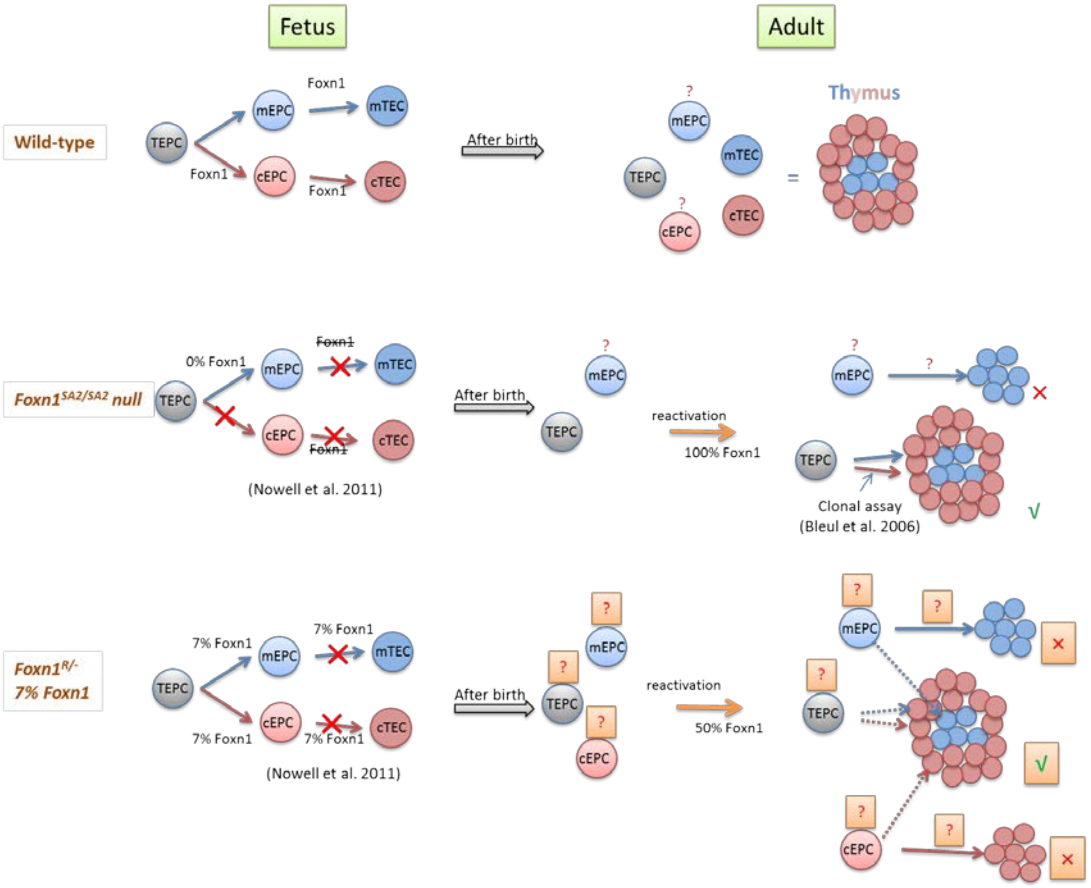

Figure 7.1 Early thymic epithelial lineage specification and persistence of common or lineage restricted progenitor cells at postnatal stage – summary of findings based on Figure 1.4. Dotted arrows represent the possible explanations. Thymus with both cortex and medulla was observed (Squared "√"). Cortical or medullary only areas were not observed in reactivated *Foxn1*$^{R/-}$*;CreERT2* thymus and thus marked by squared "×".

ES cells have the potential to generate all of the somatic cell types and are thus believed to hold great promise for regenerative medicine. Although the pluripotency of ES cells can be easily demonstrated by *in vivo* chimera analysis, determining how to generate a specific cell type by directed differentiation *in vitro* is complicated and has not been achieved for many cell types, including the TECs. In this thesis, I have demonstrated that *Foxn1* expression can be observed in ES cell-derived cells in spontaneously formed EBs, and appear to be enriched by co-culture of EBs with

fetal thymic lobes (FTL). My work, together with previous findings from this laboratory (where *Pax1* expression was also confirmed in the *Foxn1* expressing cells of the co-cultured EBs and thus exclude the possibility of skin keratinocytes contribution), strongly indicated the possibility of using ES cells to generate TECs or TEC-like cells.

As the epithelial component of the thymus is entirely derived from the third pharyngeal pouch, induction of ES cells to regionally specified anterior definitive endoderm appeared an appropriate first step for inducing TEPCs. In collaboration with G. Morrison (University of Cambridge), I used a novel ADE-specific induction protocol to differentiate ES cells to ADE cells in a monolayer adhesion culture (2i ADE differentiation). The third pharyngeal pouch (3pp) genes, such as Tbx1, Hoxa3 and Pax1 were induced, and suggesting the existence of cells with 3pp identity in the 2i ADE cell cultures. Plet-1 was also induced or up-regulated during the ADE induction. Moreover, a considerable Plet-1^{+}EpCAM^{+} cell population was observed by flow cytometry at later stages of culture. It has previously been demonstrated that cells expressing these markers in the thymic primodium at E12.5 can give rise to a functional thymus when transplanted under the kidney capsule (Bennett, Farley et al. 2002), and a single cell from this cell population could give rise to both cTECs and mTECs (Rossi, Jenkinson et al. 2006). Thus, this is the first demonstration, to my knowledge, that a cell population with the same cell surface marker expression profile as TEPCs can be induced from ES cells.

Further analysis of gene expression, and functional testing of the Plet-1^{+}EpCAM^{+} cell population, indicated that this population of cells may contain cell lineages other than TEPCs (Plet-1^{+}EpCAM^{+} cell population showed a decrease in 3pp and TEPC related gene expressions in comparison with the whole cell population in 2i ADE differentiation culture before sorting. Plet-1^{+}EpCAM^{+} cell population, when

reaggregated with the whole dissociated FTLs cells and grafted under the kidney capsule, mainly formed tube-like epithelial structure). However, given that 3pp related genes were expressed in the population of differentiated cells generated by the 2i ADE differentiation culture, and that some contribution of the ES-derived Plet-1^{+}EpCAM^{+} cells to TEC networks in the functional test was observed, it is possible that some of the Plet-1^{+}EpCAM^{+} cells may be TEPCs. Therefore, a better, thymus-specific induction of the differentiating ES cells within the 2i ADE differentiation is needed in order to generate TEPCs or TECs more efficiently. Several 3pp related genes were found to be up-regulated immediately in the differentiating ES cells when co-cultured with the FTL. Moreover, when "TEPC medium (i.e. basal medium supplemented with Egf and Fgf7)" was used for the co-culture, a considerable expression level of *Foxn1* and *IL-7* was detected in the co-cultured ES cell-derivatives. These data suggest that both FTL stimulation and the appropriate culture medium are important for inducing TEPCs/TECs. Functional testing of these co-cultured ES cell-derivatives is now needed. As *Foxn1* is also expressed in the skin, although it is unlikely that ectodermal lineages would be induced in specific ADE-induction conditions and subsequent co-cultures, the absence of gene expression related to skin needs to be confirmed to further indicate the TEPC/TEC identity of Foxn1 expressing cells. Analysis of the co-expression of Foxn1 and markers known to be expressed in TEPC and/or TEC, but not in skin keratinocyte lineages would also address this issue.

Recently, a protocol for generating anterior foregut endoderm (AFE) from human ES cells, has been reported (Green, Chen et al. 2011), and the anterior foregut endoderm derivatives such as thyroid and lung were demonstrated to be induced using this protocol (Longmire, Ikonomou et al. 2012; Mou, Zhao et al. 2012). Data from mouse, human and induced pluripotent stem (iPS) cells collectively indicate that inhibition of transforming growth factor (TGF-β) signalling after the definitive

endoderm specification results in a highly enriched AFE population. In contrast to ADE, which also contributes to pancreas and liver generation in embryo development, AFE has a more anterior character, and its contribution is limited to pharyngeal endoderm derivatives, such as thyroid, parathyroid and thymus, and respiratory system, such as trachea and lung. When this PhD project started, no AFE specific protocol had been published, and the ADE protocol had just been developed. It would be interesting to test whether the inhibition of TGF-β signalling in the later stages of our 2i ADE protocol results in induction of stronger induction of the 3pp-related genes we have already detected, and further, whether 3pp-like cells can be generated. However, the difference between human ES cells and mouse ES cells in response to signalling pathway manipulation needs to be considered. For example, bone morphogenic protein (BMP) signalling inhibition is required together with inhibition of TGF-β signalling to induce AFE in human ES, but it is not required in mouse ES cells and human iPS (Longmire, Ikonomou et al. 2012; Mou, Zhao et al. 2012). Moreover, in one of my recently conducted cultures, inhibition of BMP and TGF-β signalling at later stage of 2i ADE differentiation, resulted predominantly in generation of mesoderm cells. This suggested that TGF-β signalling can play different roles depending on the different cell states and when in cooperation with different factors, such as FGF4 and PI-103 in the 2i ADE differentiation protocol. These factors will need to be considered in further work aiming to develop an optimized protocol for generating TEPCs/TECs.

In this study, I have demonstrated the long persistence of TEPCs in mice that can express only very low levels of Foxn1. I have also characterized several ES cell differentiation protocols, with respect to their ability to support generation of cells expressing 3pp and TEPC related genes. Through consideration of the outcome of testing existing protocols, I then developed an improved protocol for supporting development of cells expressing 3pp and TEPC related genes. I showed that several

genes known to be required for thymus development were induced, and also demonstrated the expression of cell surface markers characteristic of early thymus-lineage cells, during ES cell differentiation in this novel protocol. Collectively, these results represent an important advance towards development of a protocol allowing differentiation of ES cells to thymic epithelial progenitor cells at high efficiency.

Reference

Alexander, T., C. Nolte, et al. (2009). "Hox genes and segmentation of the hindbrain and axial skeleton." Annu Rev Cell Dev Biol **25**: 431-456.

Anderson, G. and E. J. Jenkinson (2001). "Lymphostromal interactions in thymic development and function." Nat. Rev. Immunol. **1**: 31-40.

Ardavi´n, C. (1997). "Thymic dendritic cells." Immunology Today **18**(7): 350-361.

Beattie, G. M., A. D. Lopez, et al. (2005). "Activin A Maintains Pluripotency of Human Embryonic Stem Cells in the Absence of Feeder Layers." Stem Cells **23**(4): 489-495.

Bennett, A. R., A. Farley, et al. (2002). "Identification and Characterization of Thymic Epithelial Progenitor Cells." Immunity **16**(6): 803-814.

Blackburn, C. C., C. L. Augustine, et al. (1996). "The nu gene acts cell-autonomously and is required for differentiation of thymic epithelial progenitors." Proceedings of the National Academy of Sciences **93**(12): 5742-5746.

Blackburn, C. C. and N. R. Manley (2004). "Developing a new paradigm for thymus organogenesis." Nat Rev Immunol **4**(4): 278-289.

Bleul, C. C., T. Corbeaux, et al. (2006). "Formation of a functional thymus initiated by a postnatal epithelial progenitor cell." Nature **441**(7096): 992-996.

Bollag, R. J., Z. Siegfried, et al. (1994). "An ancient family of embryonically expressed mouse genes sharing a conserved protein motif with the T locus." Nat Genet **7**(3): 383-389.

Bonfanti, P., S. Claudinot, et al. (2010). "Microenvironmental reprogramming of thymic epithelial cells to skin multipotent stem cells." Nature **466**(7309): 978-982.

Borowiak, M., R. Maehr, et al. (2009). "Small molecules efficiently direct endodermal differentiation of mouse and human embryonic stem cells." Cell Stem Cell **4**(4): 348-358.

Boyd, R. L., C. L. Tucek, et al. (1993). "The thymic microenvironment." Immunology Today **14**(9): 445-459.

Brons, I. G. M., L. E. Smithers, et al. (2007). "Derivation of pluripotent epiblast stem cells from mammalian embryos." Nature **448**(7150): 191-195.

Buckingham, M. and F. Relaix (2007). "The role of Pax genes in the development of tissues and organs: Pax3 and Pax7 regulate muscle progenitor cell functions." Annu Rev Cell Dev Biol **23**: 645-673.

Buehr, M., S. Meek, et al. (2008). "Capture of Authentic Embryonic Stem Cells from Rat Blastocysts." Cell **135**(7): 1287-1298.

Chambers, I., J. Silva, et al. (2007). "Nanog safeguards pluripotency and mediates germline development." Nature **450**(7173): 1230-1234.

Chapman, D. L., N. Garvey, et al. (1996). "Expression of the T-box family genes, Tbx1–Tbx5, during early mouse development." Developmental Dynamics **206**(4): 379-390.

Chen, S., M. Borowiak, et al. (2009). "A small molecule that directs differentiation of human ESCs into the pancreatic lineage." Nat Chem Biol **5**(4): 258-265.

Chinn, I. K., C. C. Blackburn, et al. (2012). "Changes in primary lymphoid organs with aging." Seminars in Immunology **24**(5): 309-320.

Choi, E., M. R. C. Kraus, et al. (2012). "Dual Lineage-Specific Expression of Sox17 During Mouse Embryogenesis." Stem Cells **30**(10): 2297-2308.

Clegg, C. H., J. T. Rulffes, et al. (1996). "Regulation of an extrathymic T-cell development pathway by oncostatin M." Nature **384**(6606): 261-263.

D'Amour, K. A., A. D. Agulnick, et al. (2005). "Efficient differentiation of human embryonic stem cells to definitive endoderm." Nat Biotechnol **23**(12): 1534-1541.

D'Amour, K. A., A. G. Bang, et al. (2006). "Production of pancreatic hormone-expressing endocrine cells from human embryonic stem cells." Nat Biotechnol **24**(11): 1392-1401.

Depreter, M. G., N. F. Blair, et al. (2008). "Identification of Plet-1 as a specific marker of early thymic epithelial progenitor cells." Proc Natl Acad Sci U S A **105**(3): 961-966.

Dessimoz, J., R. Opoka, et al. (2006). "FGF signalling is necessary for establishing gut tube domains alongthe anterior–posterior axis in vivo." Mechanisms of Development **123**(1): 42-55.

Drukker, M., C. Tang, et al. (2012). "Isolation of primitive endoderm, mesoderm, vascular endothelial and trophoblast progenitors from human pluripotent stem cells." Nat Biotech **30**(6): 531-542.

Dudakov, J. A., A. M. Hanash, et al. (2012). "Interleukin-22 Drives Endogenous Thymic Regeneration in Mice." Science **336**(6077): 91-95.

Duijvestijn, A. M. and E. C. M. Hoefsmit (1981). "Ultrastructure of the rat thymus: The micro-environment of T-lymphocyte maturation." Cell and Tissue Research **218**(2): 279-292.

Esashi, E., T. Sekiguchi, et al. (2003). "Cutting edge: A possible role for CD4(+) thymic macrophages as professional scavengers of apoptotic thymocytes." Journal of Immunology **171**(6): 2773-2777.

Evans, M. J. and M. H. Kaufman (1981). "Establishment in culture of pluripotential cells from mouse embryos." Nature **292**(5819): 154-156.

Fontaineperus, J. C., F. M. Calman, et al. (1981). "SEEDING OF THE 10-DAY MOUSE EMBRYO THYMIC RUDIMENT BY LYMPHOCYTE PRECURSORS INVITRO." Journal of Immunology **126**(6): 2310-2316.

Foster, K., J. Sheridan, et al. (2008). "Contribution of Neural Crest-Derived Cells in the Embryonic and Adult Thymus." The Journal of Immunology **180**(5): 3183-3189.

Frank, J., C. Pignata, et al. (1999). "Exposing the human nude phenotype." Nature **398**(6727): 473-474.

Fry, T. J. and C. L. Mackall (2002). "Interleukin-7: from bench to clinic." Blood **99**(11): 3892-3904.

Ganju, R. K., S. A. Brubaker, et al. (1998). "The α-Chemokine, Stromal Cell-derived Factor-1α, Binds to the Transmembrane G-protein-coupled CXCR-4 Receptor and Activates Multiple Signal Transduction Pathways." Journal of Biological Chemistry 273(36): 23169-23175.

Gerrard, L., D. Zhao, et al. (2005). "Stably Transfected Human Embryonic Stem Cell Clones Express OCT4-Specific Green Fluorescent Protein and Maintain Self-Renewal and Pluripotency." Stem Cells **23**(1): 124-133.

Gilchrist, D. S., J. Ure, et al. (2003). "Labeling of hematopoietic stem and progenitor cells in novel activatable EGFP reporter mice." Genesis **36**(3): 168-176.

Godfrey, D. I., J. Kennedy, et al. (1993). "A developmental pathway involving four phenotypically and functionally distinct subsets of CD3-CD4-CD8- triple-negative adult mouse thymocytes defined by CD44 and CD25 expression." The Journal of Immunology **150**(10): 4244-4252.

Gonzalez, B., S. Denzel, et al. (2009). "EpCAM is involved in maintenance of the murine embryonic stem cell phenotype." Stem Cells **27**(8): 1782-1791.

Gordon, J., A. R. Bennett, et al. (2001). "Gcm2 and Foxn1 mark early parathyroid- and thymus-specific domains in the developing third pharyngeal pouch." Mechanisms of Development **103**(1–2): 141-143.

Gordon, J., V. A. Wilson, et al. (2004). "Functional evidence for a single endodermal origin for the thymic epithelium." Nat Immunol **5**(5): 546-553.

Gouon-Evans, V., L. Boussemart, et al. (2006). "BMP-4 is required for hepatic specification of mouse embryonic stem cell-derived definitive endoderm." Nat Biotech **24**(11): 1402-1411.

Grapin-Botton, A. and D. A. Melton (2000). "Endoderm development: from patterning to organogenesis." Trends in Genetics **16**(3): 124-130.

Gray, D. H. D., A. L. Fletcher, et al. (2008). "Unbiased analysis, enrichment and purification of thymic stromal cells." J Immunol Methods **329**(1–2): 56-66.

Gray, D. H. D., N. Seach, et al. (2006). "Developmental kinetics, turnover, and stimulatory capacity of thymic epithelial cells." Blood **108**(12): 3777-3785.

Green, J. B. A. and J. C. Smith (1990). "Graded changes in dose of a Xenopus activin A homologue elicit stepwise transitions in embryonic cell fate." Nature **347**(6291): 391-394.

Green, M. D., A. Chen, et al. (2011). "Generation of anterior foregut endoderm from

human embryonic and induced pluripotent stem cells." Nat Biotechnol **29**(3): 267-272.

Griffith, A. V., K. Cardenas, et al. (2009). "Increased thymus- and decreased parathyroid-fated organ domains in Splotch mutant embryos." Dev Biol **327**(1): 216-227.

Griffith, A. V., M. Fallahi, et al. (2012). "Persistent degenerative changes in thymic organ function revealed by an inducible model of organ regrowth." Aging Cell **11**(1): 169-177.

Guo, G., J. Yang, et al. (2009). "Klf4 reverts developmentally programmed restriction of ground state pluripotency." Development **136**(7): 1063-1069.

Hamazaki, Y., H. Fujita, et al. (2007). "Medullary thymic epithelial cells expressing Aire represent a unique lineage derived from cells expressing claudin." Nat Immunol **8**(3): 304-311.

Hameyer, D., A. Loonstra, et al. (2007). "Toxicity of ligand-dependent Cre recombinases and generation of a conditional Cre deleter mouse allowing mosaic recombination in peripheral tissues." Physiological Genomics **31**(1): 32-41.

Hare, K. J., E. J. Jenkinson, et al. (2000). "An Essential Role for the IL-7 Receptor During Intrathymic Expansion of the Positively Selected Neonatal T Cell Repertoire." The Journal of Immunology **165**(5): 2410-2414.

Harman, B. C., E. J. Jenkinson, et al. (2003). "Entry into the Thymic Microenvironment Triggers Notch Activation in the Earliest Migrant T Cell Progenitors." The Journal of Immunology **170**(3): 1299-1303.

Hay, D. C., D. Zhao, et al. (2008). "Efficient Differentiation of Hepatocytes from Human Embryonic Stem Cells Exhibiting Markers Recapitulating Liver Development In Vivo." Stem Cells **26**(4): 894-902.

Hay, D. C., D. Zhao, et al. (2007). "Direct differentiation of human embryonic stem cells to hepatocyte-like cells exhibiting functional activities." Cloning and Stem Cells **9**(1): 51-62.

Hetzer-Egger, C., M. Schorpp, et al. (2002). "Thymopoiesis requires Pax9 function in thymic epithelial cells." Eur J Immunol **32**(4): 1175-1181.

Hidaka, K., J.-K. Lee, et al. (2003). "Chamber-specific differentiation of Nkx2.5-positive cardiac precursor cells from murine embryonic stem cells." The FASEB Journal.

Hidaka, K., T. Nitta, et al. (2010). "Differentiation of pharyngeal endoderm from mouse embryonic stem cell." Stem Cells Dev **19**(11): 1735-1743.

Higashi, A. Y., T. Ikawa, et al. (2009). "Direct Hematological Toxicity and Illegitimate Chromosomal Recombination Caused by the Systemic Activation of CreERT2." The Journal of Immunology **182**(9): 5633-5640.

Hozumi, K., N. Negishi, et al. (2004). "Delta-like 1 is necessary for the generation of marginal zone B cells but not T cells in vivo." Nat Immunol **5**(6): 638-644.

Hu, T., H. Yamagishi, et al. (2004). "Tbx1 regulates fibroblast growth factors in the anterior heart field through a reinforcing autoregulatory loop involving

forkhead transcription factors." Development **131**(21): 5491-5502.
Inami, Y., T. Yoshikai, et al. (2011). "Differentiation of induced pluripotent stem cells to thymic epithelial cells by phenotype." Immunol Cell Biol **89**(2): 314-321.
Itoi, M., H. Kawamoto, et al. (2001). "Two distinct steps of immigration of hematopoietic progenitors into the early thymus anlage." International Immunology **13**(9): 1203-1211.
Jenkinson, W. E., S. W. Rossi, et al. (2007). "PDGFRα-expressing mesenchyme regulates thymus growth and the availability of intrathymic niches." Blood **109**(3): 954-960.
Jerome, L. A. and V. E. Papaioannou (2001). "DiGeorge syndrome phenotype in mice mutant for the T-box gene, Tbx1." Nat Genet **27**(3): 286-291.
Jiang, R., Y. Lan, et al. (1998). "Defects in limb, craniofacial, and thymic development in Jagged2 mutant mice." Genes & Development **12**(7): 1046-1057.
Jordan, V. C. (2003). "Tamoxifen: a most unlikely pioneering medicine." Nat Rev Drug Discov **2**(3): 205-213.
Kampinga, J., S. Berges, et al. (1989). "Thymic epithelial antibodies: immunohistological analysis and introduction of nomenclature." Thymus **13**(3-4): 165-173.
Kasahara, H. (1998). "Cardiac and Extracardiac Expression of Csx/Nkx2.5 Homeodomain Protein." Circulation Research.
Klug, D. B., C. Carter, et al. (1998). "Interdependence of cortical thymic epithelial cell differentiation and T-lineage commitment." Proceedings of the National Academy of Sciences **95**(20): 11822-11827.
Klug, D. B., C. Carter, et al. (2002). "Cutting Edge: Thymocyte-Independent and Thymocyte-Dependent Phases of Epithelial Patterning in the Fetal Thymus." The Journal of Immunology **169**(6): 2842-2845.
Klug, D. B., E. Crouch, et al. (2000). "Transgenic Expression of Cyclin D1 in Thymic Epithelial Precursors Promotes Epithelial and T Cell Development." The Journal of Immunology **164**(4): 1881-1888.
Koch, U., E. Fiorini, et al. (2008). "Delta-like 4 is the essential, nonredundant ligand for Notch1 during thymic T cell lineage commitment." The Journal of Experimental Medicine **205**(11): 2515-2523.
Krumlauf, R. (1994). "Hox genes in vertebrate development." Cell **78**(2): 191-201.
Kubo, A., K. Shinozaki, et al. (2004). "Development of definitive endoderm from embryonic stem cells in culture." Development **131**(7): 1651-1662.
Kunath, T., M. K. Saba-El-Leil, et al. (2007). "FGF stimulation of the Erk1/2 signalling cascade triggers transition of pluripotent embryonic stem cells from self-renewal to lineage commitment." Development **134**(16): 2895-2902.
Lai, L. and J. Jin (2009). "Generation of thymic epithelial cell progenitors by mouse embryonic stem cells." Stem Cells **27**(12): 3012-3020.
Le Lièvre, C. S. and N. M. Le Douarin (1975). "Mesenchymal derivatives of the neural crest: analysis of chimaeric quail and chick embryos." Journal of Embryology and Experimental Morphology **34**(1): 125-154.

Linton, P. J. and K. Dorshkind (2004). "Age-related changes in lymphocyte development and function." Nat Immunol **5**(2): 133-139.

Liu, Z., S. Yu, et al. (2007). "Gcm2 is required for the differentiation and survival of parathyroid precursor cells in the parathyroid/thymus primordia." Dev Biol **305**(1): 333-346.

Longmire, T. A., L. Ikonomou, et al. (2012). "Efficient derivation of purified lung and thyroid progenitors from embryonic stem cells." Cell Stem Cell **10**(4): 398-411.

Maillard, I., T. Fang, et al. (2005). Regulation of lymphoid development, differentiation, and function by the notch pathway. Annu Rev Immunol. Palo Alto, Annual Reviews. **23:** 945-974.

Mancini, S. J. C., N. Mantei, et al. (2005). "Jagged1-dependent Notch signaling is dispensable for hematopoietic stem cell self-renewal and differentiation." Blood **105**(6): 2340-2342.

Manley, N. R. and M. R. Capecchi (1995). "The role of Hoxa-3 in mouse thymus and thyroid development." Development **121**(7): 1989-2003.

Manley, N. R. and M. R. Capecchi (1998). "HoxGroup 3 Paralogs Regulate the Development and Migration of the Thymus, Thyroid, and Parathyroid Glands." Dev Biol **195**(1): 1-15.

Manley, N. R. and B. G. Condie (2010). Transcriptional Regulation of Thymus Organogenesis and Thymic Epithelial Cell Differentiation. Progress in Molecular Biology and Translational Science. L. Adrian, Academic Press. **92:** 103-120.

Manley, N. R. and B. G. Condie (2010). "Transcriptional Regulation of Thymus Organogenesis and Thymic Epithelial Cell Differentiation." **92**: 103-120.

Marks, H., T. Kalkan, et al. (2012). "The Transcriptional and Epigenomic Foundations of Ground State Pluripotency." Cell **149**(3): 590-604.

Martin, G. R. (1981). "Isolation of a pluripotent cell line from early mouse embryos cultured in medium conditioned by teratocarcinoma stem cells." Proceedings of the National Academy of Sciences **78**(12): 7634-7638.

McGrath, K. E., A. D. Koniski, et al. (1999). "Embryonic Expression and Function of the Chemokine SDF-1 and Its Receptor, CXCR4." Dev Biol **213**(2): 442-456.

McLean, A. B., K. A. D'Amour, et al. (2007). "Activin a efficiently specifies definitive endoderm from human embryonic stem cells only when phosphatidylinositol 3-kinase signalling is suppressed." Stem Cells **25**(1): 29-38.

Milicevic, N. M., Z. Milicevic, et al. (1987). "Ultrastructural-study of macrophages in the rat thymus, with special reference to the corticomedullary zone." Journal of Anatomy **150**: 89-98.

Miller, J. F. A. P. (1961). "IMMUNOLOGICAL FUNCTION OF THE THYMUS." The Lancet **278**(7205): 748-749.

Min, H., E. Montecino-Rodriguez, et al. (2006). "Reassessing the role of growth hormone and sex steroids in thymic involution." Clinical Immunology **118**(1):

117-123.
Mori, K., M. Itoi, et al. (2010). "Foxn1 is essential for vascularization of the murine thymus anlage." Cell Immunol **260**(2): 66-69.
Morrison, G. M., I. Oikonomopoulou, et al. (2008). "Anterior definitive endoderm from ESCs reveals a role for FGF signalling." Cell Stem Cell **3**(4): 402-415.
Mou, H., R. Zhao, et al. (2012). "Generation of Multipotent Lung and Airway Progenitors from Mouse ESCs and Patient-Specific Cystic Fibrosis iPSCs." Cell Stem Cell **10**(4): 385-397.
Mountford, P., B. Zevnik, et al. (1994). "Dicistronic targeting constructs: reporters and modifiers of mammalian gene expression." Proceedings of the National Academy of Sciences **91**(10): 4303-4307.
Murry, C. E. and G. Keller (2008). "Differentiation of embryonic stem cells to clinically relevant populations: lessons from embryonic development." Cell **132**(4): 661-680.
Najm, Fadi J., Josh G. Chenoweth, et al. (2011). "Isolation of Epiblast Stem Cells from Preimplantation Mouse Embryos." Cell Stem Cell **8**(3): 318-325.
Nehls, M., B. Kyewski, et al. (1996). "Two genetically separable steps in the differentiation of thymic epithelium." Science **272**(5263): 886-889.
Nehls, M., D. Pfeifer, et al. (1994). "New member of the winged-helix protein family disrupted in mouse and rat nude mutations." Nature **372**(6501): 103-107.
Nichols, J. and A. Smith (2009). "Naive and Primed Pluripotent States." Cell Stem Cell **4**(6): 487-492.
Nichols, J. and A. Smith (2011). "The origin and identity of embryonic stem cells." Development **138**(1): 3-8.
Nijhof, J. G. W., K. M. Braun, et al. (2006). "The cell-surface marker MTS24 identifies a novel population of follicular keratinocytes with characteristics of progenitor cells." Development **133**(15): 3027-3037.
Niwa, H., K. Ogawa, et al. (2009). "A parallel circuit of LIF signalling pathways maintains pluripotency of mouse ES cells." Nature **460**(7251): 118-122.
Nowell, C. S., N. Bredenkamp, et al. (2011). "Foxn1 regulates lineage progression in cortical and medullary thymic epithelial cells but is dispensable for medullary sublineage divergence." PLoS Genet **7**(11): e1002348.
Nowell, C. S., A. M. Farley, et al. (2007). "Thymus organogenesis and development of the thymic stroma." Methods in molecular biology (Clifton, N.J.) **380**: 125-162.
Odaka, C. and T. Mizuochi (2002). "Macrophages are involved in DNA degradation of apoptotic cells in murine thymus after administration of hydrocortisone." Cell Death and Differentiation **9**(2): 104-112.
Ornitz, D. M., J. Xu, et al. (1996). "Receptor Specificity of the Fibroblast Growth Factor Family." Journal of Biological Chemistry **271**(25): 15292-15297.
Owen, J. J. T. and M. A. Ritter (1969). "Tissue interaction in development of thymus lymphocytes." Journal of Experimental Medicine **129**(2): 431-&.
Peschon, J. J., P. J. Morrissey, et al. (1994). "Early lymphocyte expansion is severely

impaired in interleukin 7 receptor-deficient mice." The Journal of Experimental Medicine **180**(5): 1955-1960.

Peters, H., B. Wilm, et al. (1999). "Pax1 and Pax9 synergistically regulate vertebral column development." Development **126**(23): 5399-5408.

Petrie, H. T. (2002). "Role of thymic organ structure and stromal composition in steady-state postnatal T-cell production." Immunological Reviews **189**(1): 8-20.

Petrie, H. T. (2003). "Cell migration and the control of post-natal T-cell lymphopoiesis in the thymus." Nat Rev Immunol **3**(11): 859-866.

Petrie, H. T. and J. C. Zuniga-Pflucker (2007). "Zoned out: functional mapping of stromal signalling microenvironments in the thymus." Annu Rev Immunol **25**: 649-679.

Radtke, F., A. Wilson, et al. (1999). "Deficient T Cell Fate Specification in Mice with an Induced Inactivation of Notch1." Immunity **10**(5): 547-558.

Revest, J.-M., R. K. Suniara, et al. (2001). "Development of the Thymus Requires Signaling Through the Fibroblast Growth Factor Receptor R2-IIIb." The Journal of Immunology **167**(4): 1954-1961.

Ritter, M. A. and R. L. Boyd (1993). "Development in the thymus: it takes two to tango." Immunology Today **14**(9): 462-469.

Ritter, M. A., C. A. Sauvage, et al. (1981). "The human thymus micro-environment - invivo identification of thymic nurse cells and other antigenically-distinct sub-populations of epithelial-cells." Immunology **44**(3): 439-446.

Rodewald, H.-R., S. Paul, et al. (2001). "Thymus medulla consisting of epithelial islets each derived from a single progenitor." Nature **414**(6865): 763-768.

Rossi, S. W., W. E. Jenkinson, et al. (2006). "Clonal analysis reveals a common progenitor for thymic cortical and medullary epithelium." Nature **441**(7096): 988-991.

Savino, W., D. M. S. Villa-Verde, et al. (1993). "Extracellular matrix proteins in intrathymic T-cell migration and differentiation?" Immunology Today **14**(4): 158-161.

Schmitt, T. M. and J. C. Zúñiga-Pflücker (2002). "Induction of T Cell Development from Hematopoietic Progenitor Cells by Delta-like-1 In Vitro." Immunity **17**(6): 749-756.

Seguin, C. A., J. S. Draper, et al. (2008). "Establishment of endoderm progenitors by SOX transcription factor expression in human embryonic stem cells." Cell Stem Cell **3**(2): 182-195.

Shakib, S., G. E. Desanti, et al. (2009). "Checkpoints in the Development of Thymic Cortical Epithelial Cells." The Journal of Immunology **182**(1): 130-137.

Sheridan, J. M., S. Taoudi, et al. (2009). "A novel method for the generation of reaggregated organotypic cultures that permits juxtaposition of defined cell populations." Genesis **47**(5): 346-351.

Smith, A. G. (2001). "Embryo-derived stem cells: Of mice and men." Annu Rev Cell Dev Biol **17**: 435-462.

Spence, J. R., C. N. Mayhew, et al. (2011). "Directed differentiation of human pluripotent stem cells into intestinal tissue in vitro." Nature **470**(7332): 105-109.

Starr, T. K., S. C. Jameson, et al. (2003). "Positive and negative selection of T cells." Annu Rev Immunol **21**: 139-176.

Su, D., S. Ellis, et al. (2001). "Hoxa3 and pax1 regulate epithelial cell death and proliferation during thymus and parathyroid organogenesis." Dev Biol **236**(2): 316-329.

Tada, S., T. Era, et al. (2005). "Characterization of mesendoderm: a diverging point of the definitive endoderm and mesoderm in embryonic stem cell differentiation culture." Development **132**(19): 4363-4374.

ten Berge, D., W. Koole, et al. (2008). "Wnt signalling mediates self-organization and axis formation in embryoid bodies." Cell Stem Cell **3**(5): 508-518.

Tesar, P. J., J. G. Chenoweth, et al. (2007). "New cell lines from mouse epiblast share defining features with human embryonic stem cells." Nature **448**(7150): 196-199.

Thomas, P. Q., A. Brown, et al. (1998). "Hex: a homeobox gene revealing peri-implantation asymmetry in the mouse embryo and an early transient marker of endothelial cell precursors." Development **125**(1): 85-94.

Thomson, J. A. (1998). "Embryonic Stem Cell Lines Derived from Human Blastocysts." Science **282**(5391): 1145-1147.

Ting, J. P.-Y. and J. Trowsdale (2002). "Genetic Control of MHC Class II Expression." Cell **109**(2, Supplement 1): S21-S33.

Torres, M., E. Gomez-Pardo, et al. (1995). "Pax-2 controls multiple steps of urogenital development." Development **121**(12): 4057-4065.

Toyooka, Y., D. Shimosato, et al. (2008). "Identification and characterization of subpopulations in undifferentiated ES cell culture." Development **135**(5): 909-918.

Trigueros, C., K. Hozumi, et al. (2003). "Pre-TCR signaling regulates IL-7 receptor α expression promoting thymocyte survival at the transition from the double-negative to double-positive stage." Eur J Immunol **33**(7): 1968-1977.

Tzouanacou, E., A. Wegener, et al. (2009). "Redefining the Progression of Lineage Segregations during Mammalian Embryogenesis by Clonal Analysis." Dev Cell **17**(3): 365-376.

van Ewijk, W., B. Wang, et al. (1999). "Thymic microenvironments, 3-D versus 2-D?" Seminars in Immunology **11**(1): 57-64.

Vandewijngaert, F. P., M. D. Kendall, et al. (1984). "Heterogeneity of epithelial-cells in the human thymus - an ultrastructural-study." Cell and Tissue Research **237**(2): 227-237.

Wallin, J., H. Eibel, et al. (1996). "Pax1 is expressed during development of the thymus epithelium and is required for normal T-cell maturation." Development **122**(1): 23-30.

Walther, C., J.-L. Guenet, et al. (1991). "Pax: A murine multigene family of paired

box-containing genes." Genomics **11**(2): 424-434.
Wawersik, S. and R. L. Maas (2000). "Vertebrate eye development as modeled in Drosophila." Human Molecular Genetics **9**(6): 917-925.
Wekerle, H. and U.-P. Ketelsen (1980). "Thymic nurse cells[mdash]Ia-bearing epithelium involved in T-lymphocyte differentiation?" Nature **283**(5745): 402-404.
Wells, J. M. and D. A. Melton (1999). "Vertebrate endoderm development." Annu Rev Cell Dev Biol **15**(1): 393-410.
Wijngaert, F. P., M. D. Kendall, et al. (1984). "Heterogeneity of epithelial cells in the human thymus." Cell and Tissue Research **237**(2): 227-237.
Wilson, A., H. R. MacDonald, et al. (2001). "Notch 1–Deficient Common Lymphoid Precursors Adopt a B Cell Fate in the Thymus." The Journal of Experimental Medicine **194**(7): 1003-1012.
Wray, J., T. Kalkan, et al. (2011). "Inhibition of glycogen synthase kinase-3 alleviates Tcf3 repression of the pluripotency network and increases embryonic stem cell resistance to differentiation." Nat Cell Biol **13**(7): 838-845.
Wray, J., T. Kalkan, et al. (2010). "The ground state of pluripotency." Biochemical Society Transactions **38**(4): 1027-1032.
Xu, H., F. Cerrato, et al. (2005). "Timed mutation and cell-fate mapping reveal reiterated roles of Tbx1 during embryogenesis, and a crucial function during segmentation of the pharyngeal system via regulation of endoderm expansion." Development **132**(19): 4387-4395.
Xu, H., M. Morishima, et al. (2004). "Tbx1 has a dual role in the morphogenesis of the cardiac outflow tract." Development **131**(13): 3217-3227.
Xu, P.-X., W. Zheng, et al. (2002). "Eya1 is required for the morphogenesis of mammalian thymus, parathyroid and thyroid." Development **129**(13): 3033-3044.
Yasunaga, M., S. Tada, et al. (2005). "Induction and monitoring of definitive and visceral endoderm differentiation of mouse ES cells." Nat Biotechnol **23**(12): 1542-1550.
Ying, Q.-L., J. Nichols, et al. (2003). "BMP Induction of Id Proteins Suppresses Differentiation and Sustains Embryonic Stem Cell Self-Renewal in Collaboration with STAT3." Cell **115**(3): 281-292.
Ying, Q. L., J. Wray, et al. (2008). "The ground state of embryonic stem cell self-renewal." Nature **453**(7194): 519-523.
Zamisch, M., B. Moore-Scott, et al. (2005). "Ontogeny and Regulation of IL-7-Expressing Thymic Epithelial Cells." The Journal of Immunology **174**(1): 60-67.
Zorn, A. M. and J. M. Wells (2009). "Vertebrate endoderm development and organ formation." Annu Rev Cell Dev Biol **25**: 221-251.
Zou, D., D. Silvius, et al. (2006). "Patterning of the third pharyngeal pouch into thymus/parathyroid by Six and Eya1." Dev Biol **293**(2): 499-512.